CHARPTER 1

INTRODUCTION

1.1 Research Background and Motivation

The need to meet global energy demand (with respect to supply) has become a major challenge due to industrialisation and increase in population. This has resulted in price fluctuation for fossil fuels and its products [1-3]. Furthermore, environmental issues that pose problem to human health, arising from the use of fossil fuels have necessitated the exploration and the development of different sources of renewable energy [4-6]. Hence, efforts are being made by researchers to harness available technologies in the conversion of different sources for renewable energy [7-11]. Biomass material conversion into hydrocarbon fuel is one of such promising options [12-14]. Even though biofuel production from edible vegetable oil through esterification and transesterification has been considered, the process leading to competitiveness in food available for consumption is a setback. Therefore, research has been re-directed to liquid fuel production with the use of non-edible vegetable oils and non biodegradable materials [8, 14-16].

There are various means of converting biomass and non-biodegradable solid waste such as vehicle tyres to fuel [13-14]. An alternative option of such conversion method is the thermochemical process. After tyres have served its purpose, they are disposed off as solid waste. Used tyres (UT) make up one of the most problematic hazardous solid wastes in developing countries [17-18]. In South Africa, more than one hundred and sixty tonnes of waste tyres are generated on a yearly basis [19]. This has resulted in the national government formulating a

policy of fee charges of about $223.20 per tonne including 14% value added tax on new tyres introduced by tyre manufacturers and importers into the country [20, 21].

Difficulty in the disposal of this polymer material waste arose from its non-biodegradable nature, accompanied with the challenges of its negative impact on the environment and human health [7, 15]. Irrespective of other methods of recycling used tyres such as grinding, reclaiming, retreading and so forth being used, these methods do not utilize used tyres as an excellent material for energy recovery [8, 12]. Thus, interest in pyrolysis has been renewed since the optimisation of the process can help in deriving high value products [5-6, 14-15, 23-27]. Basically, pyrolysis encompasses the thermal degradation of organic materials such as polyisoprene, to low hydrocarbon weight components at high temperature (250–900^{o}C) in an inert environment [4, 9, 13, 28]. Apart from the possibility of performing pyrolysis under atmospheric or reduced pressure, it is also an excellent route for energy recovery. The technique is environmentally friendly and can thermally decompose a wide range of waste including used tyres [3, 5, 8-9, 18, 23, 29-41]. The basic products of pyrolysis include liquid fraction (pyrolytic oil), solid residue (char), and gases [1, 7, 23]. Solid residue can find application in the rubber industry as reinforcement agent, activated carbon production, or as solid fuel (with caution due to its sulphur content). The pyrolytic oil or liquid fraction can be used as an additive or substitute for conventional fossil fuel due to its high heating value (range of 41–44MJ/kg). Similarly, the pyrolytic oil can be a source of chemicals that is required for various industrial purposes. The gas fraction can serve as heat energy in the operation of the pyrolysis process [12-13, 28, 31, 42-45].

Although pyrolysis of used tyres has been reported in literature, there is a need to explore other means of improving the yield and composition of the liquid fraction from tyre pyrolysis. Apart from the pyrolytic oil (liquid fraction) being used as "dirty" fuel as a result of the presence of tars, sulphur and other inorganic materials; it should be upgraded and refined both as a source of clean fuel. Refining of the pyrolytic oil for wider industrial application and higher chemical value products, will help increase the market for the pyrolysis products thereby making the process more economically viable.

The major components of Natural Rubber (NR) also referred to as *latex rubber* (a term used in order to distinguish it from synthetic rubber) obtained from the species of plants known as Hevea brasiliensis [46-47] are mainly polyisoprene organic compounds, inorganic materials and water. This suggests that NR, which has found application in different areas of human activities, especially in the plastic and automobile industries [48-51], has not been reported as a source of liquid fuel or pyrolytic oil in literature [7].

Therefore, the main focus of this research was to utilize used tyres (UT), a known source of increasing solid waste currently in Africa and NR which is available in West Africa as pyrolysis feed material for production of pyrolytic oil. To produce oil from the UT and NR, catalytic pyrolysis could be used. Hence, catalyst was used to produce oil in this study. The catalyst used was zeolite NaY synthesised from Lawani Benin River Nigeria kaolin (LBK) obtained from Benin City, Edo state Nigeria. The kaolin served as a source of silica and alumina for the synthesis of the catalyst. This could help increase the market value of such clay due to the many

industrial applications of zeolites [52]. Characterisation and upgrade of the pyrolytic oil was performed so as to make it suitable as fuel for internal combustion engines (ICT).

1.2 Hypothesis

Used tyres and natural rubbers are made up of heavy molecular weight hydrocarbon compounds, which can be depolymerised to low molecular weight ones under controlled conditions using pyrolysis process. It is therefore hypothesised that pyrolysis of natural rubber will produce higher yield of low molecular weight hydrocarbon such as pyrolytic oil than used tyres.

1.3 Justification of the Study

In recent years, research on the pyrolysis of used tyres and other biomass for obtaining different products of interest (depending on the process conditions) abound in literature [2-4]. Nevertheless, investigation of natural rubber as a source of liquid fuel is yet to be reported in literature; while used tyres pyrolysis is an area that still needs to be explored and developed in Africa [21]. From available reports, almost 28 million of the used tyres generated in South Africa on a yearly basis are either burnt or discarded in unauthorized locations [20-21]. An annual increase of 9.3 million has been projected for this figure [20-21, 53].

There is also the rising demand for products made from polymeric materials due to their excellent properties in serving human needs. This has led to an increase in polyisoprene based non-biodegradable solid waste which has become a negative environmental issue and human health challenge. Thus, knowledge of this project using South African used tyres for production

of pyrolytic oil is of interest in managing such solid waste and turning them to a means of renewable energy while reclaiming and sustaining the environment. The use of NR as a means of liquid fuel will give an economic boost and help revamp the farming of natural rubber in countries like Nigeria where such plants are grown. Also the possibility of LBK as a natural material source of synthesising zeolite NaY will increase the economic value of such material.

1.4 Research Aims and Objectives

The main aim of this project was to compare the pyrolysis of used tyres and natural rubber. The accomplishment of the aim was achieved by the following objectives:

- To produce pyrolytic oil from the catalytic pyrolysis of used tyres and natural rubber using synthesised zeolite NaY (Lawani Benin River Nigeria Kaolin (LBK) was used as source for silica and alumina silicate).
- To optimize the pyrolytic oil production process from both used tyres and natural rubber
- To characterize and upgrade the pyrolytic oil to attain commercial standard as chemicals and substitute fuel energy source.
- To determine the effect of different blends of pyrolytic oil distillates from used tyres and natural rubber with conventional gasoline on the fuel consumption and fuel power in an internal combustion engine**.**

The schematic representation of the objectives is shown in Figure.1.1.

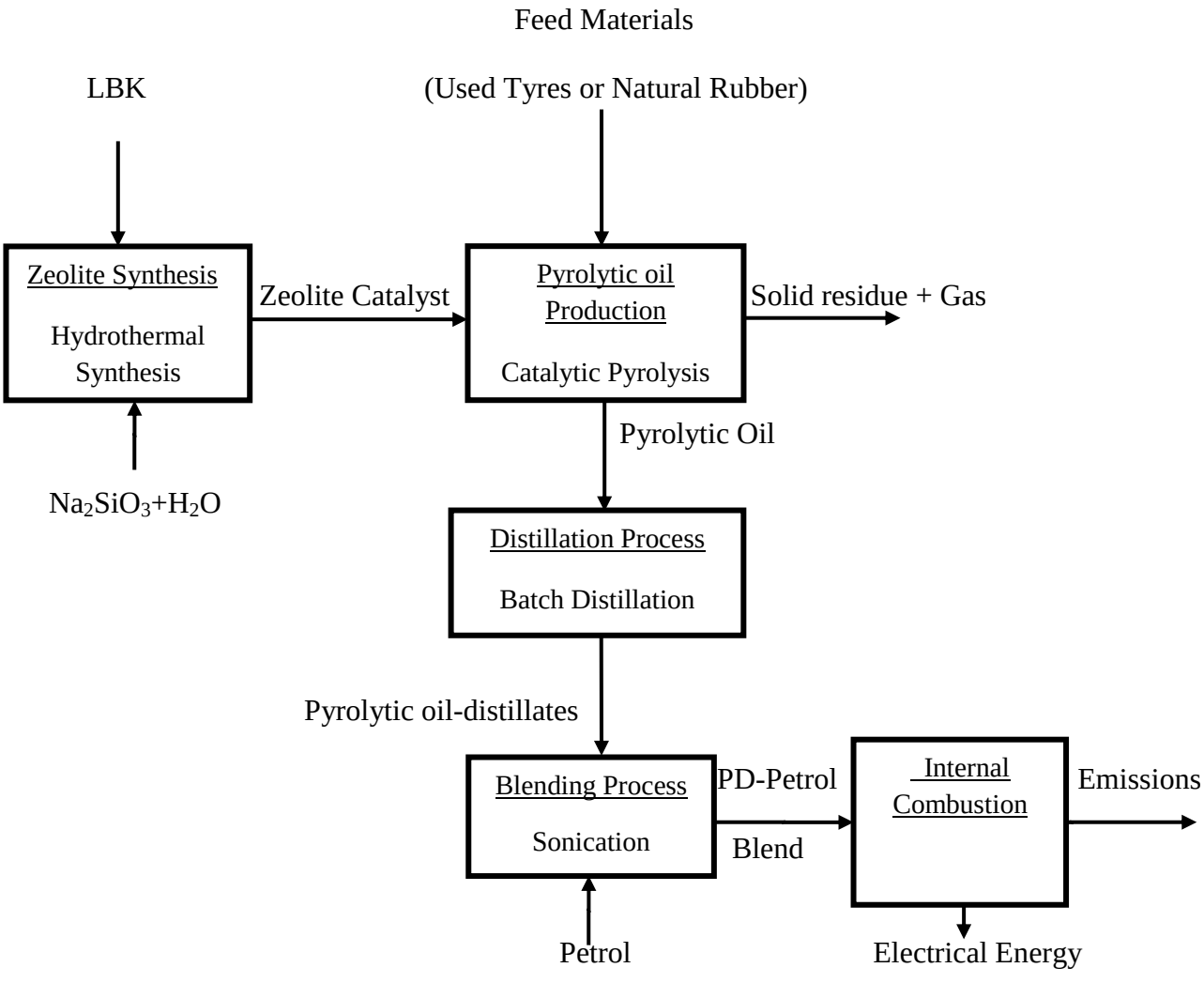

Figure 1.1: Work flowchart of objectives/activities of the study

1.5 Thesis Outline

Chapter One is the introductory chapter and contains: Research Background and Motivation, Hypothesis, Justification of the Study, Research Aims and Objectives and the Thesis Outline.

Chapter Two, entitled literature review, provides background information on natural rubber, tyre processing routes, vulcanization, fabrication, composition and disposal challenges of

used tyres, used tyre pyrolysis process description, mechanism of used tyre pyrolysis. Also, products obtained from UT pyrolysis and their compositions, influence of pyrolysis process parameters on yield and properties of products, benefits and limitations of the pyrolysis process, properties and process of zeolite synthesis and the internal combustion of blended fuel were reported.

Chapter 3 provides detailed information about the experimental procedures. It also explains the operating conditions of the equipment used in the synthesis of zeolite NaY catalysts, characterisation of the material samples, the analyses and distillation of the produced pyrolytic oils, the properties and performance of the pyrolytic oil distillate/commercial gasoline blend in an internal combustion engine. Chapter 4 contains the results and the discussion of the results tables, pictures and figures. These were interpreted and discussed with comparison to previous research studies.

Chapter 5 contains conclusion and recommendations. This chapter provides a summary of the main findings, overall conclusions drawn from the results and recommendations for future work.

References

[1] Kumaravel, S.T., Murugesan, A. and Kumaravel, A., 2016. Tyre pyrolysis oil as an alternative fuel for diesel engines–A review. *Renewable and Sustainable Energy Reviews*, *60*, pp.1678-1685.

[2] Rengga, W.D.P., Handayani, P.A., Kadarwati, S. and Feinnudin, A., 2015. Kinetic study on catalytic cracking of rubber seed (Hevea brasiliensis) oil to liquid fuels. *Bulletin of Chemical Reaction Engineering and Catalysis*, *10*(1), pp. 50-60.

[3] Martínez, J.D., Veses, A., Mastral, A.M., Murillo, R., Navarro, M.V., Puy, N., Artigues, A., Bartrolí, J. and García, T., 2014. Co-pyrolysis of biomass with waste tyres: upgrading of liquid bio-fuel. *Fuel Processing Technology*, *119*, pp. 263-271.

[4] Frigo, S., Seggiani, M., Puccini, M. and Vitolo, S., 2014. Liquid fuel production from waste tyre pyrolysis and its utilisation in a diesel engine. *Fuel*, *116*, pp. 399-408.

[5] Undri, A., Rosi, L., Frediani, M. and Frediani, P., 2014. Upgraded fuel from microwave assisted pyrolysis of waste tyre. *Fuel*, *115*, pp. 600-608.

[6] Hu, H., Fang, Y., Liu, H., Yu, R., Luo, G., Liu, W., Li, A. and Yao, H., 2014. The fate of sulfur during rapid pyrolysis of scrap tyres. *Chemosphere*, *97*, pp. 102-107.

[7] Osayi, J.I., Iyuke, S. and Ogbeide, S.E., 2014. Biocrude production through pyrolysis of used tyres-A review. *Journal of Catalysts*, *2014*, pp. 9.

[8] Onoji, S.E., Iyuke, S.E., Igbafe, A.I. and Nkazi, D.B., 2016. Rubber seed oil: A potential renewable source of biodiesel for sustainable development in sub-Saharan Africa. *Energy Conversion and Management*, *110*, pp. 125-134.

[9] Quek, A. and Balasubramanian, R., 2013. Liquefaction of waste tyres by pyrolysis for oil and chemicals —A review. *Journal of Analytical and Applied Pyrolysis*, *101*, pp. 1-16.

[10] Liu, S., Xie, Q., Zhang, B., Cheng, Y., Liu, Y., Chen, P. and Ruan, R., 2016. Fast microwave-assisted catalytic co-pyrolysis of corn stover and scum for bio-oil production with CaO and HZSM-5 as the catalyst. *Bioresource Technology*, *204*, pp. 164-170.

[11] Boxiong, S., Chunfei, W., Cai, L., Binbin, G. and Rui, W., 2007. Pyrolysis of waste tyres: The influence of USY catalyst/tyre ratio on products. *Journal of Analytical and Applied Pyrolysis*, *78*(2), pp. 243-249.

[12] Bi, J., Guo, X., Liu, M. and Wang, X., 2010. High effective dehydration of bio-ethanol into ethylene over nanoscale HZSM-5 zeolite catalysts. *Catalysis Today*, *149*(1), pp. 143-147.

[13] Brammer, J. and Bridgwater, A.V., 1999. A review of biomass drying technologies for thermal conversion. *Renewable and Sustainable Energy Reviews*, *3*(4), pp. 243-289.

[14] Jahirul, M.I., Rasul, M.G., Chowdhury, A.A. and Ashwath, N., 2012. Biofuels production through biomass pyrolysis—A technological review. *Energies*, *5*(12), pp.4952-5001.

[15] Islam, M.R., Tushar, M.S.H.K. and Haniu, H., 2008. Production of liquid fuels and chemicals from pyrolysis of Bangladeshi bicycle/rickshaw tyre wastes. *Journal of Analytical and Applied Pyrolysis*, *82*(1), pp. 96-109.

[16] Aguado, R., Olazar, M., Vélez, D., Arabiourrutia, M. and Bilbao, J., 2005. Kinetics of scrap tyre pyrolysis under fast heating conditions. *Journal of Analytical and Applied Pyrolysis*, *73*(2), pp. 290-298.

[17] Weisz, P.B., Haag, W.O. and Rodewald, P.G., 1979. Catalytic production of high-grade fuel (gasoline) from biomass compounds by shape-selective catalysis. *Science*, *206*(4414), pp. 57-58.

[18] Bajus, M. and Olahová, N., 2011. Thermal conversion of scrap tyres. *Petroleum and Coal*, *53*(2), pp. 98-105.

[19] Mastral, A.M., Murillo, R., Callen, M.S. and Garcia, T., 2000. Optimisation of scrap automotive tyres recycling into valuable liquid fuels. *Resources, Conservation and Recycling*, *29*(4), pp. 263-272.

[20] Molewa, B.E.E., 2013. National Environmental Management: Waste Act (59/2008): Approval of an Integrated Industry Waste Tyre Management Plan of the Recycling and Economic Development Initiative of South Africa. *South African National Department of Environmental Affairs*, *569*, pp. 35927.

[21] Pilusa, T.J., Shukla, M. and Muzenda, E., 2013. Tyre Derived Fuel as an Alternative fuel for CI engines. *International Conference on Environment, Agriculture and Food Sciences Kuala Lumpur, Malaysia (ICEAFS'2013*).

[22] Berrueco, C., Esperanza, E., Mastral, F.J., Ceamanos, J. and García-Bacaicoa, P., 2005. Pyrolysis of waste tyres in an atmospheric static-bed batch reactor: Analysis of the gases obtained. *Journal of Analytical and Applied Pyrolysis*, *74*(1), pp. 245-253.

[23] Williams, P.T., 2013. Pyrolysis of waste tyres: A review. *Waste Management*, *33*(8), pp.1714-1728.

[24] Harrison, G. and Ross, A.B., 1996. Use of tyre pyrolysis oil for solvent augmentation in two-stage coal liquefaction. *Fuel*, *75*(8), pp. 1009-1013.

[[25] Bhatia, V.K., Padmaja, K.V., Kamra, S., Singh, J. and Badoni, R.P., 1993. Upgrading of biomass constituents to liquid fuels. *Fuel*, *72*(1), pp. 101-104.

[26] Fix, S.R., 1980. Microwave devulcanization of rubber. *Elastomerics*, *112*(6), pp. 38-40.

[27] Phadke, A.A., Bhattacharya, A.K., Chakraborty, S.K. and De, S.K., 1983. Studies of vulcanization of reclaimed rubber. *Rubber Chemistry and Technology*, *56*(4), pp. 726-736.

[28] Isayev, A.I., Yushanov, S.P. and Chen, J., 1996. Ultrasonic devulcanization of rubber vulcanizates. I. Process model. *Journal of Applied Polymer Science*, *59*(5), pp. 803-813.

[29] Schnecko, H., 1998, December. Rubber recycling. In *Macromolecular Symposia*, 135(1), pp. 327-343.

[30] Midgley Jr, T. and Henne, A.L., 1929. Natural and synthetic rubber. I. Products of the destructive distillation of natural rubber. *Journal of the American Chemical Society*, *51*(4), pp. 1215-1226.

[31] Beecham, M., 2008. Global market review of automotive tyres—forecasts to 2014. *Aroq Limited*, UK. JA1867566, 31.

[32] Donatelli, A., Iovane, P. and Molino, A., 2010. High energy syngas production by waste tyres steam gasification in a rotary kiln pilot plant. Experimental and numerical investigations. *Fuel*, *89*(10), pp. 2721-2728.

[33] Kar, Y., 2011. Catalytic pyrolysis of car tyre waste using expanded perlite. *Waste Management*, *31*(8), pp.1772-1782.

[34] Chang, Y.M., 1996. On pyrolysis of waste tyre: degradation rate and product yields. *Resources, Conservation and Recycling*, *17*(2), pp. 125-139.

[35] de Marco Rodriguez, I., Laresgoiti, M.F., Cabrero, M.A., Torres, A., Chomon, M.J. and Caballero, B., 2001. Pyrolysis of scrap tyres. *Fuel Processing Technology*, *72*(1), pp. 9-22.

[36] Yang, J., Tanguy, P.A. and Roy, C., 1995. Heat transfer, mass transfer and kinetics study of the vacuum pyrolysis of a large used tyre particle. *Chemical Engineering Science*, *50*(12), pp. 1909-1922.

[37] Conesa, J.A., Font, R., Fullana, A. and Caballero, J.A., 1998. Kinetic model for the combustion of tyre wastes. *Fuel*, *77*(13), pp. 1469-1475.

[38] Senneca, O., Salatino, P. and Chirone, R., 1999. A fast heating-rate thermogravimetric study of the pyrolysis of scrap tyres. *Fuel*, *78*(13), pp. 1575-1581.

[39] Domínguez, A., Fernández, Y., Fidalgo, B., Pis, J.J. and Menéndez, J.A., 2008. Bio-syngas production with low concentrations of CO_2 and CH_4 from microwave-induced pyrolysis of wet and dried sewage sludge. *Chemosphere*, *70*(3), pp.397-403.

[40] Zhao, X., Song, Z., Liu, H., Li, Z., Li, L. and Ma, C., 2010. Microwave pyrolysis of corn stalk bale: A promising method for direct utilization of large-sized biomass and syngas production. *Journal of Analytical and Applied Pyrolysis*, *89*(1), pp. 87-94.

[41] Balat, M., Balat, M., Kırtay, E. and Balat, H., 2009. Main routes for the thermo-conversion of biomass into fuels and chemicals. Part 1: Pyrolysis systems. *Energy Conversion and Management*, *50*(12), pp. 3147-3157.

[42] Bridgwater, T., 2007. Pyrolysis of Biomass. IEA Bioenergy: Task 34. *Bioenergy Research Group, Aston University*, Birmingham, UK.

[43] Bridgwater, A.V., Czernik, S. and Piskorz, J., 2001. An overview of fast pyrolysis. *Progress in Thermochemical Biomass Conversion*, pp. 977-997.

[44] Aguado, R., Olazar, M., Gaisán, B., Prieto, R. and Bilbao, J., 2002. Kinetic study of polyolefin pyrolysis in a conical spouted bed reactor. *Industrial and Engineering Chemistry Research*, *41*(18), pp. 4559-4566.

[45] Cornelissen, T., Yperman, J., Reggers, G., Schreurs, S. and Carleer, R., 2008. Flash co-pyrolysis of biomass with polylactic acid. Part 1: Influence on bio-oil yield and heating value. *Fuel*, *87*(7), pp. 1031-1041.

[46] Thomas, S. and Stephen, R., 2010. Rubber nanocomposites: preparation, properties and applications. *John Wiley and Sons,*Clementi Loop, Singapore.

[47] Slack, C., 2003. Noble Obsession: Charles Goodyear, Thomas Hancock, and the Race to Unlock the Greatest Industrial Secret of the 19th Century. *Hyperion*.

[48] Haydary, J., Koreňová, Z., Jelemenský, Ľ. and Markoš, J., 2008. Thermal decomposition of waste polymers. *Thermophysics 2008*, pp. 62.

[49] Evans, M.S., 2002. Tyre compounding for improved performance, 12. *iSmithers Rapra Publishing*.

[50] Pradhan, D. and Singh, R.K., 2011. Thermal pyrolysis of bicycle waste tyre using batch reactor. *International Journal of Chemical Engineering and Applications*, *2*(5), pp. 332.

[51] Trongkaew, P., Utistham, T., Reubroycharoen, P. and Hinchiranan, N., 2011. Photocatalytic desulfurization of waste tyre pyrolysis oil. *Energies*, *4*(11), pp. 1880-1896.

[52] Kovo, A.S., Hernandez, O. and Holmes, S.M., 2009. Synthesis and characterization of zeolite Y and ZSM-5 from Nigerian Ahoko Kaolin using a novel, lower temperature, metakaolinization technique. *Journal of Materials Chemistry*, *19*(34), pp. 6207-6212.

[53] Pilusa, J., Shukla, M. and Muzenda, E., 2014. Economic assessment of waste tyres pyrolysis technology: a case study for Gauteng Province, South Africa. *International Journal of Research in Chemical, Metallurgical and Civil engineering (IJRCMCE)*, 1(1).

CHAPTER 2

LITERATURE REVIEW

This literature review chapter contains part of a review paper that has been published in the journal of Catalyst: **Julius I. Osayi**., Sunny Iyuke and Samuel E. Ogbeide (2014). Pyrolytic oil production through pyrolysis of used tyres. *Hindawi Publishing Corporation Journal of Catalysts Volume 2014*, Article ID 386371, 9 pages http://dx.doi.org/10.1155/2014/386371

2.1 Origin and General Concept of Natural Rubber

The origin of natural rubber is reportedly associated with the Native Americans as far back as the 14th century, particularly Brazil, therefore earning the plants the botanical name Hevea Brasiliensis [1-2]. This unique plant was brought to Europe by Christopher Columbus, one of Europe foremost voyagers [3-4]. Charles de la Condamine in 1736 was the first to perform a scientific study on natural rubber, a year after coming into contact with the product in Peru [4]. It was later described as nothing more than a "type of condensed resinous oil" by Fresnau, another French Engineer after he studied rubber on his home ground Guiana [3, 5]. Despite the discovery of its use as an eraser and popularity acclaimed to it by an English scientist, Joseph Priestley, which made it to become commonly known as “Indian rubber”, it did not get much attention until Macquer suggested that rubber could be used to produce flexible tubes [6]. From 1815 to 1830 rubber caught the attention of countless craftsmen and led to the establishment of the Rosburg factory in 1832. It was during this period that the famous waterproof coat known as the "Macintosh" was invented by Macintosh, who also implemented the use of benzene as a solvent,

in collaboration with Hancock [7]. The manufacture of elastic balls and rubber mattress were invented by Hancock, who also introduced an industrial scale method of cutting, rolling and pressing rubber. The role of heat during the pressing process and the suitable machine to perform it was invented by Hancock [3, 7].

However, cold and sunlight had a negative impact on the un-vulcanized rubber products which became a major setback to its demand [7]. Consequently, the discovery of vulcanization in 1840 by Charles Goodyear [1-2, 8] brought about the successful process of upgrading natural rubber. Since then, rubber has played a leading role in the world market due to its numerous applications [9]. During the 19th century, South America was the world's major supplier of the required quantity of latex rubber. However, in recent years, the major rubber producing countires are Thailand and Indonesia with an estimated amount of 62% of natural rubber produced in the world. Figure 2.1 shows the top ten countries that produce high quantities of natural rubber and their percentages.

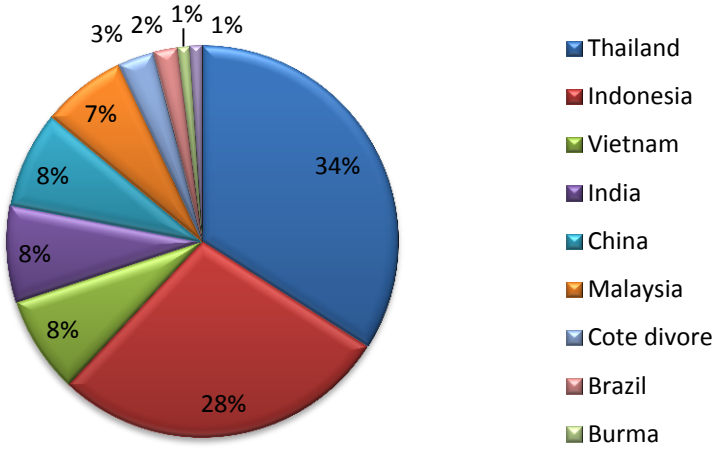

Figure 2.1: World top 10 countries in natural rubber production (in tons) as at 2013[4]

Natural rubber, commonly called latex rubber, is a product obtained from certain varieties of plant trees. These trees include Para rubber tree, Common Dandelion, Gutta Percha, Rubber fig, Panama Rubber tree and Hevea Brasiliensis [4]. However, for commercial purpose in the rubber industry, Hevea Brasiliensis is the most common and important source of natural rubber [10]. This is as a result of the high yield of between 50–100 g latex per day in a matured Hevea Brasiliensis tree [11].The term 'tapping' is used in describing the harvesting of natural rubber from trees [12]. This involves the incision of the bark of the tree with a sharp object such that the milky-like fluid can flow into a container mounted on the tree as shown in Figure 2.2(a-b). Although latex can coagulate naturally after a certain period of time, it can be aided by adding chemicals like formic acid. Coagulation is when the latex changes from liquid to a solid state. Depending on the seasonal effects and condition of the soil, typical constituents of Hevea latex is 25~35 wt% *cis*-1,4-polyisoprene (PIP), 1~1.8 wt% protein; 1~2 wt% carbohydrates; 0.4~1.1 wt% lipids, 0.5~0.8 wt% amino acids, and 50~70 wt% Water [13].

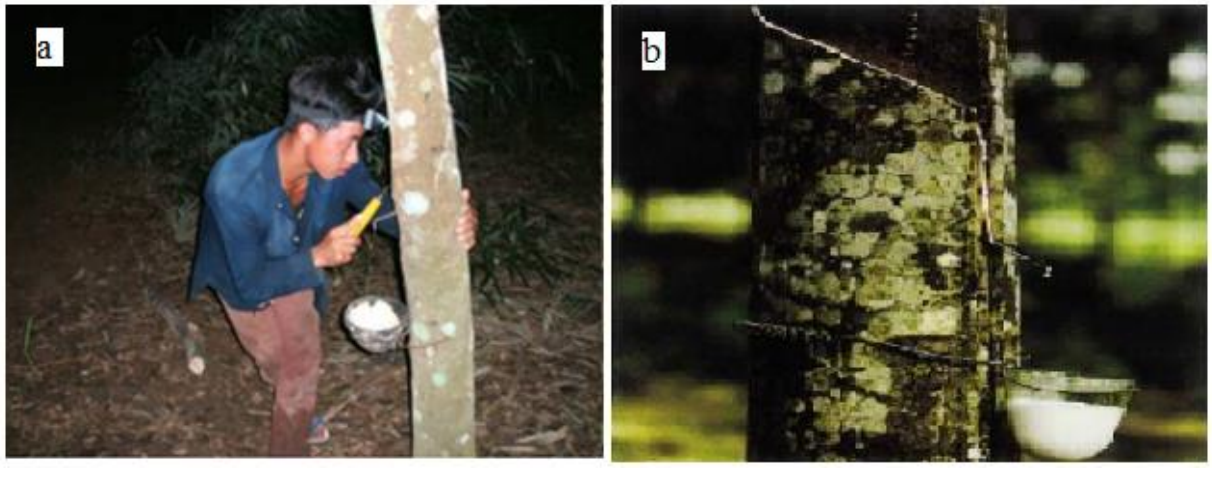

Figure 2.2: (a) Natural rubber tree latex being tapped (b) Collection of natural rubber latex after tapping [4]

2.1.1 Properties of rubber

Natural rubber possesses some exceptional physical and chemical properties that have endeared it to different areas of man's need. Since its discovery, natural rubber has played a major role in modern civilization and technology [3]. Despite attempts by researchers to formulate its chemical composition, which lead to the production of various types of synthetic rubbers and plastics, natural rubber still remains a unique elastomer [3-7]. These properties are discussed below.

2.1.1.1 Elastomeric property

NR is composed of long-chain branched natural polymer molecules [15-17].The presence of these long chain polymers and linear structure contributes to its high molecular weight of more than 100,000 g/mol to 1,000,000 g/mol [4]. The hydrocarbon cis-1, 4-polyisoprene as shown in Figure 2.3 makes up 85% of the content of these polymers. This accounts for natural rubber ability to exist in both the gel and the sol phase. This enhances its cross-linked resistance in solvents such as toluene and benzene.

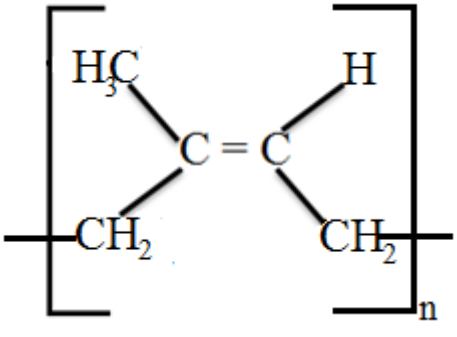

Figure 2.3: Cis-polyisoprene structure (the key component of natural rubber)

Also the low temperature and ease to crystallize exhibited by natural rubber can be attributed to its elastomeric property [4]. The tensile strength, resistance to cutting, tearing and abrasion properties of natural rubber is enhanced through crystallization [4].

2.1.1.2 Thermal property

The thermal conductivity of NR enables it to dissipate heat rapidly when stretched continuously. This loss of energy is termed hysteresis [3-4]. In general, NR is sensitive to heat such that a variation in temperature affects the latex. For instance, NR at temperature below 0^{o}C hardens, but become soft and weak at temperature above 80^{o}C, with a decrease in strength. It also becomes sticky [7].

2.1.1.3 The oxidation property

Unprocessed latex rubber and various elastomers undergo oxidation upon exposure to air which is also referred to as ozone cracking [18] or dry rotting (as shown in Figure 2.4). This is due to the fact that each isoprene unit contains multiple bonds that make it sensitive to ozone cracking and prone to vulcanization. During this process, a reaction occurs between the polymer chains and oxygen from the atmosphere with ultra violet radiation acting as catalyst [18-19]. When subjected to tensile stress, the chain length of the material polymers is hereby broken into smaller chain polymers which can result in the material failure. Antiozonants are normally added to rubber to prevent such problems [4].

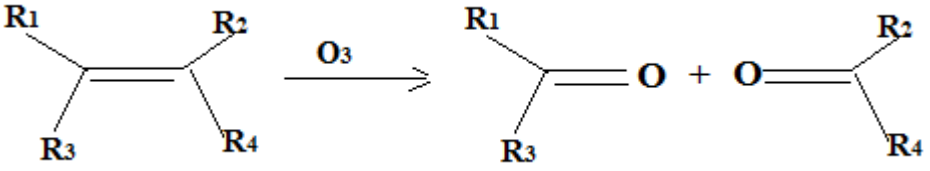

Figure 2.4: A typical Ozonolysis reaction equation [18]

2.1.1.4 The elasticity property

NR comprises of covalent cross-linked polymer chains that can elongate when under tension and also regain its original position briskly when the tension is released. Such a feature is known as elasticity [4]. This elasticity is as a result of the ability of the long chains to spread out and reconfigure themselves in response to applied stress [20]. The extreme flexibility of rubber is attributed to its elasticity property. When the applied stress exceeds the elasticity of the rubber material, a permanent deformation occurs due to the cross-linkages being broken, leading to failure or uneasiness to reconfigure chains when the stress is removed. Young's modulus of elasticity can be used to predict the extent of elongation or compression of elastomers as long as the stress does not exceed the material yield strength [20-21].

Mathematical expression for Young's modulus of elasticity, *E*,

$$E = \frac{stress}{strain} \tag{2.1}$$

$$E = \frac{\frac{F}{A}}{\frac{dL}{L}}$$

Where;

F = Force (N), A=Area of object (m^2), dL = elongation or compression (offset) of the object (m) and L = length of the object (m)

Elasticity of polymers can be affected by temperature variation. At lower temperature, the elasticity reduces due to less mobile chains in the elastomers especially when cooled to crystalline state. NR has been reported to have a tensile strength of 200 kg/cm^2 and an elasticity of 300 to 1000 % [21-22].

2.1.2 Synthetic rubbers and natural rubber

Despite a wide variety of synthetic rubbers available today as a result of technological innovation to produce different rubbers with specific properties and purpose, the most common ones are polybutadiene rubber, BR, and polystyrene-butadiene rubber, SBR. These synthesised rubbers still cannot replace natural rubber in terms of quality and performance. They are artificial rubber, made from monomers such as butadiene, styrene, isoprene, chloroprene, isobutylene, acrylonitrile, ethylene and propylene which are abundant in petroleum refining. Majority of the synthetic rubbers such as SBR are utilized for tyre production. Generally, both NR and synthetic rubbers must undergo processing for improved performance in application [4]. The difference in the process of production between synthetic rubbers and natural rubber is shown in the Figure 2.5 and 2.6

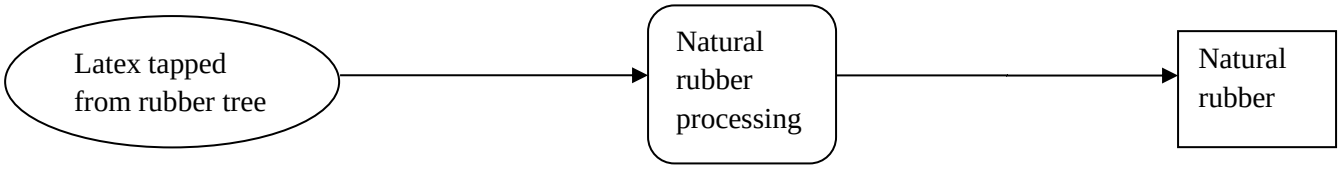

Figure 2.5: Production process of Natural rubber

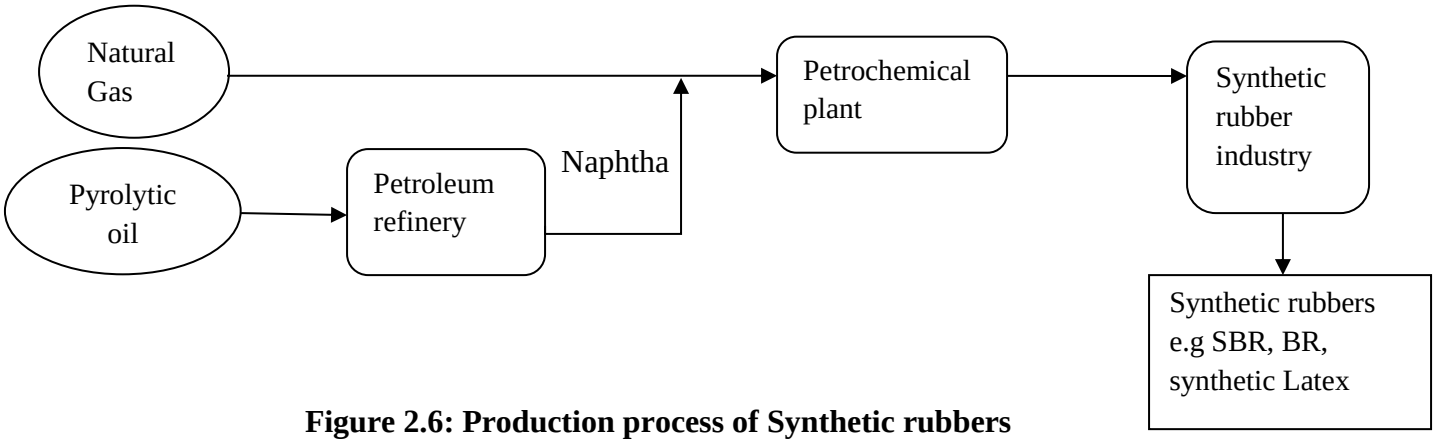

Figure 2.6: Production process of Synthetic rubbers

2.1.3 Vulcanization of rubber

Vulcanization is a process mostly undergone by NR. It involves rubber being heated along with chemicals like peroxide, sulfur, or bisphenol at a particular temperature for a specific time after which it is left to cure and assume its shape (Figure 2.7). Sulfur vulcanization is the most common form of rubber vulcanization. During this process, polysulfide crosslinks are formed between the carbon chains. The carbon-hydrogen bonds of the polyisoprene structure are then substituted by carbon-sulfur bonds. This results in rapid tightness of the chain for a particular length of strain, thereby making rubber harder and less-extensible due to an increase of the elastic force constant [23]. In order to avoid formation of brittle rubber, the crosslink density must be controlled [22]. The process of vulcanization helps to improve rubber properties such as abrasion resistance, tear strength, hardness, elasticity, tensile strength and resistance to solvents. When only sulfur is used during vulcanization, the curing time could take up to 9 hours. This could be reduced with the aid of “activators” and “accelerators” which also help in eliminating cyclic structures and shorten sulfur links to two or one sulfur atoms from seven sulfur atoms. Hence the rubber perishing properties such as poor resistance to heat is improved. ZnO and

$C_{18}H_{36}O_2$ (stearic acid) are typical activators, while accelerators commonly used in industry are $C_7H_5NS_2$ (Mercaptobenzthiazole) and $[(CH_3)_2NCS_2]_2$ (Tetramethylthiuram disulphide) [24]. In order to increase the rubber abrasion resistance, protective agents such as trialkyphenol is used along with clay, carbon black, and $CaCO_3$ which serves as fillers etc. [23-24].

The discovery of vulcanization is generally ascribed to Charles Goodyear in 1839 [2, 25].

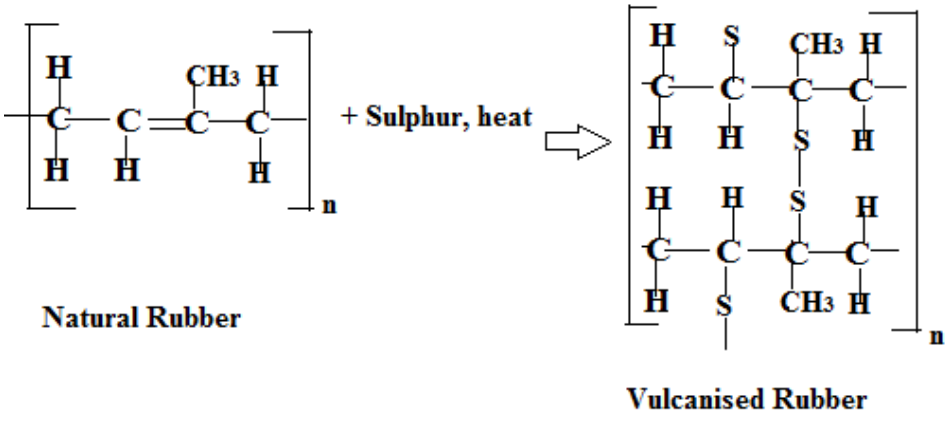

Figure 2.7: Vulcanization of Natural Rubber [25]

2.1.4 Application of natural rubber

NR is a vital and strategic industrial raw material for manufacturing a wide variety of products, ranging from household items, footwear, hospital and medical equipment, civil construction, telecommunications, automobile, aviation industry, industrial safety wears and personal protective equipment. Car tyres are made from 12-14 different rubbers, of which up to 50% of the rubber used can be NR. Aircraft and race tyres contain only NR [2-3].

2.1.5 Natural rubber as liquid fuel

Despite the number of years in which NR has been in use for different purposes, investigation of NR, also referred to as Latex rubber, solely as a source of liquid fuel has not been reported [26]. Although it is noted that as a component in used tyres, NR has undergone pyrolysis along with other components [27-28]. Hence in this research, NR will be studied as a source of pyrolytic oil that can then be upgraded as chemical feedstock and as fuel for internal combustion engine. This is expected to produce fewer pollutants (PAHs, CO_2 and H_2S) than that from petroleum.

2.2 Used Tyres

2.2.1. Tyre production process and composition of used tyres

On a global scale, the largest sector of natural rubber consumption is the tyre industry. The industry operates a process where different components are mustered on a tyre building drum and made to undergo vulcanization under heat and pressure [23]. The tyre production process, made up of two stages, could be automated or manually operated. The wrapping of the drum with inner liner, sidewalls, body piles and coupling of the assembly over the placed bead occur at the first stage. During the second stage, the belt package and tread are attached and the uncured tyre is inflated and shaped. The curing time for this process takes about sixteen minutes for car tyres and twenty four hours for heavy duty tyres [23]. Inspection with human eyes for any deformity of the tyres along with balance measurement is done with the aid of an X-ray machine at the final stage of production [23, 29]. A tyre compound is made up of rubber elastomers (55-65%) present in varying ratios, and the rest is carbon black (CB), stabilizers, antioxidants, sulphur, hydrocarbon oils, zinc oxides, textile or steel cords [30-33]. The rubber elastomers present in tyres (Figure 2.8

shows their monomers present in tyres) is a blend of NR, which is obtained from the Hevea tree, and synthetic rubbers (such as SBR and BR) which is generally obtained from petroleum based products [34-35]. Although the percentages of each component of tyres vary according to manufacturer's formulation and purpose, Table 2.1 presents the typical tyre constituents of a passenger and truck tyres [31, 36]. It is the same properties of tyres at point of manufacture that is mostly present in a used tyre.

Table 2.1: Composition of a tyre [31, 36]

Constituent	**Car tyre (wt. %)**	**Truck tyre (wt. %)**	**Remark**
Rubber	47	45	Natural rubber (polyisoprene) and different synthetic rubbers such as SBR, BR, nitrile rubber, chloroprene rubber are used
Carbon black	21.5	22	For fortification of the rubber and to withstand abrasion
Metal	16.5	21.5	Serves as cord for strength and steel belt
Fabric/textile	5.5	-	Strengthening of the tyre
Zinc oxide	1	2	Improves the physical properties of the rubber and helps (with stearic acid) to regulate the vulcanization process
Sulphur	1	1	Helps with the cross linking of rubber polymer chain in the tyre and also to solidify and resist distortion at higher temperatures
Additives	7.5	5	Clay or silica are examples of additives partly used for carbon black replacement

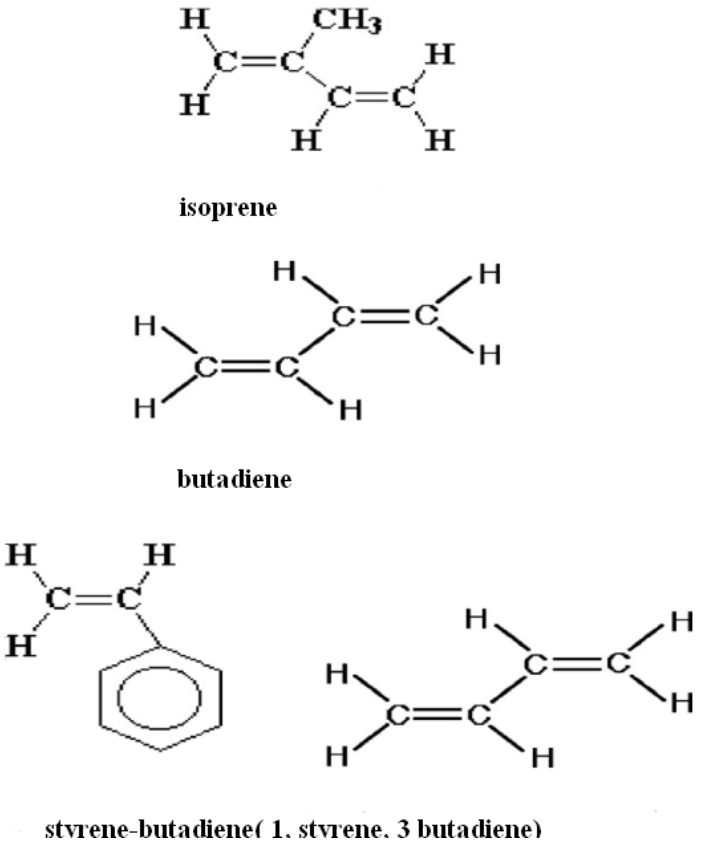

Figure 2.8: Tyre rubber monomers [35, 37]

2.2.2 Proximate and ultimate analysis of used tyres

The various amounts of volatile matter, ash content, fixed carbon and moisture content in the tyre is identified through proximate analysis. It has been reported that the volatile content indicates the suitability of the feedstock for pyrolysis conversion to liquid product where high volatile content is needed [32]. Rodriguez et al. [38] reported that the volatile content is composed of polymeric compounds that came from NR and SBR in the tyre. The ash content is the inorganic residue left after the combustion of the volatile and fixed carbon. The fixed carbon content indicates the amount of char formation in the pyrolysis process [32]. It does not represent the total carbon in the feedstock as some also escaped along with the volatiles during the thermal

decomposition. From literature, the calorific value of tyre pyrolytic liquid (Pyrolytic oil) between the range of 40-44 MJ/kg is higher than that of most conventional fuel such as coal, which could make it suitable for use as an alternative fuel [38-41].

Table 2.2 and 2.3 (on a steel free basis) show the proximate and ultimate analysis reported by various authors in literature. It is noteworthy that the difference in values is as a result of the formulation (which is unique to each manufacturer) used for the tyre production. This determines the weight percent of the different tyre components [32].

From Table 2.2, the values of the fixed carbon varied from 19.45 to 33.50%, with ash content which is between 2.40 to 19.13%, while that of the volatile matter ranges between 1.72 to 66.5% and the moisture content ranges from 0.50 to 58.80%. For the ultimate analysis, the results of H and N contents reported are similar but there was a little variation in that of C and S contents [34]. Another advantage of Tyre rubber is that it has a lower moisture and ash content than coal [42].

Table 2.2: Proximate analysis of used tyre rubber

Moisture (wt. %)	Ash (wt. %)	Volatile (wt. %)	Fixed carbon (wt. %)	HHV (MJ/kg)	Ref.
0.80	4.40	61.30	33.50	37.10	[43]
1.72	19.13	59.69	19.45	27.37	[44]
1.31	10.21	62.32	26.26	33.24	[45]
1.22	8.73	62.40	27.60	35.70	[46]
0.70	8.00	61.90	29.50	36.20	[39]
0.80	7.41	64.64	27.15	39.56	[47]
1.72	14.01	61.61	22.66	-	[48]
0.80	2.40	66.50	30.30	-	[49]

Table 2.3: Used tyre rubber ultimate analysis

Carbon (wt. %)	Hydrogen (wt. %)	Nitrogen (wt. %)	Sulphur (wt. %)	Oxygen (wt. %)	Ashes (inorganic)	Ref.
85.20	7.30	0.40	2.30	0.40	4.40	[43]
67.08	6.12	0.17	2.05	24.58	-	[44]
74.41	6.94	0.21	1.60	5.02	-	[45]
80.10	7.48	0.42	1.54	10.50	-	[46]
86.70	8.10	0.40	1.40	1.30	2.10	[39]
81.84	6.06	1.77	1.64	0.48	-	[47]
81.24	7.36	0.49	1.99	8.92	-	[48]
85.80	8.00	0.40	1.00	2.30	2.40	[49]

2.2.3 Thermogravimetric analysis of used tyres

The main objective of thermogravimetry analysis (TGA) is to get information about the general behaviour of the thermal degradation of used tyres, (UT) [50].The pyrolysis process comprises of more than one stage degradation temperature zone during the process [32, 52]. Both TG and DTG methods are acceptable techniques for measurements of tyre rubber sample mass change with respect to temperature and time [51-53]. From the TG results data (shown in Table 2.4) provided by other authors in literature, it can be estimated that the pyrolysis process for the different rubber components in the UT [55–56], which are usually NR, SBR and BR respectively, start around 200 ^{o}C and goes to completion around 550 ^{o}C.

Table 2.4: commencement and end temperatures of pyrolysis of used tyre

Pyrolysis Commencement temperature ^{o}C	Pyrolysis end temperature ^{o}C	Heating rate (^{o}C/min)	Ref.
250	550	5	[48]
250	500	5	[57]
200	500	10	[47]
200	450	5	[58]

2.3. Disposal Challenges of Used Tyres

As a result of the tyre manufacturing process, tyres are made to withstand rough mechanical usage and survive harsh weather conditions such as ozone (the most cause of damage on rubbers), light and biological organisms [34, 59]. When tyres are no longer serving its purpose, they enter the solid waste streamline; it is at this stage they are referred to as used tyres (UT). UT which can also be referred to as waste tyres (WT) is defined as tyres that have expired as a result of exceeding their production life span or are no longer safe for usage due to defects (such as damage of its physical composition/structure arising from use) and cannot be retreaded. It is one of the most problematic hazardous solid wastes modern society has to deal with, particularly in developing countries [32, 54-55, 60,]. The disposal difficulty results from the UT bulky nature, abrasion resistance and the presence of inorganic components [32, 35, 61-63].

Although, there are options for disposing UT such as land filling, stockpiling, combustion and recycling they have major setbacks [56, 64-66]. Since almost 75% of the volume of tyre is an empty space, landfilling and stockpiling of UT take a lot of space, compaction is difficult and they are non-biodegradable. The lifetime of a tyre in landfill is considered to be between four and five decades [34, 59, 67].

When UT can be combusted to serve as energy recovery, the emissions composed of dioxins, polycyclic aromatic hydrocarbons, PAH, volatile organic compounds, VoCs, particulate matter etc released during the combustion process have harmful impact on the environment and human health [30, 34-35, 37]. In the investigation of emission produced from the combustion of rubber,

Buekens [67] reported that a sizeable amount of zinc, (Zn) particles were present. When a blend of coal (80%) and tyres (20%) was used as energy for the operation of a cement manufacturing plant with a capacity of one million tons annually as a case study, Carrasco et al. [68] reported an increase of 47 and 30% in the rate of CO and SO_2 emissions alongside a decrease of 15% in NOx.

Furthermore, there was an increase in the amount of inorganic compounds such as zinc, chromium, aluminum, iron, lead and magnesium in comparison to when coal serves as the only feedstock. According to DeMarini et al. [69], the mutagenic emission factor of open air combustion of UT is 3 - 4 orders of magnitude greater than the values reported for the combustion of oil, coal or wood in utility boilers. Even the combustion of UT under controlled conditions, the PAHs emissions from UT were almost twice as high as that of coal at comparable equivalence ratios [70].

2.3.1. Methods of recycling of used tyres

Used tyres recycling methods are discussed below.

2.3.1.1 Retreading method: This method involves the smoothing off the residual tread in an expended tyre and a new tread rubber is installed through vulcanization. The term “remold” is used to describe such process. [54]. It is noteworthy that only inspected and repaired used tyres casings can be retreaded. Despite the economic advantage of this method, its major challenge is product quality confidence.

2.3.1.2 Mechanical or cryogenic method: This entails the milling of tyres to produce ground rubber of different particle sizes as a means of recycling used tyres. In the cryogenic method, the use of liquid Nitrogen enables the waste tyres to be grounded at temperatures of -80 to -100^{o}C [60]. Several areas of application abound for the use of the fine grounded rubber, but the disadvantge of the method is that it is an expensive process to operate and it has a limited market [54].

2.3.1.3. Reclaiming rubber raw materials methods: Several methods of how to reclaim rubber exist.The most relevant of them are thermomechanical reclaiming [71], microwave reclaiming [72], mechanical shearing process [73], reclaiming by biotechnological processes, ultrasonic reclaiming [74], reclaiming by renewable resource materials, reclaiming by use of different chemical agents [48], gasification and pyrolysis of waste tyre [75].

The properties exhibited by rubber obtained from the reclaiming method are similar to that of a virgin rubber. This can be attributed to the change in structure of the used tyres from an interlinked thermoset of three dimensions to two dimensional polymers. However, the process high cost of operation and industry indifference towards reclaimed rubber is a major discouragement. Even though used tyres can be combusted as solid fuel in cement kilns, the process is harmful to the environment and not economically wise [30, 35, 76].

Since tyres have been reported to have high calorific value, higher than coal and biomass [34, 77], and are composed of long-chain hydrocarbons, finding a process/route to harness this

potential will be advantageous especially in recovering hydrocarbons from the used tyres to serve as alternative energy and other chemical feedstock. This would reduce the dependence on fossil fuels and help in CO_2 emission reduction [31]. For this reason, pyrolysis is receiving renewed interest in used tyres disposal owing to the fact that this process can be optimized to produce some high value products [30-32, 35, 78-83]. Also in comparison with other methods of treating solid waste, pyrolysis is more appropriate in converting polyisoprene materials such as used tyres to different high value products.

During the pyrolysis process, organic materials decompose at high temperature under an inert atmosphere into low molecular weight components [32, 35]. Hence, pyrolysis is also referred to as destructive distillation. One of the foremost investigations on the destructive distillation of rubber was done in the 1920s when Midgley and Henne performed destructive distillation of rubber and reported that isoprene and dipentene were the main products [27, 84]. Table 2.5 gives a list of the processes used for used tyres pyrolysis for the past thirty years.

Table 2.5: Different methods of Tyre pyrolysis used within the past three decades [54]

Year	Process type	Reactor used	Ref.
1970	Destructive distillation	n.r	[84]
1972	Hydro conversion	n.r	[85]
1974	Microwave pyrolysis	Microwave	[86]
1976	Pyrolization	n.r	[87]
1978	Subatmospheric pyrolysis	n.r	[88]
1980	Pyrolysis	Fluidized bed	[89]
1982	Pyrolysis and incineration	Fluidized bed and incineration fluidized bed chamber	[90]
1984	Pyrolysis	Quartz tube	[91]
1986	Tyre copyrolysis with oil	Heated cylindrical glass flask	[92]
1988	Flash pyrolysis	Quartz tube	[93]
1990	Vacuum pyrolysis	Batch reactor	[94]
1992	Vacuum pyrolysis	Batch reactor	[95]
1994	Vacuum pyrolysis	Continuous feed reactor	[40]
1996	Pyrolysis	Fluidized bed reactor	[57]
1998	Pyrolysis and combustion	Platinum pan	[59]
2000	Pyrolysis and hydropyrolysis	Swept fixed bed	[42]
2002	Pyrolysis	Rotary kiln reactor	[96]
2004	Pyrolysis	Autoclave reactor	[41]
2006	Pyrolysis	Fixed bed reactor	[97]
2008	Vacuum pyrolysis	Fixed bed reactor	[98]
2010	Pyrolysis	Moving bed	[99]
2012	Pyrolysis	Fixed bed reactor	[100]
2014	Microwave assisted pyrolysis	Microwave oven	[30]

n.r.: not reported

2.4. Pyrolysis of Used Tyres

2.4.1 Pyrolysis description

Pyrolysis, also termed destructive distillation is a process that enables the breaking down of organic materials at high temperatures (250 to 900 ^{o}C) into low molecular-weight products in an oxygen free environment [35, 55-56]. Pyrolysis classification can be into slow, fast and flash pyrolysis with regards to the operating conditions (such as heating rate, the residence time of the volatiles and the temperature) and the environment used such as catalytic pyrolysis, vacuum pyrolysis, oxidative pyrolysis, hydro-pyrolysis and steam pyrolysis [34,79]. Despite UT pyrolysis being entirely an endothermic process; it involves a combination of endothermic and exothermic reactions [61]. It can be performed under vacuum or atmospheric pressure [79]. During the process, chemical bonds in the compounds are broken; it is also the first stage in gasification and combustion process [33]. Pyrolysis can also be referred to as reverse polymerization due to the occurrence of thermal depolymerisation or polymer cracking that occurs during the process, [101].

Amongst other methods of recycling such as combustion and gasification used to deal with solid waste, which are otherwise difficult, attention in the area of research has been given to pyrolysis due to the possibility of optimising the process conditions to yield high energy density liquids, char, and gas [32]. Also, ease of storage and transportation of the condensable fraction (pyrolytic oil) from the production location to where it can be most proficiently utilized is an advantage. Thermal degradation of used tyres can be said to be made up of more than one phase, that is, the release of volatiles and moisture which occur at low temperature, succeeded by the thermal

decomposition of NR, BR and SBR at higher temperature, respectively [28, 37]. Subject to the aim of the pyrolysis process, the following process parameters such as pressure, heating rate, temperature, feed particle sizes, catalysts, flow rate of inert carrier gas, configuration of reactor used [34], and so forth can influence the percentage weight of each fraction of pyrolysis [54, 101].

2.4.2 Types of pyrolysis

As stated earlier, the operating conditions of pyrolysis can be used to classify the process. Its difference can also be from the residence time of the pyrolysed material in the reactor, process temperature, feed particle size, heating rate [28, 102], and so forth. Further description of the types of pyrolysis includes the following.

2.4.2.1 Slow pyrolysis

The feedstock residence time in the reactor is greater than 450 – 550s for volatile materials and could be several hours or days for solid materials. The operating conditions include a heating rate of between 0.1 – 1 ^{o}C, feed particle size range of 5 – 50 mm with process temperature of 550 – 950 (^{o}C) [54, 79]. More of char production is favoured during slow pyrolysis and is unlikely to yield bio-oil of high quality. Furthermore, as a result of a long residence time, the quality of bio-oil produced could be adversely affected due to occurrence of secondary reactions arising from the cracking of the primary products [54, 103].

2.4.2.2. Fast pyrolysis

In this pyrolysis method, the condensable vapour generated by the rapid heating of the pyrolysed material at a high temperature in an inert environment is vey short. The operating conditions comprise of less than 10 s of residence time for the pyrolysed material, between 10 to 200 ^{o}C heating rate, below 5 mm feed particle size and 550 to 1200 ^{o}C reaction temperature. The effectiveness in yielding liquid fuel together with a variety of specialty and commodity chemicals has accorded much attractiveness to this technology [79]. In general when compared with other processes based on percent yield, fast pyrolysis produces 60 to 75% pyro-oil unlike 15 to 25% yield obtained from other processes; it has reasonably low investment costs and high energy efficiencies, particularly on a small scale [104].

2.4.2.3. Flash pyrolysis

During flash pyrolysis, a high heating rate of more than 200 ^{o}C, particle size below 0.2 mm, reaction temperature that exceeds 1000 ^{o}C and a less than 0.5 s solid residence time operating conditions are used. Nevertheless, the major technological setback for this process is poor thermal stability, the bio-oil containing solids, and generation of pyrolytic water [79, 103].

2.4.2.4. Catalytic pyrolysis

This is a pyrolysis process that involves the application of a catalyst. The role of the catalyst is to help improve the kinetics of pyrolysis reaction of the thermal degradation of heavy molecular weight hydrocarbon compounds to lighter hydrocarbon compounds [31]. It has been reported that the use of a catalyst in tyre pyrolysis systems can greatly influence the composition, quality, and

yield of products [31, 75]. Examples of catalysts used in tyre pyrolysis include Na_2CO_3, NaOH, MgO, $CaCO_3$, aluminium-based catalyst, perlite, CaC_2, $Cu(NO_3)_2$, zeolite-based catalyst, and so forth [31, 35]. Product distribution from the use of different catalysts can be affected by the operating conditions.

Also, the method of catalyst application during pyrolysis can be used in grouping catalytic pyrolysis methods. The first group is when the catalyst is added to the feedstock before being fed into the reactor. This is the method adopted in this study for the catalytic pyrolysis of used tyres and natural rubber. The second group is when catalyst is added after the feed is already heated up in the reactor allowing it to have immediate contact with vapors, solid, and char. The third group is when the catalyst is placed in another reactor located downstream from the pyrolysis reactor [79, 105].

Also, depending on the catalyst composition, they can be classified as dolomite catalyst, Ni-based catalysts, alkali metal catalysts and novel metal catalysts [79, 106]. These Ni and alkali metal based catalysts have been proven and reported to be effective in more than 99% heavy tar destruction and elimination but rendered inactive by carbon deposition [106]. Assessment of used tyres via catalytic pyrolysis is of significance from an economic and environmental point of view as the quality and composition of the derived gas and tyre pyrolytic oil (TPO) also referred to as used tyre pyrolytic oil (UT pyrolytic oil) can be of higher market value with lower contaminates. It also creates the opportunity to harness natural minerals such as kaolin that can a source for silica and alumina for synthezing the catalyst used for the process.

2.4.3. Chemical reaction of the catalytic pyrolysis

In catalytic pyrolysis, the chemical reaction is mainly an endothermic process. The 3 stages which happen at various temperatures in the course of the process are dehydration, fragmentation, and product formation. In order to prevent combustion, the process is performed in oxygen free environment.The reaction mechanism (reaction 2.1) and the flowchart of organic material catalytic pyrolysis (Figure 2.9) is shown below:

$$[CH_2CH=C(CH_3)CH_2]_n \xrightarrow[+\Delta H]{\text{Catalyst, No } O_2} \text{char, gas, oil} \qquad (2.1)$$

Polyisoprene Where ΔH = heat

Organic material liquefaction via Catalytic pyrolysis

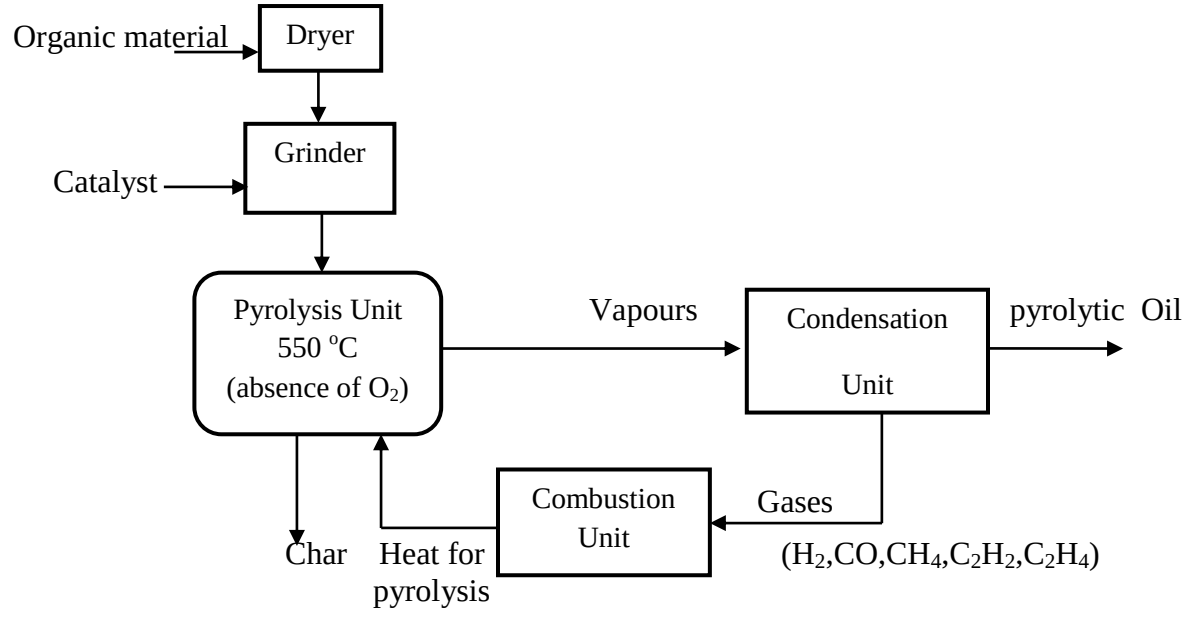

Figure 2.9: Flowchart of Organic material catalytic pyrolysis

2.4.4 Mechanism of used tyre pyrolysis

The pyrolysis process has been reported to have more than one temperature degradation zone by various authors [59, 107]. The pyrolysis mechanism of rubber tyres can then be described with the different pyrolysis temperature degradation stages which are dehydration, fragmentation and product formation. Dehydration of pyrolysis feedstock takes place within the low temperature zone (<300 ^{o}C). At this stage, the volatile additives, oil plasticizers and moisture content of the material are released. This is more of a physical process. At temperatures higher than 300 ^{o}C, fragmentation and product formation begins. Fragmentation of rubber tyre is possible due to their structural composition which is carbon atoms linked with single or double bonds [35, 108]. Hence, depolymerisation of rubber polymer sets in as a result of the carbon bond scission classified as chain scission and side group scission. But chain scission occurs mostly for the pyrolysis of the various components (NR, SBR, BR) of used tyres [109-110].

The carbon bond scission, results in the release of highly reactive free radicals. The investigation done by Chen and Qian [109] and Choi [110] further confirm that radicals, which are mostly sub-units of the source rubber molecule, are formed as a result of the scission of the carbon bonds. Dodds et al. [108] also reported that highly reactive free radicals produced from the thermal degradation of rubber tyre are the outcome of the scission of carbon bonds. Nevertheless, the formation of dimers in rubber pyrolysis is aided by the Diel-Alders mechanism. Groves et al [111] reported that the possible recombination of the monomers could also be attributed to the Diels-Alder mechanism. This was described by Rofiqul et al. [112] during their investigation of UT thermal decompositions mechanism. They reported that depolymerisation of polyisoprene

resulted in the formation of dimeric species, a short-life radical which stabilizes by formation of limonene through pyrolytic isomerisaion. The mechanism as it occurred from propylene to cyclopropene is shown in Figure 2.10.

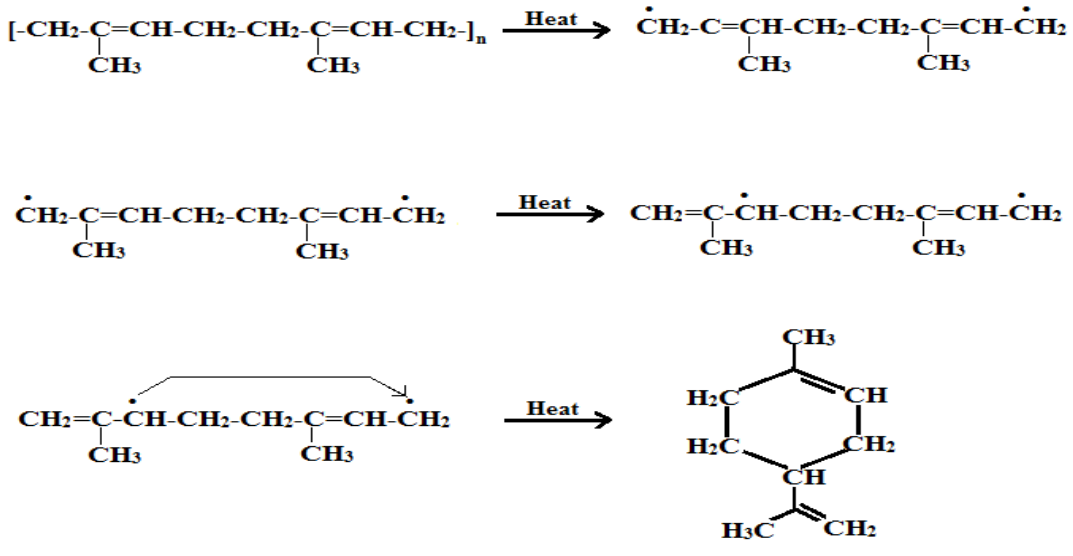

Figure 2.10: Limonene formation from dimeric species through pyrolytic isomerization [109]

In the investigation of thermal degradation mechanism of a waste tyre, Kwon and Castaldi [113] using chemical analysis, reported that the presence of heterocyclic hydrocarbons could be attributed to gas phase reaction between nitrogen (used as purge gas) and radicals such as C, CH, and CH_2 obtained from the pyrolysis of SBR at 600 ^oC. Examples of such heterocyclic hydrocarbons are shown in Figure 2.11. They suggested that the absence of C_4 hydrocarbons (saturated and unsaturated) at high temperature (>500 ^oC) could be attributed to Diel-Alders reaction. This mechanism has been suggested to also favour condition for the generation of benzene ring chemical species at higher temperature [113-114] through the reaction route shown in Figure 2.12.

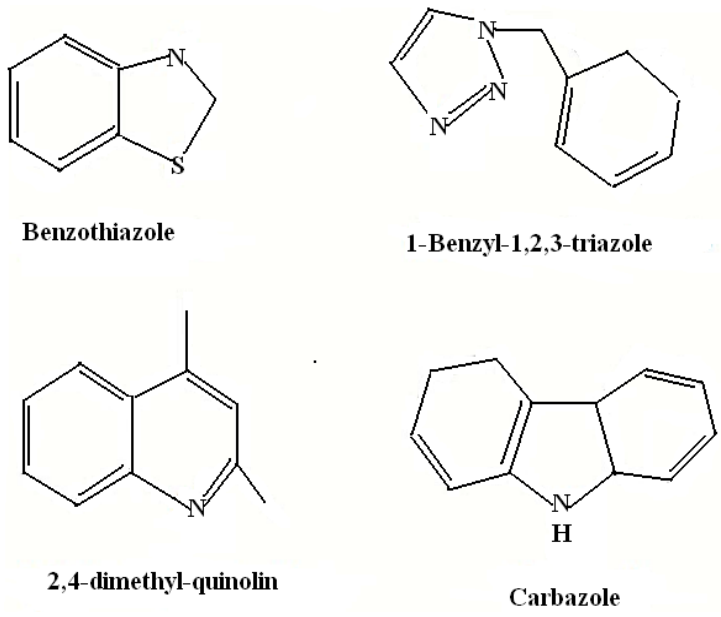

Figure 2.11: Examples of heterocyclic hydrocarbons formed from gas phase reaction in UT pyrolysis [113]

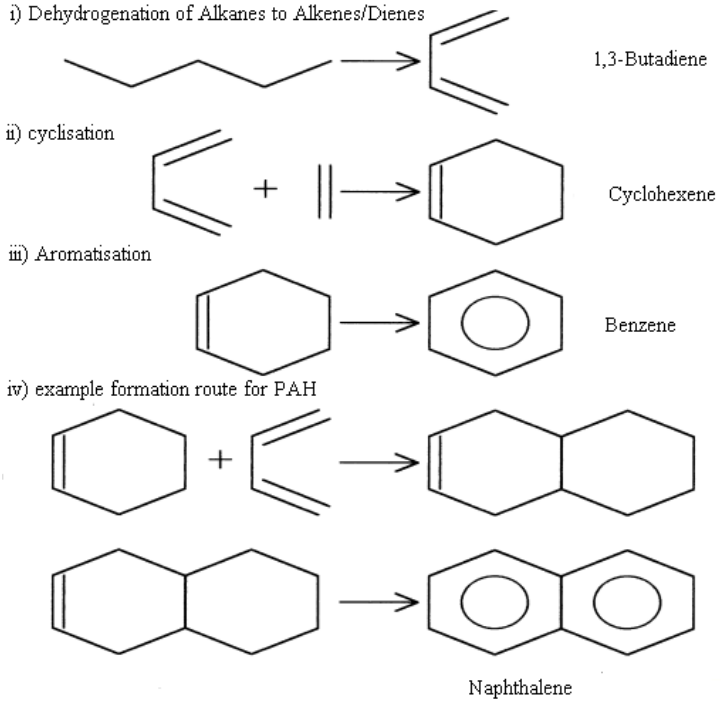

Figure 2.12: Diels–Alder reaction pathway for polycyclic aromatic hydrocarbons formation in UT pyrolysis [114]

Similarly, Pakdel et al. [115] and Williams et al. [116] explained that the production of aromatics such as benzene, xylenes, styrene, toluene, methylstyrene and trimethylbenzene at temperatures greater than 500 ^{o}C is as a result of the decomposition of limonene. This was followed by a gas phase reaction involving cyclisation of alkenes and dehydrogenation to form aromatic hydrocarbons. Hence, the increase in PAH formation at this temperature range during UT pyrolysis. Consequently, the decrease in concentration of single ring aromatic compounds may be attributed to Diels-Alder aromatization to form PAH. Figure 2.13 shows the various steps of the thermal degradation of limonene and resultant PAH formation.

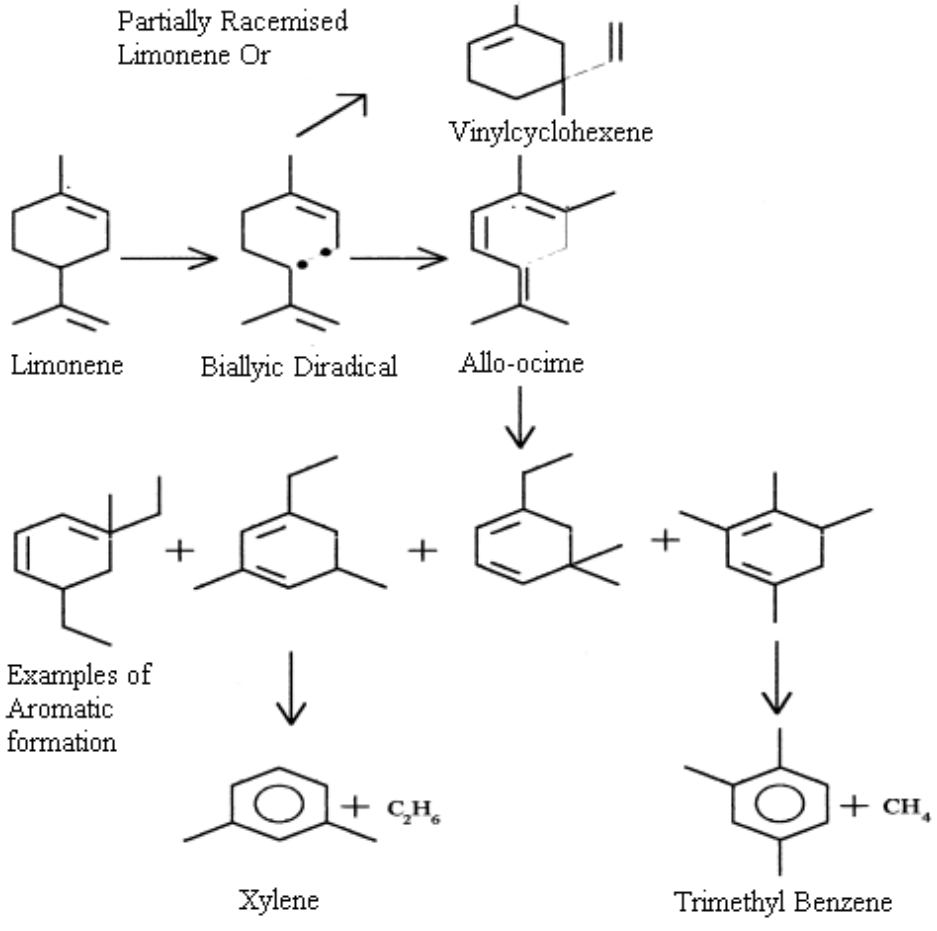

Figure 2.13: Reaction scheme of PAH formation from thermal degradation of Limonene [113]

Simply, the thermal degradation mechanism of UT occurs from the bond scission on each component monomer of the tyre, preceded by hydrogenation / dehydration and recombination by gas phase reaction [113] in relation with the pyrolysis process conditions. Nevertheless, during rubber pyrolysis, decomposition reactions occur simultaneously with depolymerisation to produce short chain hydrocarbons [35].

2.4.5 Products obtained from UT pyrolysis and their compositions

Generally, three main products are usually derived from used tyres pyrolysis. They are classified according to their physical state; solid fraction (char or carbon residue), liquid fraction (also referred to as pyrolytic oil) and the gas fraction [79]. Depending on the desired product from pyrolysis method, the process conditions could be operated to enhance the yield of any of the product fractions [48].

2.4.5.1 Pyrolysis solid fraction

The pyrolysis char, also referred to as the solid carbon residue, is a carbon-rich solid. It is mainly composed of the original carbon black (CB), other carbonized rubber polymer, non-volatile hydrocarbons and inorganic materials such as zinc, sulphur, silica, and clay which served as additives during the tyre production [31]. The pyrolytic char makes up approximately 34-38% of the feedstock used for the pyrolysis process. The yield and properties of CB (particularly the specific area) depend greatly on the manufacturers' formulation during the tyre production

process and the pyrolysis process conditions. Carbon features specifically the specific area is greatly influenced by the process temperature [48]. The elemental, proximate analysis and calorific value of the pyrolytic char reported in literature is presented in Table 2.6. Observation of the elemental results shows that there is high ash content and sulphur retention in the solid residue. Teng et al. [117], and Berrueco et al. [118] in their study of the pyrolysis of waste tyres in an atmospheric static bed reactor, reported that the amount of sulphur retained in the char is approximately 77 wt. % of the initial sulphur present in the tyre (with the rest left in the gas and liquid fraction). These two components, sulphur and ash, present in the char in high amount limit its usage as direct carbon black. Its low surface area, organic impurities and large particle structure make it less desirable for rubber compounding [39,119]. Nevertheless, the solid residue can be used as a precursor for printing ink pigment and activated carbon after physical and chemical treatment, as filler in road bitumen while the high carbon content of calorific value (27-34 MJ/kg) of the pyrolytic char makes it suitable as a source of solid fuel [32, 62].

Table 2.6: Elemental and Proximate analysis of used tyre pyrolysis solid residue reported in literature

Elemental analysis on dry basis (wt. %)				**Proximate analysis (wt. %)**					**Ref.**
C	**H**	**N**	**S**	**Ashes**	**Volatile content**	**Fixed Carbon**	**Moisture content**	**Calorific Value(MJ/kg)**	
80.82	1.46	0.53	2.41	14.58	6.92	77.22	1.28	30.00	[119]
86.30	0.30	0.30	2.80	12.50	1.80	91.30	0.40	29.70	[120]
80.08	0.42	0.17	2.84	16.50	1.20	81.30	1.00	28.57	[121]
85.31	1.77	0.34	2.13	15.33	12.78	71.89	3.57	30.71	[96]

2.4.5.2 Liquid fraction from pyrolysis

The liquid fraction, also known as pyro-oil or pyrolytic oil, is the liquid formed from the condensation of the vapour of a pyrolysis reaction. It is a dark brown/black coloured viscous liquid with a strong acrid smell. The oil is a mixture of C_6–C_{24} organic compounds (53.4–74.8%) specified to be paraffins, olefins, and aromatic compounds with some nitrogenated (2.47–3.75%) and some oxygenated compounds (2.29–4.85%) [61-62]. Elemental analysis of the liquid fraction as reported in literature is presented in Table 2.7. Due to its high heating value (HHV) of ~ 43 MJ/kg, the oil can serve directly as a fuel oil in large stationary engines such as the marine engines which can accept sulphur content up to 2%. It can also be used as an added petroleum refinery feedstock [41, 55, 101]. Presence of high value chemicals such as benzene, toluene and xylenes in the oil has been reported in literature. These chemical compounds can be used as primary feedstock in plastics production [32, 41, 63,].

Similarly, the presence of monoterpene such as limonene (1-methyl-4(1-methylethenyl)-cyclohexene) has been shown in the pyro-oil. Limonene as a high value light hydrocarbon is used in the formulation of wide range of industrial solvents [63]. It can also serve as feedstock in the production of cosmetics and fragrance-based products [62-63,117]. It is noteworthy that chemical species like limonene and 1–methyl-4-(1-methylethyl)-benzene productions from tyre pyrolysis are closely related to the polyisoprene rubber and the styrene butadiene rubber in the used tyre [113]. The elemental analysis of the pyrolytic oil reported in literature (Table 2.7) shows that it contains mainly carbon, C, hydrogen, H, nitrogen, N, sulphur, S, and some amount of oxygen, O.

Table 2.7: Elemental and calorific value of liquid fraction reported in literature

Elemental analysis (wt. %)						Ref.
C	**H**	**N**	**S**	**O**	**CV**	
85.60	10.10	0.40	1.40	2.10	42.10	[38]
84.55	9.59	0.64	1.26	3.96	41.00	[119]
85.40	11.40	0.40	0.60	n.r	43.27	[120]
84.90	9.60	0.40	1.60	3.50	40.77	[121]

2.4.5.3 Pyrolysis gas fraction

The non-condensable gas fraction evolved from the pyrolysis process is often referred to as pyrogas, effluent gas or syngas [55]. It is predominantly composed of paraffin and olefin compounds with carbon numbers ranging from C_1 to C_5 [55]. Table 2.8 shows a collection of the gases present in pyrogas as reported in literature.

Table 2.8: Composition and calorific value of pyrogas reported in literature value

Gas yield (wt. %)	CV(MJ/Nm^3)	Gas concentration (vol. %)								
		H_2	**CO**	**CO_2**	**CH_4**	**C_2H_4**	**C_2H_6**	**H_2S**	**Tempt ^oC**	**Ref.**
25.50	38.10	20.70	2.60	1.80	44.50	4.40	17.30	n.r	800	[59]
29.0	36.16	40.00	1.60	1.40	26.00	-	20.00	n.r	550	[121]
13.90	68.70	22.27	1.98	2.54	21.32	2.32	4.19	n.r	550	[120]
7.60	n.r	26.60	1.15	2.41	23.92	-	13.37	4.18	650	[103]

The presence of CO and CO_2 in the pyrogas may be as a result of the carbonylation and decarboxylation reactions or secondary oxidation reactions of carbon, while secondary aromatization is suggested for the presence of hydrogen and methane [63, 114]. Sulphur oxide, SO_2, nitrogen oxides, NO*x*, carbon monoxide, CO, and polycyclic aromatic hydrocarbons, PAHs are reported as the main pollutant gases from the combustion of used tyres [48, 108, 114]. The generated gas has been reported to have a significant higher heating value of between 34.6 and 40 MJ m^{-3} making it suitable as a source of energy in a gas motor (for electrical power generation), or as a make-up heat required by the pyrolysis process [32]. Figure 2.14 presents a used tyre pyrolysis scheme using the weight percent of the various components and that of the products fraction.

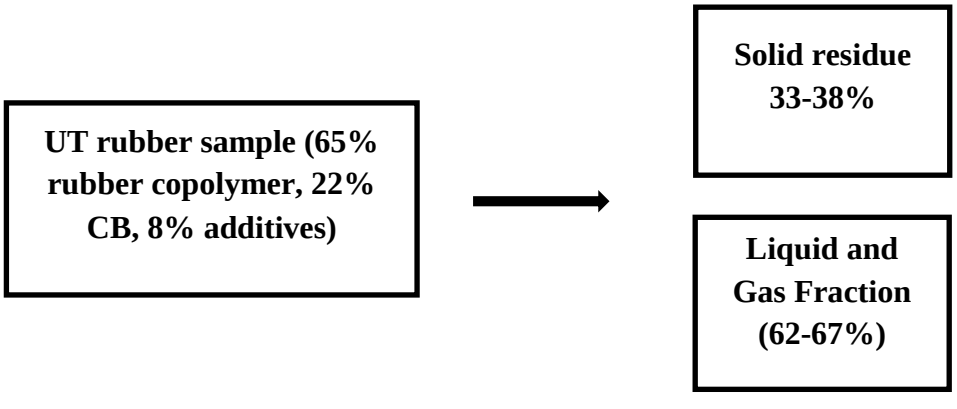

Figure 2.14: Scheme of pyrolysis according to weight percent and products fractions [31]

2.4.6 Influence of pyrolysis process parameters on yield and properties of products

Pyrolysis process product yields and their properties is influenced not only by the operating temperature used for the process, but by several variables such as; feedstock composition, configuration and type of reactor, feed particle size, heating rate, vapour residence time,

efficiency of heat transfer from the hot reactor surface to and within the feed mass, flow rate of the inert carrier gas, presence of catalyst, pressure (vacuum or atmospheric), etc [98]. Hence, with proper manipulation of these various variables the pyrolysis process could be controlled to favour or optimize the desired end product which is basically solid residue, pyrolytic oil and syngas. It is a known fact that the feed material type and composition certainly affect the product yield as it is the defragmentation and depolymerisation of the component materials that will form part of the products at the end of the process [32]. This is responsible for the variation in both proximate and elemental analysis results by different authors as tyre formulation varies according to its brand, type (passenger car tyre, truck tyre, bicycle tyre, tricycle tyre, aero tyre etc) and process method used by manufacturers [36]. Even the weight percentage yield, sulphur and naphtha content of the pyrolytic oil have been linked with the tyre composition [32, 103]. The reactor plays an important role in the pyrolysis process as it can greatly influence the pyrolysis performance, product quality and yield [34, 105]. Within the past three decades, there has been a considerable advancement in the innovation and technological development of the pyrolysis process. Researchers [79] have developed and investigated different reactors and processes to the point where pyrolysis is now an acceptable technique for the deriving of gaseous, liquid, solid fuels, and chemicals. Nevertheless, individual reactor type has unique characteristics, pyrolytic oil yielding capacity, benefits and setbacks. Table 2.9 presents the most popular reactor types and their heating source.

Table 2.9: Reactors and their heating methods [54, 79]

Reactor	Heating method
Fixed bed	Heated wall surface
Bubbling fluidized bed	Heated recycle gas
Circulating fluidized bed	Wall and sand heating
Rotating cone	Gasification of char to heat
Auger	Fire tube
Fluidized bed/quartz	Solar
Plasma	Radio frequency
Vacuum	Direct contact with hot surface
Ablative	Wall heating

The effect of a catalyst in the pyrolysis process can best be seen in terms of product composition, quality and yield [34, 64]. This is due to the ability of the catalyst to crack higher molecular weight compounds into lighter hydrocarbon products by enhancing the pyrolysis reaction kinetics as reported by Gonzalez et al. [39], and Cunliffe and Williams [62]. The use of catalyst to pyrolyse used tyres has therefore helped to produce more single ring aromatics such as benzene, toluene, and xylenes, important chemical feed stocks for the chemical industry, than the non-catalysed process. This was confirmed by the study report by Olazar et al [53] where HY and H-ZSM-5 zeolite catalyst were used to pyrolyse used tyres in a conical spouted bed reactor. The molecular weight of the oil was significantly decreased by both catalysts. This gave a high yield of olefins (specifically ethene and propene), aromatic fractions (more xylenes concentration) and low tar yield compared to the thermal (non-catalysed) pyrolysis. Also the influence of USY zeolite catalyst on pyrolysis temperature, heating rate and products yields of used tyres pyrolysis was investigated by Shen et al [123]. The outcome revealed that zeolite USY catalyst lead to a

decrease in the liquid fraction yield and a resultant increase in gas yield as the catalyst/tyre ratio and pyrolysis temperature increased.

Williams and Brindle [124] have also shown the effect of ZSM-5 zeolite and two zeolite Y- type catalysts with different Si/Al ratios and pore size on the liquid fraction composition and products yields. Their report revealed that zeolite Y with lower Si/Al ratio gave a significant higher amount of benzene, toluene, xylenes, naphthalene and alkylated naphthalene than ZSM-5 zeolite catalyst. These could be due to the acidity and larger pore size possessed by the zeolite Y than the ZSM-5 Zeolite catalyst. The effect of basic catalysts, magnesium oxides and calcium carbonate (V) on pyrolysis of used tyres has also been researched by Shah et al [125]. Results showed that both catalysts, MgO and $CaCO_3$ produced tyre pyrolytic oil (TPO) with fuel properties comparable with fossil diesel. The TPO produced from MgO as catalyst gave 55% aromatic hydrocarbons while 50% aromatic hydrocarbons were recorded for TPO produced from $CaCO_3$ catalyst.

In the conversion of used tyres for recovery of value-added products via catalytic pyrolysis investigated by Shah et al [126], a mixture of an acidic catalyst, SiO_2 and basic catalyst, Al_2O_3 was used. The yield of produced gas, oil and solids were studied in relation to the amount of catalyst, temperature and time. It was reported that Al_2O_3 catalyst gave higher concentration of polar hydrocarbons (40%) than SiO_2 (30%), while SiO_2 gave a higher concentration of aliphatic hydrocarbons (40%) than the Al_2O_3 (30%) in the obtained liquid fraction. An equal amount of Al_2O_3:SiO_2 catalyst mixture produced a TPO of equal concentration of polar (35%) and aliphatic (35%) hydrocarbons.

Pressure increase on the pyrolysis process can aid more viscous liquid with a higher coking tendency as well as more secondary and dehydrogenation reactions. Vacuum pyrolysis will reduce the occurrence of secondary reactions in the vapour phase compared to pyrolysis at atmospheric pressure [119]. This is due to the fact that residence time of the volatile pyrolysis products is shorter and so the secondary reactions are limited [96,103]. Similarly, the amount of liquid produced is more under vacuum process than in atmospheric process with a lower char and gas yield [98,119]. Although lower operating pressure results in reduction of secondary reactions, it does not eradicate it totally. A decrease in the pressure could also result in the process temperature reduction thereby, decreasing the pyrolysis process thermal energy demand [34].

Effect of Particle size on the pyrolysis process could be related to the reaction time, volatiles residence time, heating rate and temperature [32]. From available studies, small particle size is preferred in order to minimize the mass and energy phenomena effects thereby achieving a higher conversion grade and primary pyrolysis products. Nevertheless, smaller particle sizes can lead to speedy devolatilisation rate and consequently possible secondary reactions, depending on the heating rate and the volatiles residence time [34]. Heating rate is also a crucial parameter which affects the reaction rate and determines the temperature profile within the particles during the pyrolysis reaction. An increase in the heating rate generally leads to a shift towards higher temperature in the weight loss profile of the thermogravimetry analysis [58-59, 61]. This implies that the thermal decomposition rate increases as the heating rate is increased, also the commencement and end temperature for the maximum devolatilisation of the process is affected by the heating rate [41, 58-59, 61]. Williams and Besler [33] attributed the phenomenon to the combined effects of the heat transfer and the changes in the kinetics of the decomposition,

resulting in delayed degradation. Therefore, higher heating rates in fast pyrolysis, apart from promoting an increase in the amount of volatiles cumulatively released [58], lead to an increase in the process temperature when compared with slow pyrolysis. In contrast, higher heating rates require more energy with a decrease in pyrolysis time while lower heating rate requires a lower amount of energy with increase in the pyrolysis time [34]. The characteristics of the reactor and the process also have a direct relationship with the heating rate.

The effect of the operating temperature is one of the key variables in the pyrolysis process. This has been studied by several researchers [34]. It is a major determining factor in the amount of the different fractions' yield produced. For instance, pyrolysis conducted at a temperature range of 375 to 575 ^{o}C [32, 63] reveals that as the temperature increases there was a decrease in char yield and an increase in the liquid and gas fraction yield. The optimum temperature range for the pyrolytic oil yield is between 520 to 575 ^{o}C, probably as a result of strong cracking within this temperature range. Hence tyre pyrolysis is said to be incomplete at temperatures below 450 ^{o}C as most of the tyre components such as SBR and BR have not been decomposed [61]. Beyond this optimum temperature, the solid residue remains constant with a decrease in liquid yield contributing to increase in the gas yield due to the devolatilisation of the oil vapours into permanent gases and secondary repolymerisation and/or carbonization reactions of pyrolytic oil hydrocarbons into char [32]. Once the temperature exceeds 900 ^{o}C, the gas fraction will be the dominate product with little or no liquid and char as carbon decompose completely beyond this temperature. Therefore, depending on the pyrolysis process conditions the desired product yields can be optimized and their composition greatly influenced.

2.4.7 Benefits and limitations of the pyrolysis process

Compared to other thermochemical processes such as combustion and gasification, pyrolysis is more environmentally friendly for handling a wide range of solid waste including used tyres due to its low emissions [42, 48]. Also the recovery of solid, liquid and gaseous fractions that has high potential for other application is possible. It is a viable means of harnessing the high volatile content and heating value (33-38 MJ/kg) property of used tyres as an excellent material for energy recovery [48]. The benefit of the pyrolysis process also lies in the opportunity of being able to operate and manage the process conditions to favour any of the expected solid, liquid and gas products unlike other process such as combustion. In addition, the produced liquid fuel, a major product from UT pyrolysis, can be produced and stored, making it possible for the product to be utilized outside the pyrolysis plant site [32, 62]. Furthermore, the significant reduction in gas production compared with the combustion process makes it more advantageous in terms of smaller gas cleaning system being needed than that of incineration plants. Also the generated gas can be burned to generate energy for the process thereby reducing energy cost.

There is also the possibility of preventing the release of hazardous inorganic matter such as zinc and sulphur (present in the tyre) into the environment as they are retained within the solid fraction (up to 90% of sulphur and 100% zinc). This can enable control of such elements into the environment. The generation of polycyclic aromatic hydrocarbons (PAHs) and CO_2 is lower in UT pyrolysis than in combustion when the volatile fractions (liquid and gas) obtained are burnt helping in reduction of CO_2 responsible for the greenhouse effect. Moreover, the absence or low level of oxygen during the pyrolysis process helps inhibit the formation of dioxins and furans

[31, 37]. Despite these numerous benefits of the pyrolysis process, its economic viability depends on the possible market for the three derived main products [35]. The pyrolytic oil must be further refined to make it free of char contamination, reduce its sulphur content in order to compete with conventional fuel obtained from pyrolytic oil oil in terms of price given the current world energy demand situation. There is also the challenge of marketing the solid residue as CB due to its unfavourable properties resulting from the presence of inorganic impurities, high ash content, low surface area, large particle size and lack of the particle structure desired for rubber compounding [34,57,63,].

2.5 Zeolite Structures, Synthesis, Properties and its Uses

2.5.1 General overview of zeolites

Zeolites were first discovered as natural minerals in 1756 by Cronstedt A. Fredrik, a Swedish mineralogist. He used the term ‘intumescence’ to describe the visible loss of water behaviour by the silicate minerals when heated. Hence, the name zeolite is a Greek word meaning ‘boiling stone’ [127]. They are a member of the significant class of natural and synthetic hydrated aluminosilicate minerals of group I and II elements in the periodic table [128].

Zeolites are mainly crystalline solids composed of silicon, aluminum and oxygen structures that form fundamental building blocks of tetrahedral SiO_4 and AlO_4 which results in an open three dimensional framework [128-129]. The presence of cavities and channels in the framework

allows cations (positively charged atoms or atomic clusters), water and/or small molecules to reside in them. The structural formula is given as

$$\mathbf{M}_{a/n}\,[(AlO_2)_{\mathbf{a}}(SiO_2)_{\mathbf{b}}]\,\mathbf{c}H_2O$$

Where; **M** is the cation of valence **n, C** is the number of water molecules, **b/a** is the silica to alumina ratio and (**a+b**) is the number of tetrahedral present in the unit cell.

The framework composition is represented by the square brackets [1]. Since they have no fixed compositions, zeolites are typical non stoichiometric compounds. The presence of a cation in the zeolite framework resulted from the isomorphous substitution of Si^{4+} by Al^{3+} which needs to be compensated by extra framework cation. The unique properties of zeolite and other zeolite-like materials are attributed to the presence and mobility of this cation and its aluminosilicate framework which is not destroyed upon removal or exchange of ions and molecules present in its cavity [127-129].

2.5.2 Structures of zeolites

Generally**,** zeolites can be portrayed as a three dimensional structural material with a framework atom linked with four oxygen atoms tetrahedrally [130]. Silicon (Si) and aluminium (Al) are the common framework atoms but can be replaced by other metals such as gallium, germanium, boron and titanium [129]. Figure 2.15 shows a typical zeolite represented by its primary building unit (PBU), TO4 where T stands for the framework atom.

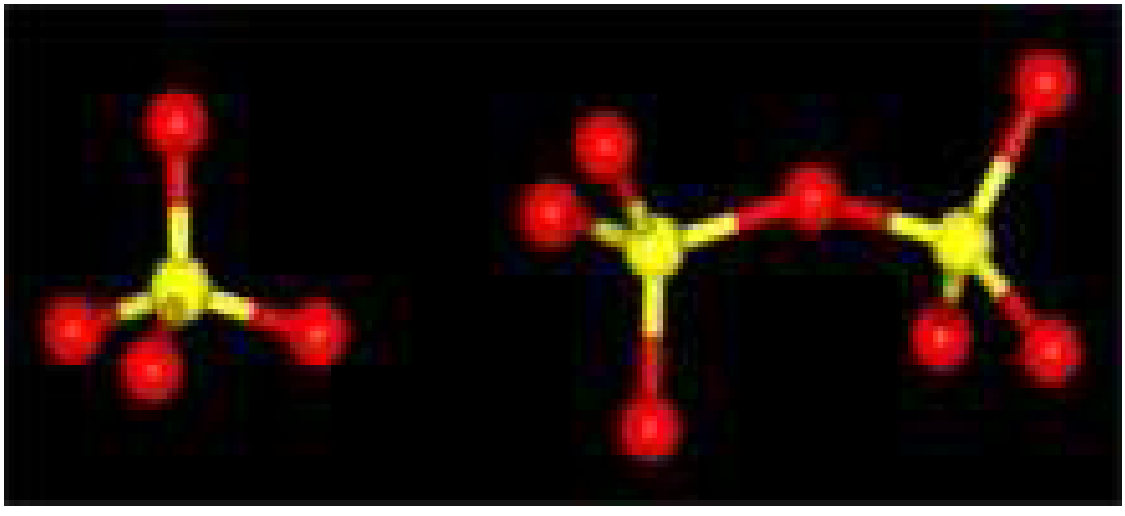

Figure 2.15: The primary building unit TO4 is depicted on the left side while the right side shows two TO4 units linked together to form larger structures [131].

The clusters of the primary building units, TO4 to form similar repeating units gives rise to polyhedral units also called the secondary building units (SBU) which are further connected to build up the entire framework [129]. Although the SBUs cannot describe the presence of cations and other molecules such as water within the framework cavities and holes, zeolite structures are mainly described by these SBUs. Nevertheless, the water molecules within the zeolites framework can be removed reversibly at temperatures below 500 ^{o}C upon dehydration since they are highly mobile. The stability of some zeolite material is maintained at temperatures within 700 to 800 ^{o}C [130].

The nine known SBUs that denote all known zeoilte framework are represented in Figure 2.16. From the SBUs the zeolite structure could be equi-dimensional, sheet-like or chainlike. Unlike other silicates, zeolites structures are less dense with a range of 20 to 50 percent volume of the

structure being void. Apart from quartz and feldspars, due to their three dimensional tetrahedral framework, zeolites are termed tectosilicates [129].

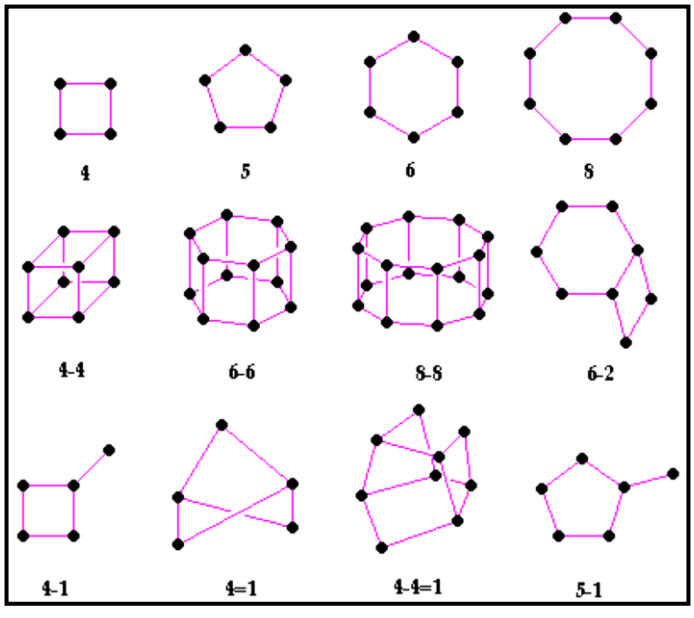

Figure 2.16: Secondary building units (SBUs) that describe known zeolite frameworks [131]

2.5.3 Types of zeolites

Zeolites can be grouped according to their source of occurrence or methods of formation [132]. This is because zeolites which were reported as naturally occurring minerals close to three centuries ago are now produced in the laboratory and in industry in commercial scale. According to reports [131-133], over 200 unique laboratory synthesised zeolites frameworks have been identified and over 40 zeolites frameworks of natural occurrence are known. Hence zeolites can be grouped as natural and synthetic/artificial zeolites as discussed in the following sections.

2.5.3.1 Natural zeolites

The formation of natural zeolites is attributed to several natural occurring geological environmental activities such as interaction between alkaline ground water and volcanic rocks, minerals or ash layers, desert alkaline lakes and soils, modification of marine sediment due to low temperature variation over several thousands of years and low level burial metamorphism amongst others [128]. Hence, natural occurring zeolites are rarely pure and contaminated with other compounds such as quartz, metals or other zeolites which limits their applications on large scale where uniformity and purity are significant. Also, their low or medium silica to alumina ratio is another setback when compared with their synthetic counterparts [132]. Natural zeolites such as clinoptilolite $(Na,K)AlSi_5O_{12}.3H_2O$ are best used for ion exchange especially in radioactive treatments, while mordenite are used for agricultural activities and as absorbent [128]. The present global production of natural zeolite exceeds 50,000 metric ton/yr with an expectation that sales will attain additional 40,000 metric ton/yr in future [133-134].The most significant factors that have encouraged the large scale use of zeolites are the large reserve of zeolite-rich rock at cheap cost and non-competitive materials. The ore is mined by the conventional open pit method and processed by grinding to specific sizes, milled and dried before being packaged.

2.5.3.2 Synthetic/artificial zeolites

Synthetic zeolites are formed as a result of sol-gel processing [131]. It is the slow crystallization of heated aqueous solutions of silica-alumina gel in the presence of an alkali such as sodium hydroxide (NaOH). In some cases organic templates and other elements (metals, metal oxides)

apart from Si and Al can be introduced into the framework of the synthesised zeolite [129]. Factors that can greatly determine the product properties include the crystallisation temperature, ageing or time of reaction, composition of reactants/starting materials, templates used, and process medium pH [130,135-137]. Synthetic zeolites possess some unique advantages compared to their natural counterparts. Their production can be done in a consistent phase-pure condition, at a shorter process formation time and the possibility to produce zeolite structures that do not exist naturally [132]. Zeolite A (shown in Figure 2.17) is a well-known case of a zeolite structure that does not exist in nature. Also, the possibility to supply zeolites is practically limitless as the main raw materials used for their production, alumina and silica, are amongst the most abundant mineral components on earth [134].

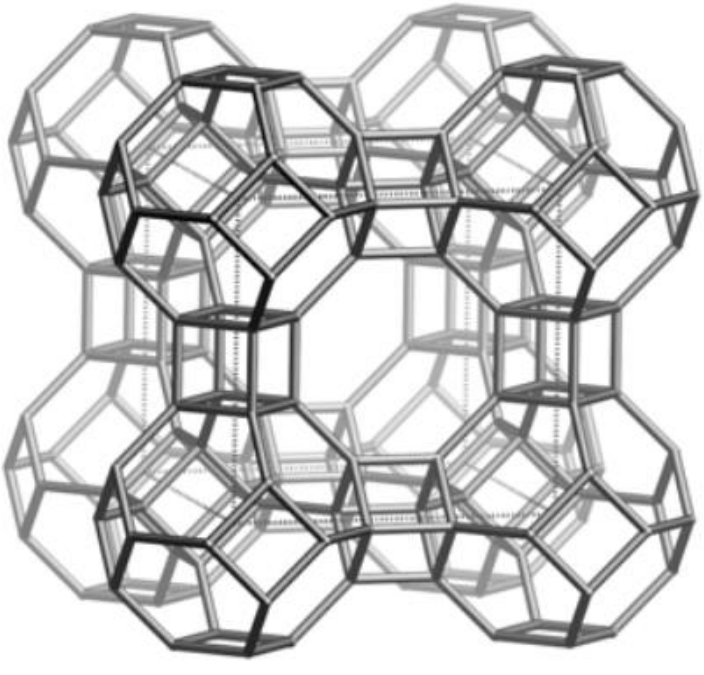

Figure 2.17: structure of zeolite A [131]

2.5.3.3 Properties and uses of zeolites

Natural and synthetic zeolites have found a wide range of application as a result of their unique properties (ion exchange, adsorption and catalytic properties). Zeolites are applied as additives in detergent industry, in agriculture, water and waste-gas purification, radioactive waste treatment, as additives in asphalts and cements during construction and as catalyst in petrochemical industry [134]. This is due to their ability to be involved in a wide range of reactions such as fluid catalytic cracking, hydrocracking, isomerisation and alkylation as a result of their adjustable acidity and well-defined pore structure [129]. During catalytic cracking, the catalyst helps in breaking down heavy molecular weight hydrocarbons to small molecules of hydrocarbon that is within gasoline and diesel range without being involved in the reaction. The catalyst can be regenerated and recycled back into the reactor [135]. Typical zeolites (shown in Figure 2.18a and b) used in the petrochemical industry are ZSM-5 zeolite, a member of MFI, and zeolite NaY, a member of the FAU. In this study, zeolite NaY will be synthesised using Lawani River Benin Nigeria kaolin (LBK) as a precursor for silica-alumina source.

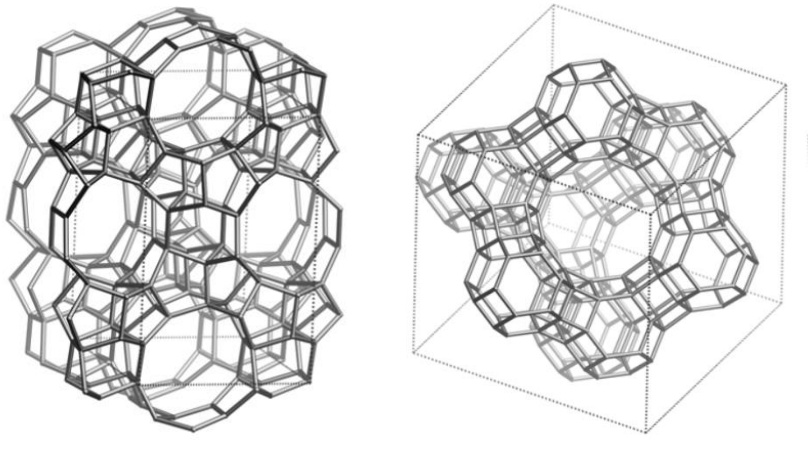

(a) (b)

Figure 2.18(a): Zeolite ZSM-5 structure (b): Zeolite structure type FAU [131,138]

2.5.4 Zeolite synthesis techniques

Since the first time synthetic zeolite was synthesised by Steclaire Deville in 1862 where he carried out hydrothermal treatment of potassium silicate and sodium aluminate in a glass tube to synthesise Levynite zeolite, several reports by researchers on synthetic zeolite as a topic abound in literature [128-129, 137]. The most popular techniques employed in synthetic zeolites preparation include solvothermal, hydrothermal and ionothermal [129,138]. In the hydrothermal technique, water is used as solvent during zeolite synthesis; solvothermal uses organic solvents such as alcohol and amine; and ionothermal technique uses ionic or eutectic liquids as solvents during zeolite synthesis [139]. However, in this present study were the Lawani River Benin Nigeria Kaolin (LBK) will be used to synthesis Zeolite NaY for the catalytic pyrolysis of used tyres, and natural rubber, the hydrothermal technique will be utilized.

2.5.4.1 Hydrothermal technique

The technique produces a very stable silicalite sol and is an easy process to scale up for large scale production [140]. It uses water as a solvent for the zeolite synthesis process. Hydrothermal synthesis can be performed at mild temperature range of 100 to 240 ^{o}C or at temperature region of 1000 ^{o}C, but zeolite synthesis takes place at low temperatures and autogeneous pressure [129]. According to Byrappa and Yoshimura [140], synthesis of zeolite by a hydrothermal method can be broadly classified into two basic stages; the aluminosilicate gel formation stage followed by the gel crystallisation process stage. During this process, copolymerisation also referred to as condensation-polymerisation mechanism, is responsible for the gel formation.

A standard method for hydrothermal synthesis of zeolites (depicted in Figure 2.19) includes, gel formation by thorough mixing of reactant materials (silica, alumina or metakaolin as a precursor for silica and alumina) in a strong basic environment (mainly aqueous NaOH) [140-141].

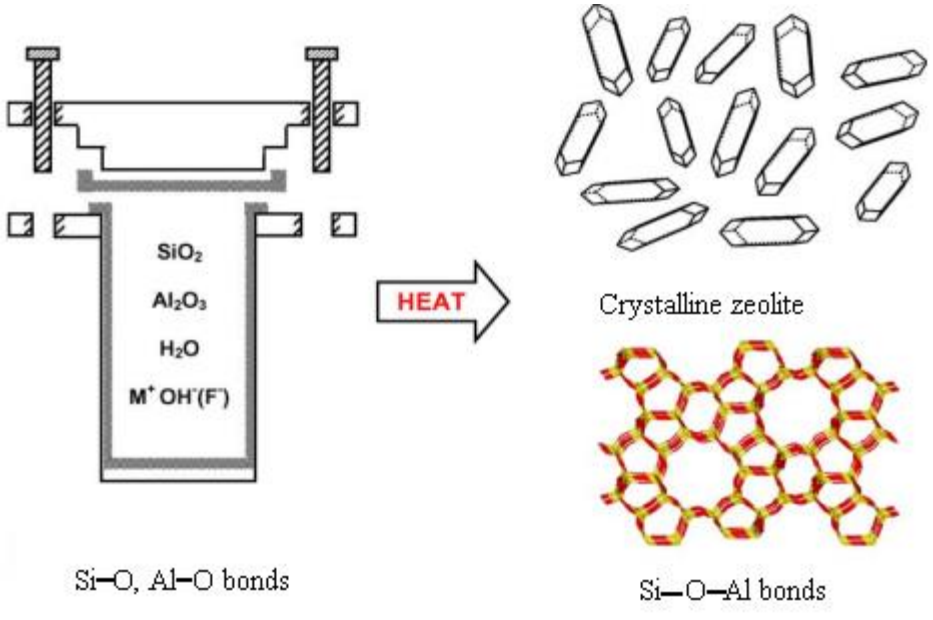

Figure 2.19: Pictorial scheme of hydrothermal synthesis [137]

After the gel is aged, it is allowed to crystallize over a certain time period in a sealed autoclave at temperature range of 90 to 110 ^{o}C [141]. The synthesised zeolite is recovered by washing and drying the filtrate. Figure 2.20 shows a reaction scheme for both the gel formation and crystallisation process from Na_2O-Al_2O_3-SiO_2-H_2O.

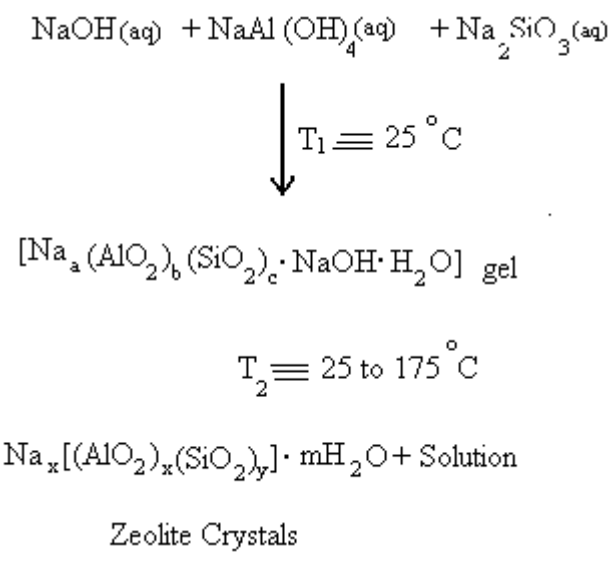

Figure 2.20: Reaction schemes for gel formation and zeolite crystallization [131]

2.6 Pyrolysed Tyre Oil as Fuel in Internal Combustion Engine

The application of the liquid fraction also referred to as tyre pyrolytic oil, TPO, or UT pyrolytic oil, for this study obtained from used tyres pyrolysis as fuel in an internal combustion engine, has been performed. This is due to the similar fossil fuel properties presented by TPO [142]. Results showed that TPO can serve as fuel either directly or when blended with conventional fuel such as diesel in internal combustion engines without modification of the engine [142-143]. Typical fuel properties of different TPO and diesel blends available from literature are shown in Table 2.10

Table 2.10: TPO and diesel blend fuel properties [144]

Property	Diesel	TPO100	TPO05	TPO10	TPO15	TPO20
Density(Kg/m^3 at 20 ^oC)	820	920	825	830	835	840
Kinematic Viscosity (cSt @ 40^oC)	2-4.0	5.4	3.12	3.24	3.36	3.48
Calorie Value (MJ/kg)	43.8	39.2	43.57	43.34	43.11	42.88
Flash point by Abel Method (^oC)	50	43	49.65	49.3	48.95	48.6
Cetane Number	45-50	25-30	44-49	43-48	42-47	41-46

From the investigation done by Dogan et al. [102] on a direct injection (DI) diesel engine using TPO/diesel fuel blends, the result revealed a reduction in carbon monoxide emissions, smoke opacity and unburnt hydrocarbon with blends up to 90% TPO/diesel fuel. Increasing nitrogen oxides emissions was recorded with increasing TPO content in the fuel blends. Assessment of TPO as energy source was also done by Murugan et al [75] using fuel blends of 10, 30 and 50 percent of TPO and diesel fuel (DF) in a single cylinder DI diesel engine. An increase in the cylinder pressure from 71.4 to 73.8 bars and brake thermal efficiency was observed with increase of the TPO in the TPO-DF blend compared with DF. A longer ignition delay and high aromatic content at higher loads led to increased nitrogen oxides, carbon monoxides, hydrocarbons and smoke emissions as the concentration of TPO increases in the fuel blend. Nevertheless, an improved combustion performance and reduction in emissions were achieved when the pyrolytic oil TPO was desulphurised and distillated before being used either as direct or blended fuel in the DI diesel engine. Two different blends of 30% TPO and 70% DF (TPO30) as well as 30% distilled TPO and 70% DF (DTPO30) was the case studied by Murugan et al [74]. The DTPO30

gave about 8% NOx reduction compared to the TPO30 and a decrease of 10% compared with DF. Hydrocarbon emissions were also 2% less for the DTPO30 than the TPO30 case study. DTPO gave higher smoke emissions than both TPO30 and DF.

Similarly, from the investigation conducted by Pradhan and Singh [50] on the use of TPO obtained from waste bicycle tyres and tubes (10 to 50% blend with DF) in a DI diesel engine performance test, results revealed that emissions characteristics from the engine was lower for all ratios of the tube pyrolytic oil-diesel blend (TUPO10 to TUPO50) than diesel fuel. An optimum blend of 40% tube pyrolytic oil with diesel was noted as the engine failed to run smoothly above this percent ratio. The TUPO blends also gave higher peak pressure values than diesel fuel. The study conducted by Nabi et al [144], on the application of purified TPO (Tyre Pyrolytic Oil) and its use in a diesel engine, a blend of TPO10 (10% tyre pyrolytic oil and 90% diesel fuel) and TPO20 were successfully combusted directly in the diesel engine with a slightly lower brake thermal efficiency than diesel fuel without any engine modifications. Other investigations done by Pilusa et al [145], Wongkhorsub et al [146] and Patel et al [147], revealed that limited amount of tyre pyrolytic oil blended with diesel can be used as a fuel in diesel engines without modification of the engines. In addition, production of TPO from used tyres would be a suitable route for used tyre disposal (with additional energy benefits).

From the literature review, the three fractions obtainable from pyrolysis of used tyres have limitations in terms of yield and composition. The main setback for the liquid fraction serving as direct fuel is the presence of sulphur and other aromatic compounds which have been linked to

environmental pollution and health complications. This has resulted in adopting desulphurization and other purification methods that could lead to an increase in the cost price of the pyrolytic oil.

Although co-pyrolyis of biomass and used tyres have been investigated by different researchers, the aim of having higher yield and improved liquid fraction composition has not been encouraging. There is the need to explore other pyrolysable materials which can give high yield and better composition of liquid fraction compared to that obtained from used tyres pyrolysis. Such material to be investigated in this research is latex NR (obtained from Hevea Brasiliensis) which is expected to give more liquid fraction yield (containing less pollutant) with better fuel properties composition and engine performance compared to UT pyrolytic oil. An increase in liquid fraction yield could encourage an expansion in terms of investment for the pyrolysis products, thereby making the process more economically feasible.

Also, the thermogravimetric analysis, (TGA) equipment which is a standard method used for determining the thermal behavior of a pyrolysable material such as rubber can only provide information based on weight loss with change in time and temperature (occurring simultaneously). This implies that the rate at which the temperature changes is dependent on time which has a direct effect on the material weight loss. Hence, most researchers have only used the data derived (over a certain temperature range and heating rate) from the TGA in determining kinetic parameters such as activation energy and pre-exponential factor. This limitation prevents the TGA equipment from being used to analyse the weight change of a material at a fixed temperature over a period of time. This research will attempt to address this restriction by developing a mathematical model that will make it possible for the TGA to predict the weight

loss behavior of a material at a constant temperature over a period of time. This can be an analytical means of operating the TGA as a dynamic apparatus to predict weight change of a material as it degrades with time at a fixed temperature.

References

[1] Hosler, D., Burkett, S.L. and Tarkanian, M.J., 1999. Prehistoric polymers: rubber processing in ancient Mesoamerica. *Science*, *284*(5422), pp. 1988-1991.

[2] Hobhouse, H., 2005. Seeds of Wealth: Five Plants that Made Men Rich. *Counterpoint Press*.

[3] Chiang, C.C.K., 2013. Natural Rubber Biosynthesis: Perspectives from Polymer Chemistry. (Doctoral dissertation, *University of Akron,* Ohio, USA*).*

[4] Mensah, G., 2014. Analysis of environmental threats during rubber processing in Ghana: case study of Ghana Rubber Estate limited (A degree dissertation, *University of Arcada,* Helsinki, Finland).

[5] Moss, F.H., 1920. The Rubber Industry: The History, Manufacture and Marketing. (Doctoral dissertation, *University of Indiana,* Bloomington, USA).

[6] Müller, I. and Strehlow, P., 2004. 11 History of Rubber and Its Use. In Rubber and Rubber Balloons. *Springer Berlin Heidelberg*, pp. 105-110.

[7] Morel, E.D., 1907. Red Rubber: The Story of the Rubber Slave Trade Flourishing on the Congo in the Year of Grace 1907. *TF Unwin*.

[8] Bird, S.A., Clary, D., Jajam, K.C., Tippur, H.V. and Auad, M.L., 2013. Synthesis and characterization of high performance, transparent interpenetrating polymer networks with polyurethane and poly (methyl methacrylate). *Polymer Engineering and Science*, *53*(4), pp.716-723.

[9] Ciesielski, A., 1999. An introduction to rubber technology. *iSmithers Rapra Publishing*.

[10] Cornish, K., 2001. Biochemistry of natural rubber, a vital raw material, emphasizing biosynthetic rate, molecular weight and compartmentalization, in evolutionarily divergent plant species. *Natural Product Reports*, *18*(2), pp. 182-189.

[11] Rao, P.S., Saraswathyamma, C.K. and Sethuraj, M.R., 1998. Studies on the relationship between yield and meteorological parameters of para rubber tree (Hevea brasiliensis). *Agricultural and Forest Meteorology*, *90*(3), pp.235-245.

[12] Stern, H.J., 1967. Rubber: natural and synthetic. *Maclaren and Sons Ltd*, London.

[13] Subramaniam, A., 1995. The chemistry of natural rubber latex. *Immunology and Allergy Clinics of North America*, *15*(1), pp.1-20.

[14] Manivong, V., 2007. The economic potential for small holder rubber production in Northern Laos. (Master dissertation, *University of Queensland,* Brisbane, Australia*).*

[15] Campos‐López, E. and Angulo‐Sánchez, J.L., 1976. Molecular weight characterization of natural guayule rubber by gel‐permeation chromatography. *Journal of Polymer Science: Polymer Letters Edition*, *14*(11), pp. 649-652.

[16] Angulo-Sanchez, J.L. and Cabaulero-Mata, P., 1981. Long chain branching in natural Hevea rubber-determination by gel permeation chromatography.*Rubber Chemistry and Technology*, *54*(1), pp. 34-41.

[17] Fuller, K.N.G. and Fulton, W.S., 1990. The influence of molecular weight distribution and branching on the relaxation behaviour of uncrosslinked natural rubber. *Polymer*, *31*(4), pp. 609-615.

[18] Lake, G.J., 1970. Ozone cracking and protection of rubber. *Rubber Chemistry and Technology*, *43*(5), pp.1230-1254.

[19] Tucker, H., 1959. The reaction of ozone with rubber. *Rubber Chemistry and Technology*, *32*(1), pp. 269-277.

[20] Gent, A.N., 2005. Strength of elastomers. *Science and Technology of Rubber*, pp. 419-454.

[21] Tobolsky, A.V. and Mark, H.F., 1971. Polymer Science and Materials (1). *John Wiley and Sons*, New York, USA.

[22] Jain, P.C., 1976. Engineering Chemistry. *Dhanpat Rai Pub Company*, 11, Pp. 165-173.

[23] Groover, M.P., 2007. Fundamentals of modern manufacturing: materials processes, and systems. *John Wiley and Sons*. USA

[24] Peralta, J., Silva, H.M., Williams, R.C., Rover, M. and Machado, A.V., 2013. Development of an innovative bio-binder using asphalt-rubber technology. *International Journal of Pavement Research and Technology*, *6*(4), pp.447-456.

[25] Slack, C., 2003. Noble Obsession: Charles Goodyear, Thomas Hancock, and the Race to Unlock the Greatest Industrial Secret of the 19th Century. *Hyperion*.

[26] Rengga, W.D.P., Handayani, P.A., Kadarwati, S. and Feinnudin, A., 2015. Kinetic study on catalytic cracking of rubber seed (Hevea brasiliensis) oil to liquid fuels. *Bulletin of Chemical Reaction Engineering and Catalysis*, *10*(1), pp. 50-60.

[27] Midgley Jr, T. and Henne, A.L., 1929. Natural and synthetic rubber. I. Products of the destructive distillation of natural rubber. *Journal of the American Chemical Society*, *51*(4), pp. 1215-1226.

[28] Mui, E.L., Cheung, W.H. and McKay, G., 2010. Tyre char preparation from waste tyre rubber for dye removal from effluents. *Journal of Hazardous Materials*, *175*(1), pp. 151-158.

[29] Kaliske, M., Serafinska, A. and Zopf, C., 2013. Optimized and robust design of tyres based on numerical simulation. *Tyre Science and Technology*, *41*(1), pp. 21-39.

[30] Undri, A., Rosi, L., Frediani, M. and Frediani, P., 2014. Upgraded fuel from microwave assisted pyrolysis of waste tyre. *Fuel*, *115*, pp. 600-608.

[31] Williams, P.T., 2013. Pyrolysis of waste tyres: a review. *Waste Management, 33*(8), pp.1714-1728.

[32] Islam, M.R., Tushar, M.S.H.K. and Haniu, H., 2008. Production of liquid fuels and chemicals from pyrolysis of Bangladeshi bicycle/rickshaw tyre wastes. *Journal of Analytical and Applied Pyrolysis*, *82*(1), pp. 96-109.

[33] Williams, P.T. and Besler, S., 1995. Pyrolysis-thermogravimetric analysis of tyres and tyre components. *Fuel, 74*(9), pp.1277-1283.

[34] Martínez, J.D., Veses, A., Mastral, A.M., Murillo, R., Navarro, M.V., Puy, N., Artigues, A., Bartrolí, J. and García, T., 2014. Co-pyrolysis of biomass with waste tyres: upgrading of liquid bio-fuel. *Fuel Processing Technology*, *119*, pp. 263-271.

[35] Quek, A. and Balasubramanian, R., 2013. Liquefaction of waste tyres by pyrolysis for oil and chemicals—a review. *Journal of Analytical and Applied Pyrolysis*, *101*, pp. 1-16.

[36] Evans, A. and Evans, R., 2006. The Composition of a Tyre: Typical Components. *The Waste and Resources Action Programme.*Banbury Oxford, UK.

[37] Ochmann, N., 2002. Scrap tyre management: tyre demand estimation (Doctoral dissertation, *College of Agriculture, Montana State University*-Bozeman, USA).

[38] de Marco Rodriguez, I., Laresgoiti, M.F., Cabrero, M.A., Torres, A., Chomon, M.J. and Caballero, B., 2001. Pyrolysis of scrap tyres. *Fuel Processing Technology*, *72*(1), pp. 9-22.

[39] González, J.F., Encinar, J.M., Canito, J.L. and Rodríguez, J.J., 2001. Pyrolysis of automobile tyre waste. Influence of operating variables and kinetics study. *Journal of Analytical and Applied Pyrolysis*, *58*, pp. 667-683.

[40] Pakdel, H. and Roy, C., 1994. Simultaneous gas chromatographic—Fourier transform infrared spectroscopic—mass spectrometric analysis of synthetic fuel derived from used

tyre vacuum pyrolysis oil, naphtha fraction. *Journal of Chromatography A*, *683*(1), pp. 203-214.

[41] Laresgoiti, M.F., Caballero, B.M., de Marco, I., Torres, A., Cabrero, M.A. and Chomón, M.J., 2004. Characterization of the liquid products obtained in tyre pyrolysis. *Journal of Analytical and Applied Pyrolysis*, *71*(2), pp. 917-934.

[42] Mastral, A.M., Callén, M.S., Murillo, R. and GarcÍa, T., 1999. Combustion of high calorific value waste material: Organic atmospheric pollution. *Environmental Science and Technology*, *33*(23), pp. 4155-4158.

[43] Donatelli, A., Iovane, P. and Molino, A., 2010. High energy syngas production by waste tyres steam gasification in a rotary kiln pilot plant. Experimental and numerical investigations. *Fuel*, *89*(10), pp. 2721-2728.

[44] Kar, Y., 2011. Catalytic pyrolysis of car tyre waste using expanded perlite. *Waste Management*, *31*(8), pp.1772-1782.

[45] Chang, Y.M., 1996. On pyrolysis of waste tyre: degradation rate and product yields. *Resources, Conservation and Recycling*, *17*(2), pp. 125-139.

[46] Trongkaew, P., Utistham, T., Reubroycharoen, P. and Hinchiranan, N., 2011. Photocatalytic desulfurization of waste tyre pyrolysis oil. *Energies*, *4*(11), pp. 1880-1896.

[47] Su, Y. and Zhao, B., 2010, June. Pyrolysis of waste tyre and its model. In *Bioinformatics and Biomedical Engineering (iCBBE), 2010 4th International Conference*, Chengdu, China. IEEE, pp. 1-4.

[48] Juma, M., Koreňová, Z., Markoš, J., Annus, J. and Jelemenský, L., 2006. Pyrolysis and combustion of scrap tyre. *Petroleum and Coal*, *48*(1), pp.15-26.

[49] Williams, P.T. and Bottrill, R.P., 1995. Sulfur-polycyclic aromatic hydrocarbons in tyre pyrolysis oil. *Fuel*, *74*(5), pp.736-742.

[50] Pradhan, D. and Singh, R.K., 2011. Thermal pyrolysis of bicycle waste tyre using batch reactor. *International Journal of Chemical Engineering and Applications*, *2*(5), pp. 332.

[51] Chen, J.H., Chen, K.S. and Tong, L.Y., 2001. On the pyrolysis kinetics of scrap automotive tyres. *Journal of Hazardous Materials*, *84*(1), pp. 43-55.

[52] Llompart, M., Sanchez-Prado, L., Lamas, J.P., Garcia-Jares, C., Roca, E. and Dagnac, T., 2013. Hazardous organic chemicals in rubber recycled tyre playgrounds and pavers. *Chemosphere*, *90*(2), pp. 423-431.

[53] Olazar, M., Lopez, G., Arabiourrutia, M., Elordi, G., Aguado, R. and Bilbao, J., 2008. Kinetic modelling of tyre pyrolysis in a conical spouted bed reactor. *Journal of Analytical and Applied Pyrolysis*, *81*(1), pp. 127-132.

[54] Osayi, J.I., Iyuke, S. and Ogbeide, S.E., 2014. Biocrude production through pyrolysis of used tyres. *Journal of Catalysts*, *2014*, pp. 9.

[55] Frigo, S., Seggiani, M., Puccini, M. and Vitolo, S., 2014. Liquid fuel production from waste tyre pyrolysis and its utilisation in a Diesel engine. *Fuel*, *116*, pp. 399-408.

[56] Boxiong, S., Chunfei, W., Cai, L., Binbin, G. and Rui, W., 2007. Pyrolysis of waste tyres: The influence of USY catalyst/tyre ratio on products. *Journal of Analytical and Applied Pyrolysis*, *78*(2), pp. 243-249.

[57] Conesa, J.A. and Marcilla, A., 1996. Kinetic study of the thermogravimetric behavior of different rubbers. *Journal of Analytical and Applied Pyrolysis*, *37*(1), pp. 95-110.

[58] Senneca, O., Salatino, P. and Chirone, R., 1999. A fast heating-rate thermogravimetric study of the pyrolysis of scrap tyres. *Fuel*, *78*(13), pp. 1575-1581.

[59] Leung, D.Y.C. and Wang, C.L., 1998. Kinetic study of scrap tyre pyrolysis and combustion. *Journal of Analytical and Applied Pyrolysis*, *45*(2), pp. 153-169.

[60] Haydary, J., Koreňová, Z., Jelemenský, Ľ. and Markoš, J., 2008. Thermal decomposition of waste polymers. *Thermophysics 2008*, pp. 62.

[61] Aguado, R., Olazar, M., Vélez, D., Arabiourrutia, M. and Bilbao, J., 2005. Kinetics of scrap tyre pyrolysis under fast heating conditions. *Journal of Analytical and Applied Pyrolysis*, *73*(2), pp. 290-298.

[62] Cunliffe, A.M. and Williams, P.T., 1999. Influence of process conditions on the rate of activation of chars derived from pyrolysis of used tyres. *Energy and Fuels*, *13*(1), pp.166-175.

[63] González, J.F., Encinar, J.M., Canito, J.L. and Rodríguez, J.J., 2001. Pyrolysis of automobile tyre waste. Influence of operating variables and kinetics study. *Journal of Analytical and Applied Pyrolysis*, *58*, pp. 667-683.

[64] Karthikeyan, S., Sathiskumar, C. and Moorthy, R.S., 2012. Effect of process parameters on tyre pyrolysis: a review. *Journal of Scientific and Industrial Research*, *71*(5), pp. 309-315.

[65] Li, X., Berger, W., Musante, C. and Mattina, M.I., 2010. Characterization of substances released from crumb rubber material used on artificial turf fields.*Chemosphere*, *80*(3), pp. 279-285.

[66] Lin, J.P., Chang, C.Y. and Wu, C.H., 1998. Pyrolysis kinetics of rubber mixtures. *Journal of Hazardous Materials*, *58*(1), pp. 227-236.

[67] Buekens, A.G., 1977. Some observations on the recycling of plastics and rubber. *Conservation and Recycling*, *1*(3-4), pp. 247-271.

[68] Carrasco, F., Bredin, N., Gningue, Y. and Heitz, M., 1998. Environmental impact of the energy recovery of scrap tyres in a cement kiln. *Environmental Technology*, *19*(5), pp. 461-474.

[69] DeMarini, D.M., Lemieux, P.M., Ryan, J.V., Brooks, L.R. and Williams, R.W., 1994. Mutagenicity and chemical analysis of emissions from the open burning of scrap rubber tyres. *Environmental Science and Technology*, *28*(1), pp.136-141.

[70] Levendis, Y.A., Atal, A., Carlson, J., Dunayevskiy, Y. and Vouros, P., 1996. Comparative study on the combustion and emissions of waste tyre crumb and pulverized coal. *Environmental Science and Technology*, *30*(9), pp. 2742-2754.

[71] Aguado, R., Olazar, M., Gaisán, B., Prieto, R. and Bilbao, J., 2002. Kinetic study of polyolefin pyrolysis in a conical spouted bed reactor. *Industrial and Engineering Chemistry Research*, *41*(18), pp. 4559-4566.

[72] Cornelissen, T., Yperman, J., Reggers, G., Schreurs, S. and Carleer, R., 2008. Flash co-pyrolysis of biomass with polylactic acid. Part 1: Influence on bio-oil yield and heating value. *Fuel*, *87*(7), pp. 1031-1041.

[73] Khoo, H.H., 2009. Life cycle impact assessment of various waste conversion technologies. *Waste Management*, *29*(6), pp. 1892-1900.

[74] Murugan, S., Ramaswamy, M.C. and Nagarajan, G., 2008. Performance, emission and combustion studies of a DI diesel engine using distilled tyre pyrolysis oil-diesel blends. *Fuel Processing Technology*, *89*(2), pp. 152-159.

[75] Murugan, S., Ramaswamy, M.C. and Nagarajan, G., 2009. Assessment of pyrolysis oil as an energy source for diesel engines. *Fuel Processing Technology*, *90*(1), pp. 67-74.

[76] Bianchi, M., Bortolani, G., Cavazzoni, M., De Pascale, A., Montanari, I., Nobili, M., Peretto, A., Tosi, C. and Vecci, R., 2014. Preliminary design and numerical analysis of a scrap tyres pyrolysis system. *Energy Procedia*, *45*, pp. 111-120.

[77] Al-Salem, S.M., Lettieri, P. and Baeyens, J., 2009. Kinetics and product distribution of end of life tyres (ELTs) pyrolysis: A novel approach in polyisoprene and SBR thermal cracking. *Journal of Hazardous Materials*, *172*(2), pp.1690-1694.

[78] Hu, H., Fang, Y., Liu, H., Yu, R., Luo, G., Liu, W., Li, A. and Yao, H., 2014. The fate of sulfur during rapid pyrolysis of scrap tyres. *Chemosphere*, *97*, pp.102-107.

[79] Jahirul, M.I., Rasul, M.G., Chowdhury, A.A. and Ashwath, N., 2012. Biofuels production through biomass pyrolysis—a technological review. *Energies*, *5*(12), pp.4952-5001.

[80] Harrison, G. and Ross, A.B., 1996. Use of tyre pyrolysis oil for solvent augmentation in two-stage coal liquefaction. *Fuel*, *75*(8), pp.1009-1013.

[81] Alsaleh, A. and Sattler, M.L., 2014. Waste Tyre Pyrolysis: Influential Parameters and Product Properties. *Current Sustainable and Renewable Energy Reports*, *1*(4), pp.129-135.

[82] Fix, S.R., 1980. Microwave devulcanization of rubber. *Elastomerics*, *112*(6), pp.38-40.

[83] Phadke, A.A., Bhattacharya, A.K., Chakraborty, S.K. and De, S.K., 1983. Studies of vulcanization of reclaimed rubber. *Rubber Chemistry and Technology*, *56*(4), pp. 726-736.

[84] Gotshall, W.W., 1972. Reinforcing agent from scrap rubber char. *U.S Patent*,*3*, pp.131.

[85] Alpert, S.B., Hydrocarbon Research Inc, 1972. Hydroconversion of waste natural and synthetic rubbers. *U.S. Patent,* 3,704, 108.

[86] Grannen, E.A. and Robinson, L., 1974. Microwave pyrolysis of wastes. *U.S Patent*, 3843457.

[87] Crane, G. and Kay, E.L., The firestone tyre and rubber company, 1976.Pyrolization. *U.S Patent* 3,966,487.

[88] Herbold, O. and Dittloff, D., Helma Lampl, 1978. Method and apparatus for the pyrolysis of waste products. *U.S. Patent,* 4,084,521.

[89] Kaminsky, W., 1980. Pyrolysis of plastic waste and scrap tyres in a fluid bed reactor. *Resource Recovery and Conservation*, *5*(3), pp. 205-216.

[90] Ito, K., Hirayama, Y., Ishii, Y. and Ando, N., Ebara Corporation, 1982. Pyrolyzing apparatus. *U.S. Patent,* 4,324,620.

[91] Engman, H., Mayfield, H.T., Mar, T. and Bertsch, W., 1984. Classification of bacteria by pyrolysis-capillary column gas chromatography-mass spectrometry and pattern recognition. *Journal of Analytical and Applied Pyrolysis*, *6*(2), pp. 137-156.

[92] Bouvier, J.M. and Gelus, M., 1986. Pyrolysis of rubber wastes in heavy oils and use of the products. *Resources and Conservation*, *12*(2), pp. 77-93.

[93] Chou, I.M., Lake, M.A. and Griffin, R.A., 1988. Flash pyrolysis of coal, coal maceral, and coal-derived pyrite with on-line characterization of volatile sulfur compounds. *Journal of Analytical and Applied Pyrolysis*, *13*(3), pp. 199-207.

[94] Roy, C., Labrecque, B. and de Caumia, B., 1990. Recycling of scrap tyres to oil and carbon black by vacuum pyrolysis. *Resources, Conservation and Recycling*, *4*(3), pp. 203-213.

[95] Roy, V., de Caumia, B. and Roy, C., 1992. Development of a gas-cleaning system for a scrap-tyre vacuum-pyrolysis plant. *Gas Separation and Purification*, *6*(2), pp. 83-87.

[96] Galvagno, S., Casu, S., Casabianca, T., Calabrese, A. and Cornacchia, G., 2002. Pyrolysis process for the treatment of scrap tyres: preliminary experimental results. *Waste Management*, *22*(8), pp. 917-923.

[97] Murillo, R., Aylón, E., Navarro, M.V., Callén, M.S., Aranda, A. and Mastral, A.M., 2006. The application of thermal processes to valorise waste tyre. *Fuel Processing Technology*, *87*(2), pp.143-147.

[98] Zhang, X., Wang, T., Ma, L. and Chang, J., 2008. Vacuum pyrolysis of waste tyres with basic additives. *Waste Management*, *28*(11), pp. 2301-2310.

[99] Aylón, E., Fernández-Colino, A., Murillo, R., Navarro, M.V., García, T. and Mastral, A.M., 2010. Valorisation of waste tyre by pyrolysis in a moving bed reactor. *Waste Management*, *30*(7), pp. 1220-1224.

[100] Aydın, H. and İlkılıç, C., 2012. Optimization of fuel production from waste vehicle tyres by pyrolysis and resembling to diesel fuel by various desulfurization methods. *Fuel*, *102*, pp. 605-612.

[101] Scheirs, J. and Kaminsky, W. eds., 2006. Feedstock recycling and pyrolysis of waste plastics. *John Wiley and Sons*.

[102] Doğan, O., Çelik, M.B. and Özdalyan, B., 2012. The effect of tyre derived fuel/diesel fuel blends utilization on diesel engine performance and emissions. *Fuel*, *95*, pp. 340-346.

[103] Ucar, S., Karagoz, S., Ozkan, A.R. and Yanik, J., 2005. Evaluation of two different scrap tyres as hydrocarbon source by pyrolysis. *Fuel*, *84*(14), pp. 1884-1892.

[104] Fernández, A.M., Barriocanal, C. and Alvarez, R., 2012. Pyrolysis of a waste from the grinding of scrap tyres. *Journal of Hazardous Materials*, *203*, pp. 236-243.

[105] Bridgwater, A.V., Czernik, S. and Piskorz, J., 2001. An overview of fast pyrolysis. *Progress in Thermochemical Biomass Conversion*, pp. 977-997.

[106] Han, J. and Kim, H., 2008. The reduction and control technology of tar during biomass gasification/pyrolysis: an overview. *Renewable and Sustainable Energy Reviews*, *12*(2), pp. 397-416.

[107] Conesa, J.A., Font, R., Fullana, A. and Caballero, J.A., 1998. Kinetic model for the combustion of tyre wastes. *Fuel*, *77*(13), pp. 1469-1475.

[108] Dodds, J., Domenico, W.F., Evans, D.R., Fish, L.W., Lassahn, P.L. and Toth, W.J., 1983. Scrap tyres: a resource and technology evaluation of tyre pyrolysis and other selected alternate technologies (No. EGG-2241). *EG and G Idaho, Inc.*, Idaho Falls,USA.

[109] Chen, F. and Qian, J., 2002. Studies on the thermal degradation of cis-1, 4-polyisoprene. *Fuel*, *81*(16), pp. 2071-2077.

[110] Choi, S.S., 2000. Characterization of bound rubber of filled styrene-butadiene rubber compounds using pyrolysis-gas chromatography. *Journal of Analytical and Applied Pyrolysis*, *55*(2), pp. 161-170.

[111] Groves, S.A., Lehrle, R.S., Blazsó, M. and Székely, T., 1991. Natural rubber pyrolysis: Study of temperature-and thickness-dependence indicates dimer formation mechanism. *Journal of Analytical and Applied Pyrolysis*, *19*, pp. 301-309.

[112] Rofiqul, I.M., Haniu, H. and Rafiqul, A.B.M., 2007. Limonene-rich liquids from pyrolysis of heavy automotive tyre wastes. *Journal of Environment and Engineering*, *2*(4), pp. 681-695.

[113] Kwon, E. and Castaldi, M.J., 2009. Fundamental understanding of the thermal degradation mechanisms of waste tyres and their air pollutant generation in a N_2 atmosphere. *Environmental Science and Technology*, *43*(15), pp. 5996-6002.

[114] Cypres, R. and Bettens, B., 1989. Production of benzoles and active carbon from waste rubber and plastic materials by means of pyrolysis with simultaneous post-cracking. *Pyrolysis and Gasification*, pp. 209-229.

[115] Pakdel, H., Roy, C., Aubin, H., Jean, G. and Coulombe, S., 1991. Formation of dl-limonene in used tyre vacuum pyrolysis oils. *Environmental Science and Technology*, *25*(9), pp.1646-1649.

[116] Williams, P.T. and Taylor, D.T., 1993. Aromatization of tyre pyrolysis oil to yield polycyclic aromatic hydrocarbons. *Fuel*, *72*(11), pp.1469-1474.

[117] Teng, H., Serio, M.A., Wojtowicz, M.A., Bassilakis, R. and Solomon, P.R., 1995. Reprocessing of used tyres into activated carbon and other products. *Industrial and Engineering Chemistry Research*, *34*(9), pp. 3102-3111.

[118] Berrueco, C., Esperanza, E., Mastral, F.J., Ceamanos, J. and García-Bacaicoa, P., 2005. Pyrolysis of waste tyres in an atmospheric static-bed batch reactor: Analysis of the gases obtained. *Journal of Analytical and Applied Pyrolysis*, *74*(1), pp. 245-253.

[119] Li, S.Q., Yao, Q., Chi, Y., Yan, J.H. and Cen, K.F., 2004. Pilot-scale pyrolysis of scrap tyres in a continuous rotary kiln reactor. *Industrial and Engineering Chemistry Research*, *43*(17), pp. 5133-5145.

[120] López, F.A., Centeno, T.A., Alguacil, F.J. and Lobato, B., 2011. Distillation of granulated scrap tyres in a pilot plant. *Journal of Hazardous Materials*, *190*(1), pp. 285-292.

[121] Dıez, C., Martınez, O., Calvo, L.F., Cara, J. and Morán, A., 2004. Pyrolysis of tyres. Influence of the final temperature of the process on emissions and the calorific value of the products recovered. *Waste Management*, *24*(5), pp. 463-469.

[122] Zhao, X., Song, Z., Liu, H., Li, Z., Li, L. and Ma, C., 2010. Microwave pyrolysis of corn stalk bale: A promising method for direct utilization of large-sized biomass and syngas production. *Journal of Analytical and Applied Pyrolysis*, *89*(1), pp. 87-94.

[123] Shen, B., Wu, C., Wang, R., Guo, B. and Liang, C., 2006. Pyrolysis of scrap tyres with zeolite USY. *Journal of Hazardous Materials*, *137*(2), pp. 1065-1073.

[124] Williams, P.T. and Brindle, A.J., 2003. Aromatic chemicals from the catalytic pyrolysis of scrap tyres. *Journal of Analytical and Applied Pyrolysis*, *67*(1), pp.143-164.

[125] Shah, J., Jan, M.R. and Mabood, F., 2008. Catalytic pyrolysis of waste tyre rubber into hydrocarbons via base catalysts. *Iranian Journal of Chemistry and Chemical Engineering* ,*27*(2).

[126] Shah, J., Jan, M.R. and Mabood, F., 2009. Recovery of value-added products from the catalytic pyrolysis of waste tyre. *Energy Conversion and Management*, *50*(4), pp. 991-994.

[127] Tschernich, R.W., 1992. Zeolites of the World. *Geoscience Press. Inc.*, Phoenix, Arizona, USA.

[128] Brek, D., 1974. Zeolite Molecular Sieves: Structure, Chemistry and Use. *John Wiley and Sons*, New York, USA

[129] Xu, R., Pang, W., Yu, J., Huo, Q. and Chen, J., 2009. Chemistry of zeolites and related porous materials: synthesis and structure. *John Wiley and Sons,* Clementi loop Singapore.

[130] Dyer, A., 1988. An introduction to zeolite molecular sieves. *John Wiley and Sons*, Chichester, New York, USA

[131] Kovo, A.S., 2011. Development of Zeolites and Zeolite membranes from Ahoko Nigerian Kaolin. (Doctoral dissertation, *University of Manchester,* Manchester, UK)

[132] Auerbach, S.M., Carrado, K.A. and Dutta, P.K., 2003. Handbook of zeolite science and technology. *CRC press*, New York, USA.

[133] Zorpas, A.A., Inglezakis, V.J. and Loizidou, M., 2008. Heavy metals fractionation before, during and after composting of sewage sludge with natural zeolite. *Waste Management*, *28*(11), pp. 2054-2060.

[134] Sand, L.B. and Mumpton, F.A., 1978. Natural zeolites: occurrence, properties, and use (No. CONF-760626-(Exc.)). *Pergamon Press, Inc*., Elmsford, New York, USA.

[135] Weitkamp, J. and Puppe, L. eds., 2013. Catalysis and zeolites: fundamentals and applications. *Springer Science and Business Media.*

[136] Ginter, D.M., Went, G.T., Bell, A.T. and Radke, C.J., 1992. A physicochemical study of the againg of colloidal silica gels used in zeolite Y synthesis. *Zeolites*, *12*(6), pp.733-741.

[137] Cundy, C.S. and Cox, P.A., 2005. The hydrothermal synthesis of zeolites: Precursors, intermediates and reaction mechanism. *Microporous and Mesoporous Materials*, *82*(1), pp.1-78.

[138] Morris, R.E., 2008. Concepts in the ionothermal synthesis of zeolites and metal organic frameworks. *Studies in Surface Science and Catalysis*, *174*, pp. 33-42.

[139] Parnham, E.R. and Morris, R.E., 2007. Ionothermal synthesis of zeolites, metal–organic frameworks, and inorganic–organic hybrids. *Accounts of Chemical Research*, *40*(10), pp.1005-1013.

[140] Byrappa, K. and Yoshimura, M., 2001. Handbook of hydrotermal technology. A technology for crystal growth and materials processing. *Byrappa, M. Yoshimura-Noyes Publications,* Park Ridge, New Jersey, USA.

[141] Miladinović, Z., Zakrzewska, J., Kovačević, B. and Bačić, G., 2007. Monitoring of crystallization processes during synthesis of zeolite A by in situ 27 Al NMR spectroscopy. *Materials Chemistry and Physics*, *104*(2), pp. 384-389.

[142] Williams, P.T., Bottrill, R.P. and Cunliffe, A.M., 1998. Combustion of tyre pyrolysis oil. *Process Safety and Environmental Protection*, *76*(4), pp. 291-301.

[143] Lucas, N., Bienaime, C., Belloy, C., Queneudec, M., Silvestre, F. and Nava-Saucedo, J.E., 2008. Polymer biodegradation: Mechanisms and estimation techniques–A review. *Chemosphere*, *73*(4), pp. 429-442.

[144] Nabi, A.R., Masud, M.H. and Alam, Q.I., 2014. Purification of TPO (Tyre Pyrolytic Oil) and its use in diesel engine. *IOSR Journal of Engineering*, *4*(3), pp.1.

[145] Pilusa, T.J., Shukla, M. and Muzenda, E., 2013. Tyre derived fuel as an alternative fuel for CI engines. *International Conference on Environment, Agriculture and Food Sciences (ICEAFS'2013)*, Kuala Lumpur, Malaysia.

[146] Wongkhorsub, C., Chindaprasert, N. and Peanprasit, S., 2014. Engine performance and economic impact study of gasoline-like tyre pyrolysis oil in Thailand. *Advances in Environmental Sciences, Development and Chemistry*, pp.340-345.

[147] Patel, J.M., Patel, K.J., Patel, V.V. and Vaghela, K.V., Performance studies of tyre pyrolysis oil blends with Diesel Fuel. *International Journal of Engineering and Advanced Technology (IJEAT) ISSN*, pp.2249-8958.

CHAPTER 3

METHODOLOGY AND EXPERIMENTAL PROCEDURE

3.1 Materials and Methods

Zeolite NaY catalyst, car used tyres and natural rubber (also known as latex rubber) were the raw materials used for the catalytic pyrolysis process. South African made car tyre was collected from a selected, dump site in Johannesburg, South Africa; while the natural rubber lump was sourced from a rubber tree plantation located at Iyanomo village near Benin City, Edo state, Nigeria. The materials were washed to remove debris, stones and sand. The natural rubber and used tyres samples were cut into different sizes of 2, 4, 6, 8 and 10 mm. The chopped pieces representatives of the used tyres contained no wire cord but the fabrics thread. Before pyrolysis, both the natural rubber and used tyres sample materials were taken for proximate and ultimate analysis.

The zeolite NaY catalyst used for this study was produced in the laboratory of the School of Chemical and Metallurgical Engineering, University of the Witwatersrand by the hydrothermal method. Kaolin (clay) obtained from Lawani River located in Benin City Edo state Nigeria (LBK) served as precursor for the aluminum and silicon oxides. The produced catalyst was characterised according to an international standard. In order to achieve the aims of this study the following steps were followed:

- Firstly, the zeolite NaY catalyst was synthesised followed by the production of pyrolytic oil from used tyres, natural rubber using pyrolysis (with and without catalyst)

- Secondly, the obtained pyrolytic oil from both catalytic and non-catalytic pyrolysis were characterised for physical and fuel properties

- Thirdly, the pyrolytic oil from the first step was distilled using batch distillation to obtain pyrolytic oil distillates (PD)

- Fourthly, the PD from step three were blended with petrol and then

- tested in an internal combustion engine for fuel consumption and fuel power study.

The grade 95 unleaded petrol used in this study was bought from a Caltex filling station, Braamfontein, Johannesburg – South Africa.

3.2 Zeolite NaY Synthesis and Characterisation

The raw Lawani River Benin Nigeria Kaolin (LBK) was refined using sedimentation method to remove unwanted and foreign materials such as quartz which was trapped within the mineral aggregates.The clay was spread on an oven pan and placed in the oven at a set temperature of 50 ^{o}C. After two hours and thirty minutes, the oven temperature was raised to 110 ^{o}C and maintained at that temperature for approximately four hours. The oven pan was then removed and placed in a desiccator and allowed to cool. This is done so as to help reduce the water content in the clay as much as possible before it can be crushed to the desired size and calcined in a furnace. Crushing of the dried clay was done in a ceramic mortal using a ceramic piston. The grounded clay was then sieved using 38 µm sieves to obtain particle size of 38 µm. A pictorial description of the process is depicted in Figure 3.1.

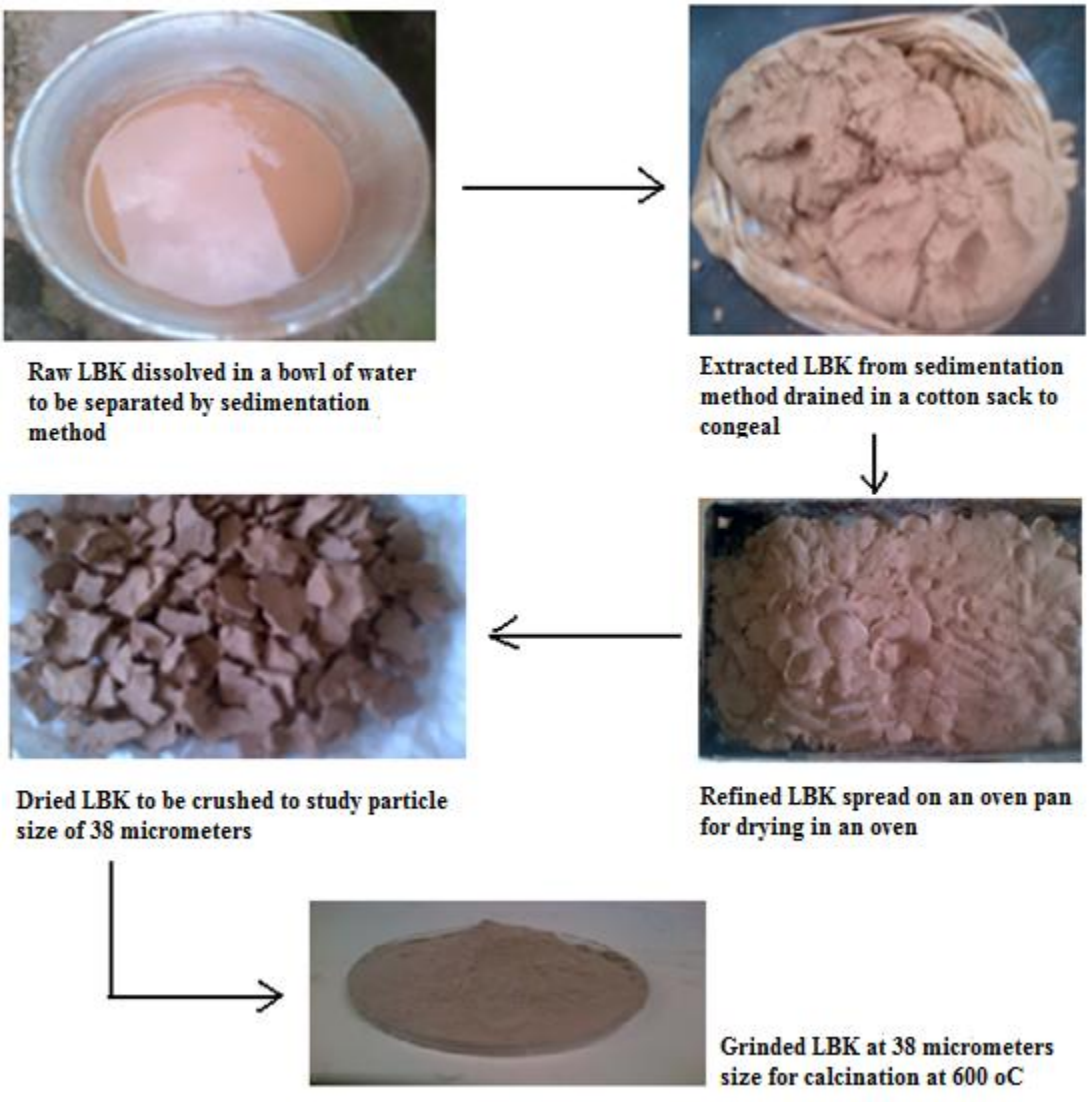

Figure 3.1: Process description of the refinement of raw LBK to particle size reduction before calcination

The ground clay of 38 µm size was placed in a crucible and loaded into a furnace for calcining at 600^{o}C at a heating rate of 10 ^{o}C/min and kept constant for two hours. It was then removed and placed in a desiccator to cool. According to Franco et al. [1], this would help to remove the hydration water, better disordering of the kaolinite molecule structure and formation of a non-

crystalline phase. At this stage, the metakaolin can be said to be an amorphous material comprising of free silica and free alumina [2]. The calcined LBK also referred to as LBK metakaolin was characterised with the following equipment: XRF, XRD and SEM.

The synthesis of zeolite NaY from the LBK metakaolin was performed using the aluminosilicate molar ratio shown below and hydrothermal method [3-4].

$$15Na_2O: Al_2O_3:15SiO_2:450H_2O$$

Sodium hydroxide pellets (99 %w/w) and anhydrous sodium metasilicate (Sigma-Aldrich) which served as source of alkaline medium and additional silica were both supplied by Sigma-Aldrich. LBK Metakaolin served as a combined source of alumina and silica. 28.59 g of deionised water was measured and divided into two equal parts. 0.60 g of sodium hydroxide pellets was dissolved in the first halve of the deionised water, this was followed by dissolving 1 g of LBK metakaolin. 5.45 g of anhydrous sodium metasilicate was measured and added to the second halve of the deionised water. Both sets of precursors were subsequently mixed together to form a homogenous aluminosilicate gel. The gel was then aged with continuous stirring at room temperature. The different ageing times investigated was 0, 0.5, 1, 3, 6, 9, 12 and 24 h. The aged gel was crystallised for 9 h at 100 ^{o}C in a teflon autoclave as shown in Figure 3.2.

Figure 3.2: Autoclave used for zeolite NaY synthesis in this study

At the end of the hydrothermal treatment, the autoclave was removed from the oven and the sample taken out, filtered and washed with deionised water until the pH was between 7 and 8 [4]. The washed sample was subsequently dried overnight at 60 ^{o}C. The products obtained were characterised with XRD, SEM and TEM. Synthesis calculation is shown in Appendix A.

3.3. Physical Characterisation of the Raw Used Tyre and Natural Rubber Samples

Gross calorific values, proximate and ultimate analyses were used to study the physical characterisation of the used tyres and natural rubber raw material samples. The DryCal modular

calorimeter, model 2010, was used to obtain the gross calorific values (GCV), the Perkin Elmer precisely STA6000, Shelton USA simultaneous Analyzer was used to obtain the proximate analysis value (with experimental conditions; N_2 gas as purge gas at 40 ml/min, heating rate of 65 ^oC/min, temperature range of 30 to 800 ^oC). The Thermo Scientific Flash 2000 elemental analyzer was used to obtain the elements present in the samples.

3.3.1 Thermogravimetric (TGA/DTG) analysis

Thermogravimetric analysis (TGA) and differential thermogravimetric analysis (DTG) is a thermal analysis method which helps in the study of the degradation behaviour of materials during heating. It investigates the mass variation of sample as a function of time and temperature [7-8]. In this study, thermogravimetric analysis was performed in a TG/DTG analyzer SDT-Q600 from TA instruments. Sample weights of 10 to 20 mg were used. Nitrogen gas at a flow rate of 40 ml/min was used to maintain inert atmosphere for the thermal degradation. The temperature range for the pyrolysis investigation was 30 to 800 ^oC using different heating rates (15, 20 and 30^oC/ min).

3.3.2 Catalytic pyrolysis setup

Figure 3.3 (a) and (b) shows the schematic diagram and pictorial representation of the experimental setup used to produce pyrolytic oil from the catalytic pyrolysis of used tyres/ natural rubber.

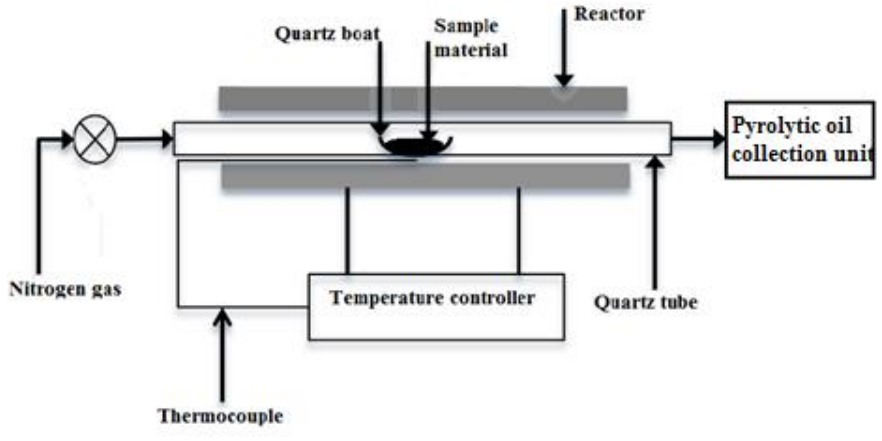

(a)

(b)

Figure 3.3 (a) Schematic diagram and (b) Pictorial scheme of experimental setup for pyrolytic oil production from used tyres and natural rubber in the Nanotechnology laboratory of the University of the Witwatersrand, Johannesburg

Number	Description
1	Reactor unit
2	Glass quartz tube
3	Temperature controller
4	Ice blocks Container for cooling
5	Round bottom flask for pyrolytic oil collection immersed in ice block container
6	Exit to fume hood/ gas collection point
7	Reactor exit linked to three-neck round bottom flask for volatile fraction
8	Nitrogen gas regulator
9	Nitrogen gas inlet to reactor unit
10	Nitrogen gas cylinder
11	Fume hood

Using the experimental setup shown in Figure 3.3, both thermal (without catalyst) pyrolysis and catalytic pyrolysis process was performed on the used tyres or natural rubber separately and in batches so as to be able to compare the quantity of pyrolytic oil obtained from the two sources with and without catalyst. The following parameters were investigated:

- Effect of the catalyst: feedstock (used tyres and natural rubber) ratio on the pyrolytic oil yield
- The concentration weight % of 1, 2.5, 5, 6, 7.5 and 10 wt. % of catalyst: feedstock

- Temperature effect on products obtained from the pyrolysis process (ranging from 375 to 750 ^{o}C)
- Feedstock particle sizes (2, 4, 6, 8 and 10 mm) effect on pyrolysis products.

Nitrogen gas baseline supplied by Afrox (Pty) ltd South Africa at a flowrate of 150ml/min was used both as a carrier gas and to keep the process inert. The pyrolytic oil produced was analysed and characterised using suitable equipment and standard laboratory procedures.

3.3.3 Experimental procedure for pyrolytic oil production from used tyres and natural rubber

The sample material, used tyres/natural rubber (10g/ batch) was placed in a glass crucible and introduced into a glass quartz tube positioned in a horizontal fixed-bed reactor chamber.The reactor chamber (which was heated by an electric system) had a K-type thermocouple and a P96 temperature controller connected to it. One end of the glass tube was connected to the N_2 gas cylinder to serve as inlet for the N_2 gas, while the other end served as an outlet for the liquid and volatile fractions (to the collection unit). The N_2 gas helped to ensure an inert environment and act as a carrier gas for the process.

Once the sample was in the reactor, the system was purged with N_2 gas at a flow rate of 150ml/min to remove air for about 15min before the experiment commenced. The reactor heater was switched on and the set value or operating temperature studied were 375, 450, 525, 600, 675 and 750 ^{o}C at a heating rate of 15^{o}C/min as programmed on the temperature controller. The

reactor temperature was kept constant once the process attains the set value temperature for 30 mins or till no visible flow of liquid was observed before it begins to cool to 20^{o}C. This was to allow all possible liquid and vapour products to exit the reactor to the collection unit. Nitrogen gas was continuously supplied in order to keep the reactor inert and also to sweep away the pyrolysed liquid and vapour products to the collection unit. The collection unit was made up of a three neck round bottom flask, placed in a bowl of ice. Both the pyrolytic oil and the gas fraction entered into the flask from the end connected to the reactor outlet via a flexible hose. The ice helps to retrieve the condensable fraction of the gas fraction while the non-condensable gases were collected for analysis (when needed) or allowed to escape through the outlet of the flask connected to the fume hood.

At the completion of the pyrolysis, N_2 gas flow was stopped and the reactor power was turned off. Upon cooling of the system, the round bottom flask was disconnected from the quartz glass tube reactor and the liquid fraction or pyrolytic oil was collected in a glass bottle and weighed. Also the char left on the glass crucible in the reactor chamber was collected, weighed and kept in a glass bottle. The amount of gas was determined by the difference between the sum of the pyrolytic oil and char weight from total weight of the feedstock. Afterwards the system was made ready for the next run by positioning the collection unit.

3.4 Characterisation of Used Tyres and Natural Rubber Pyrolysis Products

3.4.1 Chemical characterisation of used tyres and natural rubber pyrolytic oil

The chemical characterisation of the pyrolytic oil produced from used tyres and natural rubber via catalytic and non-catalytic process was performed using the following methods/equipments.

3.4.1.1 Fourier transform infrared spectroscopy (FTIR)

Fourier Transform Infrared spectroscopy (FT-IR) was used to analyse the chemical composition of the pyrolytic oil produced from used tyres and natural rubber.The FT-IR instrument, Bruker Tensor 27 model with Opus software was used to generate the IR spectra (range of 500 – 4000 cm^{-1}) and identify the functional groups present in the pyrolytic oil.

3.4.1.2 GC-MS analysis

A GC Agilent© 7890B and MS Pegasus 4D GCxGC from Leco was used for the identification of the compounds present in the pyrolytic oil and the distillates fractions. The GC had a Capillary configuration (Rxi-5silms) of column length 29.77m (30m), with internal diameter of 250µm, with film thickness of 0.25 µm and maximum temperature of 350 ^{o}C. The front inlet type was Split/Splitless with a split mode of 20:1 with an inlet temperature of 200 ^{o}C. Helium gas of 99.95% purity was used as carrier gas at a constant flow rate of 1.51 ml/min. The initial oven temperature of 70 ^{o}C was maintained for 2 min and ramped at 10^{o}C/min to 300 ^{o}C and held at 300 ^{o}C for 0.5min. Transfer line temperature was 260 ^{o}C.

The Mass Spectrometer method acquisition delay of 4 min, mass range of between 40 - 450 m/z, with acquisition rate of 10 spectra/second and electron energy (ionization energy) of -70eV was used. The ion source temperature was 250 ^{o}C.

Data processing method base line offset of 1 (just above the noise) was used, with a peak width of 4 secs and signal to noise (S/N) ratio of 500. The library search mode was normal and forward. The number of library hit was 10, while the minimum molecular weight allowed was 40 and maximum molecular weight was 450. Mass threshold was 2% and minimum similarity before name was assigned was 50%. The library used was Replib and mainlb from NIST.

3.4.1.3 NMR analysis

The ^{1}H NMR and ^{13}C NMR analyses of the pyrolytic oil were performed using the Bruker Advance III 400 equipment operating at 400.132 MHz for ^{1}H and 100.623 MHz for ^{13}C. Samples were prepared in 5ml NMR tubes using $PDCl_3$ as solvent.

3.4.2 Physical characterisation of used tyres and natural rubber pyrolytic oil

Physical properties such as density, kinematic viscosity, flash point, pour point, calorific value, sulphur content, and distillation boiling range of the used tyres and natural rubber pyrolytic oil was determined according to the American Society for Testing and Materials (ASTM) standard methods as shown in Table 3.1.

Table 3.1: Standard Methods for Physical Property Analysis

Physical Property	Method	Process description
Density	ASTM D1298-12b	Use of hydrometer placed in a constant temperature bath
Kinematic viscosity	ASTM D445 - 15	Use of calibrated glass viscosity tube submerged in a water bath at 40 ^{o}C
Flash point	ASTM D93 - 15a	Use of Pensky-Martens Closed test cup filled up to its mark with the test sample. The temperature shall be at least 18 °C below the expected flash point for the test sample and the cup.
Pour Point	ASTM D97 - 15	Use of test Jar glass which held the sample. Samples are first heated and then cooled at a specific rate at decrements of 3°C. The temperature 3°C above the point the oil stops moving is noted as the pour point
Gross Calorific Value	ASTM - E711	Use of the Parr oxygen bomb calorimeter
Sulphur Content	ASTM D7039 - 15a	Method based on measurement of the specific wavelength from excitation of sulfur, which can accurately measure the concentrations of sulfur from 2 to 500 ppm.
Distillation Boiling Range	ASTM D86-15	120 mL sample is distilled under prescribed conditions and observed temperature and volumes of condensate are reported.

3.5 Characterisation of Used Tyres and Natural Rubber Pyrolytic Solid Residue

3.5.1 Proximate and ultimate analysis of the used tyres and natural rubber pyrolytic solid residue

The proximate analysis was done according to ASTM D3172-73 with the Perkin Elmer precisely STA6000, Shelton USA simultaneous Analyzer and theThermo Scientific Flash 2000 elemental

analyzer was used to obtain the elements present in the samples according to ASTM D3176 - 15. Calorific value of the raw material was found by ASTM E711 using the DryCal modular calorimeter, model 2010.

3.5.2 SEM Analysis

Used tyres and natural rubber pyrolytic residue were characterised for surface morphology by Zeiss ultra60 FE-SEM Scanning Electron Microscope located at the School of Chemical and Metallurgical Engineering of the University of the Witwatersrand. The instrument was also used for the LBK and synthesised zeolite NaY catalyst characterisation. The size and shape of synthesised zeolite crystals were measured using the Zeiss ultra60 FE-SEM Scanning Electron Microscope. A thin layer of gold-palladium was used to coat the zeolite crystals in a BAL-TEC SPD-050 instrument before measurement.

3.6 Distillation of Used Tyres and Natural Rubber Pyrolytic Oil

3.6.1 Distillation set up

The pyrolytic oil obtained from the pyrolysis process (with/without catalyst) of used tyres and natural rubber was distilled according to the set up shown in Figure 3.4 (a) and (b).

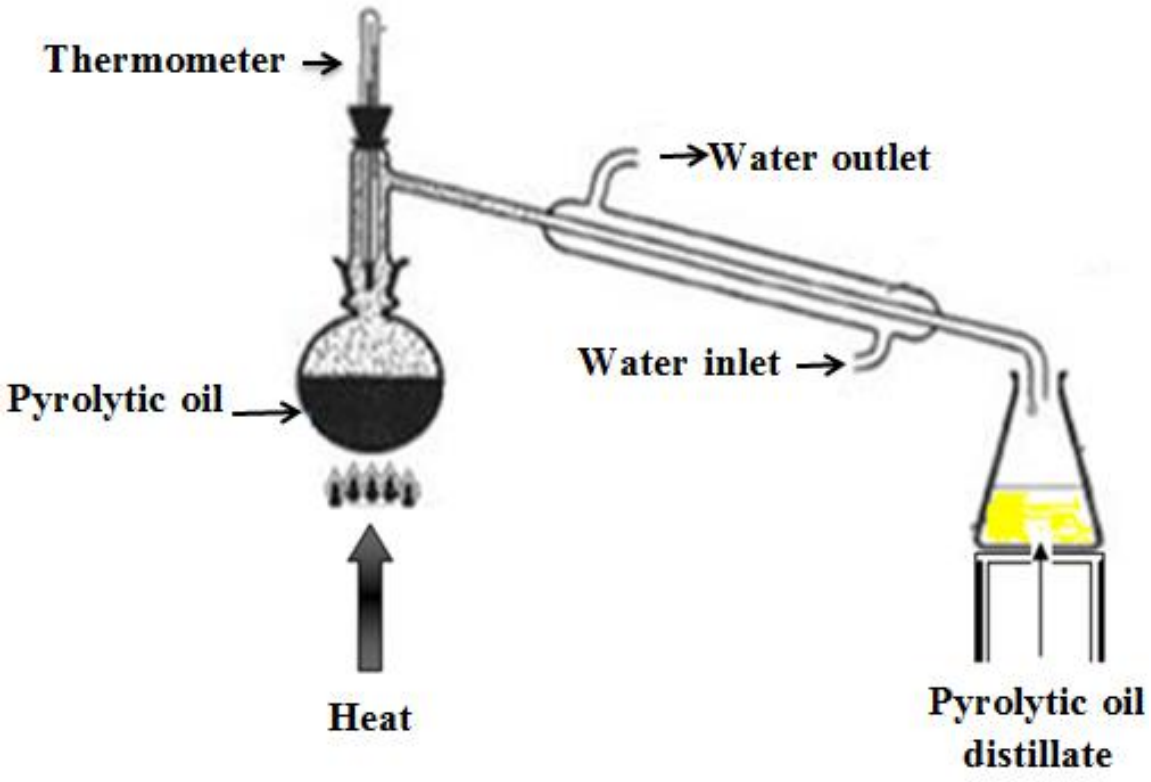
Thermometer
Water outlet
Water inlet
Pyrolytic oil
Heat
Pyrolytic oil distillate

(a)

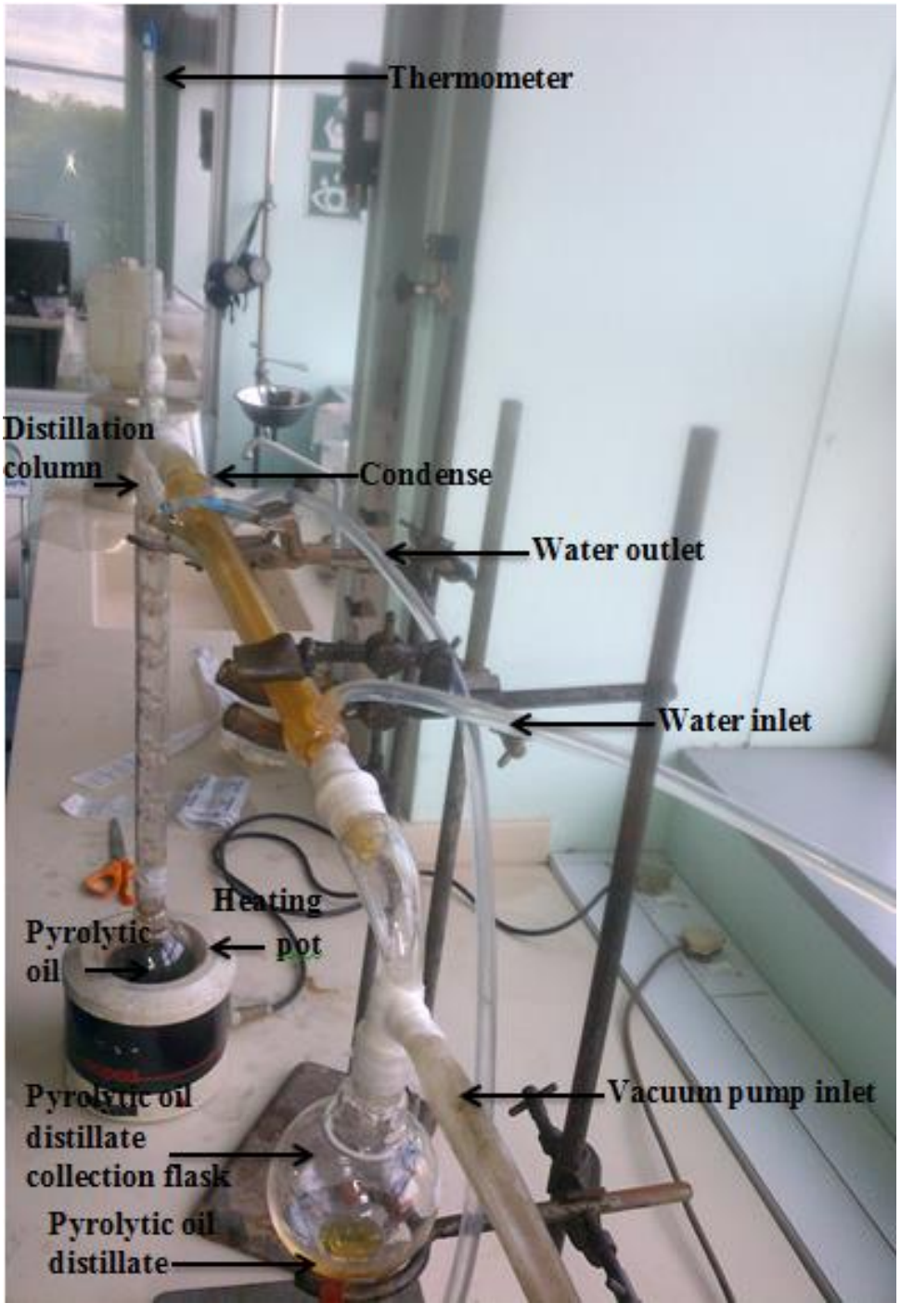

Figure 3.4 (a) Schematic and (b) pictorial set-up of batch distillation of pyrolytic oil from used tyres and natural rubber set up

3.6.2 Distillation experimental procedure

A volume of 120 ml of pyrolytic oil obtained from the thermal and catalytic pyrolysis of used tyres and natural rubber at 600 ^{o}C at a heating rate of 15^{o}C/min was poured into a round bottom flask seated in a heating mantle and distilled (under vacuum) with the aid of a vacuum pump as shown in Fig 3.3 (a and b). This was done so as to help reduce pressure build up in the batch distillation unit. The total volume of distillates obtained at different temperature from the 120 ml of the different pyrolytic oil was noted. The obtained pyrolytic oil distillates were then characterised using GC-MS.

3.7 Fuel blend Technique for Pyrolytic Oil Distillates and Petrol

The experimental set up for the fuel blend technique of pyrolytic oil distillates and petrol is depicted in Figure 3.5. It consists of a glass blender, a thermometer and an ultrasonicator.The ultrasonicator horn is 33 cm high with diameter of 0.7 cm, and operates at 24 kHz. The thermometer was positioned at 3 cm from the ultrasonicator horn (which was placed at the middle of the blender).

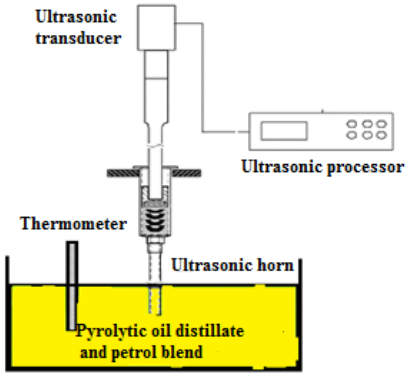

Figure 3.5: Setup for blending of pyrolytic oil distillates and petrol

Pyrolytic oil distillates obtained from used tyres/natural rubber and petrol were blended in different amounts ranging from 0 to 20% pyrolytic oil distillates. For each blend, the required volume of petrol was first poured into the batch blender. The ultrasonicator horn was then lowered to a depth of 2 cm within the petrol before being switched on. The temperature of the petrol was maintained at 26 °C, and then the appropriate volume of pyrolytic oil distillates was added to the petrol at a constant rate and allowed to blend for duration of 5 min before switching off the ultrasonicator. The obtained fuel mixture in the batch blender was emptied into a measuring cylinder to be tested in an internal combustion engine.

3.8 Combustion of Pyrolytic Oil Distillates and Petrol Blend in Internal Combustion Engine

3.8.1 Experimental set up for fuel blend study

A Sinemaster IG2600 BUNDU POWER (AC generator) was used to power a Martlet 375 W heavy duty 150 mm Bench Grinder, model MD 150BG for the internal combustion engine study of the various blended fuel as shown in Figure 3.6. The generator is a 4-stroke single cylinder, air-cooled spark ignition engine runs on 95unleaded-petrol with a fuel tank capacity of 4.6 L. Its manufacturer's engine specification is presented in Table 3.2.

Figure 3.6: (a) A Sinemaster IG2600 BUNDU POWER (AC Generator) (b) Bench Grinder powered during the combustion study

Table 3.2: Specification and characteristics of the internal combustion engine

Model type	KG166 (Single cylinder, air-cooled 4 stroke, gasoline engine)
Displacement (BorexStroke)	171 cc (66 x 50 mm)
Compression ratio	8.5:1
Rated power (kW/(r/min))	3.3/3600
Ignition system	Transistor-Controlled Ignition **(**TCI**)**
Spark plug	Bosch - WR7DC
Starting system	Recoil starter
Fuel type	Automotive unleaded gasoline
Fuel consumption (g/kW-h)	500
Lube oil	PD grade or SAE 10W-30, 15W-40
Fuel tank capacity (L)	4.6
Continuous running time	3 hours (at rated output)
Overall dimension (L x W x H) mm (inches)	564x317x453 (22.2x12.5x17.8)
Dry weight (kg (lbs))	26 (57.2)

3.8.2 Experimental procedure for fuel blend test in the internal combustion engine

For the fuel blend test in the internal combustion engine, Pyrolytic oil distillates and petrol blend with different proportion of Pyrolytic oil distillates (0, 5, 10, 15 and 20%) were prepared using ultrasonication-enhanced blending method for internal combustion test. Before running the blends, the engine was run on commercial or un-blended petrol for 60 min in order to flush the fuel line and internal combustion system. The electricity generator improvised tank was filled

with a volume of 200 ml of the blended fuel and then the engine was switched on to run for approximately 50 min. The parameters studied include the generator fuel consumption rate and fuel power under load. The volume of the fuel in the tank was measured and recorded at different time interval (0, 5, 10, 15, 20, 25, 30, 35, 40, 45 and 50 min) to determine the fuel consumption with the aid of a calibrated dipstick in the fuel tank.

References

[1] Franco, F., Pérez-Maqueda, L.A. and Pérez-Rodrí, J.L., 2003. The influence of ultrasound on the thermal behaviour of a well ordered kaolinite.*Thermochimica Acta, 404*(1), pp. 71-79.

[2] Brindley, G.W. and Nakahira, M., 1959. The Kaolinite - Mullite Reaction Series: II, Metakaolin. *Journal of the American Ceramic Society, 42*(7), pp. 314-318.

[3] Chandrasekhar, S. and Pramada, P.N., 2004. Kaolin-based zeolite Y, a precursor for cordierite ceramics. *Applied Clay Science, 27*(3), pp. 187-198.

[4] Kovo, A.S., 2011. Development of Zeolites and Zeolite Membranes from Ahoko Nigerian Kaolin. **(**Doctoral dissertation, *University of Manchester*, Manchester, UK).

[5] Islam, M.R., Tushar, M.S.H.K. and Haniu, H., 2008. Production of liquid fuels and chemicals from pyrolysis of Bangladeshi bicycle/rickshaw tyre wastes. *Journal of Analytical and Applied Pyrolysis, 82*(1), pp. 96-109.

[6] Kar, Y., 2011. Catalytic pyrolysis of car tyre waste using expanded perlite. *Waste Management, 31*(8), pp. 1772-1782.

CHAPTER 4

RESULTS AND DISCUSSION

4.1 Zeolite NaY Synthesis and Characterisation

Zeolite NaY catalyst used in this study was synthesised using a natural raw material, LBK as precursor for silicon and alumina. After refinement, the calcined LBK at 600 ^{o}C with exposure time of 2 hours was sent for analysis. The catalyst synthesised using the calcined LBK was performed at different ageing time (0, 0.5, 1, 3, 6, 9, 12 and 24 h). A constant crystallization temperature and time of 100 ^{o}C and 9 h reported in literature [1-3] as the optimum temperature and time for zeolite NaY synthesis (which is also used in the industry) was adopted for this study [4-5]. The synthesised zeolites at different ageing was characterised using XRF, SEM and XRD. These are discussed in sections 4.1.1 – 4.1.3.

4.1.1 XRF characterisation of calcined LBK

XRF analysis was performed on the calcined LBK in order to determine the chemical constituent weight percent present in the LBK. Table 4.1 shows the chemical constituents present in the LBK metakaolin produced at 600 ^{o}C revealed by the XRF.

Table 4.1: XRF chemical constituent present in LBK Metakaolin

Chemical constituent	Weight %
SiO_2	68.93
Al_2O_3	24.32
Na_2O	0.11
MgO	0.24
Fe_2O_3	0.22
MnO	0.02
CaO	0.08
K_2O	0.30
TiO_2	3.09
P_2O_5	0.10
Cr_2O_3	0.05
NiO	0.0022
Total	99.22
LOI	2.01

From Table 4.1, the LBK metakaolin main chemical constituent is silicon expressed as silicon oxides, 68.93 wt. % and aluminium expressed as alumina, 24.32 wt. % (with the presence of trace oxides at very low weight percent). The Si/Al ratio of approximately 2.83 obtained in this study was higher than that needed in synthesising commercial zeolite (Si/Al > 1.5) [2-4] and that reported by Kovo [1] which was approximately 2 when he synthesised zeolite NaY using kaolin as silicon and alumina source. This makes LBK a suitable source for silica and alumina in zeolite synthesis. With the XRF result, the amount of external silica source needed to boost the silica in the LBK metakaolin and other components needed in the zeolite NaY synthesis was calculated as shown in Appendix A.

4.1.2 SEM and XRD characterisation of refined and calcined LBK

The SEM morphology and XRD analysis pattern of the refined LBK Metakaolin was obtained as shown in Figure 4.1 and 4.2

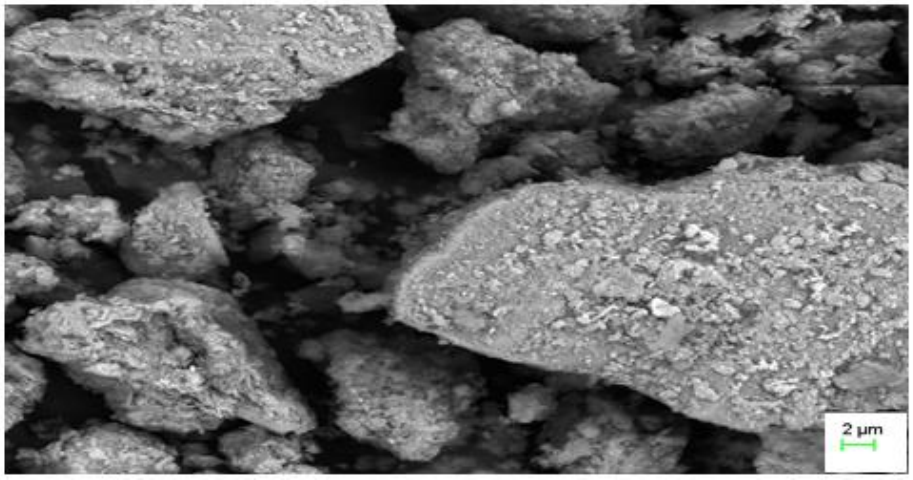

Figure 4.1: SEM image of LBK Metakaolin used in this study (Scale bar = 2µm)

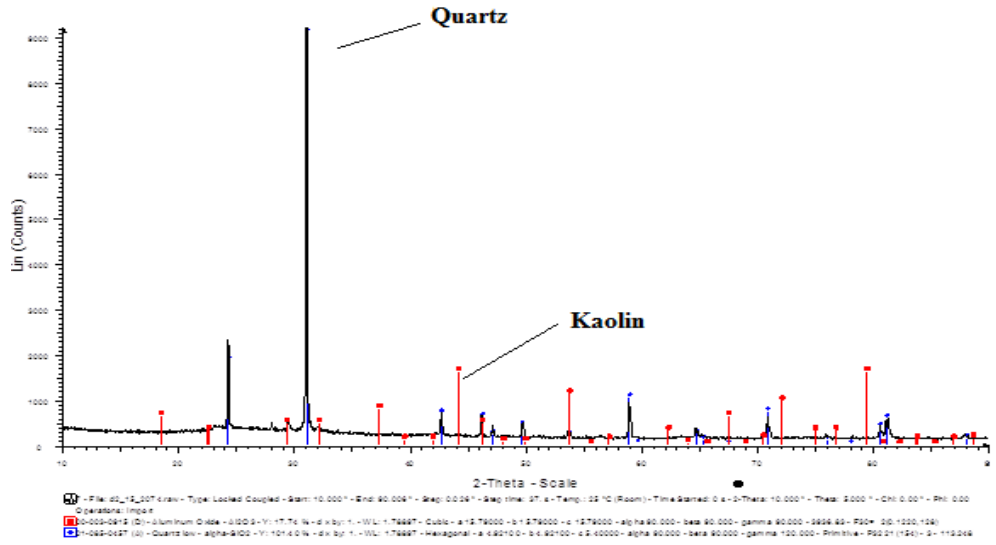

Figure 4.2(a): XRD pattern of the LBK Metakaolin used in this study for zeolite NaY synthesis

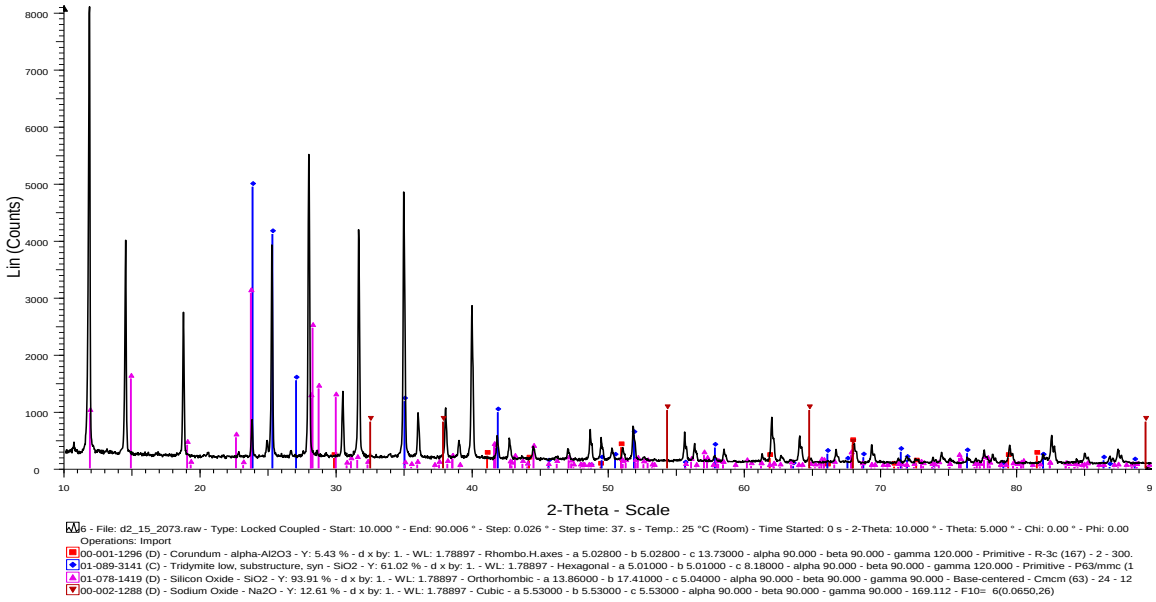

Figure 4.2(b): XRD pattern of reference commercial zeolite NaY showing its composition

From the XRD pattern, the presence of silicon and aluminium were identified. The EDAX result gave a Si/Al ratio of 1.6 which is higher than that required (≥1.5) for the synthesis of commercial zeolite. This made the LBK metakaolin a suitable material for zeolite NaY synthesis. From this characterisation of the LBK, noticeable changes undergone by the LBK Metakaolin (as aluminosilicate gel) in the formation of zeolite NaY will be compared with respect to the commercial zeolite.

4.1.3 SEM and XRD characterisation of the synthesised zeolite NaY from LBK Metakaolin

The SEM images of synthesised zeolite NaY obtained at different ageing time at a constant crystallization temperature and time of 100 ^{o}C and 9 h respectively using LBK metakaolin as precursor for silicon and alumina is shown in Figure 4.3(a) – (h). Commercial zeolite NaY (supplied by Sigma-Aldrich) SEM image was also obtained to serve as the reference zeolite NaY in this study.

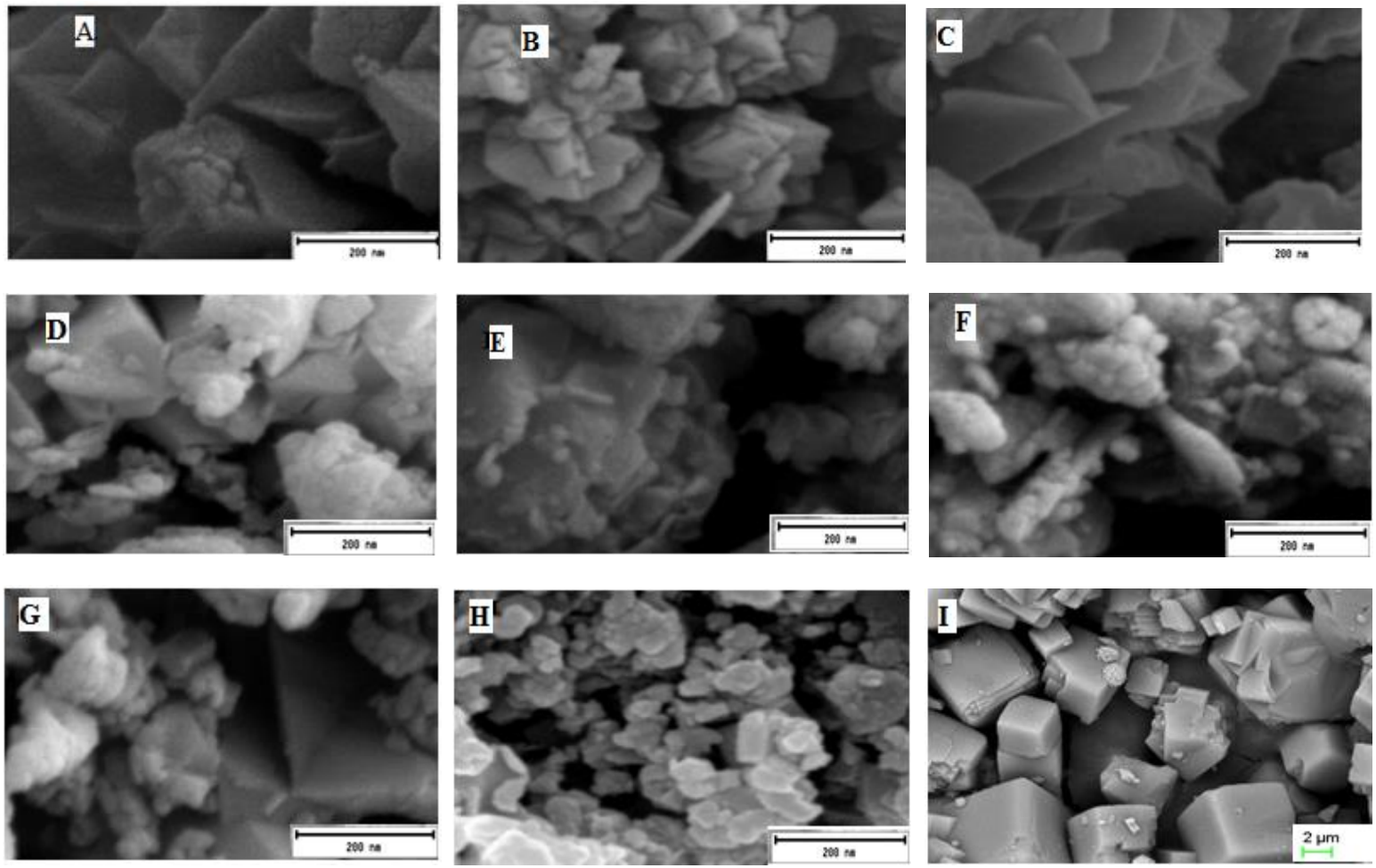

Figure 4.3: SEM image of zeolite NaY from LBK metakaolin (effect of ageing time A = 0, B = 0.5, C = 1, D = 3, E = 6, F = 9,G = 12, H = 24 h) and I is commercial zeolite NaY.

The SEM images reveal the presence of crystals even at 0 h ageing time with 9 h crystallization at 100 ^{o}C without seeding to induce zeolite formation. It was observed that the crystal sizes continued to grow with increasing ageing time. Fig 4.4 presents the role of increased ageing time on the aluminosilicate gel formation in the strong basic environment (NaOH used in this study) in the increase of particle size of the zeolite NaY formed.

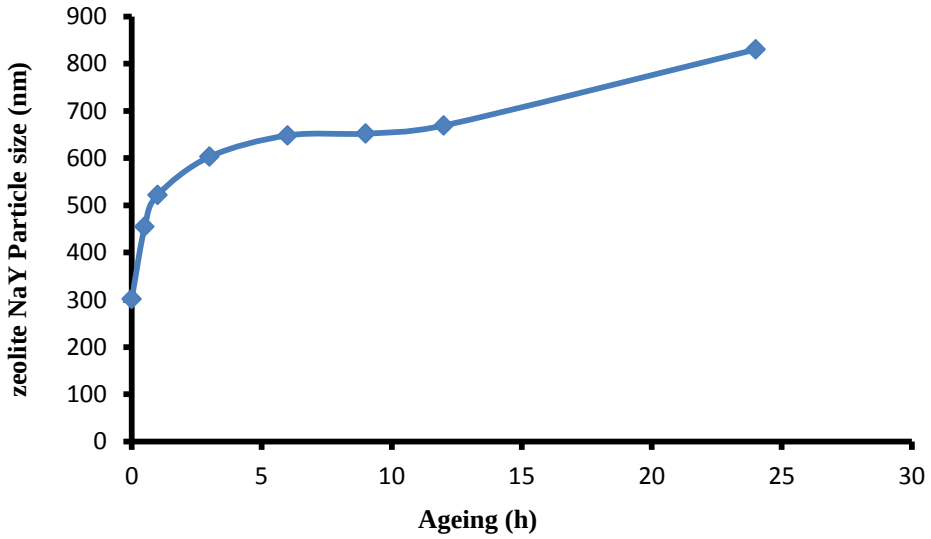

Figure 4.4: Effect of aging on zeolite NaY particle size

From Figure 4.4, the plot reveals that zeolite NaY crystallization and crystal growth commenced from as low as few minutes ageing time (0 h) and continued till 6 h ageing time. Upon further ageing from 6 – 9 h, it was observed that there was no more crystal growth, which was why the curve became flat. However, from 9 – 24 h ageing time, the crystals started agglomerating to form globules. This is probably due to hydrogen or van

der Waal force of hydrogen and oxygen found in AlO_2 and mH_2O moieties in $Mx/n[(AlO_2)x(SiO_2)y].mH_2O$, respectively.

Nevertheless, ageing is necessary in zeolite NaY synthesis as it assist in promoting and enhancing the chance of nucleation and crystallization [2]. This was confirmed in this study by synthesising the aluminosilicate gel at 0 h ageing time at room temperature. The SEM morphology of the synthesised sample displayed absence of zeolite crystals as presented in Fig 4. 5.

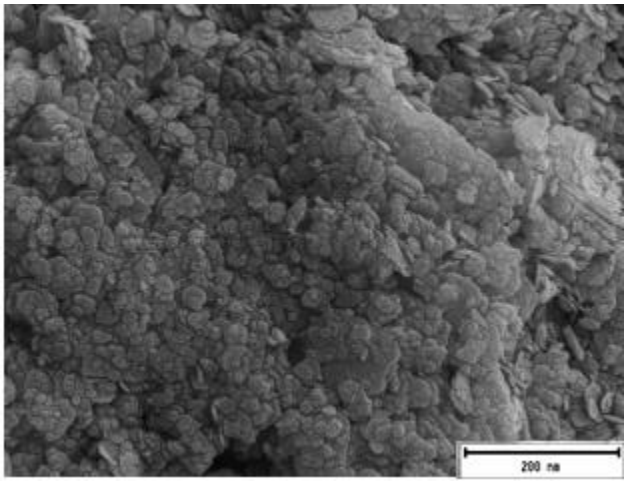

Figure 4.5: SEM image of 0 h aging at room temperature of 25 ^{o}C

The well-defined octahedral crystal shapes obtained for the zeolites NaY obtained at the ageing time lower than 1 h upward have similarity with that reported in literature by Chandrasekhar et al [2] and the commercial zeolite NaY used as reference zeolite NaY in this study. It is also worthy to note that the SEM scale bar of 200 nm was used for the capturing of all the synthesised zeolite NaY in this study shown in Figure 4.3(A) – (H) while a scale bar of 2µm was used for the SEM image of the commercial zeolite NaY.

This is because the synthesised Zeolite NaY came out as nanoscale particle sizes range as confirmed by the TEM images shown in Figure 4.6 below. For better comprehension, the SEM image at 2µm of the sizes of the synthesised zeolite NaY is found in Appendix B.

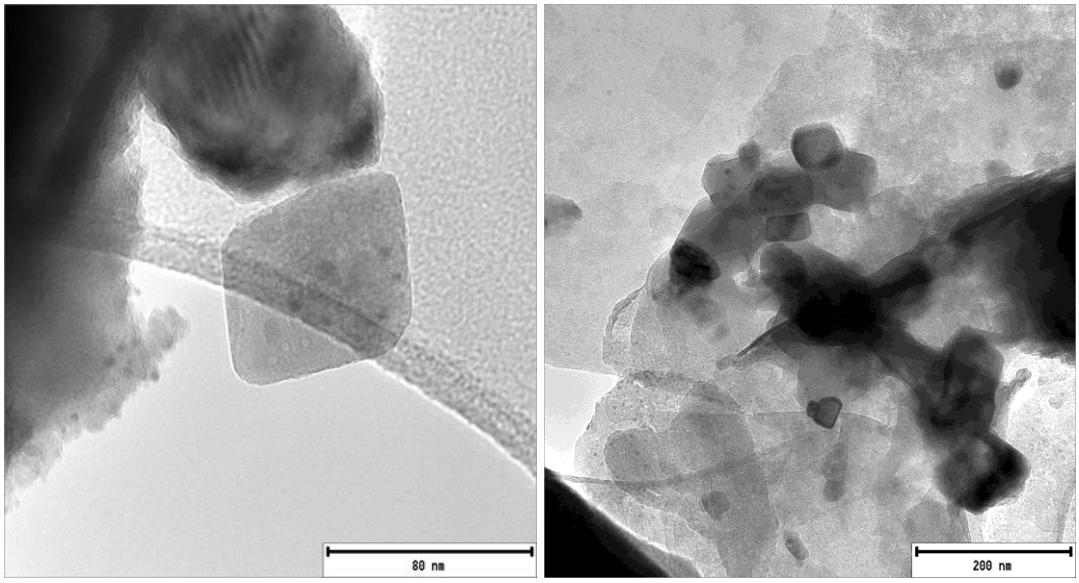

Figure 4.6: TEM image of synthesised zeolite NaY with particles nanoscale sizes

Also the X-ray diffraction pattern for the Zeolite NaY produced at different ageing time during this study as presented in Figure 4.7; support the SEM report of the formation of zeolite NaY even at 0 h ageing time at 100 ^{o}C and 9 h crystallisation time.

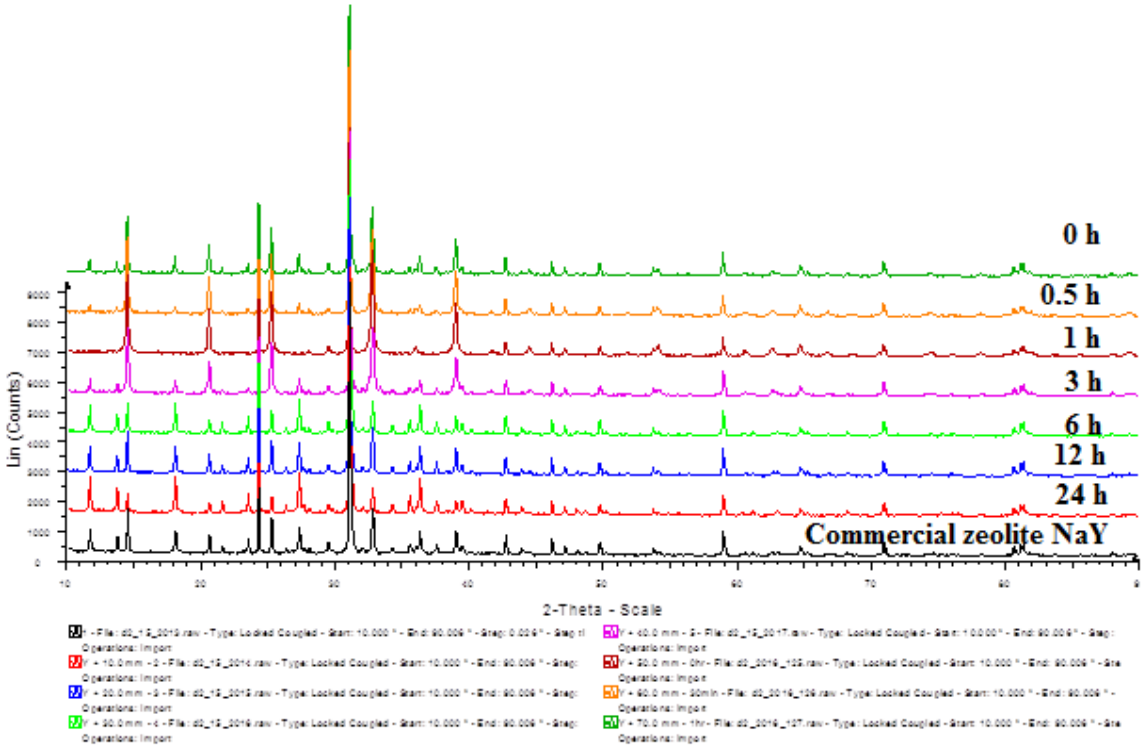

Figure 4.7: XRD pattern for the synthesised Zeolite NaY from LBK produced at different ageing time at constant crystallisation time and temperature

All the obtained XRD patterns match well with that of the commercial zeolite NaY supplied by Sigma-Aldrich which served as a reference standard in this study. From the synthesised zeolite NaY diffraction pattern, the intensity of the peaks for ageing time of below 1 h and above were a near perfect match with that of the reference commercial zeolite NaY (used as standard). This implies that the calcination of the LBK resulted in the release of free silica and alumina from the kaolin structure which made the aluminosilicate to be very reactive in the base environment [3]. The role of ageing can be said not to be responsible for the zeolite formation has shown in this study. Other conditions such as autogenous pressure, crystallization time, temperature and the

reactivity of the aluminosilicate gel formed from the LBK metakaolin and the strong base, NaOH could be the controlling factors [4].

4.1.4 Summary of zeolite NaY synthesised from LBK Metakaolin

Generally, use of kaolin in the synthesis of faujasite has not yielded much success except for zeolite X [1, 3-5]. This could be attributed to several factors such as nature of the raw kaolin, quantity and composition of other materials such as alkali medium required for zeolite Y synthesis. Nevertheless in this study, the outcomeof the use of LBK metakaolin as a precursor for alumina and silica in the synthesis of zeolite NaY via hydrothermal method was achieved. This was confirmed by the SEM and XRD results. Hence, reaffirming the assertion that the physicochemical property of the kaolin material determines to what extent such kaolin can be converted to zeolite NaY [2]. Despite ageing period of more than 9 h has been reported as necessary for other kaolin in literature [3], LBK metakaolin was reactive enough to form zeolite nucleus within a short time of less than 1 h. Also the nano sizes of the synthesised zeolite NaY particle was obtained at the first 3 h of ageing in this study. These synthesised zeolites NaY of different particle sizes would be used in the catalytic pyrolysis of used tyres and natural rubber.

4.2 Proximate and Ultimate Analysis and GCV of Used Tyres and Natural Rubber

Both the proximate analysis and heating value of natural rubber and used tyre rubber samples are presented in Table 4.2. The obtained results for the proximate analysis of

natural rubber and used tyre samples reveal that these raw materials are suitable for pyrolysis, which is in agreement with the data presented by many authors [6–10] Nevertheless, the ash content of natural rubber was much lower than that of the used tyre in this study as well as those reported in literature [11]. This is owing to the fact that the natural rubber sample studied had no additive and other inorganic content (such as zinc, clay, silica) which are usually present in tyre rubber according to manufacturers' formulation [11-12]. With the low ash content in natural rubber, a higher mass of product yield should be expected. The fixed carbon content of the natural rubber was almost thrice that available in literature but with a very low volatile content which could be due to the absence of oil based additives, plasticizers and anti-oxides in the sample [9]. The GCV of natural rubber (39.00 MJ/kg) and car used tyre (31.22 MJ/kg) were higher than that of lignite coal (15.00 MJ/kg) and wood (21.70 MJ/kg) making them a better source of solid fuel but lower than that of conventional diesel (44.80 MJ/kg).

Table 4.2 Proximate and ultimate analysis of natural rubber and used tyres

Proximate analysis %	**This study**		**Ref. [6]**
	Natural rubber	Used Tyre	Car tyre
Moisture content	1.50	0.50	0.70
Ash	0.70	16.00	8.00
Fixed carbon	89.10	27.10	29.50
Volatile content	8.70	56.40	61.90
Ultimate analysis %			
Carbon (C)	87.90	85.00	86.70
Hydrogen (H)	7.90	5.50	8.10
Nitrogen (N)	3.20	0.21	0.40
Sulphur (S)	-	1.20	1.40
Oxygen (O)	1.00	8.09	1.30
GCV (MJ/kg)	39.00	31.22	36.20

4.3. Degradation of Used Tyres and Natural Rubber

The thermogravimetric (TGA) and differential thermogravimetric (DTG) analyses curves with respect to reaction temperature, T, at a heating rate of 15^{o}C/min for used tyres and natural rubber samples are shown in Figure 4.8 and 4.9

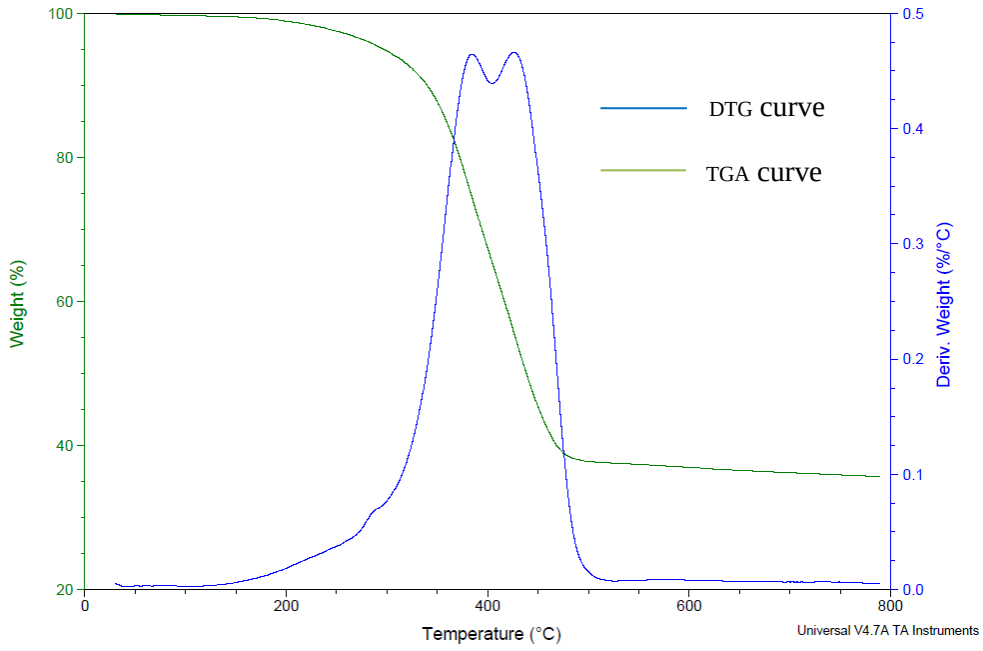

Figure 4.8: TGA/DTG curve of UT at heating rate of 15^{o}C/min

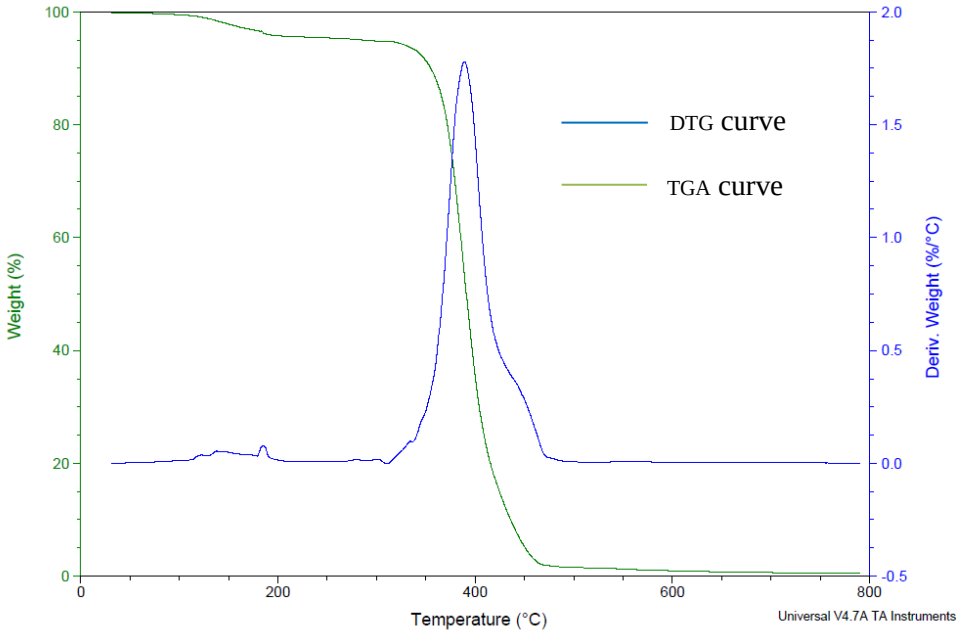

Figure 4.9: TGA/DTG curve of NR at heating rate of 15^{o}C/min

For the temperature range of 30 to 800 ^{o}C, more than one temperature degradation zone were observed for the both used tyres and natural rubber. This is in agreement with reports by different authors [8, 13-14] that there exists more than one degradation temperature zone during tyre rubber pyrolysis. The TGA curve of both samples shows that the thermal decomposition begins at a temperature of 200 ^{o}C for natural rubber, 210 ^{o}C for used tyre and complete at 500 ^{o}C for natural rubber and 520 ^{o}C for used tyre. The DTG curve (Fig 4.8 and 4.9) also gave a single peak of 386.70 ^{o}C for natural rubber and two dominant peaks of 385.64 and 425 ^{o}C for used tyre rubber. When these results are compared with values of thermal degradation of individual kind of rubbers in literature [9, 11, 14] (375 ^{o}C for NR, 445 ^{o}C for SBR and 465 ^{o}C for BR), it is evident that the single

peak in natural rubber DTG curve shows the decomposition of only NR in the sample and further confirms the absence of any type of synthetic rubber as the natural rubber investigated was in its raw form. That of the used tyres DTG curve reveals that the first peak indicates the degradation of NR and the second dominant peak gives the degradation of SBR and BR, a major type of polymer in car tyre formulation [9, 14].

The degradation of NR involves two main phases. The first phase can be attributed to the loss of volatile components (moisture and oil), and the second phase as active pyrolytic zone. While the first stage degradation of UT includes loss of plasticizers and other volatile additives in the tyre. The second degradation stage involves mainly cracking and rapid degradation of the rubber components present in the UT [15]. It is at this period that carbon bond scission of weaker chemical bonds and intermolecular associations occur. Heavy weight molecular hydrocarbons are depolymerised, hydrogenated/dehydrogenated into smaller lower weight hydrocarbon molecules in form of liquid and gas phase. From the dominant peaks revealed by both DTG curves, significant conversion takes place at this stage as well as secondary depolymerisation. Beyond this stage, the sample is mainly left as ash shown by the constant weight displayed in the TGA/DTG curves. This is in accordance with the study done by Williams et al. [16] on thermogravimetric analysis with two distinct areas of weight loss signifying a lower and higher temperature of degradation.

4.4 Thermal Pyrolysis of Used Tyres and Natural Rubber

In this study, optimum heating rate and mass of the sample used were determined experimentally (Appendix C). This obtained optimum heating rate and mass of sample were then kept constant in order to determine optimum values for other parameters (as discussed in sections 4.4.1 to 4.4.4) such as feed material particle size, operating temperature, and catalyst (concentration and particle size) effect on feed material pyrolysis yield and pyrolytic oil compoisition. Eureqa^{TM} mathematical programing software was then used to propose a fit equation for the pyrolytic oil yield in relationship with the different sets of parameters.

4.4.1 Determination of feed material optimum particle sizes on thermal pyrolysis of used tyres

Figure 4.10 (a) shows the effect of feed size on UT pyrolysis products yield performed at 600 ^{o}C at a heating rate of 15^{o}C/min. The data plotted (in Table C3 in Appendix C) are the mean value and standard deviation of the pyrolytic oil, char and gas yields for the various feed material particle sizes. It was observed that the pyrolytic oil yield increased progressively from 24.5 ± 0.17 to 34.4 ± 2.18 wt. % for 2 to 6mm feed particle size respectively. A steady decrease for the pyrolytic oil yield was observed for the feed particle size greater than 6 mm. Nevertheless, there was a steady decrease in gas and increase in solid residue yield from 2 to 10 mm. The increase in solid residue for size 2 to 10 mm may probably be due to less exposed surface area which reduced the breaking of

hydrocarbon molecules and lower thermal conductivity within the UT materials which prevented even distribution of heat within the entire material for more reaction [9, 21].

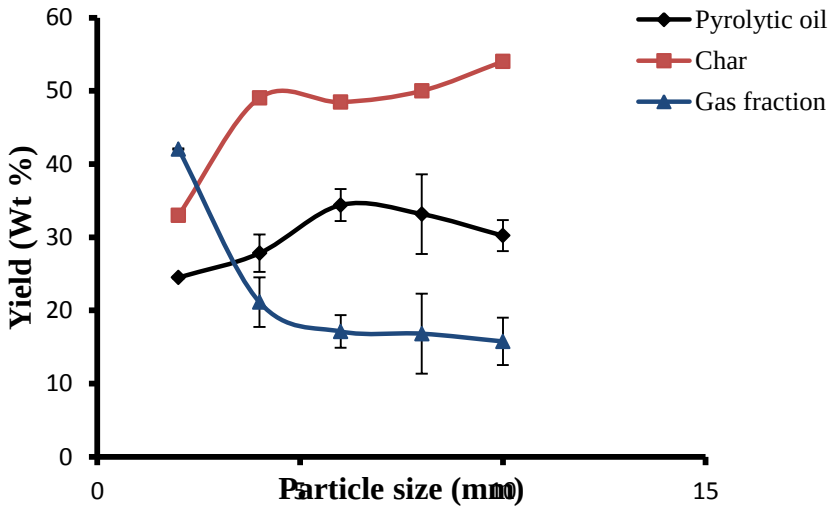

(a)

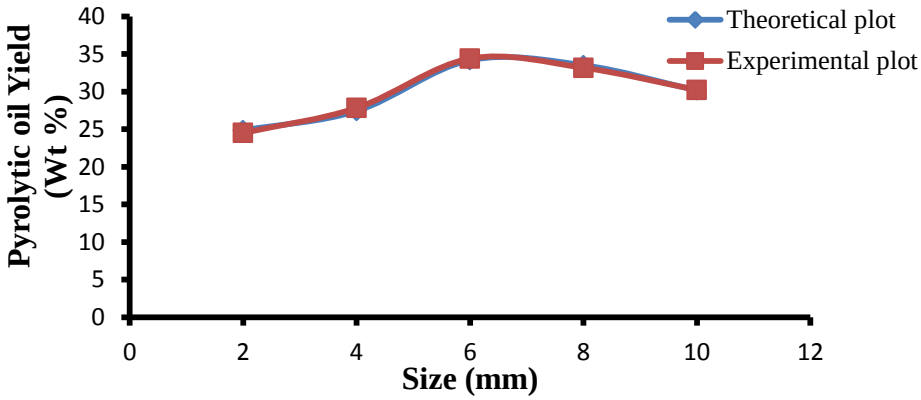

(b)

Figure 4.10: (a) Particle size effect on UT pyrolysis yield (b) Experimental and theoretical plot of size effect on UT pyrolytic oil production

(STD: Pyrolytic oil = 4.01, Char = 7.92, Gas = 11.05)

Hence, this led to carbonisation or incomplete degradation of the larger UT sizes resulting in increase in solid char produced and reduction in pyrolytic oil and gas yields. For the smaller sizes, especially 2 mm, the increase in gas yield could be as a result of the wider reaction surface area available thereby enabling rapid spread of heat and speedy degradation of the UT to happen [17,29]. Also the pyrolytic oil and solid residue produced had sufficient time to undergo secondary reaction in the reactor resulting in more gas yield and decrease in solid char and pyrolytic oil produced. The results obtained in this study are in accordance with that reported by Barbooti et al. [29] where amount of heat on a core of large pieces was restricted from the heat source. Also Islam et al. [30] reported that 8 cm^3 produced a higher char yield with corresponding lower gas and liquid yield than those of 4 cm^3. In the same way, Dai et al. [31] found that there was a higher amount of char produced for 0.8 mm tyre sample with lower gas and oil yield than that obtained for 0.32 mm sample. Therefore, it can be concluded for this study that 6 mm is the optimum feed size for degradation of UT feed stock to complete with less chances of secondary reaction at the optimum reaction temperature of 600 ^oC and heating rate of 15^oC/min. It was this feed size that was applied for the natural rubber pyrolysis in order to compare their products yield.

To predict the pyrolytic oil yield produced at a given used tyres particle size, Eureqa Newtonian software was used. The proposed equation (4.1) satisfied the experimental data as can been seen in Figure 4.10 (b)

$$Y = 21.84 + 1.68\,S + 0.43\,S\cos(S) - 4.89e^{-6}\,S^6 \qquad (4.1)$$

Where; Y = pyrolytic oil yield and S = Used tyres particle size

Figure 4.10 (b) Compares the experimental plot and the predicted from equation (4.1) with R^2 goodness of fit = 0.99, Correlation Coefficient = 0.99, Maximum Error = 0.41, Mean Squared Error = 0.09, Mean Absolute Error = 0.28 and complexity = 28.

4.4.2 Temperature effect on product yield of thermal pyrolysis of used tyres

The product distribution from the thermal pyrolysis of 10 g of used tyres at a heating rate of 15^{o}C/min for temperature range of 375 to 750 ^{o}C at every 75 ^{o}C elevation in temperature for feed size of 6 mm was studied. This was performed in order to determine the pyrolysis optimum operating temperature. The process was repeated thrice for each temperature. The process reaction temperature, and weight fractions for the various products yield, pyrolytic oil, char and gas fractions have been plotted together in Figure 4.10 (a).The data plotted (in Table C4 in Appendix C) are the mean value and standard deviation of the pyrolytic oil, char and gas yields for the various temperatures.

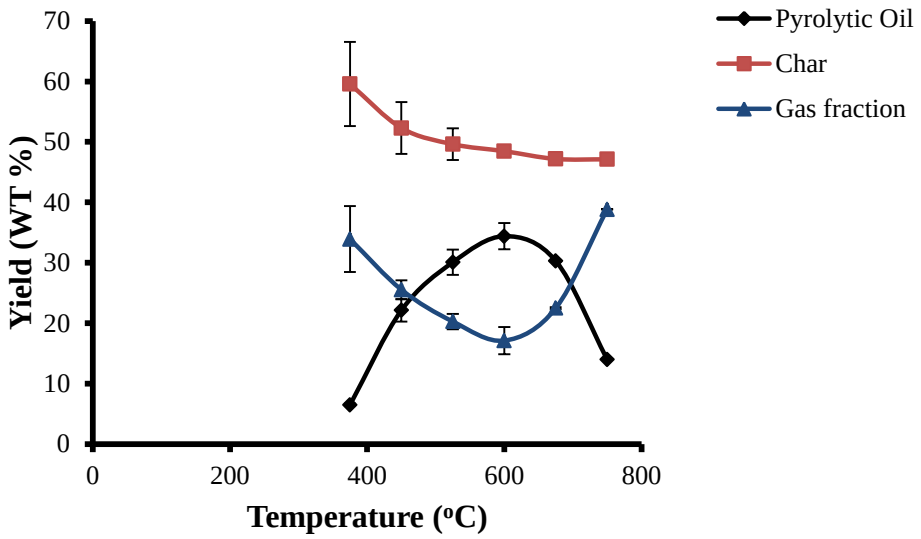

(a)

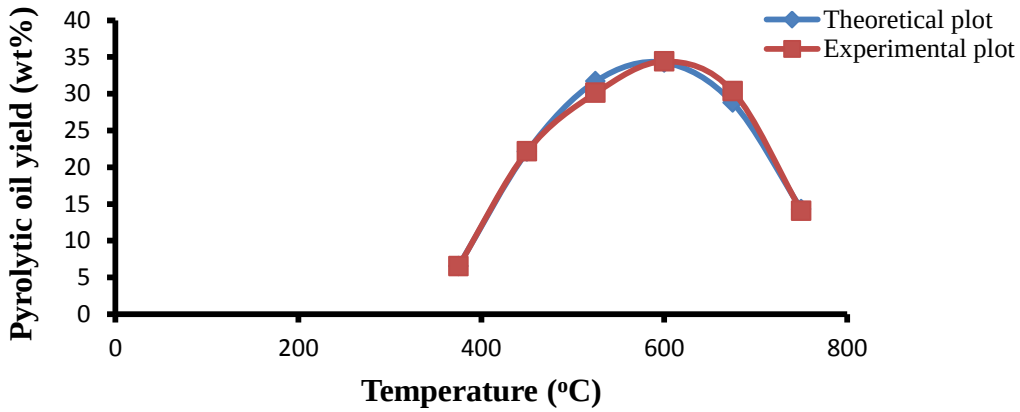

(b)

`Figure 4.11: (a) Effect of temperature on UT pyrolysis product yield. (b) Experimental and theoretical plot of temperature effect on UT pyrolytic oil production (STD: Pyrolytic oil = 10.84, Char = 4.75, Gas = 8.38)

From Figure 4.11(a) it was observed that with an increase in temperature from 375 to 750 ^{o}C, the yield of pyrolytic oil increased from 6.49 ± 0.21 to an optimum value of 34.40± 2.18 wt. % at 600 ^{o}C and then reduces to 14.03 ± 0.13 wt. % at 750 ^{o}C. The solid char yield decreased from 59.58 ± 6.98 wt. % to 47.12 ± 0.16 wt. % over the entire temperature range, while the gas yield increased from 33.93 ± 5.46 to 38.85 ± 0.07 wt. %. It is observable that a maximum exists at the temperature where optimum yield of pyrolytic oil was attained possibly as a result of strong cracking of used tyres at this temperature, 600 ^{o}C. Secondary reactions that occurred within the reactor must have led to formation of more gases which resulted in a decrease in pyrolytic oil yield at higher temperatures more than 600 ^{o}C. This was also in agreement with the optimum temperature obtained by Pradhan and Singh [17] in their investigation of thermal pyrolysis of used tyres rubber over a temperature range of 450 to 700 ^{o}C.

Hence, it can be proposed that used tyres rubber is not completely degraded during thermal pyrolysis at a temperature below 600 ^{o}C. The low pyrolytic oil yield at, 375 ^{o}C is not unexpected as most of the used tyres rubber components (SBR, BR and NR) degradation temperature except for NR is even higher than the operating temperature of 375 ^{o}C as revealed in the DTG curve of Figure 4.8. Also, the presence of high amount of gas (33.93 ± 5.46 wt. %) even at low temperature of 375 ^{o}C, shows that the used tyres has high volatile materials such as moisture, plasticizers and other additives which can easily volatilise at low temperature (as obtained from the proximate analysis results in Table 4.2) . The solid char yields over the temperature range 600 to 750 ^{o}C were almost

equivalent to the values derived from the TGA of used tyres in Figure 4.7. Since the solid char yield did not reduce over the temperature range of 600 to 750 ^{o}C, a conclusion can be reached that used tyres rubber degradation is completed.

The decline in pyrolytic oil yields and increase in gas above 600 ^{o}C could be attributed to the degradation of fractions of the pyrolytic oil into non-condensable gases [9], along with secondary reaction involving carbonization of hydrocarbons in the pyrolytic oil into char [9,18-19]. The further loss in char at higher temperatures could also contribute to high gas yield at higher temperatures making the gas fraction to be more prominent at such temperatures [20-21]. Nevertheless, 600 ^{o}C can be said to be the maximum operating temperature for the thermal pyrolysis of used tyres to obtain optimum pyrolytic oil yield in this study since degradation is completed and gas yield becomes dominating due to the outcome of the effect of temperature on the thermal pyrolysis of used tyres.

The production of pyrolytic oil from used tyres pyrolysis at different operating temperature was proposed using Eureqa Newtonian software. The proposed equation fitted the experimental data as shown in Figure 4.10 (b), which described the production yield as a third order polynomial equation. This can serve as basis for the prediction of pyrolytic oil production using the pyrolysis method. The coefficients of equation (4.2) are related to the experimental conditions and these conditions should be investigated further.

$$Y=0.41T-126.67-3.96e^{-7}T^{3} \quad (4.2)$$

Where; Y = pyrolytic oil yield and T = operating temperature

Figure 4.11 (b) compares the experimental and the predicted data from equation (4.2) with R^2 goodness of fit = 0.99, Correlation Coefficient = 0.99, Maximum Error = 1.58, Mean Squared Error = 0.83, Mean Absolute Error = 0.60 and complexity = 13.

The third order polynomial regression equation (4.3) was also obtained using the results of Islam et al (2008):

$$Y = 0.38\ T - 74.30 - 5.48e^{-7}\ T^3 \quad (4.3)$$

With R^2 goodness of Fit = 0.95, Correlation Coefficient = 0.98, maximum Error =1.62, Mean Squared Error = 0.54, Mean Absolute Error = 0.38 and Complexity = 13. This is in accordance with the results obtained in this study.

4.4.3 Temperature effect on the product yield of natural rubber thermal pyrolysis

Correspondingly, the thermal pyrolysis of natural rubber (latex rubber) generated the three pyrolysis products which are pyrolytic oil, solid char and gas. The product distribution from the thermal pyrolysis of 10 g of natural rubber at a heating rate of 15^{o}C/min for temperature range of 375 to 750 ^{o}C at every 75 ^{o}C elevation in temperature for an average feed size of 6 mm was studied. The process was repeated thrice for each temperature. The process reaction temperature, and weight fractions for the various products yield, pyrolytic oil, char and gas fractions have been plotted together in Figure 4.12(a). The data plotted are the mean value and standard deviation of the pyrolytic oil, char and gas yields for the different temperature as shown in Table C5 in Appendix C.

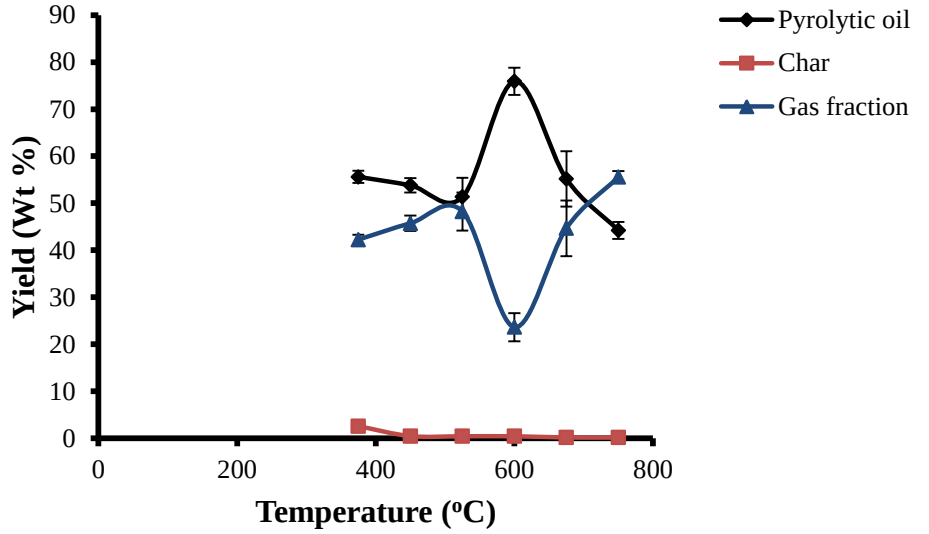

(a)

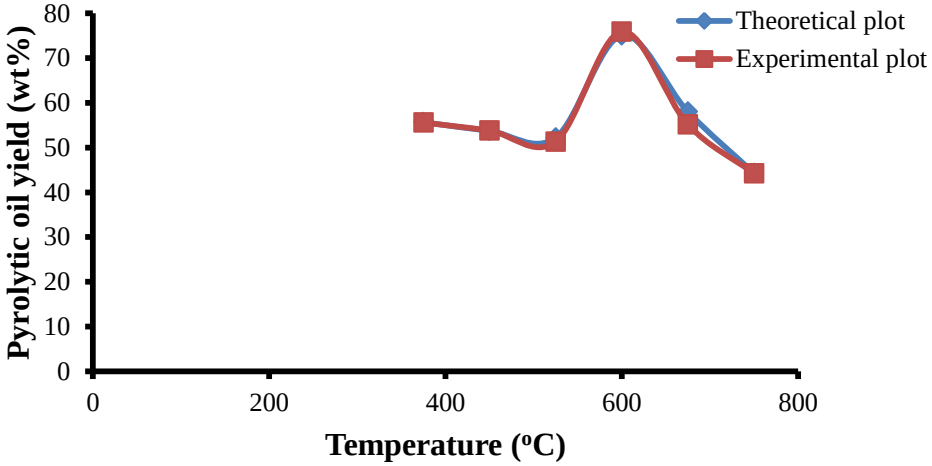

(b)

Figure 4.12: (a) Effect of Temperature on NR pyrolysis products yield (b). Experimental and theoretical plot of temperature effect on NR pyrolytic oil production (STD: Pyrolytic oil = 10.61, Char = 0.92, Gas = 10.69)

Considering the product yield results, pyrolytic oil optimum was obtained at 600 ^{o}C. This could be as a result of strong cracking of the natural rubber and dehydrogenation/ hydrogenation of the carbon bond at this temperature due to Diel Alder's mechanism described in Section 2.4.5. From the results, NR gave pyrolytic oil yield of 75.93 ± 2.88 wt. % which was almost thrice that obtained for the thermal pyrolysis of used tyres as shown in Figure 4.11(a). This yield is almost twice the amount obtained from pyrolysis of used tyres and other polyisoprene based materials reported in literature. Shen et al. [22] reported a liquid fraction yield of 52.0 wt. %, char yield of 36.1 wt. % and gas yield of 11.9 wt. % at 500 ^{o}C during the thermal pyrolysis of scrap tyres. A related result was also presented by Williams and Brindle [23] when used tyres were pyrolysed in a fixed bed reactor. Roy and Unsworth [24] reported a liquid fraction yield of 56.6 wt. % from the vacuum pyrolysis of used tyres at 415 ^{o}C. Kawakami et al. [25] reported 53 wt. % of oil yield at temperature range of 540 to 640 ^{o}C from the pyrolysis of used tyres in a rotary kiln reactor.

The gas fraction weight percent obtained in this study increased from 23.63 ± 2.99 to 55.58 ± 1.23 wt. % over the temperature range of 600 to 750 ^{o}C which was also higher than that obtained for used tyres in this study as reported in Figure 4.11 (a). This is another potential of natural rubber to provide energy in form of gas which can be used as source of heating/ fuel [9]. Natural rubber gave low solid residue of 0.43 ± 0.12 wt. % at optimum pyrolytic oil yield temperature of 600 ^{o}C which is within the proximate analysis result. This will make it less challenging in terms of chars volume turn out which is

normally associated with UT pyrolysis process. This further confirms that yields from pyrolysis and their distributions can be greatly influenced by the feedstock composition amongst other factors, therefore making results from different authors to vary [12, 14].

In order to predict pyrolytic oil production from NR at different pyrolysis temperature, the Eureqa Newtonian software was used. As shown in Fig 4.12 (b) the theoretical plot obtained from equation (4.4) fitted the experimental data.

$$Y = 44.45 + 0.03T + 22.36 \times \cos(0.23T) - 0.06\ T \cos(0.23\ T) \quad (4.4)$$

Where; Y = pyrolytic oil yield and T = operating temperature

Figure 4.12 (b) Compares the experimental and the theoretical plots with R^2 goodness of fit = 0.98, Correlation Coefficient = 0.99, Maximum Error = 2.86, Mean Squared Error = 1.61, Mean Absolute Error = 0.80 and complexity = 25.

4.4.4 Catalyst concentration effect on the pyrolysis of used tyres and natural rubber

The catalyst used in this study was zeolite NaY synthesised as discussed in Section 3.1. The aim was to investigate the possibility of using Lawani River Benin Nigerian kaolin (LBK) as a precursor for Si/Al source in the synthesis of zeolite NaY. The success of LBK as precursor for zeolite can attract industrial usage thereby creating economic value to the Nigerian raw material source. Also the catalyst was used in order to improve product yield of used tyres and natural rubber pyrolysis at optimum temperature. The

catalyst to UT and NR ratio range investigated was from 1 to 10 wt. % of the catalyst concentration to the feed stock.

From the study, it was observed that the pyrolytic oil yield for the thermal pyrolysis of used tyres (as shown in Figure 4.11(a) and that of natural rubber (as shown in Figure 4.12 (a)) at optimum temperature of 600 ^{o}C was higher than that obtained during catalytic pyrolysis of the two materials at same temperature throughout the entire catalyst for feed stock range studied (as reported in Figure 4.13(a) and 4.14(a)). The data plotted are the mean value and standard deviation of the pyrolytic oil, char and gas yields for the varied catalyst concentration as shown in Table C6 and C7 in Appendix C.

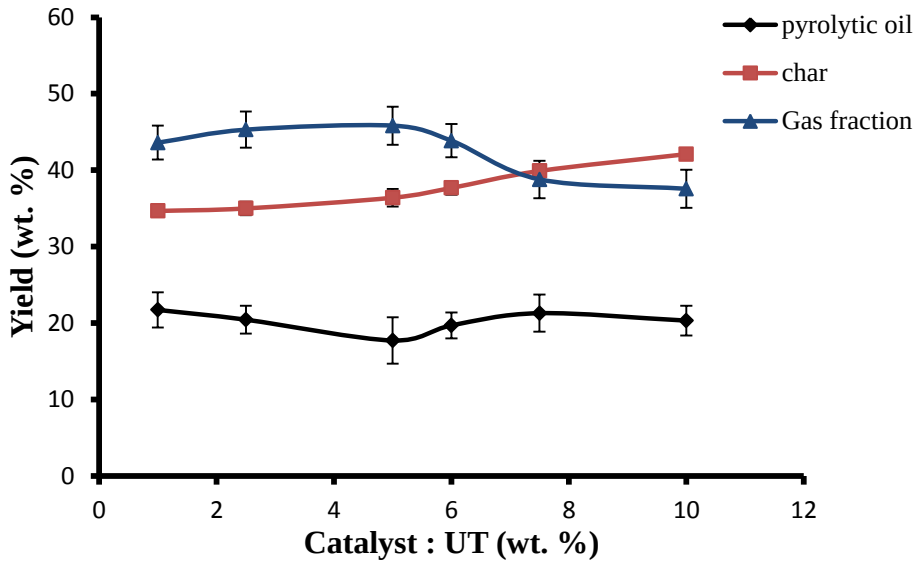

(a)

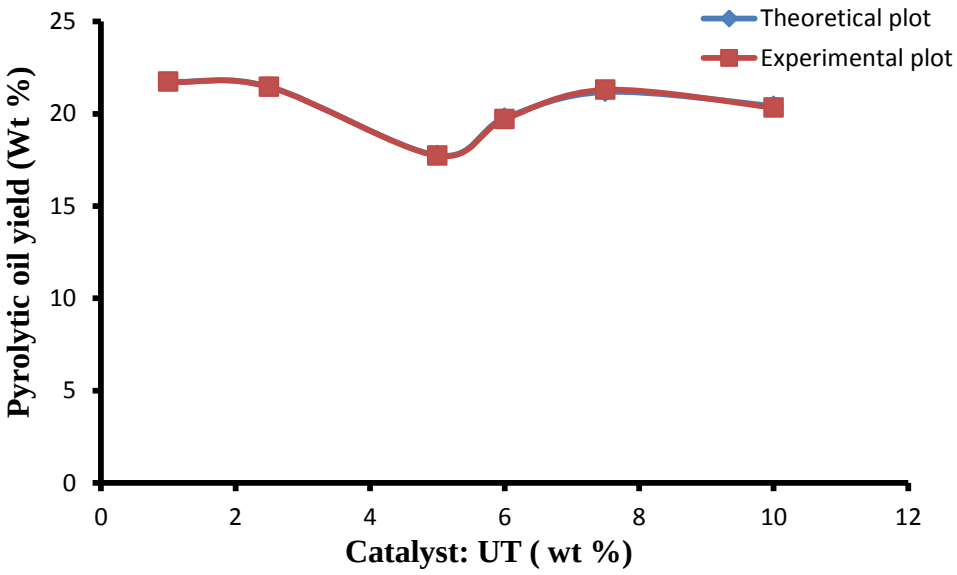

(b)

Figure 4.13: (a) Catalyst concentration effect on UT pyrolysis at 600°C (b). Experimental and theoretical plot of catalyst effect on UT pyrolytic oil production (STD: Pyrolytic oil = 1.41, Char = 2.91, Gas = 3.46)

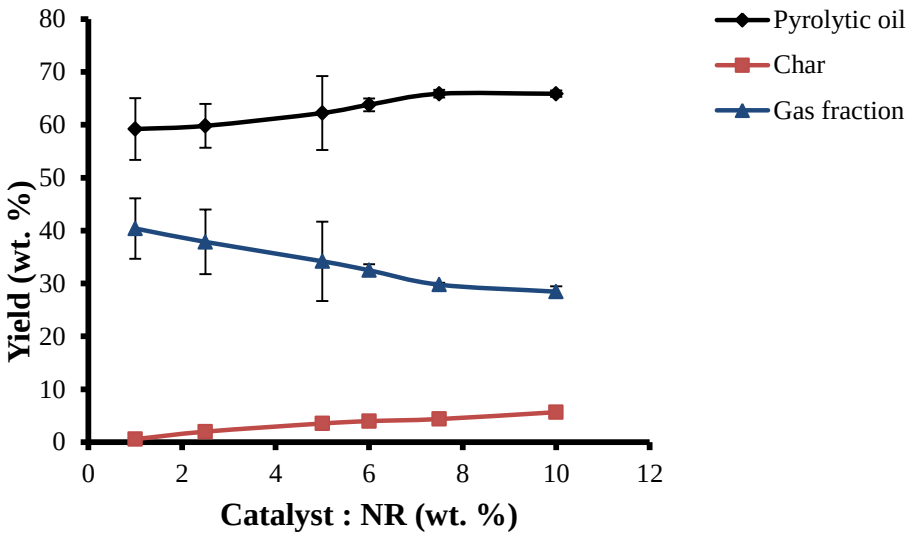

(a)

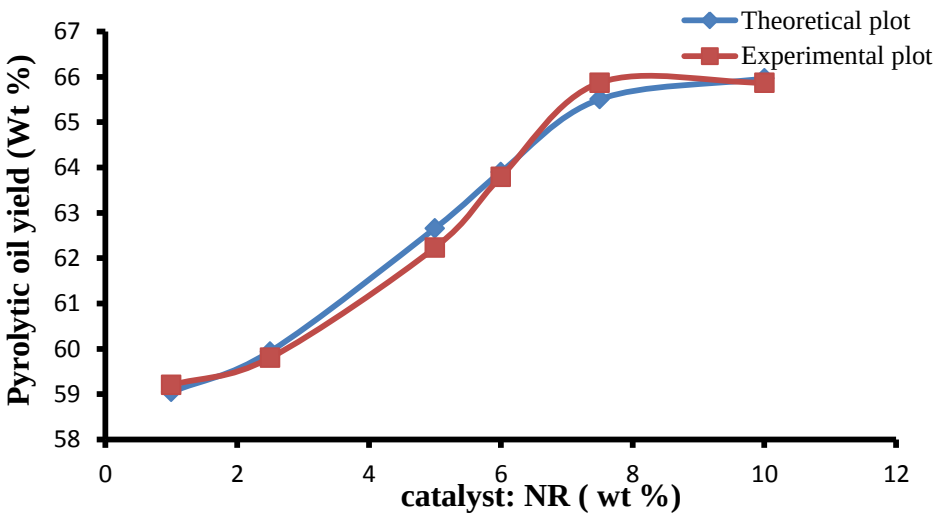

(b)

Figure 4.14: (a) Catalyst concentration effect on natural rubber pyrolysis at 600 ^{o}C and (b). Experimental and theoretical plot of catalyst effect on NR pyrolytic oil production (STD: Pyrolytic oil = 2.90, Char = 1.81, Gas = 4.62)

The presence of catalyst only resulted in lower value of pyrolytic oil and gas yield with a corresponding increase in solid char yield for both used tyres and natural rubber compared to the thermal pyrolysis. It is note worthy that most of the solid residue obtained during the catalytic pyrolysis of used tyres and natural rubber contained deposit of catalyst homogeneously mixed with the feed material before pyrolysis.

From Figure 4.13 (a), there was a steady increase for gas and solid char yield and a decrease for pyrolytic oil yield till 5 wt. % of the catalyst: UT ratio. A decrease in both gas and pyrolytic oil and an increase in solid char were observed for catalyst: UT ratio from 5 to 10 wt. %. This could be due to more deposit of catalyst as a result of increased weight percent in the reactor and coke formation from secondary reaction of the pyrolytic oil. Also for that of catalysed NR pyrolysis, Figure 4.14(a) shows a steady increase in pyrolytic oil yield from 1 to 7.5 wt. % catalyst: NR ratio with a decrease in the gas yield throughout the 1 to 10 wt. % catalyst: NR ratio. While there was a continuous increase in the solid char yield beyond 7.5 wt. %, a constant yield value of pyrolytic oil (65.87± 0.73) was observed for catalyst: NR ratio beyond 7.5 to 10 wt. % indicating no effect of the catalyst on the pyrolytic oil yield.

This is in agreement with the study conducted and reported by Pradhan et al. [17] on catalytic pyrolysis of used tyres and tube rubbers at 600 and 700 ^{o}C using SiO_2-AlO_2 Kaolin, CaO and MgO catalyst. The authors reported that none of the catalysts used

showed significant effect in increasing the oil yield compared to the thermal pyrolysis of the studied materials. Similarly, in the two-staged pyrolysis of used tyres using catalysts reported by Shen et al. [22], the authors observed that the presence of zeolite USY catalyst caused a reduction in the oil yield and an increase in gas yield with coke formation on the catalyst.

For the effect of catalyst concentration on the production behavior of pyrolytic oil from used tyres, the Eureqa Newtonian software was used. A well fitted theoretical plot with the experimental data was obtained using equation (4.5) as shown in Fig 4.13 (b).

$$Y = 23.16 - 0.49\ A - 3.15 \sin(4.78 + 1.80\ A) \quad (4.5)$$

Where; Y = pyrolytic oil yield and A = Catalyst concentration

Figure 4.13 (b) compares the experimental and the theoretical plots with R^2 goodness of fit = 0.99, Correlation Coefficient = 0.99, Maximum Error = 0.12, Mean Squared Error = 0.01, Mean Absolute Error = 0.06 and complexity = 16.

Similarly, the Eureqa Newtonian software was also used to propose the production behavior of natural rubber with respect to the catalyst concentration. Both the experimental and theoretical plots as shown in Figure 4.14 (b) fitted well the data using equation (4.6).

$$Y = 58.87 + 0.18\ A^2 - 0.001\ A^4 \quad (4.6)$$

Where; Y = pyrolytic oil yield andA = Catalyst concentration

Figure 4.14 (b) Compares the experimental and the model plots with R^2 goodness of fit = 0.99, Correlation Coefficient = 0.99, Maximum Error = 0.43, Mean Squared Error = 0.09, Mean Absolute Error = 0.26 and complexity = 17.

Since in this study, zeolite NaY catalyst had no significant increase in pyrolytic oil yield during the catalytic pyrolysis of natural rubber and used tyres in comparison with thermal pyrolysis, the effect of the different particle sizes of the synthesised zeolite NaY on the pyrolytic oil composition in terms of gasoline hydrocarbon range was investigated.

4.4.5 Effect of Zeolite NaY particle size on biogasoline yield from produced pyrolytic oil

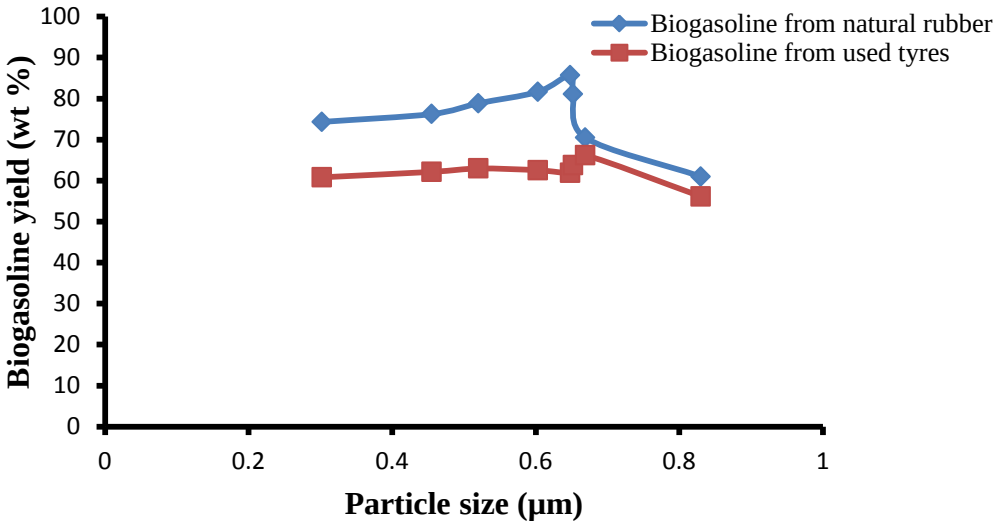

Figure 4.15: Effect of zeolite NaY catalysts particle sizes on Pyrolytic oil composition

From the results shown in Figure4.15, the particle sizes of 0.648 μm and 0.669 μm of zeolite NaY produced the maximum possible yield of 85.73 and 66.17 wt. % biogasoline from natural rubber and used tyres respectively. The catalytic activity can then be seen from the levels of C_6 to C_{12} hydrocarbon produced from the pyrolysis reaction. Particle sizes greater than the optimum size resulted in lower biogasoline yield, this implies that the greater the particle diameter the less its catalytic activity. These could be as a result of mass transfer limitations and external diffusion at increasing size. Similarly, catalyst with smaller particle size than the optimum size flows easily with the pyrolytic oil produced or are stuck to the wall of the reactor. These catalyst particles which were retained on the reactor wall or flowed along with the pyrolytic oil could reduce the amount of active site of the catalyst available for the reactants resulting in fewer long hydrocarbon chains being broken into short hydrocarbon.

The yield of biogasoline range obtained at these different sizes of synthesised zeolite NaY was compared with the yield of biogasoline range obtained from the use of commercial zeolite NaY (size of 4.113 μm) on natural rubber and used tyres. From the product formed, 53.17 and 51.77 wt. % of biogasoline range was obtained for NR and UT using commercial zeolite NaY.Thus the synthesised zeolite NaY gave pyrolytic oil with a higher yield of biogasoline range than the commercial zeolite. This could be due to less internal mass transfer limitation for the synthesised zeolites associated with their particle sizes which favoured higher catalytic activity as a result of more access to active sites than the commercial zeolite NaY. The sudden drop in biogasoline yield observed for both

NR and UT from Figure 4.15 can be accounted for by the decrease in available surface area of the catalyst. Also the catalyst performance in terms of high biogasoline yield from NR compared to UT can be attributed to the higher amount of polyisoprene present in NR than in UT.

4.5 Characterisation of Produced Pyrolytic Oil

The pyrolytic oil produced from both thermal and catalytic pyrolysis of used tyres and natural rubber (shown in Figure 4.16 (a) and (b)) was an oily dark-brown-color liquid with acrid smoky smell [9,17]. It was observed that pyrolytic oil from used tyres had a stronger acrid smell than the natural rubber pyrolytic oil probably due to the sulphur content in it [9, 17, 26]. There was no remarkable phase separation noticed in the NR and UT pyrolytic oil. The pyrolytic oil was characterised in terms of both fuel and chemical properties (as discussed in Sections 4.4.1 and 4.4.2).

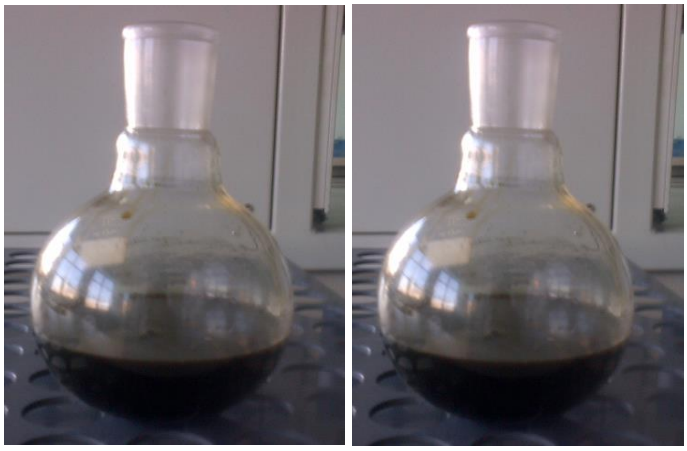

(a) UT pyrolytic oil (b) NR pyrolytic oil

Figure 4.16 Pyrolytic oil from: (a) Used tyres and (b) Natural rubber

4.5.1 Physical properties of produced pyrolytic oil

The physical properties of the pyrolytic oil obtained by the thermal and catalytic pyrolysis were analysed for their fuel properties. This is to determine their suitability as liquid fuel and potentials for other uses. The fuel properties were determined by using ASTM methods. Table 4.3 shows the fuel properties of the natural rubber pyrolytic oil and used tyre pyrolytic oil obtained in this study in comparison with that of tyre pyrolytic oil reported by other researchers and commercial automotive (No. 2) diesel. From the table, the following were observed about the pyrolytic oil physical properties;

Density

It is a measure of the mass of a liquid per unit volume at a specific temperature. Density can give an indication of the fuel volume ratio and other fuel properties of a liquid in

terms of engine performance. As shown in Table 4.3, the density of natural rubber pyrolytic oil (876 ± 0.01 kg/m^3) was slightly higher than that of the commercial diesel (820-860 kg/m^3) but lower than that obtained from used tyre pyrolytic oil in this study (890 ± 0.02 kg/m^3) and heavy fuel oil (980 kg/m^3). Since high density is dependent on the molecular weight of the fuel molecules, this implies that natural rubber pyrolytic oil has heavier molecules than that of conventional diesel and gasoline but lower than that of UT.

Viscosity

The viscosity which is a measure of a fluid frictional property is an important factor in considering the performance of a liquid fuel with respect to resistance to shear, fuel atomization, and flow in engines and spray burner, must not be too high [30]. In this study the viscosity of NR and UT pyrolytic oil was 4.65 and 5.18 cSt respectively, which were both above the maximum range for diesel and gasoline fuel but similar to light fuel oil [11]. This could be attributed to the presence of heavy compounds in both pyrolytic oil [17]. As proposed by Rofiqul et al. [30], this low viscosity is an advantageous characteristic in the handling and transportation of the pyrolytic oil.

Refractive Index

It is an important factor to consider as it affects the auto ignition of fuel vapour [32]. The refractive index of 1.500 and 1.520 were obtained for NR and UT pyrolytic oil, while 1.508 and 1.514 were obtained for the catalysed NR and UT pyrolytic oil. These values obtained for the refractive index of both the thermal and catalytic NR and UT pyrolytic

oil did not deviate much from the acceptable values for that of commercial diesel (1.45-1.475).

pH Value

This is a measure of the acidity or alkalinity level in the fuel. It is important due to the challenges of corrosion such fuel could have on storage systems and the metal components of an engine. The pH value (5.76 and 5.46) of both the thermal and catalytic pyrolytic oil for UT was higher than that for the thermal and catalytic pyrolytic oil of NR (7.68 and 7.64). This revealed the non-acidic nature of NR pyrolytic oil perhaps due to the absence of acidic agents like sulphur.

Pour Point

The pour point helps to determine the lowest temperature at which the liquid fuel can no longer flow. Reports have shown that pour point is always lower than cloud point. It is the temperature at which fuel gelling occurs resulting in fuel pump failure. Pour point temperature of -26 and -12 ^{o}C respectively was obtained for the NR and UT pyrolytic oil. This implies that the pyrolytic oil would not be problematic for engines in hot and dry regions.

Sulphur content

The absence of sulphur in the composition of the natural rubber pyrolytic oil makes it a cleaner fuel than used tyre pyrolytic liquid and fossil heavy fuel oil. The sulphur content obtained for the thermal and catalysed UT pyrolysis pyrolytic oil was 0.035 ± 0.004 and

1.35 ± 0.05 weight percent. The results are within the sulphur content range of 0.11 and 1.54 wt% for used tyre pyrolytic oil [11] and similar to that of light fuel oil.

Flash Point

The flash point of a liquid is the temperature at which sufficient vapour is evolved from the liquid which can ignite in air. This determines the flammability of the liquid and is a measure of its fire hazard in terms of storage and handling. Considering the flash point of ≤36 ^{o}C obtained for NR pyrolytic oil and ≤30 ^{o}C for the UT pyrolytic oil, both pyrolytic oil are comparable with that reported for used tyre pyrolytic oil in literature [17,28] but are lower than that of fossil fuels such as commercial diesel, >55 and light oil which is 79 ^{o}C [9,28]. The low flash points can be attributed to the fact that the pyrolytic oil is composed of a mixture of compounds with a wide distillation temperature range [9,19].

Higher heating value (HHV)

This is also referred to as gross calorific value (GCV) or higher calorific value (HCV). It helps to determine the amount of heat that can be released when a specific amount (at 25 ^{o}C) of fuel is combusted and its product temperature returns to 25 ^{o}C. The HHV of 44.13 ± 1.08 and 45.11 ± 1.22 was obtained for the thermal and catalysed NR pyrolytic oil which was higher than that of thermal and catalysed (42.72 ± 0.05 and 42.60 ± 0.37) UT pyrolytic oil, and tyre pyrolytic oil reported in literature [28]. The NR pyrolytic oil HHV value was within the range for that of commercial diesel (44.0 – 46.00 MJ/kg) making it a viable alternative source of liquid fuel which can be used directly for electricity generation, industrial furnaces, boilers and static engines.

Table 4.3: Fuel properties of NR pyrolytic oil in comparison to used tyre pyrolytic oil and commercial diesel

Fuel Properties	This study (NR pyrolytic oil)	This study (UT Pyrolytic oil)	Ref. [17]	Ref. [30]	Light fuel oil	Commercial No.2 Diesel
Density (kg/m^3)	876 ± 0.01^a	890 ± 0.05^a	917.9^b	970	890	820-860
Viscosity (cSt)	4.65^d	5.18^d	5.31^d	4.90^d	21^c	$2.0\text{-}4.5^d$
Refractive index	1.50, 1.508	1.520, 1.514	-	N/A	-	1.45-1.475
Flash point (^oC)	≤36	≤ 30		≤32	79	>55
Pour point (^oC)	-26	-12	-87	-3	-	-40 to -30
pH value	7.68, 7.64	5.76, 5.46	-	4.80	-	N/A
Sulphur content (wt %)	-	0.035 ± 0.004, 1.35 ± 0.05	1.38	1.36	1.4	1.2
HHV (MJ/kg)	44.13, 45.11	42.72, 42.60	34.61	40.80	44.8	44.0 - 46.0

a =20 ^{o}C, b =15 ^{o}C, c = 30 ^{o}C and d = 40 ^{o}C

4.5.2 Chemical properties of produced pyrolytic oil

In determining the chemical composition of the thermal and catalytic UT and NR pyrolytic oil produced at a temperature of 600 ^{o}C at a heating rate of 15^{o}C/min, recent methods and analytical techniques employed by almost all researchers in identifying and quantifying possible components in pyrolytic liquid derived from different types of organic materials was used. These include FT-IR, NMR and GC-MS analytical techniques as discussed below in sections 4.5.2.1 to 4.5.2.3.

4.5.2.1 FT-IR analysis of UT and NR pyrolytic oil

The FT-IR certainly may not be the most suitable analytical technique to check for saturated, aromatic and polar components [6, 9, 17, 30, 34]. However, this analysis operates on the principle of infrared light absorption by most molecules which helps to reveal the chemical properties of the liquid [17]. Apart from monatomic (Helium, Neon, Argon etc) and homopolar diatomic molecules (Hydrogen, Nitrogen, oxygen etc) that does not absorb infrared light, other chemical molecules present in the pyrolytic oil respond to infrared light by bond stretching and contracting in a specific wavelength range independent of the structures of other molecules. Using this principle, the identification of the functional groups present in the pyrolytic oil was achieved.

The FT-IR transmittance spectrum for UT and NR pyrolytic oil (thermal and catalysed) are shown in Figure 4.17, 4.18, 4.19 and 4.20, while data results performed on the NR and UT pyrolytic oil compared to those of other authors are presented in Table 4.4. The aliphatic C-H stretched vibrations at 3000 – 2800 cm^{-1} and C-H deformation vibrations at 1451 - 1375 cm^{-1} indicate the presence of alkanes. The presence of aromatic compounds is indicated by C-H in-plane bending in the 1155 - 1016 cm^{-1} zones, and the C-H out-of-plane bending peaks in the 965 - 795 cm^{-1} zone. The peaks between 1650 – 1635 cm^{-1} and 965 - 795 cm^{-1}, represents C=C stretching vibrations, and are indicative of alkenes. The data reveal therefore that both the thermal and catalysed pyrolytic oil obtained from used tyres and natural rubber comprise mainly of aliphatic and aromatic compounds with

the presence of other hydrocarbon compounds in low proportion. It was also observed from the peaks height in the transmittance spectrum that both pyrolytic oils obtained from natural rubber have more aliphatic hydrocarbon functional group than that of used tyres pyrolytic oil. These compounds identified in this study have also been detected by other researchers but in different proportions [6, 16, 28, 36].

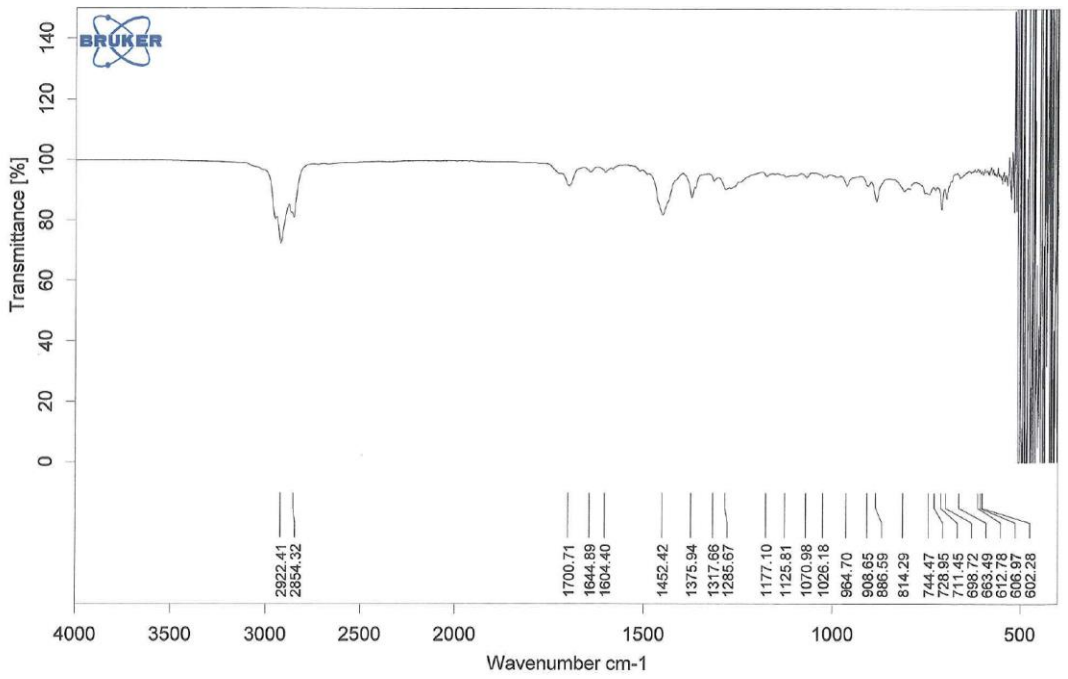

Figure 4.17: FTIR transmittance spectrum for used tyres pyrolytic oil

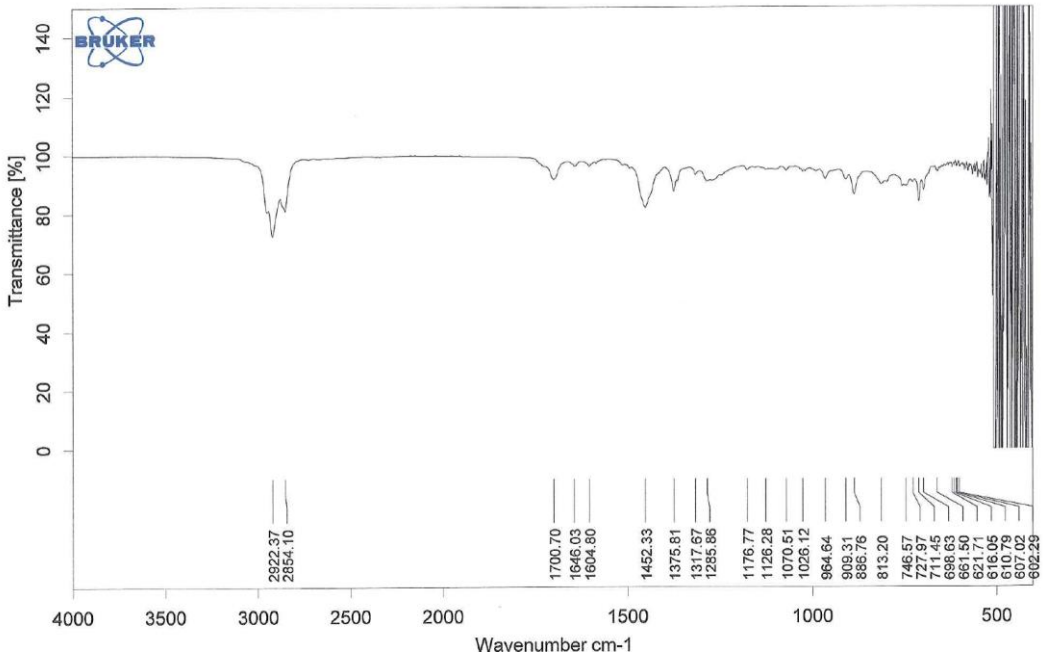

Figure 4.18: FTIR transmittance spectrum of catalysed used tyres pyrolytic oil

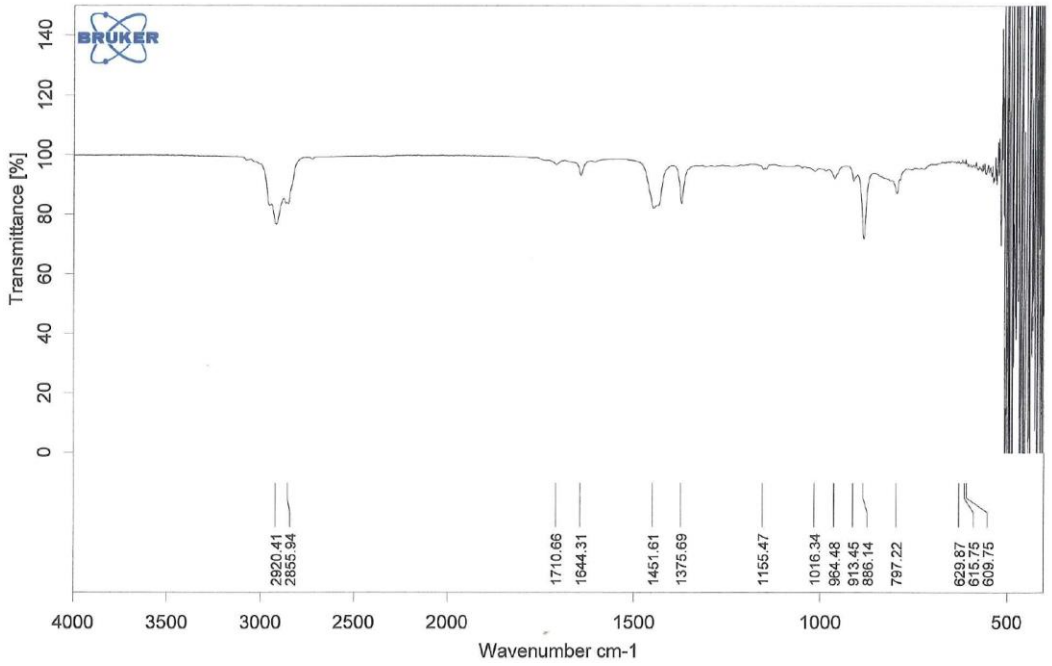

Figure 4.19: FTIR transmittance spectrum for natural rubber pyrolytic oil

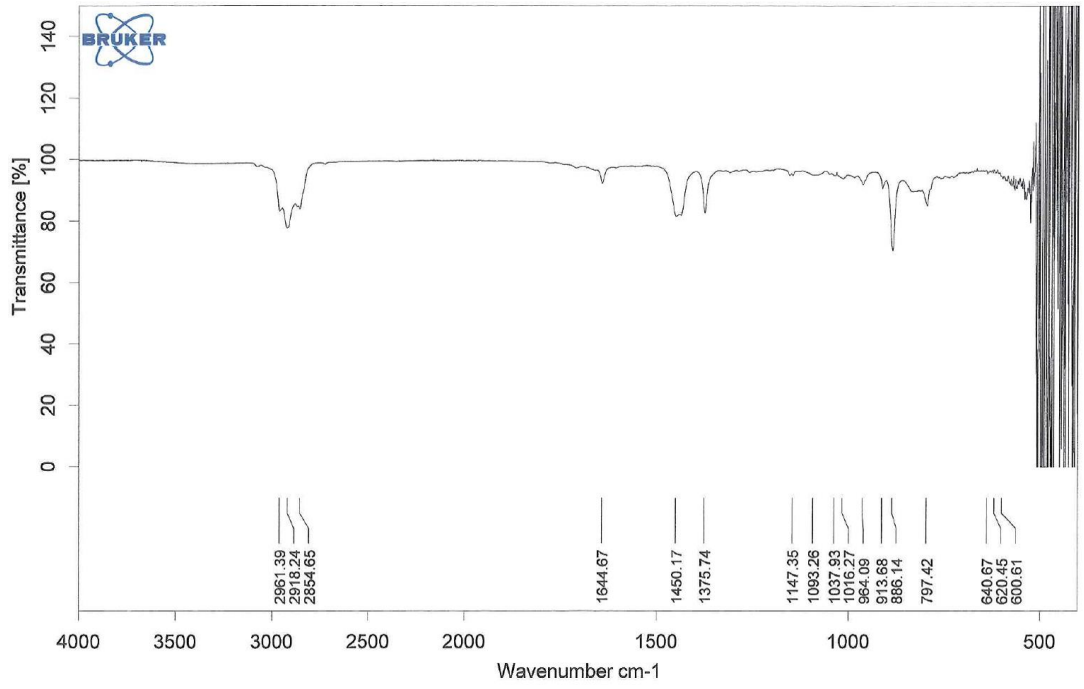

Figure 4.20: FTIR transmittance of catalysed natural rubber pyrolytic oil

Table 4.4: The FTIR functional groups and the indicated compounds of this study pyrolytic oil with other pyrolysis liquids

Wavelength number (cm^{-1})				Functional groups	Class of compounds
This study	Islam et al. [9]	Gonzalez et al. [6]	Williams et al. [16]		
-	-	3600-3250	-	O-H stretching	Alcohols, phenols or carboxylic acids
-	-	3250-3100	-	C-H stretching	Aromatic compounds
-	3100-3005	-	-	C=C stretching	Alkenes
3000-2800	3000-2800	3000-2800	3000-2800	C-H stretching	Alkanes
1750-1700	-	-	1750-1650	C=O	Aldehydes or Ketones
1650-1635	1680-1635	1670-1580	1675-1575	C=C stretching	Alkenes
-	1600-1530	1600-1500	1625-1575	carbon-carbon stretching	Aromatic compounds
1451-1375	1520-1115	1480-1360	1475-1350	C-H bending	Alkanes
1155-1016	-	1150-1000	-	C-H in plane bending	Aromatic compounds
965-795	1030-835	960-870	950-875	C=C stretching	Alkenes
630-609	830-655	900-675	900-675	C-H out-of-plane bending	Aromatic compounds

4.5.2.2 NMR analysis of UT and NR pyrolytic oil

^{1}H NMR and ^{13}C NMR were performed on the pyrolytic oil produced thermally and catalytically from used tyres and natural rubber. Figure 4.21, 4.22, 4.23 and 4.24 illustrate the hydrogen and carbon spectrum obtained from the NMR for natural rubber and used tyres pyrolytic oil with their various protons and carbon content shown in Table 4.5 and 4.6.

Since quantitative proton NMR analysis was used (interpulse delay was greater than $5xT_1$ relaxation). Therefore the area of the NMR signal quantitatively represents the hydrogen in that environment (chemical shift range). The mole percent of hydrogen for each chemical shift range was calculated using equation (4.7)

$$mol\%\ H_2 = \frac{Area\ under\ the\ peaks\ of\ region\ (chemical\ shift)}{Total\ hydrogen\ integration} \times 100 \quad (4.7)$$

Results revealed that the various pyrolytic oil produced is a mixture of aromatics, olefins, paraffins and a small amount of Alcohols (species containing Hydroxyl group). The aliphatic protons not bonded to aromatic constitute more than 50% of the total hydrogen (0.4 – 1.8 ppm chemical shift range), whereas the aliphatic adjacent to aromatic/ alkenes group was more than 20% (3.3 – 1.8 ppm chemical shift range). A higher amount of aromatic hydrogen greater than 7 % (9.0 – 6.5 ppm chemical shift range) was recorded from UT pyrolytic oil than that of natural rubber (which was less than 2.10 %) as shown

in Tables 4.5 and 4.6. This could be attributed to the polymer nature of the natural rubber compound which is mainly poly isoprene (most often cis-1, 4-polyisoprene).

From Table 4.5, the natural rubber pyrolytic oil obtained from thermal pyrolysis gave higher aliphatic carbon content, 84.38 % and low aromatic carbon content, 15.62 % (a source of polycyclic aromatic hydrocarbon, PAHs, which are pollutants) than the pyrolytic oil produced from UT as determined by quantitative ^{13}C NMR analysis (no NOE enhancement for quantitative ^{13}C pulse sequence). The decrease in the aliphatic carbon content from 84.34% to 69.58 % revealed by the catalysed natural pyrolytic oil can be related to the role of hydrocracking performed by the zeolite NaY catalyst during the catalytic pyrolysis of the natural rubber [22]. This confirms that the catalyst helped in cracking the pyrolytic oil hydrocarbon and also favoured the formation of aromatic compounds.

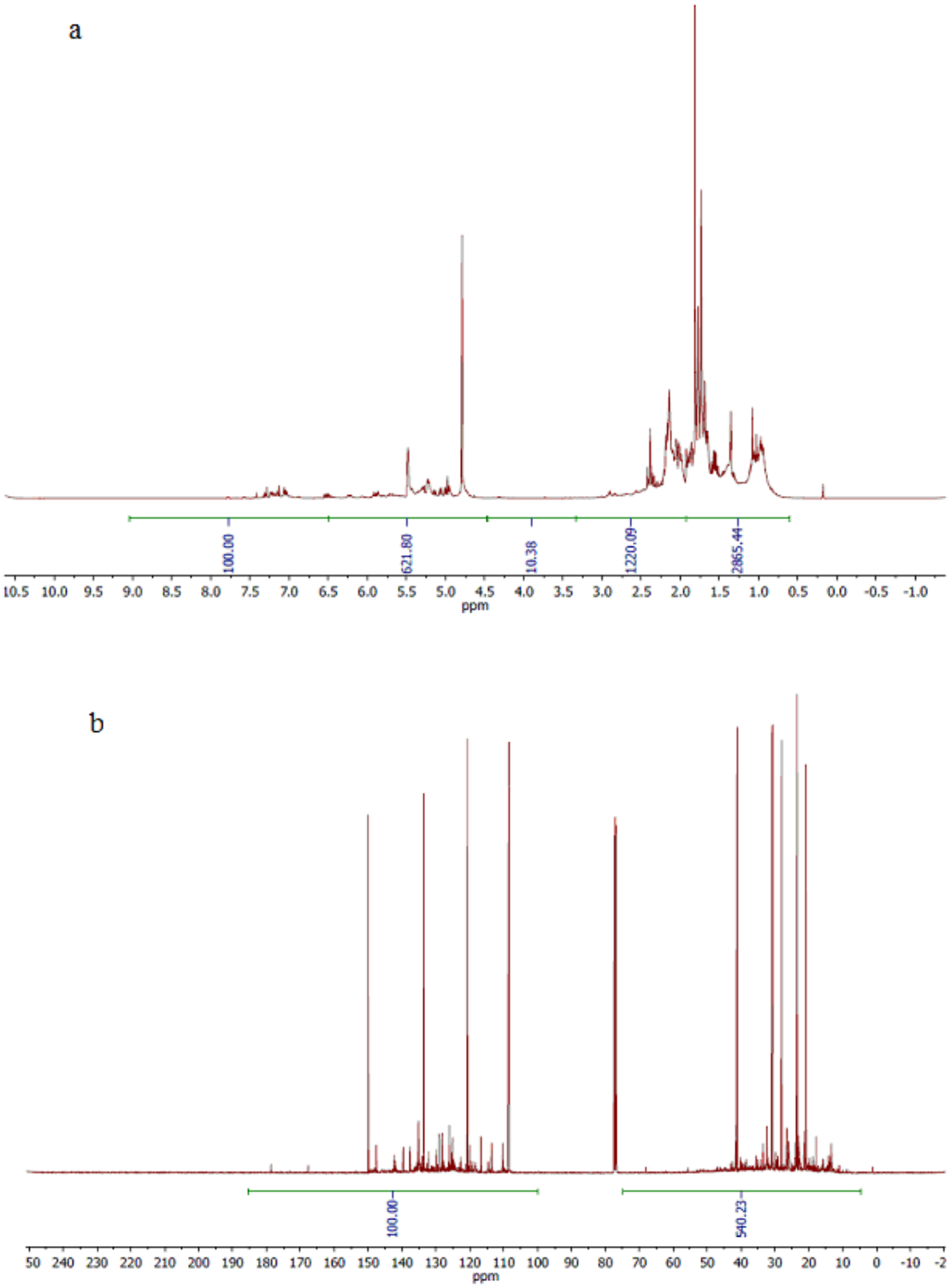

Figure 4.21 (a-b):^{1}H (a) and ^{13}C (b) NMR spectra of NR pyrolytic oil

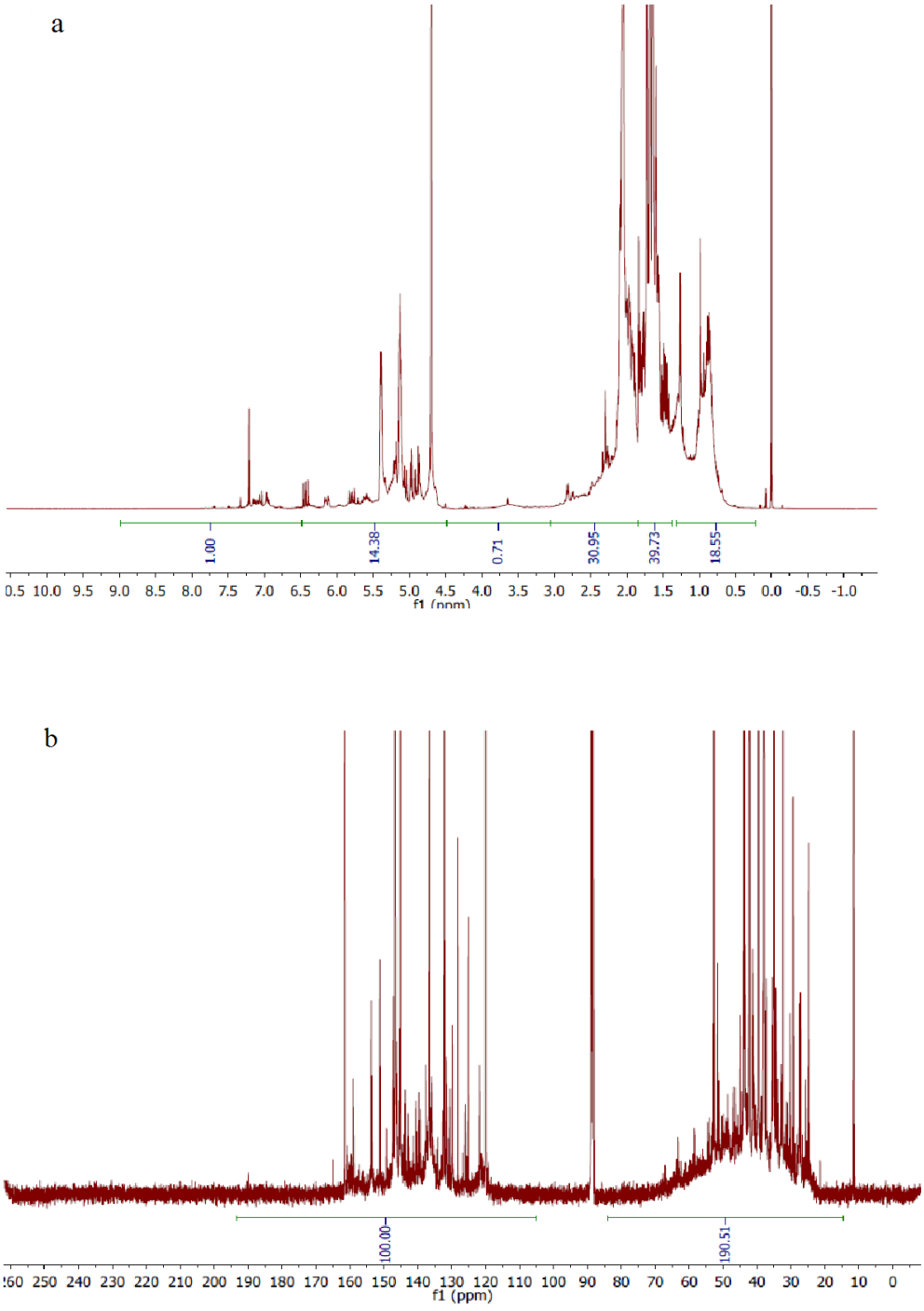

Figure 4.22(a-b):^{1}H (a) and ^{13}C (b) NMR spectra of NRZ pyrolytic oil

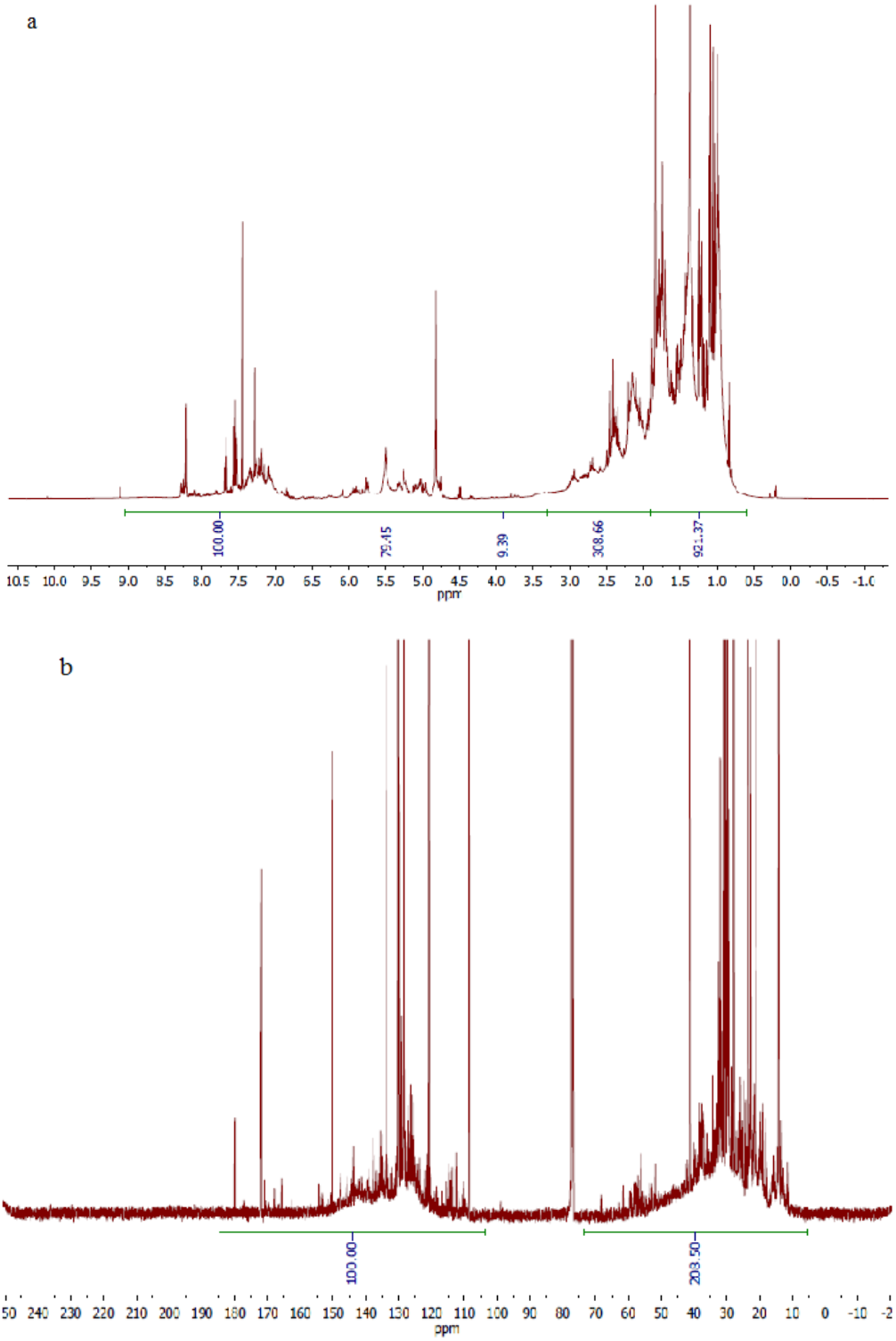

Figure 4.23 (a-b):^{1}H (a) and ^{13}C (b) NMR spectra of UT pyrolytic oil

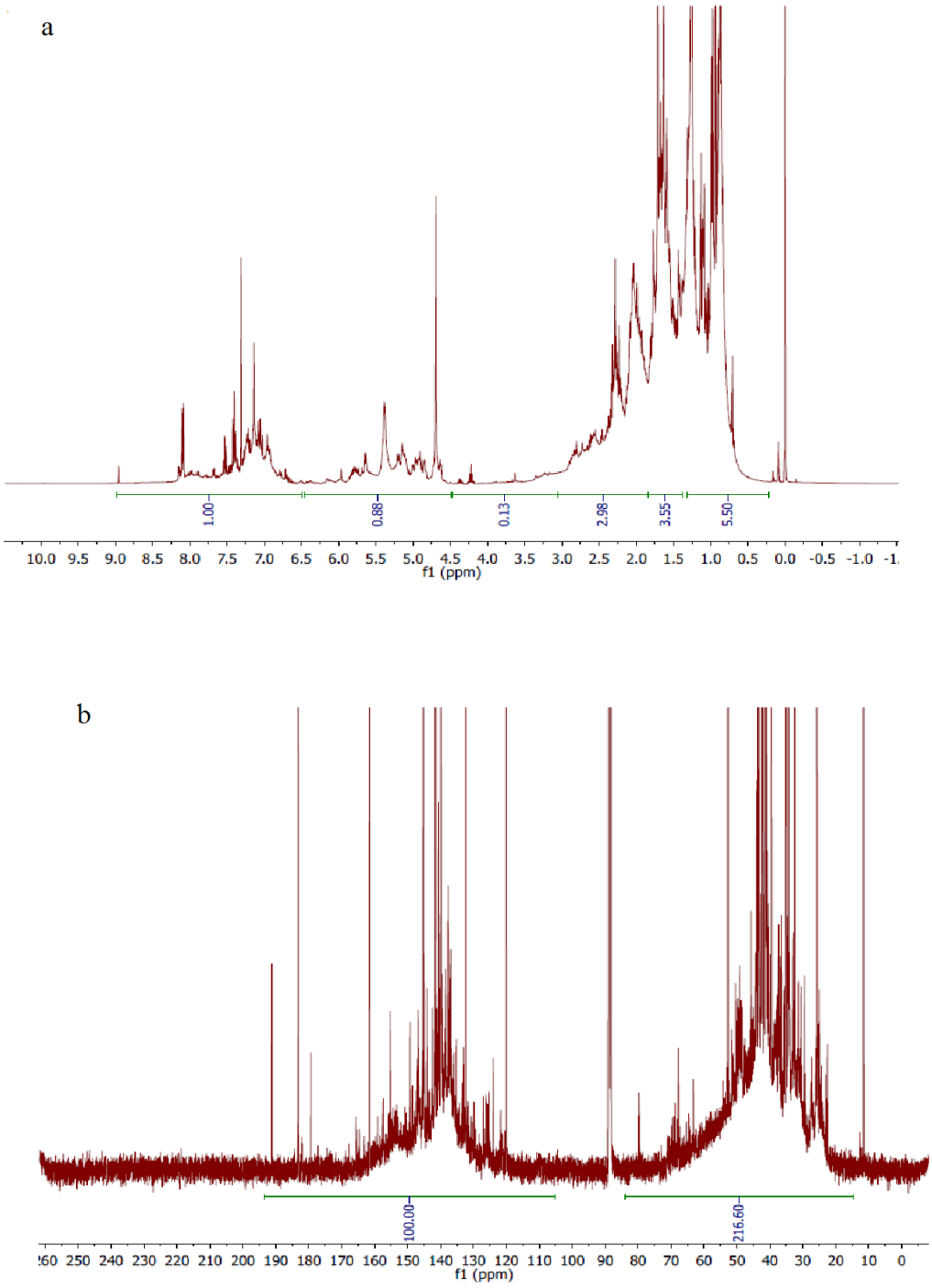

Figure 4.24 (a-b):^{1}H (a) and ^{13}C (b) NMR spectra of UTZ pyrolytic oil

Table 4.5:^{1}H and ^{13}C NMR Results for NR pyrolytic oil and Catalysed NR pyrolytic oil obtained at 600 ^{o}C

NR Pyrolytic oil		
Types of Hydrogen	**Chemical Shift (ppm)**	**Percent of Total Hydrogen (mol %)**
Aromatic	9.0 – 6.5	2.08
Phenolic (OH) or Olefinic portion	6.5 – 4.5	12.91
Aliphatic adjacent to Oxygen/hydroxyl group	4.5 – 3.3	0.22
Aliphatic adjacent to aromatic/alkene group	3.3 – 1.8	25.33
Other aliphatic (bonded to aliphatic only)	1.8 – 0.4	59.48
Types of carbon		
Aliphatics	75.0 – 5.0	84.38
Aromatics	185.0 – 100	15.62
NRZ Pyrolytic oil		
Types of Hydrogen	**Chemical Shift (ppm)**	**Percent of Total Hydrogen (mol %)**
Aromatic	9.0 – 6.5	0.95
Phenolic (OH) or Olefinic portion	6.5 – 4.5	13.65
Aliphatic adjacent to Oxygen/hydroxyl group	4.5 – 3.3	0.67
Aliphatic adjacent to aromatic/alkene group	3.3 – 1.8	29.39
Other aliphatic (bonded to aliphatic only)	1.8 – 0.4	55.34
Types of carbon		
Aliphatics	75.0 – 5.0	65.58
Aromatics	185.0 – 100	34.42

Table 4.6: ^{1}H and ^{13}C NMR Results for UT pyrolytic oil and Catalysed UT Pyrolytic oil obtained at 600 ^{o}C

UT Pyrolytic oil		
Types of Hydrogen	**Chemical Shift (ppm)**	**Percent of Total Hydrogen (mol %)**
Aromatic	9.0 – 6.5	7.0
Phenolic (OH) or Olefinic portion	6.5 – 4.5	5.60
Aliphatic adjacent to Oxygen/hydroxyl group	4.5 – 3.3	0.66
Aliphatic adjacent to aromatic/alkene group	3.3 – 1.8	21.75
Other aliphatic (bonded to aliphatic only)	1.8 – 0.4	64.94
Types of carbon		
Aliphatics	75.0 – 5.0	67.59
Aromatics	185.0 – 100	32.41
UTZ Pyrolytic oil		
Types of Hydrogen	**Chemical Shift (ppm)**	**Percent of Total Hydrogen (mol %)**
Aromatic	9.0 – 6.5	7.12
Phenolic (OH) or Olefinic portion	6.5 – 4.5	6.27
Aliphatic adjacent to Oxygen/hydroxyl group	4.5 – 3.3	0.93
Aliphatic adjacent to aromatic/alkene group	3.3 – 1.8	21.23
Other aliphatic (bonded to aliphatic only)	1.8 – 0.4	64.45
Types of carbon		
Aliphatics	75.0 – 5.0	68.41
Aromatics	185.0 – 100	31.59

4.5.2.3 GC-MS analysis of UT and NR pyrolytic oil

The GC-MS analysis was performed on the catalysed and un-catalysed pyrolytic oil obtained for natural rubber and used tyres in this study with the aim of identifying the nature and type of compounds present in them. The different sample pyrolytic oil derived compounds chromatogram peaks shown in Figure 4.25 to 4.28 were analysed with NIST search software, with over 400 compounds identified. Considering the area % of compounds identified by the GC-MS, compounds with a match peaks ≥ 75% and an area percent ≥0.1 were reported. Table D1, D2, D3 and D4 presented in Appendix D show the identified compounds and their chromatogram area percent which is an indication of their concentration in the pyrolytic oil. A few of these compounds are shown in Table 4.7 (a and b) and 4.8 (a and b). The compounds identified in this study are in accordance with that published in literature [11, 22-23].

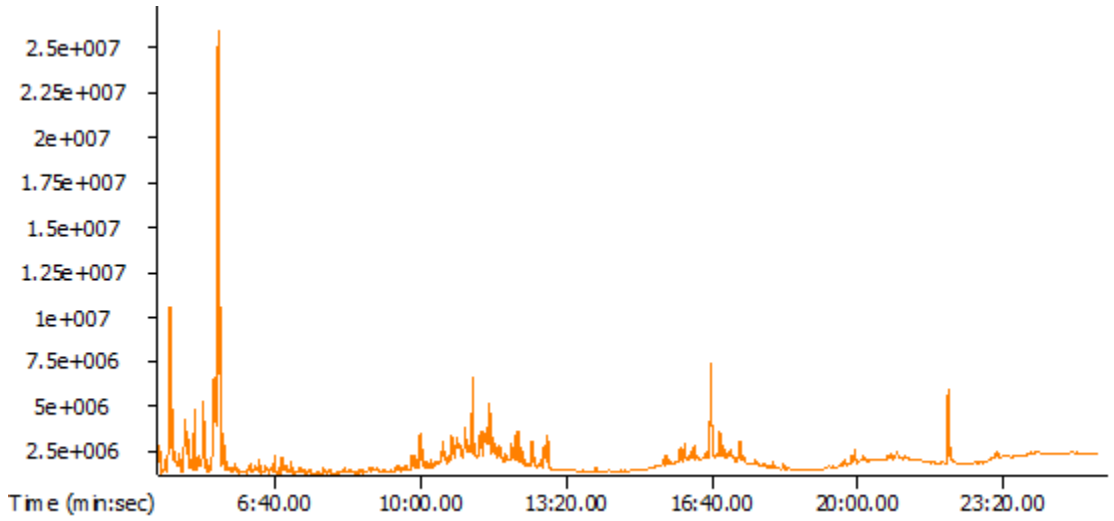

Figure 4.25: GC-MS Total compound chromatogram for NR pyrolytic oil obtained at 600^{o}C

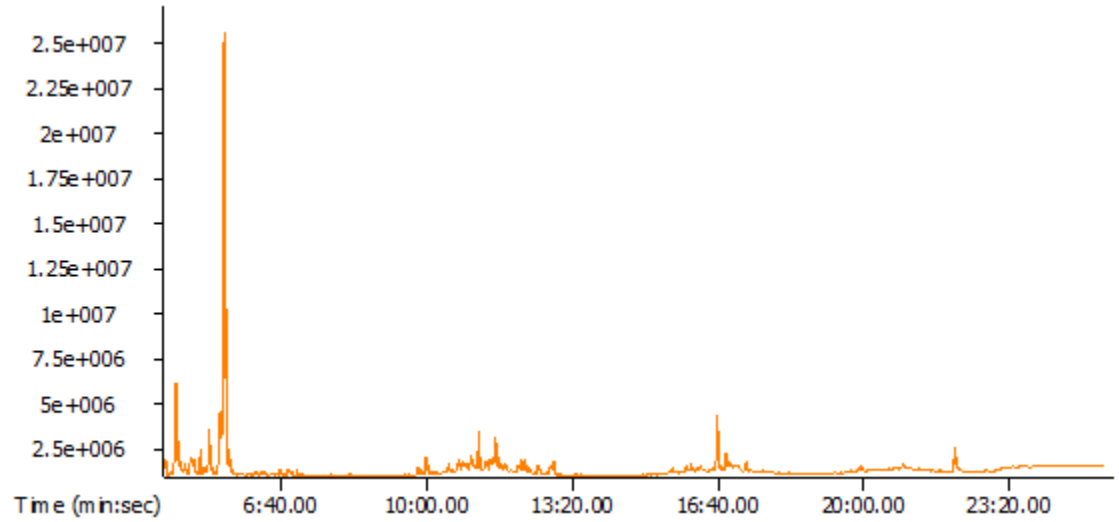

Figure 4.26: GC-MS Total compound chromatogram of NRZ pyrolytic oil obtained at 600^{o}C

Table 4.7(a): Some of the compounds identified by GC-MS characterisation of NR pyrolytic oil

Peak #	Name	R.T. (min:sec)	Area %	Formula
1	1,3,6-Heptatriene, 2,5,5-trimethyl-	04:01.5	0.4426	$C_{10}H_{16}$
27	2,6-Dimethyl-1,3,6-heptatriene	05:01.5	0.98112	C_9H_{14}
52	1-Penten-3-yne, 2-methyl-	07:01.4	0.20269	C_6H_8
28	1,3-Cyclopentadiene, 5,5-dimethyl-2-propyl-	05:04.9	0.3613	$C_{10}H_{16}$
71	1,7-Octadiene, 2,7-dimethyl-3,6-bis(methylene)-	10:00.2	0.12479	$C_{12}H_{18}$
29	2,6-Dimethyl-1,3,5,7-octatetraene, E,E-	05:05.5	0.15227	$C_{10}H_{14}$
43	1,3,5-Cycloheptatriene, 3,7,7-trimethyl-	06:06.1	0.30222	$C_{10}H_{14}$
89	Furan, 3-(4,8-dimethyl-3,7-nonadienyl)-, (E)-	11:01.1	1.0142	$C_{15}H_{22}O$
2	2-Cyclohexen-1-ol, 4-ethyl-1,4-dimethyl-	04:10.5	0.84296	$C_{10}H_{18}O$
113	cis-à-Bisabolene	12:03.8	0.10683	$C_{15}H_{24}$
90	(3S,6R)-3-Hydroperoxy-3-methyl-6-(prop-1-en-2-yl)cyclohex-1-ene	11:06.3	0.45876	$C_{10}H_{16}O_2$
91	Naphthalene, 1,7-dimethyl-	11:07.0	0.13136	$C_{12}H_{12}$
131	Squalene	16:02.5	0.87178	$C_{30}H_{50}$
31	Benzene, 1-ethyl-2-methyl-	05:14.6	0.56069	C_9H_{12}
3	Cyclohexene, 1-methyl-4-(1-methylethenyl)-, (S)-	04:16.2	8.207	$C_{10}H_{16}$
32	Cyclohexene, 3-methyl-6-(1-methylethyl)-	05:16.0	0.31605	$C_{10}H_{18}$
33	(1S)-2,6,6-Trimethylbicyclo[3.1.1]hept-2-ene	05:16.6	1.5327	$C_{10}H_{16}$
92	(3E,7E)-4,8,12-Trimethyltrideca-1,3,7,11-tetraene	11:10.7	1.5109	$C_{16}H_{26}$
93	ç-Elemene	11:11.0	0.17198	$C_{15}H_{24}$
4	Benzene, 1-ethyl-2-methyl-	04:18.4	0.33184	C_9H_{12}
46	Benzene, 1-methyl-4-(1-methylethenyl)-	06:17.5	0.29391	$C_{10}H_{12}$
7	Benzene, 1,2,3-trimethyl-	04:21.2	0.26541	C_9H_{12}
117	Cyclohexane, 1-ethenyl-1-methyl-2,4-bis(1-methylethenyl)-	12:13.8	0.32085	$C_{15}H_{24}$
118	anti-10-Methyl-endo-tricyclo[5.2.1.0(2.6)]decane	12:14.3	0.76028	$C_{11}H_{18}$
145	Diisooctyl phthalate	22:04.4	6.7325	$C_{24}H_{38}O_4$
8	1,3-Dimethyl-1-cyclohexene	04:23.2	0.243	C_8H_{14}
34	Limonene	05:22.9	42.609	$C_{10}H_{16}$
36	Benzene, 1,2,3-trimethyl-	05:24.9	0.15205	C_9H_{12}
9	Benzene, 1,2,3-trimethyl-	04:26.0	0.18654	C_9H_{12}

Table 4.7(b): Some of the compounds identified by GC-MS characterisation of NRZ pyrolytic oil

Peak #	Name	R.T. (min:sec)	Area %	Formula
1	1,3,6-Heptatriene, 2,5,5-trimethyl-	04:01.6	0.30856	$C_{10}H_{16}$
20	2,6-Dimethyl-1,3,6-heptatriene	05:01.5	0.87031	C_9H_{14}
34	2,4,6-Octatriene, 2,6-dimethyl-, (E,Z)-	07:01.5	0.21984	$C_{10}H_{16}$
37	1,7-Octadiene, 2,7-dimethyl-3,6-bis(methylene)-	10:00.1	0.79883	$C_{12}H_{18}$
21	2,6-Dimethyl-1,3,5,7-octatetraene, E,E-	05:05.4	0.11845	$C_{10}H_{14}$
44	(3E,7E)-4,8,12-Trimethyltrideca-1,3,7,11-tetraene	11:00.9	0.85701	$C_{16}H_{26}$
2	2-Cyclohexen-1-ol, 4-ethyl-1,4-dimethyl-	04:10.5	0.21119	$C_{10}H_{18}O$
61	anti-10-Methyl-endo-tricyclo[5.2.1.0(2.6)]decane	12:05.4	0.33091	$C_{11}H_{18}$
73	trans-Farnesol	16:02.5	0.74242	$C_{15}H_{26}O$
22	Mesitylene	05:14.6	0.306	C_9H_{12}
3	Cyclohexene, 1-methyl-4-(1-methylethenyl)-, (S)-	04:16.1	6.5379	$C_{10}H_{16}$
23	Cyclohexene, 3-methyl-6-(1-methylethyl)-	05:15.9	0.29224	$C_{10}H_{18}$
63	Bicyclo[3.1.1]heptane, 6,6-dimethyl-3-methylene-	12:08.9	0.32341	$C_{10}H_{16}$
24	(1S)-2,6,6-Trimethylbicyclo[3.1.1]hept-2-ene	05:16.5	0.33779	$C_{10}H_{16}$
79	4,8,12-Tetradecatrien-1-ol, 5,9,13-trimethyl-	17:04.6	0.23275	$C_{17}H_{30}O$
46	Cyclohexane, 1-ethenyl-1-methyl-2,4-bis(1-methylethenyl)-	11:10.6	1.3417	$C_{15}H_{24}$
4	Benzene, 1,2,3-trimethyl-	04:18.4	0.14847	C_9H_{12}
30	Benzene, 1-methyl-4-(1-methylethenyl)-	06:17.3	0.12066	$C_{10}H_{12}$
6	Benzene, 1,4-diethyl-	04:21.2	0.22763	$C_{10}H_{14}$
64	Cyclohexene, 1-methyl-4-(1-methylethenyl)-, (S)-	12:13.9	0.19425	$C_{10}H_{16}$
65	5-Hepten-1-ol, 2-ethenyl-6-methyl-	12:14.2	0.45075	$C_{10}H_{18}O$
85	Diisooctyl phthalate	22:04.2	3.893	$C_{24}H_{38}O_4$
7	trans,cis-1,7-Dimethylspiro[4.5]decane	04:23.3	0.15007	$C_{12}H_{22}$
25	Limonene	05:22.7	66.274	$C_{10}H_{16}$
47	2,6,9,11-Dodecatetraenal, 2,6,10-trimethyl-, (E,E,E)-	11:19.9	0.13224	$C_{15}H_{22}O$
48	1,5-Heptadiene, 2,6-dimethyl-	11:20.3	0.4911	C_9H_{16}
9	Bicyclo[2.2.1]heptane, 2,2-dimethyl-3-methylene-, (1R)-	04:27.4	0.28681	$C_{10}H_{16}$
74	1,3-Bis-(2-cyclopropyl,2-methylcyclopropyl)-but-2-en-1-one	16:16.2	0.28873	$C_{18}H_{26}O$
49	1-Cyclohexyl-1-pentyne	11:21.8	0.11196	$C_{11}H_{18}$
10	3,4-Octadiene	04:29.8	0.1834	C_8H_{14}
27	Cyclohexene, 4-methyl-1-(1-methylethenyl)-	05:29.4	0.12879	$C1_0H_{16}$
11	trans-3-Caren-2-ol	04:35.2	0.26577	$C_{10}H_{16}O$
51	(3E,7E)-4,8,12-Trimethyltrideca-1,3,7,11-tetraene	11:28.7	0.64462	$C_{16}H_{26}$
82	(1,2,3-Trimethyl-cyclopent-2-enyl)-methanol	17:23.2	0.16199	$C_9H_{16}O$
12	2,6-Octadiene, 2,6-dimethyl-	04:36.5	1.4042	$C_{10}H_{18}$

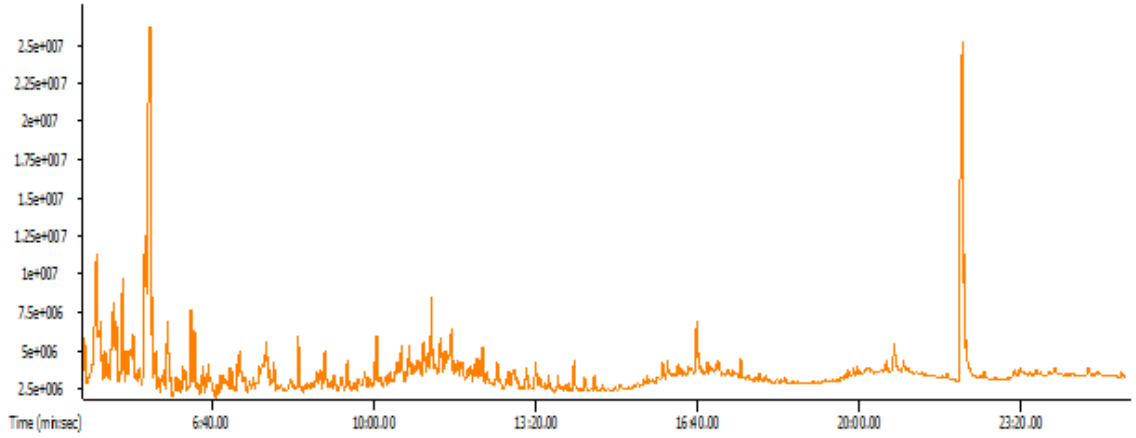

Figure 4.27: GC-MS Total compound chromatogram for UT pyrolytic oil obtained at 600^{o}C

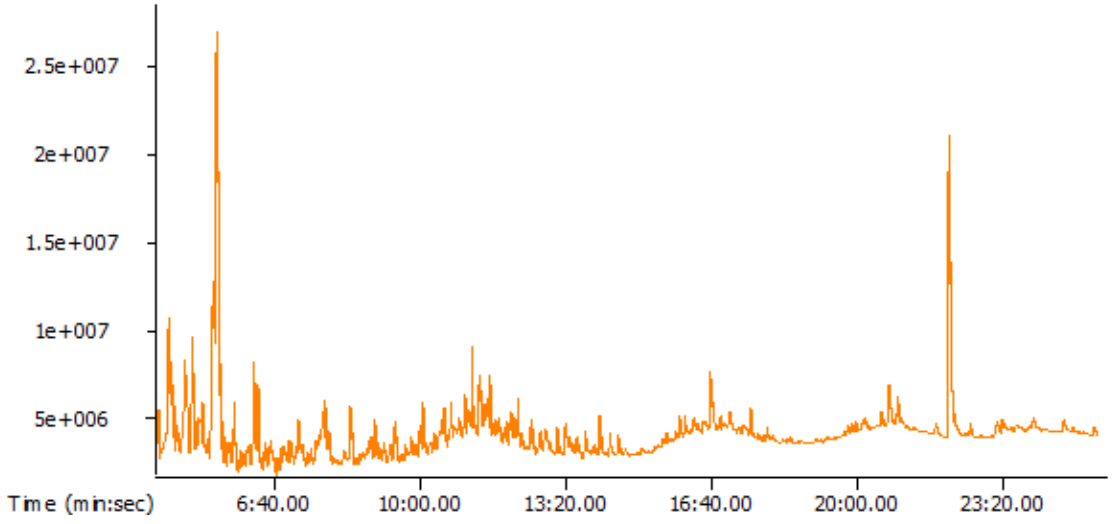

Figure 4.28: GC-MS Total compound chromatogram for UTZ pyrolytic oil obtained at 600^{o}C

Table 4.8(a): Some of the identified compounds by GC-MS characterisation of UT pyrolytic oil

Peak #	Name	R.T. (min:sec)	Area %	Formula
1	1,3,6-Heptatriene, 2,5,5-trimethyl-	04:01.9	0.27622	$C_{10}H_{16}$
2	Camphene	04:02.8	0.1468	$C_{10}H_{16}$
46	2-Methyl-1-nonene-3-yne	05:01.9	0.36244	$C_{10}H_{16}$
115	2,4,6-Octatriene, 2,6-dimethyl-, (E,Z)-	07:01.9	0.25266	$C_{10}H_{16}$
80	p-Cresol	06:03.2	0.3688	C_7H_8O
170	4-Isopropyl-1-phenyl-hexa-1,5-dien-3-ol	09:00.4	0.10126	$C_{15}H_{20}O$
5	1,1,3,3,5-Pentamethylcyclohexane	04:06.2	0.23291	$C_{11}H_{22}$
205	Isomyocorene	10:07.7	0.17025	$C_{10}H_{16}$
118	1,2,3,4,5,8-Hexahydronaphthalene	07:11.0	0.11379	$C_{10}H_{14}$
85	Benzene, 2-ethyl-1,3-dimethyl-	06:12.2	0.32995	$C_{10}H_{14}$
119	Phenol, 2,3-dimethyl-	07:11.4	0.2892	$C_8H_{10}O$
338	Squalene	16:02.8	0.36331	$C_{30}H_{50}$
86	Cyclohexene, 1-methyl-4-(1-methylethylidene)-	06:13.4	0.39596	$C_{10}H_{16}$
51	Benzene, 1,2,3-trimethyl-	05:14.9	1.6238	C_9H_{12}
176	1H-Indene, 2,3-dihydro-4,7-dimethyl-	09:11.0	0.26573	$C_{11}H_{14}$
12	Cyclohexene, 1-methyl-4-(1-methylethenyl)-, (S)-	04:16.5	2.5857	$C_{10}H_{16}$
88	o-Isopropenyltoluene	06:14.6	0.46476	$C_{10}H_{12}$
324	Sulfurous acid, butyl cyclohexylmethyl ester	14:06.9	0.90262	$C_{11}H_{22}O_3S$
277	1,3,6,10-Dodecatetraene, 3,7,11-trimethyl-, (Z,E)-	12:09.0	0.21258	$C_{15}H_{24}$
121	Naphthalene, 1,2-dihydro-	07:14.3	0.33148	$C_{10}H_{10}$
13	Cyclohexene, 1-methyl-4-(1-methylethenyl)-, (S)-	04:17.3	0.59849	$C_{10}H_{16}$
52	Cyclohexene, 3-methyl-6-(1-methylethyl)-	05:16.4	0.24432	$C_{10}H_{18}$
304	Sulfurous acid, cyclohexylmethyl hexyl ester	13:08.6	0.50938	$C_{13}H_{26}O_3S$
122	5H-5-Methyl-6,7-dihydrocyclopentapyrazine	07:15.0	0.12562	$C_8H_{10}N_2$
53	o-Cymene	05:17.3	3.7413	$C_{10}H_{14}$
14	Benzene, 1-ethyl-2-methyl-	04:18.8	0.33273	C_9H_{12}
91	Benzene, 1-methyl-4-(1-methylethenyl)-	06:17.8	0.56752	$C_{10}H_{12}$
54	2-Decene, 5-methyl-, (Z)-	05:19.3	0.91225	$C_{11}H_{22}$
55	Limonene	05:19.8	1.3456	$C_{10}H_{16}$
124	Benzene, pentyl-	07:18.4	0.22583	$C_{11}H_{16}$
149	Benzene, 1-methyl-3-(1-methyl-2-propenyl)-	08:17.5	0.13419	$C_{11}H_{14}$
378	Heptacosane	24:01.8	0.14024	$C_{27}H_{56}$
57	Limonene	05:23.5	14.275	$C_{10}H_{16}$
180	Benzene, 4-(2-butenyl)-1,2-dimethyl-, (E)-	09:19.9	0.14735	$C_{12}H_{16}$
366	Diisooctyl phthalate	22:07.2	6.6322	$C_{24}H_{38}O_4$

Table 4.8(b): Some of the identified compounds by GC-MS characterisation of UTZ pyrolytic oil

Peak #	Name	R.T. (min:sec)	Area %	Formula
1	1,3,6-Heptatriene, 2,5,5-trimethyl-	04:02.1	0.24514	$C_{10}H_{16}$
2	2-Methyl-1-nonene-3-yne	04:03.0	0.11745	$C_{10}H_{16}$
109	2,4,6-Octatriene, 2,6-dimethyl-, (E,Z)-	07:01.9	0.25173	$C_{10}H_{16}$
79	Benzyl alcohol	06:03.2	0.18381	C_7H_8O
162	4-Isopropyl-1-phenyl-hexa-1,5-dien-3-ol	09:00.4	0.10059	$C_{15}H_{20}O$
163	1H-Indene, 2,3-dimethyl-	09:00.9	0.10958	$C_{11}H_{12}$
187	Tricyclo[3.3.0.0(2,8)]octan-3-one, 4-methyl-4-(2-methyl-2-propenyl)-	10:00.4	0.11512	$C_{13}H_{18}O$
110	3,4-Dimethylcumene	07:04.6	0.10434	$C_{11}H_{16}$
188	3-Penten-1-ol, 2,2,4-trimethyl-	10:03.7	1.1644	$C_8H_{16}O$
48	1,3-Cyclohexadiene, 1-methyl-4-(1-methylethyl)-	05:09.5	0.34969	$C_{10}H_{16}$
330	Squalene	16:02.9	0.39697	$C_{30}H_{50}$
84	ç-Terpinene	06:13.4	0.44049	$C_{10}H_{16}$
51	Benzene, 1-ethyl-2-methyl-	05:14.9	1.4766	C_9H_{12}
167	1H-Indene, 2,3-dihydro-4,7-dimethyl-	09:11.0	0.27705	$C_{11}H_{14}$
344	Dibutyl phthalate	17:03.2	0.22591	$C_{16}H_{22}O_4$
114	1H-Indene, 2,3-dihydro-4-methyl-	07:13.3	0.74024	$C_{10}H_{12}$
10	Cyclohexene, 1-methyl-4-(1-methylethenyl)-, (S)-	04:16.6	2.4334	$C_{10}H_{16}$
86	Indan, 1-methyl-	06:14.7	0.45638	$C_{10}H_{12}$
307	Sulfurous acid, butyl cyclohexylmethyl ester	14:07.1	1.0533	$C_{11}H_{22}O_3S$
116	5H-5-Methyl-6,7-dihydrocyclopentapyrazine	07:15.1	0.11195	$C_8H_{10}N_2$
225	4,8,12-Tetradecatrien-1-ol, 5,9,13-trimethyl-	11:11.1	0.78057	$C_{17}H_{30}O$
53	o-Cymene	05:17.3	3.6405	$C_{10}H_{14}$
12	Benzene, 1-ethyl-2-methyl-	04:18.9	0.32468	C_9H_{12}
346	Cyclohexane, 1-bromo-4-methyl-	17:06.0	0.13808	$C_7H_{13}Br$
88	Benzene, 1-methyl-4-(1-methylethenyl)-	06:17.8	0.64512	$C_{10}H_{12}$
55	D-Limonene	05:19.9	0.87397	$C_{10}H_{16}$
118	Benzene, pentyl-	07:18.4	0.23006	$C_{11}H_{16}$
142	1H-Indene, 2,3-dihydro-1,1-dimethyl-	08:17.5	0.14803	$C_{11}H_{14}$
15	Benzene, 1-ethyl-3-methyl-	04:21.5	0.5109	C_9H_{12}
367	Diisooctyl phthalate	22:06.2	3.888	$C_{24}H_{38}O_4$
56	Limonene	05:23.3	14.059	$C_{10}H_{16}$
359	trans-Geranylgeraniol	20:08.7	0.13648	$C_{20}H_{34}O$

From the data in Table D1 to D4 in Appendix D, it can be observed that pyrolytic oil obtained from the thermal and catalytic pyrolysis of used tyres and natural rubber are complex mixtures dominated by different aliphatic and aromatic compounds. Examples of such compounds are alkanes, alkenes, alkynes, single ring benzene and its derivatives, naphthalene, oxygenated compounds, nitrogen containing compounds and sulphur compounds like thiophene, and quinoline. These GC-MS results conform well to the FTIR [Table 4.4] and ^{1}H NMR [Table 4.5 and 4.6] analyses results. The non-catalysed and catalysed natural rubber pyrolytic oil gave 79.87 and 65.76 % concentrations of aliphatic, 12.45 and 14.84 % aromatic concentrations and PAHs concentration of 1.98 and 0.79 % while the non-catalysed and catalysed used tyres pyrolytic oil had 42.20 and 32.09 % concentrations of aliphatic, 34.49 and 38.80 % aromatic concentrations and PAHs concentrations of 17.84 and 22.82 %, rescpectively.

Similar to other studies [34, 38-39], other compound species were also present in the obtained pyrolytic oil but in low proportions. The high aromatic and PAHs recorded in both used tyres pyrolytic oil could be attributed to the nature of rubber component used in the manufacture of the sample used tyre that was pyrolysed. A typical example is polystyrene butadiene (SBR) which could be additional benzene ring source and the dehydrogenation reaction that leads to cyclization of olefin structures during pyrolysis process [38]. This is because rubber samples containing high amount of aromatics will yield liquids with high aromatic content under the same condition [6, 18, 29]. Kyari et al. [39] in their investigation have reported that different types and brands of tyres will yield different concentrations of a benzene ring and PAHs in their products oil. Similarly, high

aromatic content for pyrolysed used tyres oil in a fixed bed reactor was also reported by Rodriquez et al. [38]. Their study revealed that the pyrolysed oil obtained at 500 ^{o}C had 62.4 wt. % of aromatic compounds, 31.6 wt. % aliphatic compounds, 4.2 wt. % nitrogen-containing compounds, and 1.8 wt. % sulphur-containing compounds. Rofiqul et al. [34] also reported used tyres pyrolysis liquid fraction as a complex mixture composed of 49.54 % aliphatic and 16.65 % aromatic hydrocarbons.

In this study, Limonene identified in the GC-MS analysis, is one of the most important compounds [6, 23, 38-42] which could increase the market value of the pyrolytic oil. The amount of Limonene obtained from the pyrolysis of natural rubber is greater than that reported by other researchers for used tyres pyrolysis [17, 34].

From the FTIR, NMR and GC-MS analyses, the pyrolytic oil produced from the thermal and catalytic pyrolysis of used tyres and natural rubber at 600 ^{o}C at a heating rate of 15^{o}C/min can be concluded to be a very complex mixture of organic compounds of aliphatic (C_5 – C_{30} majority being C_8-C_{10}), aromatics, PAHs and a small fraction of oxygen, nitrogen and sulphur containing compounds. Pyrolytic oil from natural rubber due to the absence of sulphur, its relatively low amount of aromatic and PAHs could be less source of pollution when combusted directly as liquid fuel than pyrolytic oil from used tyres.

4.6 Batch Distillation of UT and NR Pyrolytic Oil

Table 4.9 shows the total fractional volume percent of distillates obtained from the thermal and catalytic pyrolysis NR and UT pyrolytic oil at different ranges of temperature during distillation. As stated above in Section 3.6.2, a total volume of 120 ml of the various produced pyrolytic oil was distilled in batches. For the NR pyrolytic oil, a total fractional volume percent of 41.31% was obtained over the distillation temperature range of 60 to 175 ^{o}C while the remaining 58.69 % formed part of the pyrolytic oil lost to evaporation and the heavy residue in the round bottom flask. Similarly, batch distillation of the catalysed NR pyrolytic oil gave a fractional yield of 50 %, which was 9 % more than that obtained from the thermal pyrolysed NR pyrolytic oil but within close temperature range of 50 to 175 ^{o}C.

The distillates of the NR pyrolytic oil and NRZ pyrolytic oil can be categorised to be more of light naphtha and middle distillates with no heavy fuel, wax or solid gel produced. For the distillation of the UT and UTZ pyrolytic oil, a temperature range of 30 to 208 ^{o}C and 30 to 251 ^{o}C respectively was recorded. This could be attributed to the different rubber components and other compounds used in the tyre formulation. The high distillation temperature range observed for the UTZ pyrolytic oil could be linked to the cracking of the pyrolytic oil by the zeolite NaY to give high boiling point compounds.

The fractional volume percent of distillates made up of liquids and wax gel obtained for the UT and UTZ pyrolytic oil was 62.97 and 71.38 % respectively. The volume % of the light naphtha was less than 34 % for the UT pyrolytic oil with 48.9 % heavy fuel oil and 17.10 % solid gel. That of the UTZ pyrolytic oil had 36.26 % of light naphtha and 63.74 % of heavy fuel oil. This is also in accordance with the report by Laresgoiti et al. [43] that car tyre-derived pyrolytic oil had light naphtha, heavy naphtha and middle distillates of 20, 10 and 35 %, respectively. Ucar et al. [44] also found 40, 15 and 45 % as the respective values in their truck tyre-derived pyrolytic liquids. The higher amount of heavy fuel oil distillates could be responsible for the wide application of UT pyrolytic oil as diesel fuels and heating oil. Figure 4.29 shows the different distillates.

The GC-MS was also used to determine the compounds present in the various pyrolytic oil distillates. Figure 4.31 to 4.34 and Tables D5 to D8 shows the GC-MS total chromatogram and the compounds identified by NIST library with a similarity peak match of ≥ 75 % and an area percent ≥0.1 were regarded as valid and reported. These identified compounds are presented in Table D5 to D8 in Appendix D. They are similar to the compounds identified in the pyrolytic oil but at different proportions. The main hydrocarbon group present, aliphatic, aromatic and PAHs with their different proportions are shown in Figure 4.30.

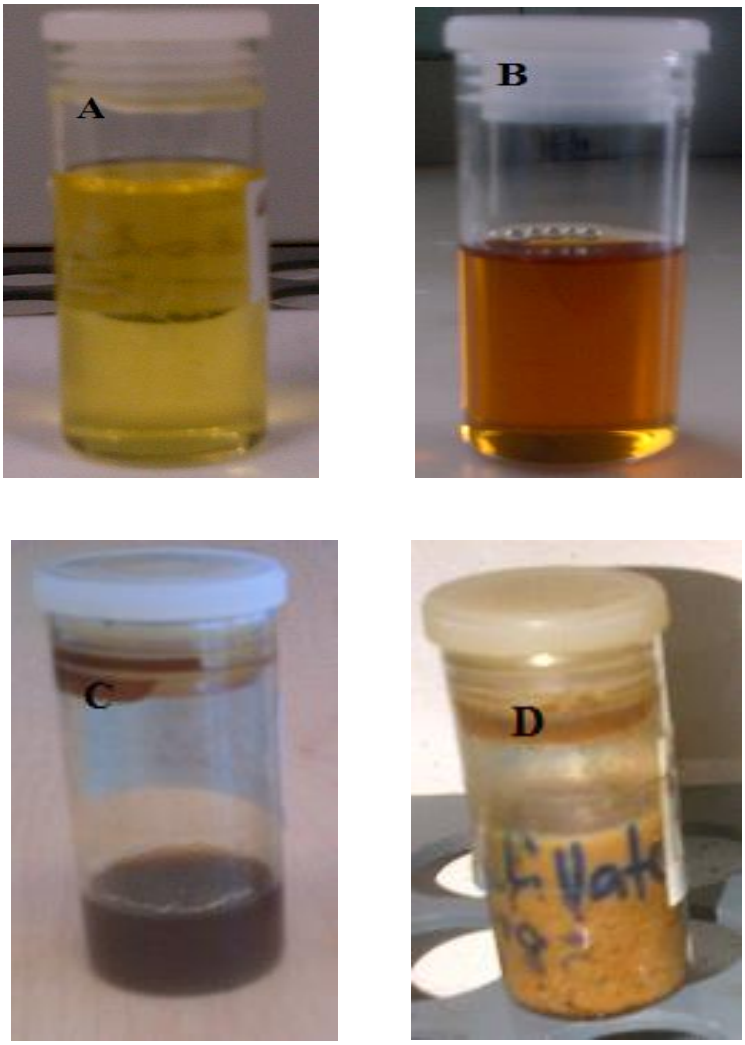

Figure 4.29: Different distillates obtained from distillation of NR and UT pyrolytic oil (A= clear fraction/light naphtha, B = middle distillate, C= heavy naphtha/fuel oil and D= wax/solid gel)

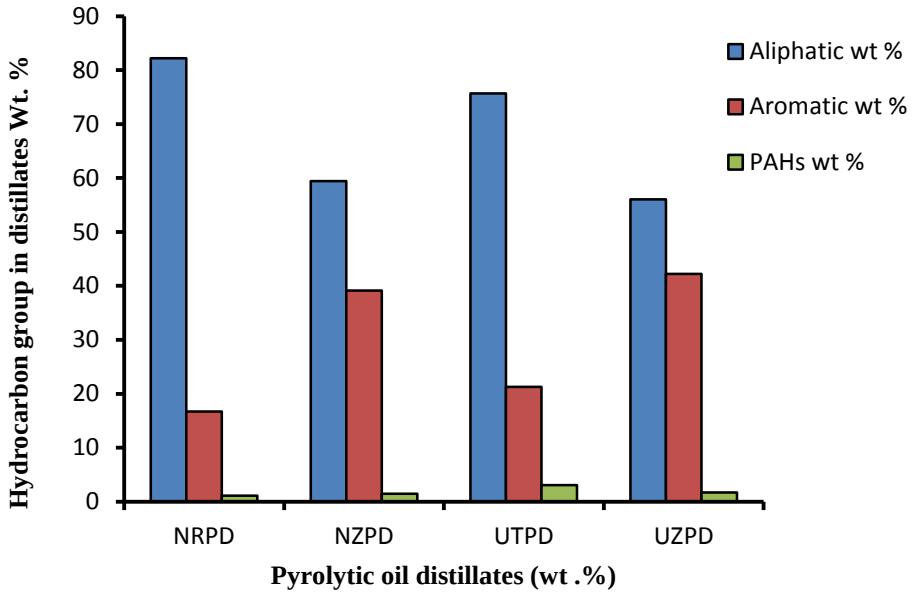

Figure 4.30: Hydrocarbon groups present in distillate obtained from various pyrolytic oil

From Figure 4.30, the percentage in which the different hydrocarbon groups are present in the distillates revealed that NRPD had a higher concentration of aliphatics and lower values for aromatics and PAHs than all the other distillates. This is not unexpected because the NMR analysis results shown in Table 4.9 and Table 4.10 also confirm this.

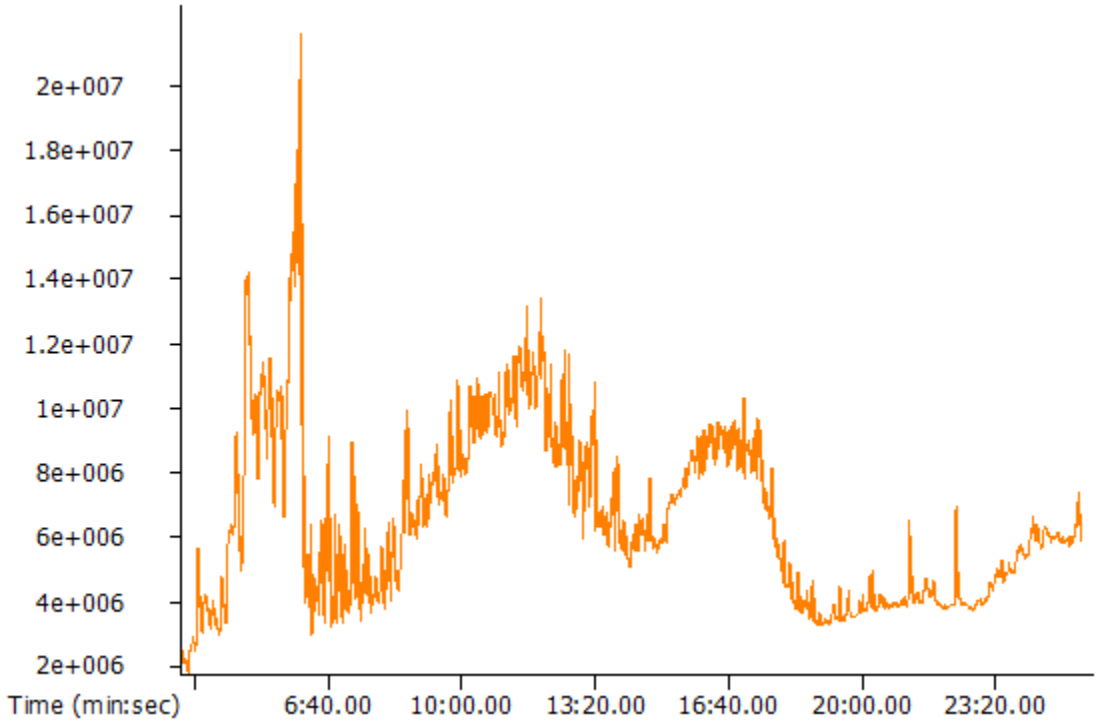

Figure 4.31: GC-MS total compound chromatogram for NR pyrolytic oil distillates

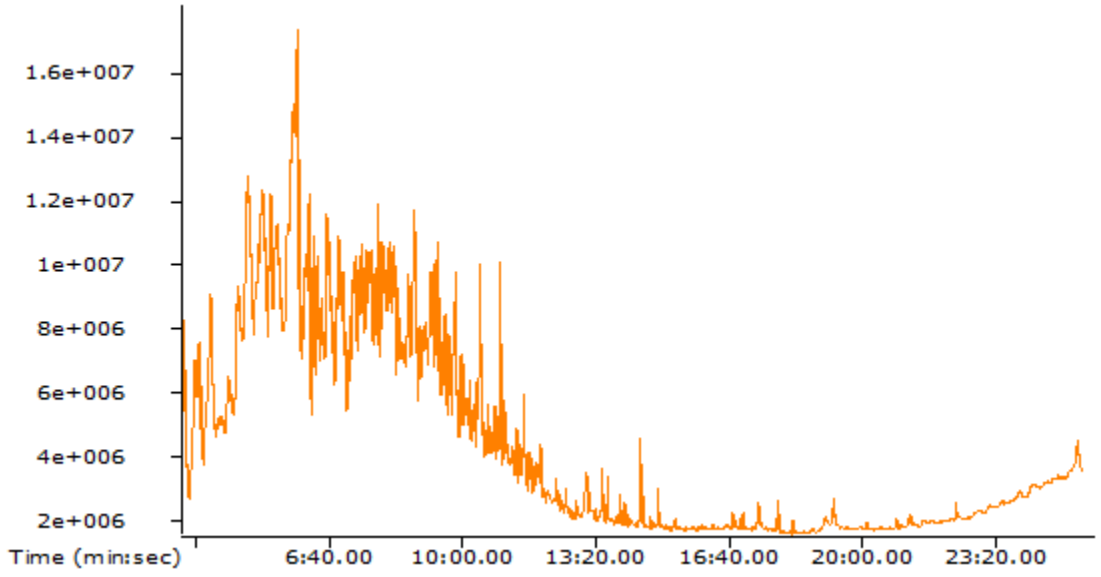

Figure 4.32: GC-MS total compound chromatogram for NRZ pyrolytic oil distillates

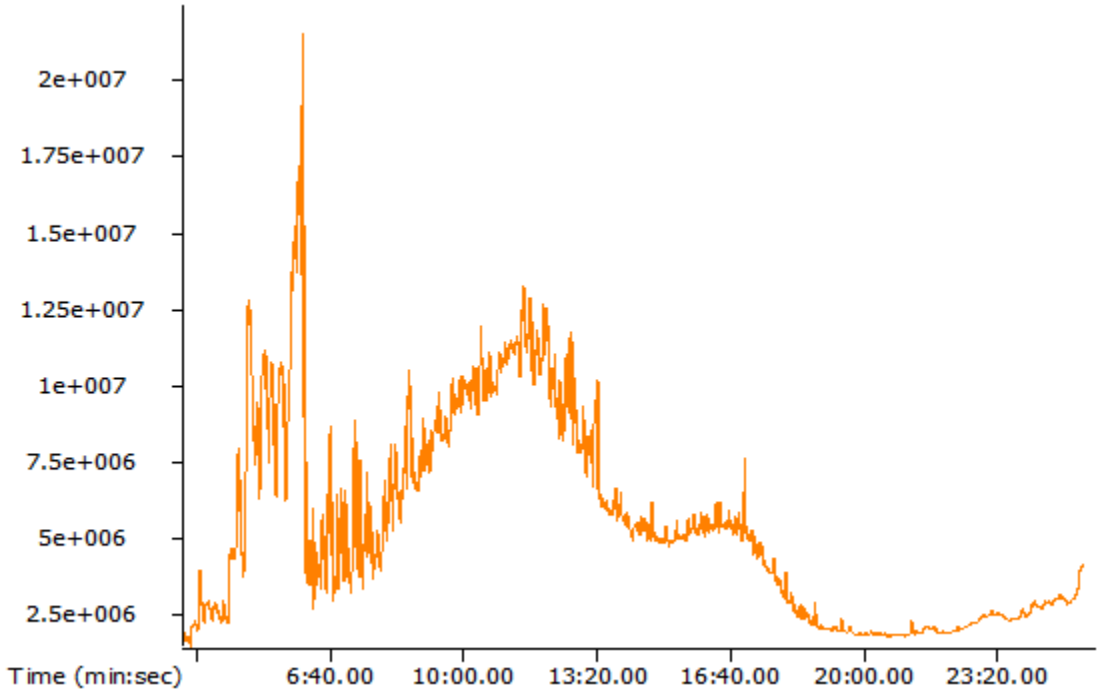

Figure 4.33: GC-MS total compound chromatogram for UT pyrolytic oil distillates

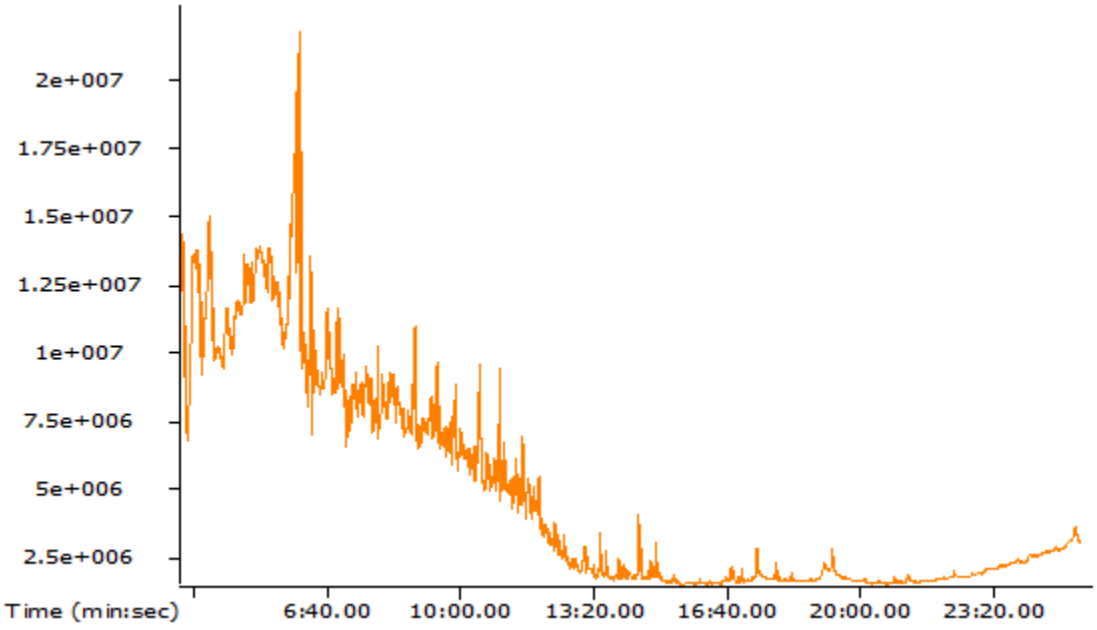

Figure 4.34: GC-MS total compound chromatogram for UTZ pyrolytic oil distillates

Table 4.9: Temperature range and distillate volume% obtained for the batch distillation of the different pyrolytic oil produced

NR Pyrolytic oil	
Temperature range (^{o}C)	Fractional Volume %
60 – 87	23.32
90 – 100	15.82
105 – 161	51.12
155 – 175	9.74
NRZ pyrolytic oil	
50 – 126	48.48
95 – 148	26.52
135 – 148	7.57
140 – 175	17.43
UT Pyrolytic oil	
Temperature range (^{o}C)	Fractional Volume %
30 – 144	43.12
162 – 198	11.98
180 – 208	5.98
UTZ Pyrolytic oil	
30 – 146	42.26
158 – 178	16.90
190 – 251	38.50

In summary, the NRZ pyrolytic oil and NR pyrolytic oil had more distillates yield within the temperature range for light naphtha compared to that of UTZ pyrolytic oil and UT pyrolytic oil. This is in accordance with the GC-MS analysis results that lower molecular weight hydrocarbon compounds were obtained in the distillates than in the pyrolytic oil. Also, the batch distillation of the UTZ pyrolytic oil gave more heavy oil liquid fraction than the UT pyrolytic oil. This could be attributed to the role of the zeolite NaY catalyst to further crack the heavy hydrocarbon compounds in the pyrolytic oil to lighter hydrocarbon compounds which is in accordance with the use of zeolite NaY as a catalyst in the cracking of pyrolytic oil oil in the petroleum industry.

4.7 Characterisation of UT and NR Solid Residue

The solid residue obtained from the thermal and catalytic pyrolysis of used tyres and natural rubber at 600 ^{o}C and heating rate of 15^{o}C/min was characterised using proximate and ultimate analysis. The scanning electron microscopy (SEM) images were also analysed.

4.7.1 Proximate and ultimate analysis and heating value of UT and NR solid residue

The proximate analysis was performed on both chars obtained from UT and NR pyrolysis. This helped in determining the fixed carbon content, volatile material, ash and moisture while the ultimate analysis was used to determine the elemental composition such as carbon, hydrogen, nitrogen, sulphur and oxygen present in the char and the HHV of the

char as reported in Table 4.10. The char obtained from both UT and NR pyrolysis had a higher heating value suitable for it to be an alternative source of heating fuel [17].

Table 4.10: HHV, Proximate and Ultimate analysis of UT and NR

Property	**Natural rubber (this study)**	**Used tyres (This study)**	**Li et al. [38]**
	Proximate analysis (wt. %)		
Moisture	0.7	0.18	2.35
Volatiles	8.90	17.0	16.14
Ash	4.0	32.3	12.32
Fixed carbon	86.4	50.52	-
	Ultimate Analysis (wt. %)		
Carbon	89.0	88.28	82.17
Hydrogen	9.4	8.5	2.28
Nitrogen	1.6	2.4	0.61
Sulphur	-	0.82	2.32
HHV (MJ/kg)	39.0	34.8	31.5

4.7.2 SEM analysis of UT and NR solid residue

Scanning electron microscopy (SEM) is an important technique used to determine the microstructure/ surface morphology of solid materials such as carbon. Hence, the solid residue obtained from the thermal and catalytic pyrolysis of used tyres and natural rubber at 600 ^{o}C and heating rate of 15^{o}C/min were analysed for their surface morphology at a

magnification of 150X as shown in Figure 4.35 (a-d).The Figure 4.35(a) and 4.35(b) reveals the presence of pores spread evenly across the residue rough surface with a distribution of particles of different sizes ranging from 132.9 to 632.3µm for the UT only residue and 149.4 to 267.3µm for the catalysed UT solid residue. The EDAX results showed that the main element in the UT only residue was zinc with 100 wt. % presence while Na (7.56 wt. %), Al (8.79 wt. %), Si (44.97 wt. %), Fe (7.69 wt. %) and Zn (31 wt. %) was identified for the catalysed UT. This confirms the retaining of the zeolite which was mixed homogenously with the UT sample before pyrolysis. The SEM for the NR solid residue (Figure 4.35(c)) and catalysed NR solid residue (Figure 4.35(d)) also revealed the presence of pores distributed evenly across the residue rough surface with a particle size distribution of 72.27 to 188.5µm.

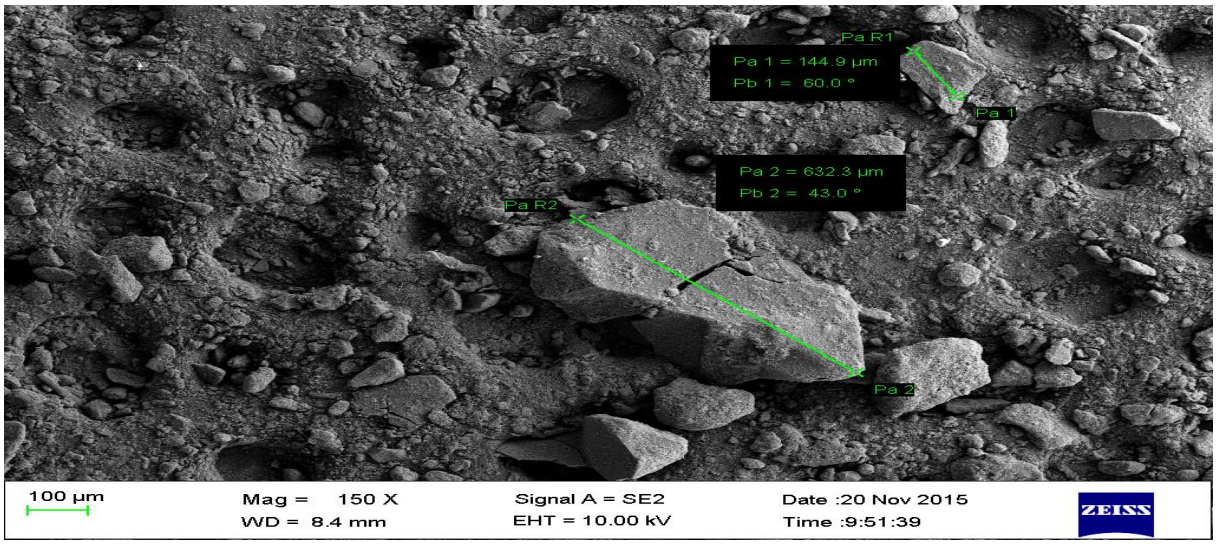

Figure 4.35 (a): SEM image of UT solid residue at 150X

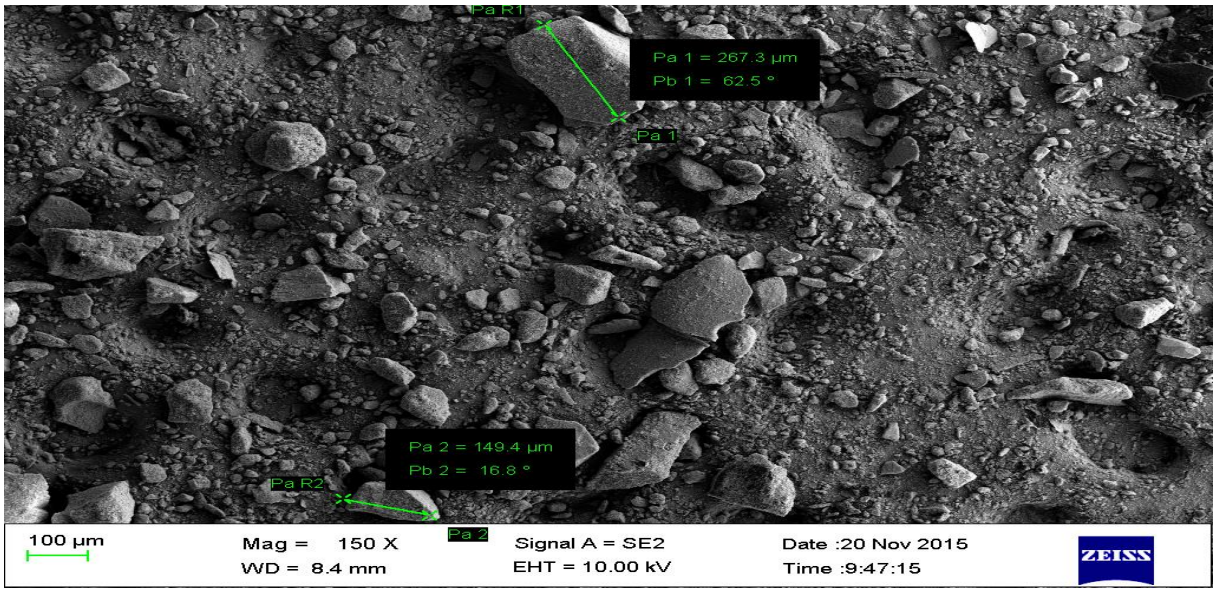

Figure 4.35(b): SEM image of Catalysed UT solid residue at 150X

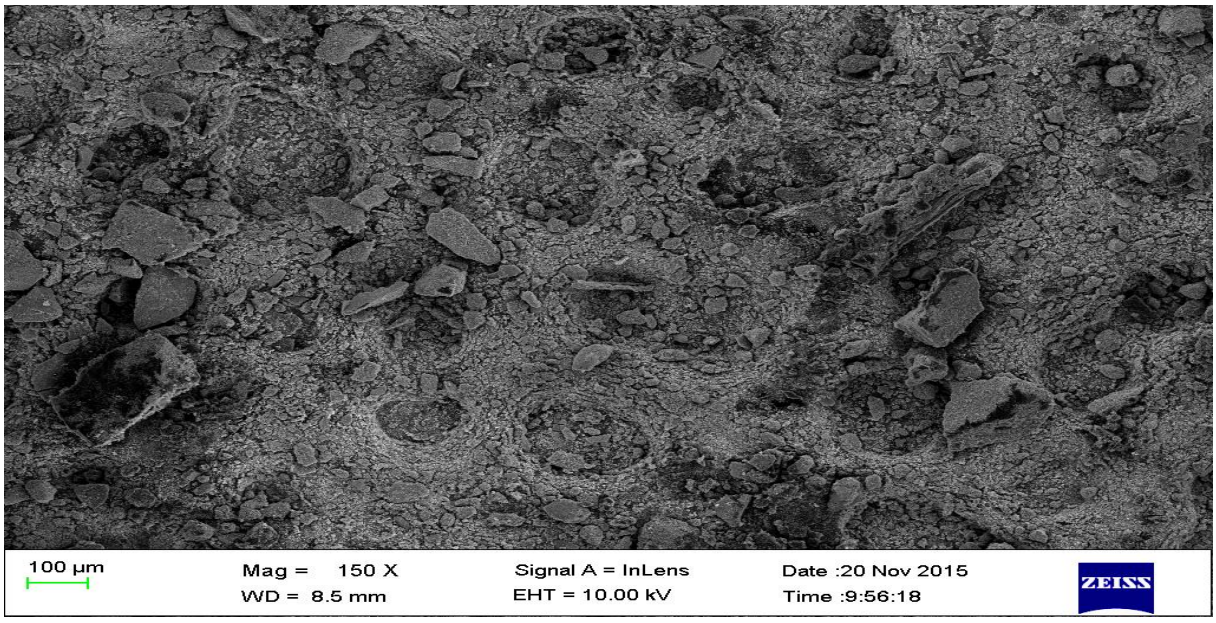

Figure 4.35(c): SEM image of natural rubber solid residue at 150X

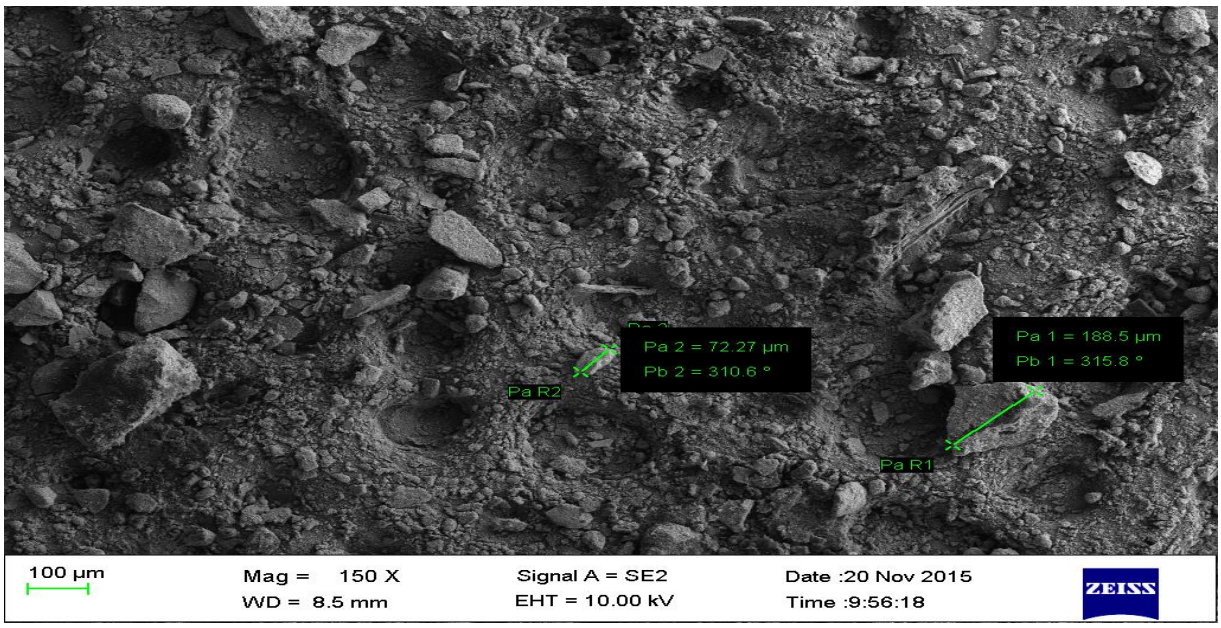

Figure 4.35(d): SEM image of catalysed natural rubber solid residue at 150X

4.8 Kinetic study of Thermal Degradation

In this study, kinetics of UT and NR thermal degradation study was performed using the TGA/DTG analysis equipment. Different heating rates (15, 20 and 30 ^{o}C/min) over a temperature range of 30 to 800 ^{o}C were investigated.

4.8.1 Kinetics of thermal degradation

An understanding of the thermal degradation kinetics of used tyres and natural rubber can contribute immensely in improving their thermal behaviour. Hence, the study of the used tyres and natural rubber pyrolysis kinetics will provide significant basis in predicting their behaviour in a pyrolysis reactor. The generally accepted technique for such kinetic

study of thermal degradation is the thermogravimetric analysis (TGA/DTG). This is because the main objective of thermogravimetric analysis is to get information on the general behaviour of the thermal degradation of used tyres [17]. Also the activation energy and pre-exponential factors can be determined from the data obtained from the TGA analysis. Since mechanisms of rubber materials pyrolysis involve complex reactions (as explained in section 2.4.5 of this study), it is not all reaction that results in the release of volatile component as some only alter the rubber material mechanical properties [46]. In thermogravimetric analysis, it is only the mass change as a function of temperature and time that is being measured, meaning only those reactions effecting a mass change are considered [46-48].

4.8.2 Mechanism and determination of kinetic parameters

Typically, the thermal degradation of polymeric materials occurs in more than one stage with multiple reactions. With the aid of the TGA, one can find the kinetic parameters and also measure the overall kinetics rather than individual reactions. Hence, Arrhenius equation and obtained thermogravimetric data are used to form the basis of the models. In this study, the kinetic analysis of the data for the used tyres and natural rubber degradation, a one-step mechanism kinetic model with a first order reaction and integral method was used to determine their kinetic parameters. The assumption of a first order reaction in thermal degradation is normally adopted by researchers [6, 17, 49-52].

Thus for the degradation of a material:

A (Solid) $\longrightarrow$ B (Solid) + C (Volatiles) (4.8)

The first order reaction is given as;

$$\frac{dX}{dt} = k(1-x)^n \quad (4.9)$$

Where n is the reaction order and X is defined as the weight loss by mass unit of the initial amount of tyre:

$$X_n = \frac{W_o - W_t}{W_o - W_f} \quad (4.10)$$

Where W_o(mg) is the initial mass of the tyre, W_f(mg) is the final mass and W_t(mg) is the mass at a given time, t (min) is the time and k is the kinetic rate constant which can also be expressed as;

$$k = k_o \exp\left(\frac{E_a}{RT}\right) \quad (4.11)$$

Where K_o is the pre-exponential factor (min^{-1}), R is the universal gas constant (8.314 J/kmol), T is the temperature of reaction (K) and $E_a$is the activation energy (kJ/mol) with a linear heating rate A (K/min) given as;

$$A = \frac{dT}{dt} \quad (4.12)$$

By substituting (4.11) in (4.9) and Integrating, equation (4.9) becomes,

$$\mathrm{Ln}[-\ln(1-X)] = \mathrm{Ln}[\left(\frac{koRT}{AEa}\right) * \left(1 - \frac{2RT}{Ea}\right)] - \frac{Ea}{RT} \quad (4.13)$$

A plot of the term on the left hand side of (4.13) against 1/T should give a straight line with slope ($-E_a$/R) which can be used to obtain the activation energy E_a. The pre-exponential factor k_o can be calculated using the exponential energy and the intercept of the plot. Figure 4.36, 4.37, 4.38 and Figure 4.39, 4.40, 4.41 represents the kinetic plots of Ln[-Ln(1-X)] versus 1/T calculated from the TGA data for natural rubber and used tyres at different heating rates of 15, 20 and 30^{o}C/min over a temperature range of 30 to 800 ^{o}C in order to determine the Activation energy for the different degradation stages. The trend line equations and regression coefficients derived from the kinetic plots for the various stages of used tyres and natural rubber degradation is shown in Table 4.11.

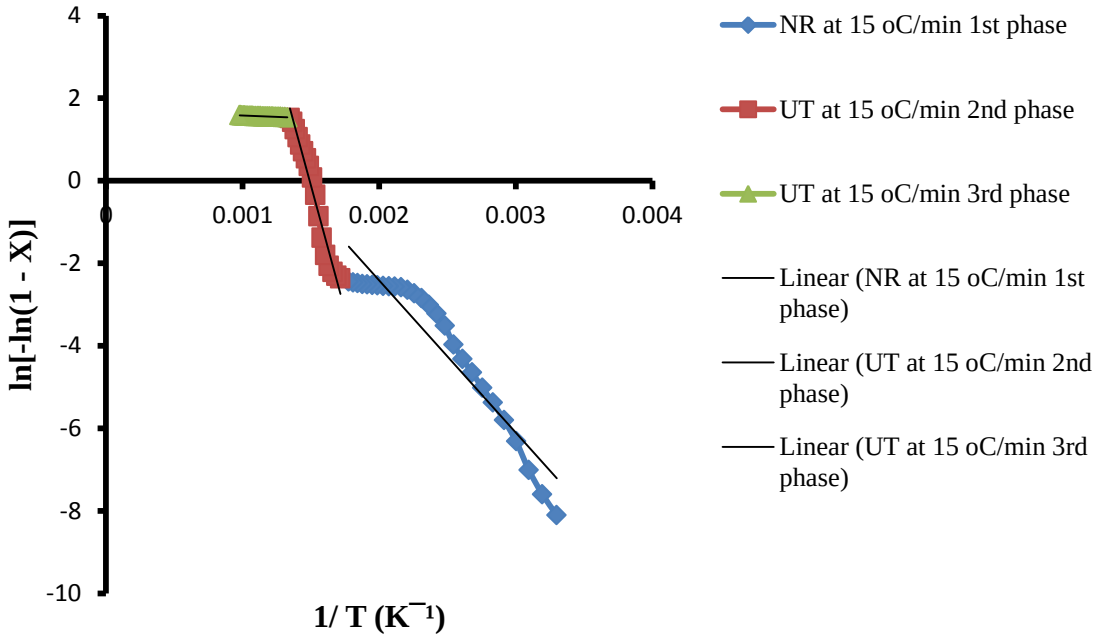

Figure 4.36 Kinetic plots of different phase of NR at heating rate of 15^{o}C/min

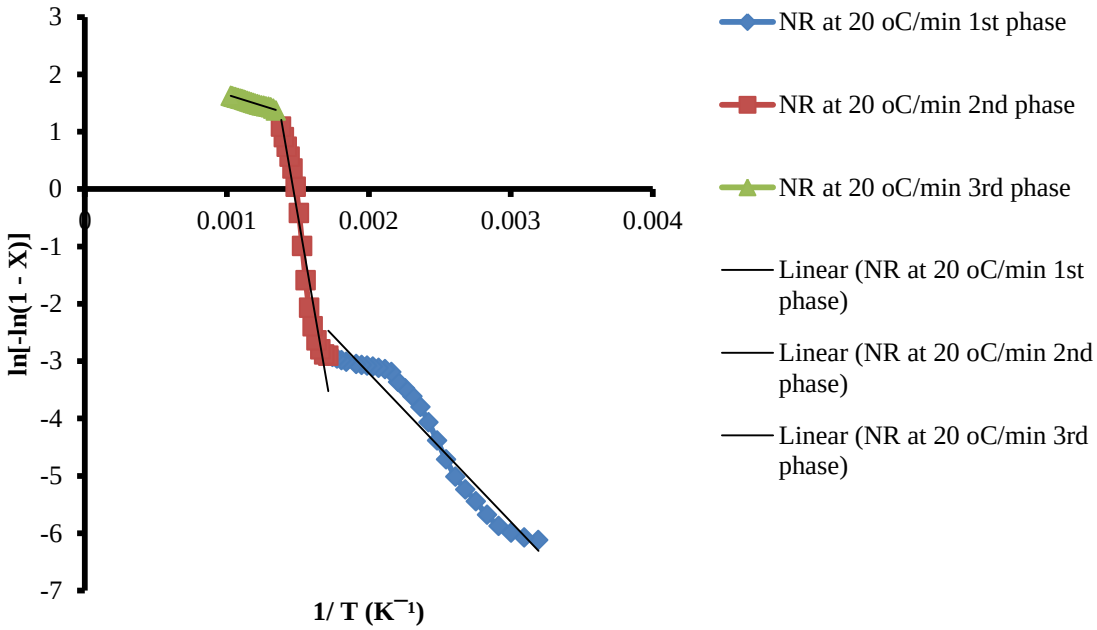

Figure 4.37 Kinetic plots of different phase of NR at heating rate of 20°C/min

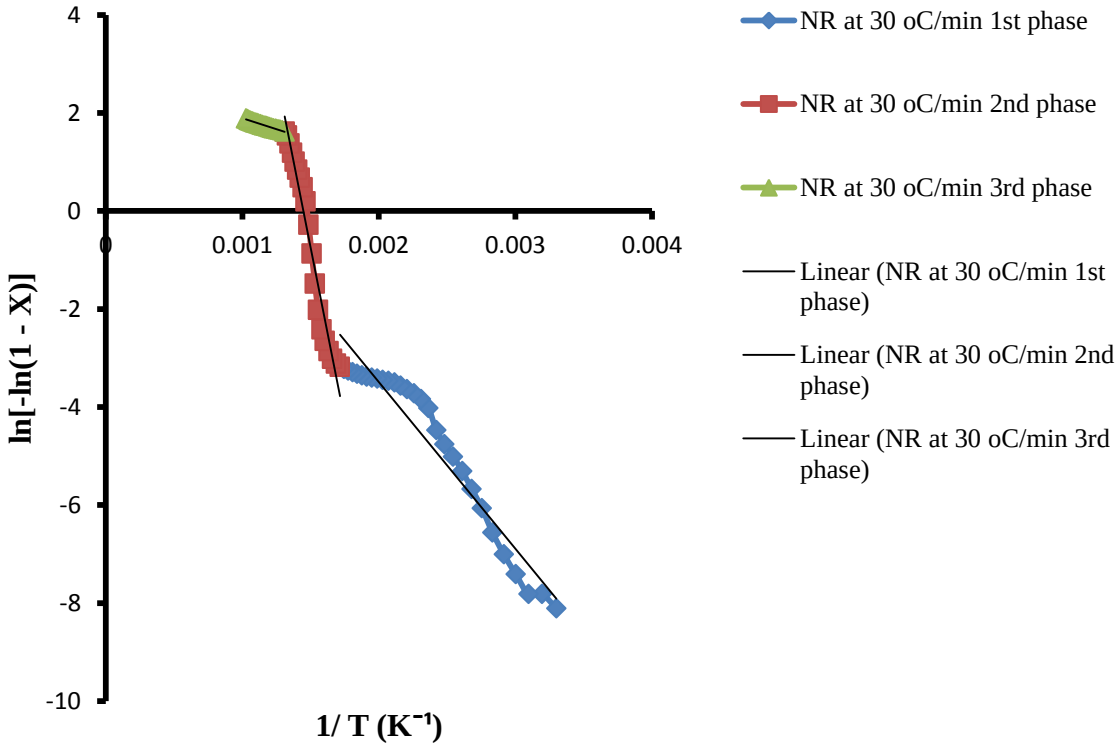

Figure 4.38 Kinetic plot of different phase of NR at heating rate of 30°C/min

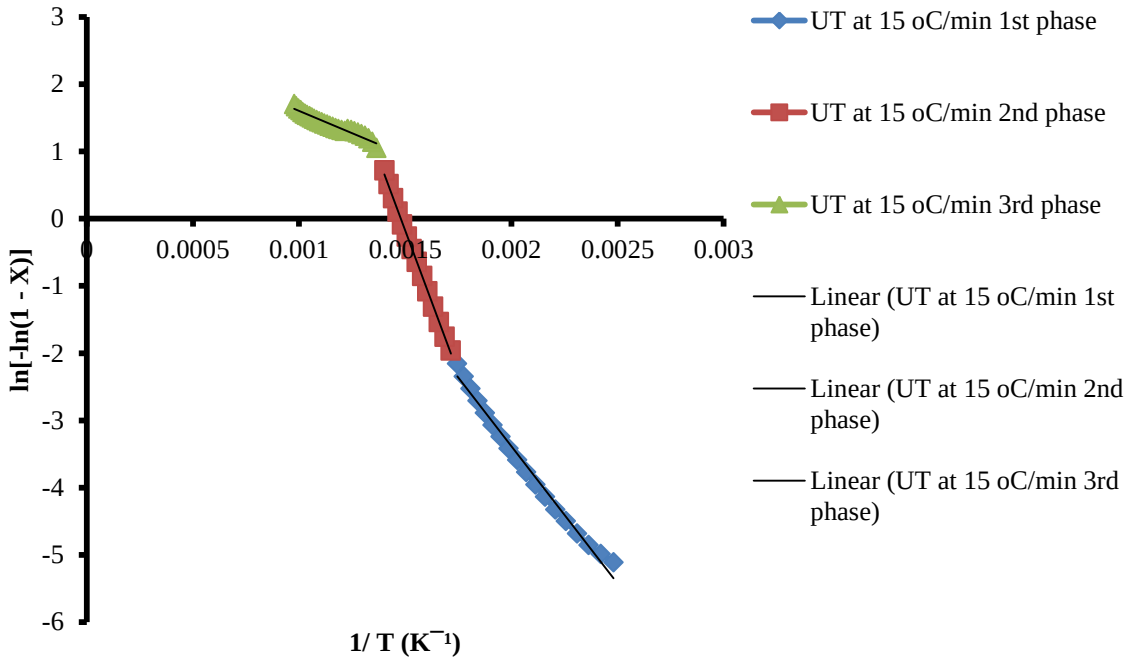

Figure 4.39 Kinetic plots of different phases of UT at heating rate of 15°C/min

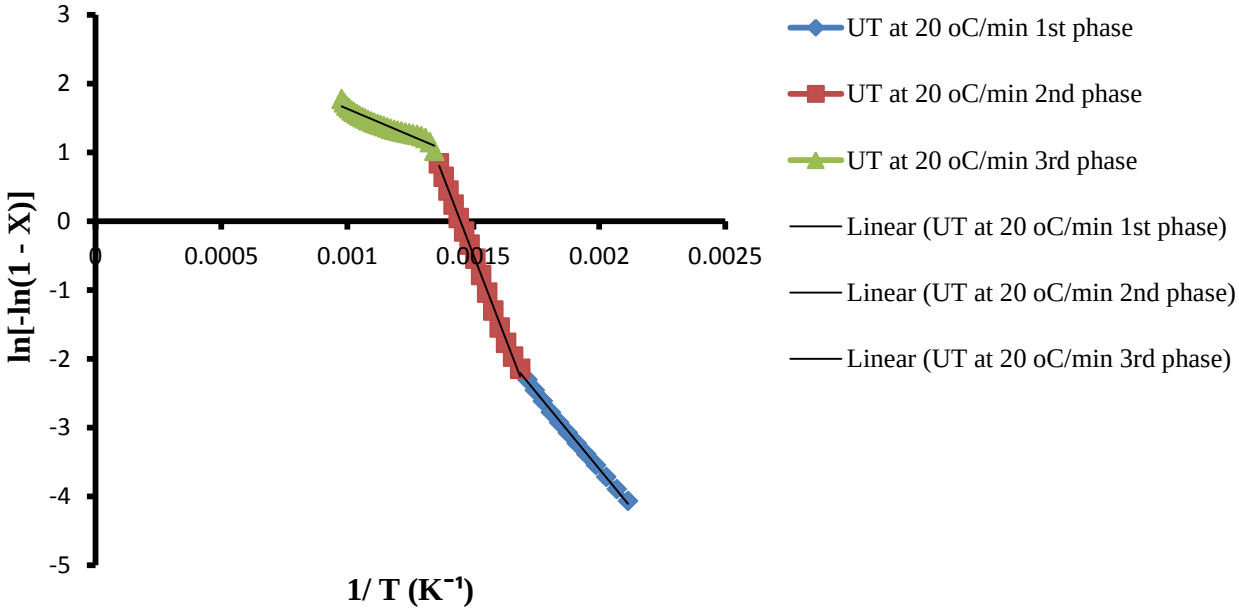

Figure 4.40 kinetic plots of the different phases of UT at heating rate of 20°C/min

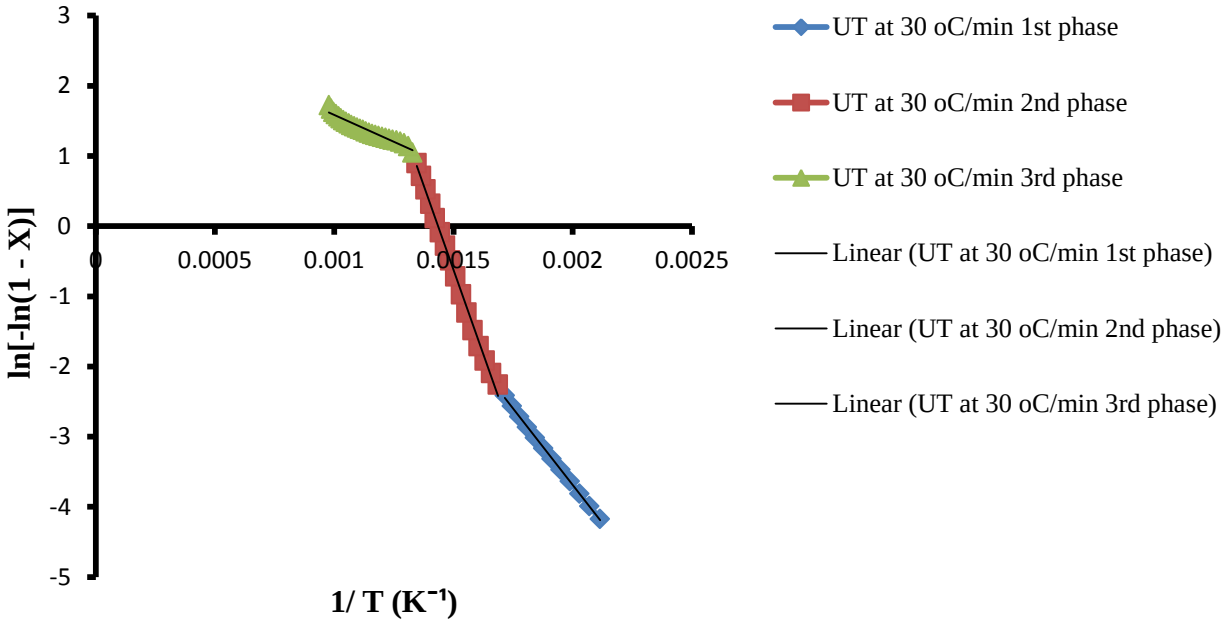

Figure 4.41 kinetic plots of different phases of UT at heating rate of 30^{o}C/min

The determined activation energy for both used tyres and natural rubber is shown in Table 4.12 and 4.13. These were used to determine the average of the three stages of both the activation energy and pre-exponential factor at the different heating rates for used tyres and natural rubber as shown in Table 4.14 and discussed below.

Table 4.11: Trend line equations and Regression coefficients for UT and NR

Heating rate (^oC/min)	1st Stage	2nd Stage	3rd Stage
	Used tyres sample		
15	Y = -3853.3 + 4.17	Y = -9092.2X + 13.20	Y = -1382X + 3.12
	R^2 = 0.98	R^2 = 0.96	R^2 = 0.99
20	Y = -4325.8X + 05.05	Y = -9538X + 13.82	Y = -1557.7 + 3.19
	R^2 = 0.99	R^2 = 0.99	R^2 = 0.95
30	Y = -4368X + 05.05	Y = -9621.7X + 13.81	Y = -1544.1X + 3.13
	R^2 = 0.99	R^2 = 0.99	R^2 = 0.95
	Natural rubber sample		
15	Y = -2708.7X + 1.57	Y = -13414X + 19.83	Y = -1208.9X + 3.13
	R^2 = 0.99	R^2 = 0.96	R^2 = 0.99
20	Y = -2941X + 2.9045	Y = -14251X + 20.92	Y = -757.97X + 2.4029
	R^2 = 0.96	R^2 = 0.96	R^2 = 0.99
30	Y = -3920.4X + 4.73	Y = -14799X + 21.52	Y = -893X+ 2.79
	R^2 = 0.96	R^2 = 0.95	R^2 = 0.99

Table 4.12: Activation energy and pre-exponential factor of used tyres sample

Heating rate (^{o}C/min)	Activation energy (kJ/mol)		
	1St Stage	2nd Stage	3rd Stage
15	32.04	75.59	11.49
20	35.96	79.30	12.95
30	36.32	79.99	12.84
Pre-exponential factor (min^{-1})			
15	3.20×10^{12}	3.51×10^{16}	2.55×10^{11}
20	2.80×10^{12}	6.66×10^{16}	1.89×10^{11}
30	4.29×10^{12}	9.43×10^{16}	2.65×10^{11}

Table 4.13: Activation energy and Pre-exponential factor of natural rubber sample

Heating Rate (^{o}C/min)	Activation energy (kJ/mol)		
	1St Stage	2nd Stage	3rd Stage
15	22.52	111.52	10.05
20	24.45	118.48	6.30
30	32.59	123.04	7.42
Pre-exponential factor (min-1)			
15	0.58×10^{12}	0.38×10^{20}	22.7×10^{10}
20	107×10^{12}	1.58×10^{20}	1.50×10^{10}
30	1.09×10^{12}	2.45×10^{20}	25×10^{10}

Table 4.14: Average Activation energy and Pre-exponential factor for used tyres and natural rubber

Used tyres sample		
Heating rate (^oC/min)	**Activation energy (kJ/mol)**	**Pre-exponential factor (min^{-1})**
15	39.71 ± 26.69	1.17×10^{16}
20	42.74 ± 27.51	2.22×10^{16}
30	43.05 ± 27.82	3.14×10^{16}
Natural rubber sample		
15	48.03 ± 45.18	1.25×10^{19}
20	49.74 ± 49.17	5.28×10^{19}
30	54.35 ± 49.65	8.17×10^{19}

From Table 4.12 and Table 4.13, it was observed that the value of activation energy for the 2nd stage of used tyres and natural rubber was higher than that recorded for the 1st and 3rd stages. This could be related to the fact that depolymerisation of the used tyres and natural rubbers in form of bond scission and decarbonylation occurred more at this stage requiring more energy for degradation. The result is in agreement with report by Pradhan and Sighn [17] on their use of a TGA/DTG for the investigation of tyre rubber and tube rubber. Also, the average activation energy for natural rubber at the different heating rates of 15, 20 and 30^{o}C/min was higher than that obtained for the used tyres sample in this study. This implies more energy is needed to depolymerise natural rubber due to its heavy molecular weight of up to a 1,000,000 g/mol than the used tyres with lower molecular weight [53-55]. Also, from the calculated average results reported in Table

4.14, the activation energy increases as the heating rate increases. This could explain how the heating rate affect the peak curve of components (from the DTG graph), which shift further away from their expected peak temperature to higher temperature zone resulting in more energy needed for their degradation. This was also reported by Leung and Wang [53] from their experimental results that as the heating rate increases, the activation energy and frequency factor also increases due to a shift of the reactions to higher temperature range and the temperature corresponding to peak value of sample weight loss increases making degradation more difficult. Figure 4.42 and 4.43 show the DTG graph variation of the peak temperature for the different degradation/peak temperature of the used tyres and natural rubber components.

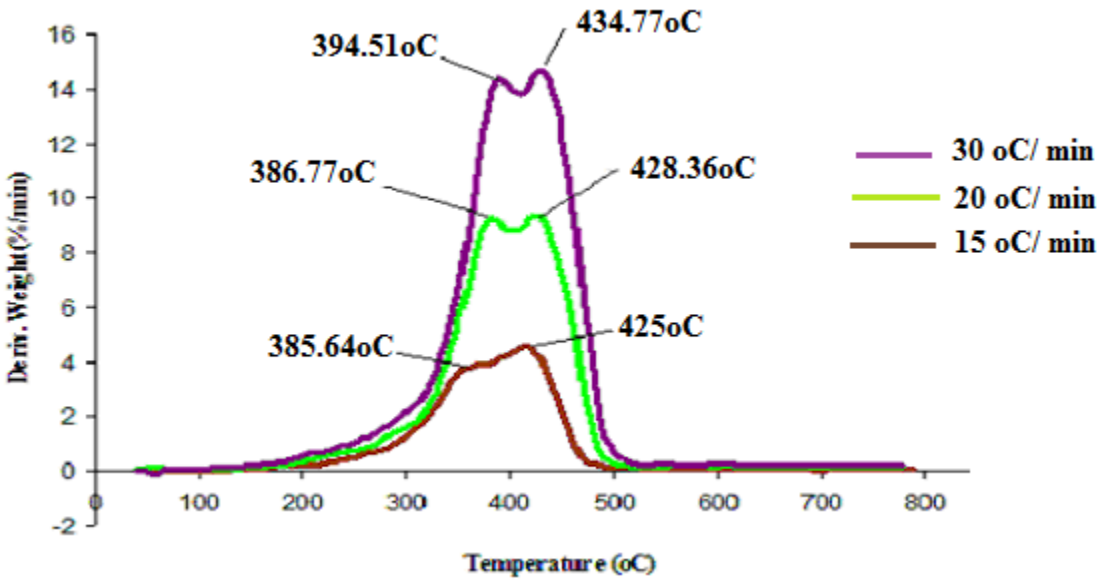

Figure 4.42: Effect of heating rate on Temperature degradation of UT

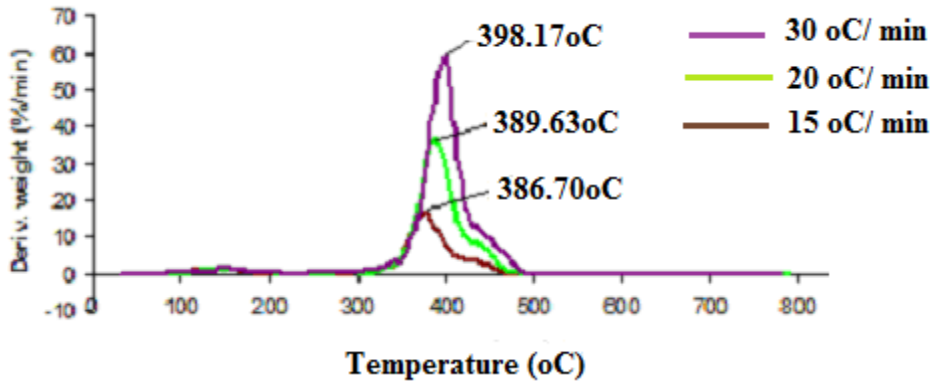

Figure 4.43: Effect of heating rates on temperature degradation of NR

From the DTG graph for used tyres, Figure 4.42, as the heating rate increased from 15, 20 to 30^{o}C/min over the temperature range of 30 to 800 ^{o}C, the two prominent temperature peaks shifted from 385.64 and 425 ^{o}C for 15^{o}C/min to 386.77 and 428.36 ^{o}C for 20^{o}Cmin to 394.51 and 434.77 ^{o}C for the heating rate of 30^{o}C/min. The same was observed for the natural rubber, Figure 4.43, at different heating rates of 15, 20 and 30^{o}C/min for the same temperature range of 30 to 800 ^{o}C. The single prominent peak in the DTG graph of NR shifted from 386.70 ^{o}C at heating rate of 15^{o}C/min to 389.63 ^{o}C at 20^{o}C/min and 398.17 ^{o}C at 30^{o}C/min. This could be related to the increase in activation energy as the heating rate increases resulting in more energy required to depolymerise the rubber components at higher peak temperature. A similar situation was also reported by Aguado et al. [28] when they studied the kinetics of scrap tyres under fast heating conditions. It was noted that as they increase the heating rate, the maximum peaks in their DTG curves displaces to higher temperatures (707K at 2K min^{-1}, 711K at 5 K min^{-1}, 721K at 10 Kmin^{-1} and 727K at 20K min^{-1}). Thus from the activation energy results

obtained with the use of the TGA/DTG data in this study, the thermal degradation of UT was found easier than that of NR. Also, it can be concluded from the kinetic study that as the heating rate increases the activation energy and the pre-exponential factor also increases.

4.9 Testing of Pyrolytic Oil Distillates and Petrol Blends

The pyrolytic oil distillates, PD, obtained from the distillation of the thermal and catalysed pyrolysis of UT and NR pyrolytic oil were blended with commercial petrol (in the ratio 0, 5, 10, 15 and 20%) and tested in a generator set. Sections 4.9.1 to 4.9.2 discuss the investigation performed during the combustion study of the PD/Petrol blend.

4.9.1 Fuel consumption over time as a function of fuel blend composition.

In order to determine the fuel consumption over time, the generator was made to power a Martlet 375 watt heavy duty 150 mm bench Grinder machine as shown in Figure 3.6 through out the sets of experiments. First, the commercial unleaded petrol was used to run the generator in order to set a reference level of fuel consumed over time against that of the blends. This was then followed by using the blend of 0, 5, 10, 15 and 20% of the NRPD, NZPD, UTPD and UZPD with petrol.This was presented as change in fuel level with time as shown in Figure 4.44 to 4.51 while the data plotted are presented in Appendix E. During the engine combustion performance test, it was evident that both the distillates from thermal and catalysed pyrolytic oil of UT and NR combusted in the spark ignition engine. This is a different approach as most reports in literature are on the use of

the pyrolytic oil and its distillates from UT in compression diesel engines. Nevertheless, as the ratio of the PD increases in the blend mixture, there were more gaseous emissions associated with that of the non-catalysed UTPD than the others. This could probably be due to the high amount heavier hydrocarbon compounds and aromatics present in it than the others from the NMR and GC-MS analyses results. The NRPD and NRZPD petrol blend of 5 to 20% had similar emission colour with that of commercial petrol. From Figure 4.44, an increase in the NRPD from 5 to 20% in blends with commercial petrol showed a decrease in the consumption of fuel. The consumption behaviour of the 20% NRDP-Petrol blends was comparative with the commercial petrol consumption until 25 min of the generator run. Afterwards, the consumption of the commercial petrol was higher than that of the 20% NRPD-Petrol blend as shown in Figure 4.45. For that of NZPD-Petrol blend consumption in Figure 4.46, a similar trend with that of NRPD-Petrol blend was observed.

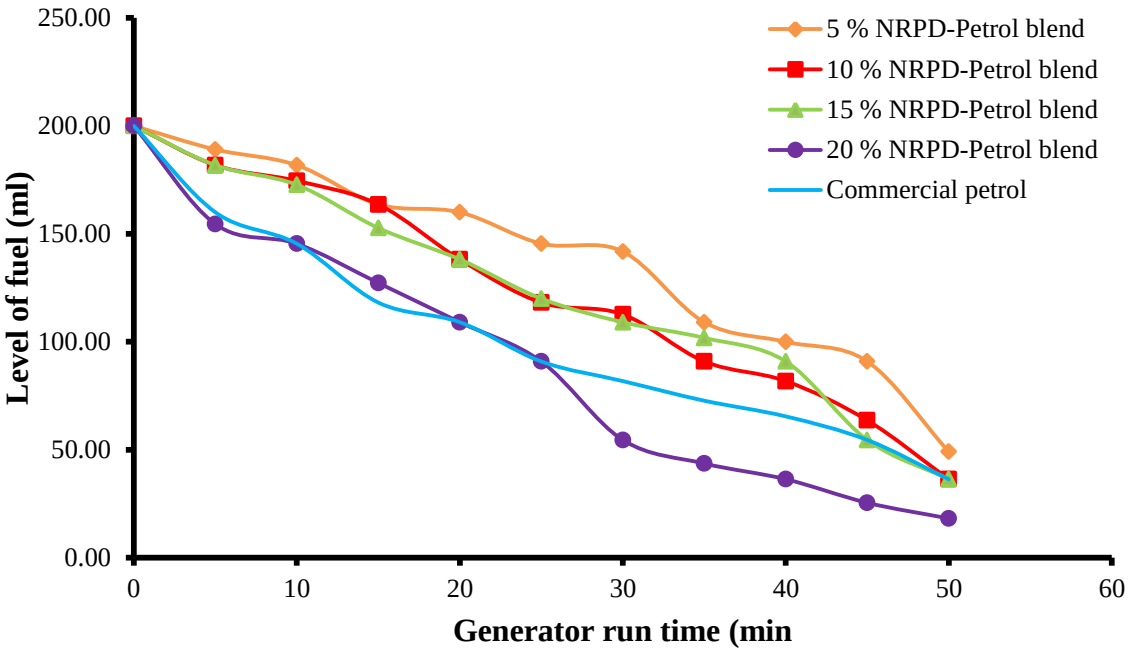

Figure 4.44: Fuel consumption rate as a function of NRPD-Petrol fuel composition

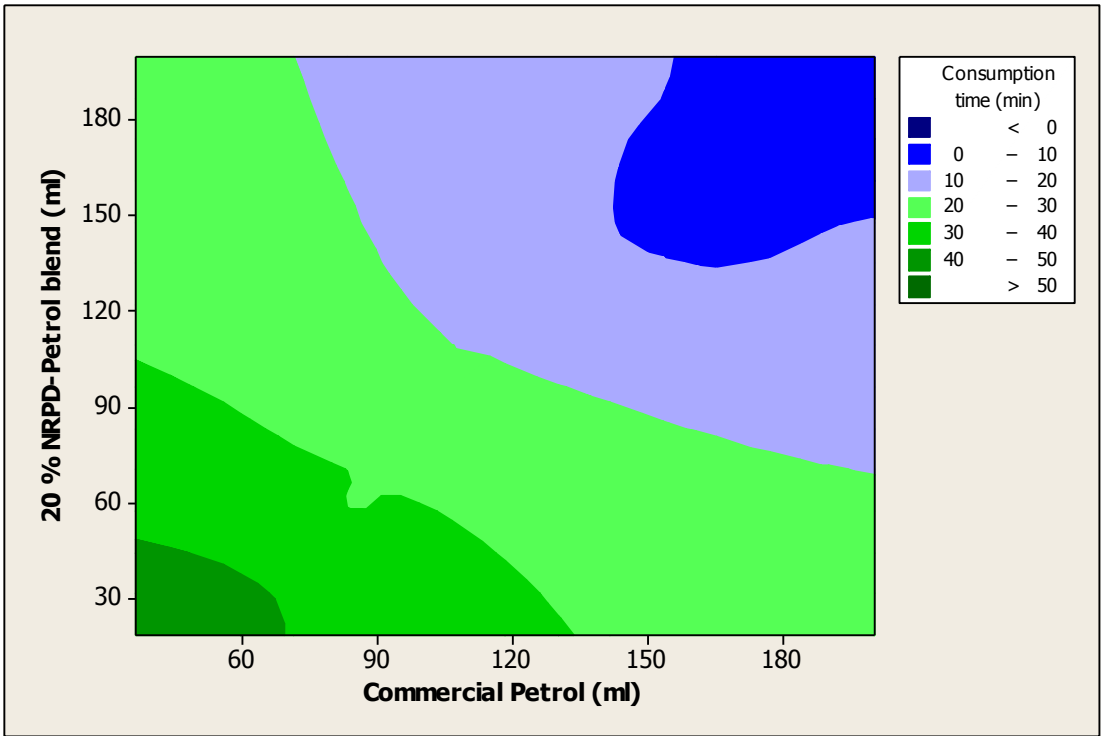

Figure 4.45: Contour Plot of Consumption time vs 20 % NRPD-Petrol, Commercial Petrol (ml)

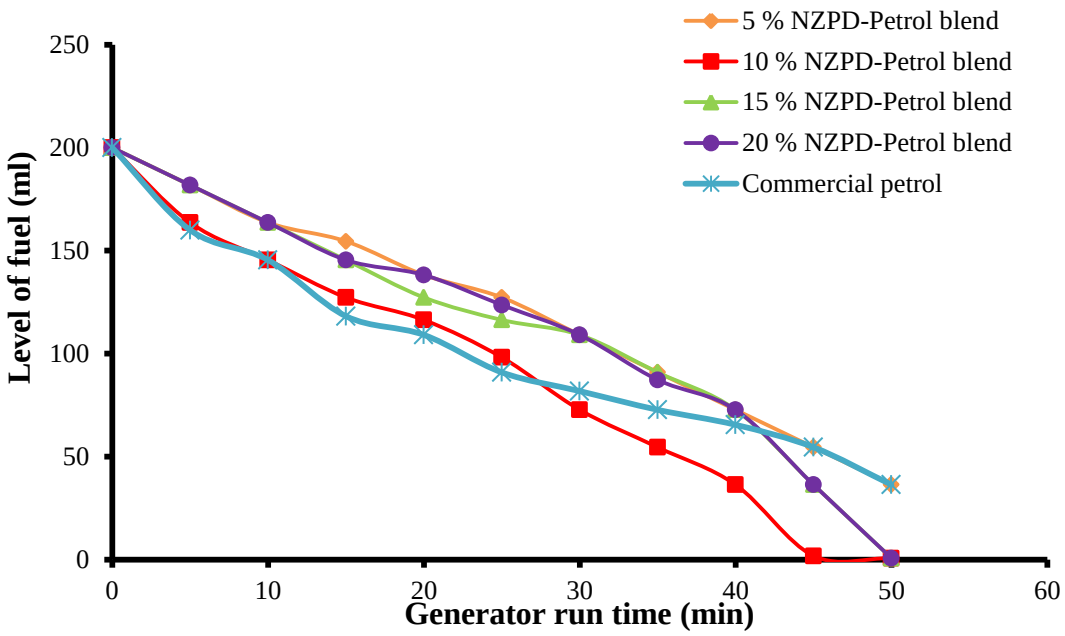

Figure 4.46: Fuel consumption rate as a function of NZPD-Petrol fuel composition

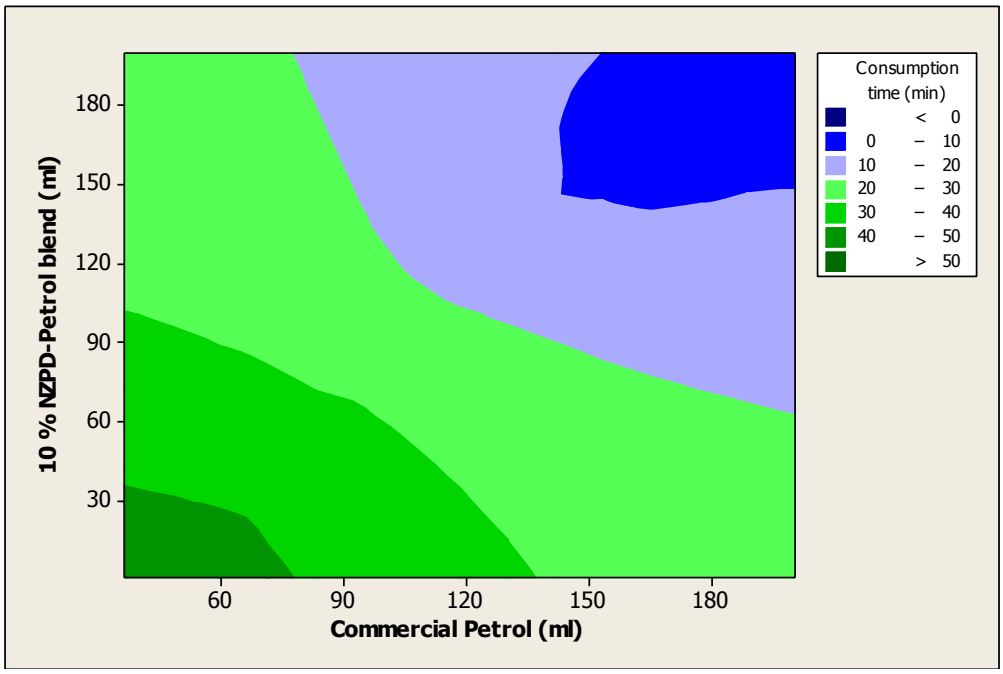

Figure 4.47: Contour Plot of Consumption time vs 10 % NZPD-Petrol, Commercial Petrol (ml)

Nevertheless, it was the 10 % NZPD-Petrol blend that had comparative consumption behaviour with that of the commercial petrol till about 30 min of the generator run. Afterwards, the commercial petrol displayed faster consumption rate than the 10 % NZPD-Petrol blend as shown in Figure 4.47.

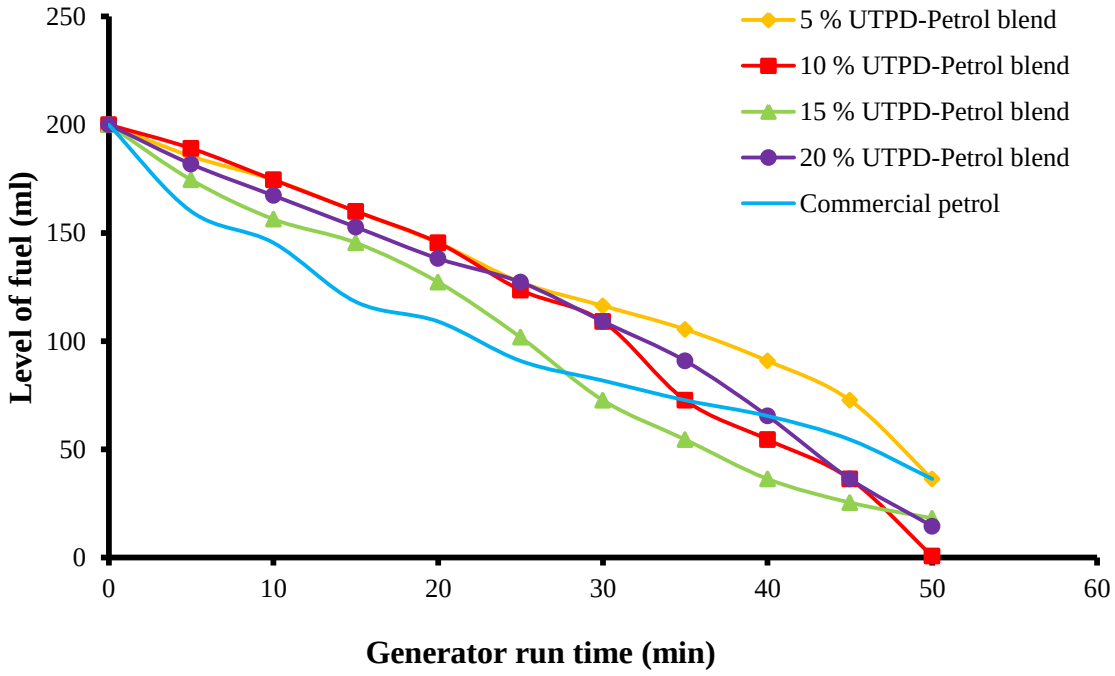

Figure 4.48: Fuel consumption rate as a function of UTPD-Petrol fuel composition

The consumption rate of the UTPD-Petrol blend represented in Figure 4.48 reveals that none of the blends had comparative fuel consumption behaviour with that of the commercial petrol until after about 30 min of the generator run. Although a decrease in consumption rate was later observed for the blend than the commercial petrol after 30 min run time upward, except for the 5% UTPD-Petrol blend. Figure 4.49 displays the

comparative consumption behaviour for the 15% UTPD-Petrol blend which had a closer behaviour pattern with the commercial petrol after 30 min run time.

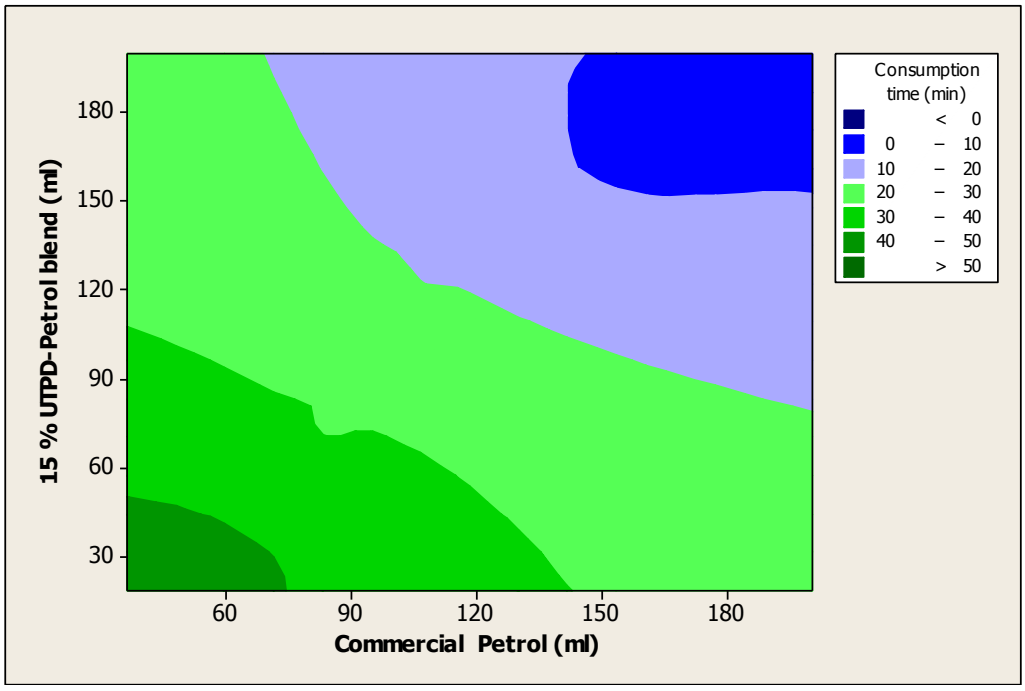

Figure 4.49: Contour Plot of Consumption time vs 15 % UTPD-Petrol, Commercial Petrol (ml)

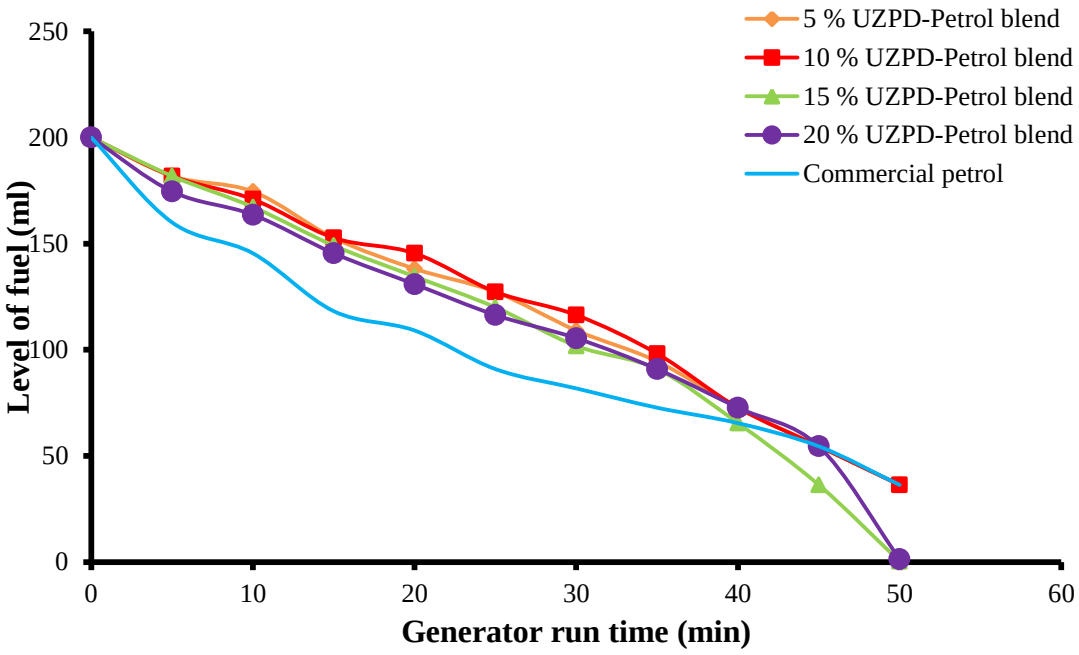

Figure 4.50: Fuel consumption rate as a function of UZPD-Petrol fuel composition

For the case of the UZPD-Petrol blend shown in Figure 4.50, there was no much deviation observed from the UTPD-Petrol blend pattern represented in Figure 4.49.

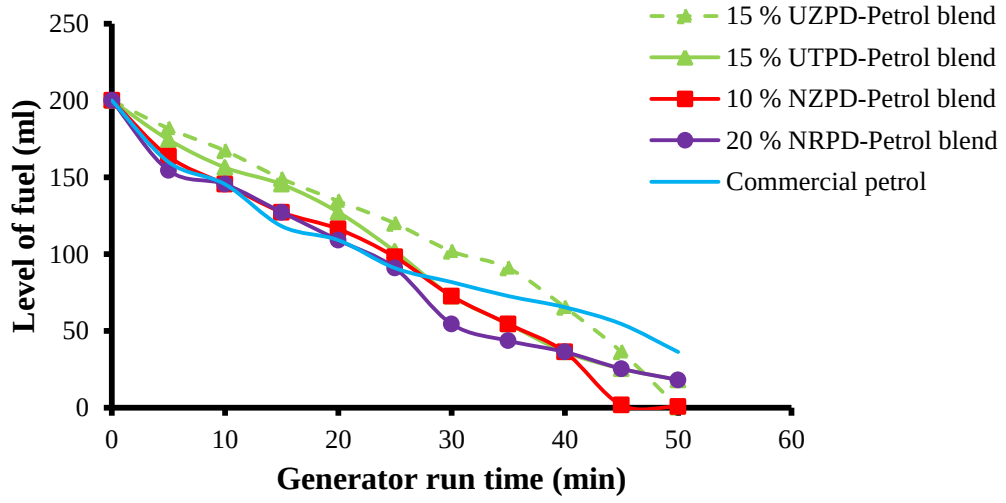

Figure 4.51: Fuel consumption rate for observed optimum PD-Petrol blend fuel

4.9.2 Fuel power as a function of PD composition in the fuel blend

Figure 4.52 to 4.55 shows the graph of the calculated Fuel power as a function of the various PD concentrations in the PD-Petrol blend fuel. The plot data and other relevant values are represented in a Tables E5 and E6 in appendix E.

From below figures (Figure 4.52 to 4.55), it was observed that the fuel power increases as the concentration of the different PD increases in the PD-Petrol fuel blend. An optimum fuel power performance value of 2.02, 2.20, 2.20 and 2.22 kJ/s was obtained at 20% for the NRPD-Petrol blend fuel, 10% for the NZPD- Petrol blend fuel, 15% for the UTPD-Petrol blend fuel and 15% for the UZPD-Petrol blend fuel. When compared with that of the commercial petrol, 1.79kJ/s, the composition of the PD in the fuel mixture resulted in a higher fuel power in the generator.

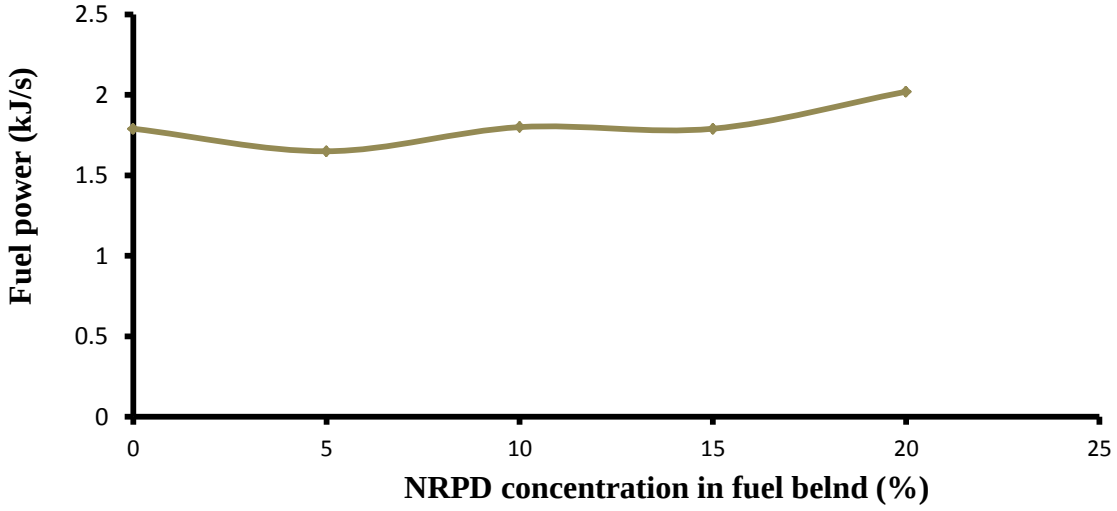

Figure 4.52: Curve showing the fuel power as a function of NRPD concentration in the fuel blend

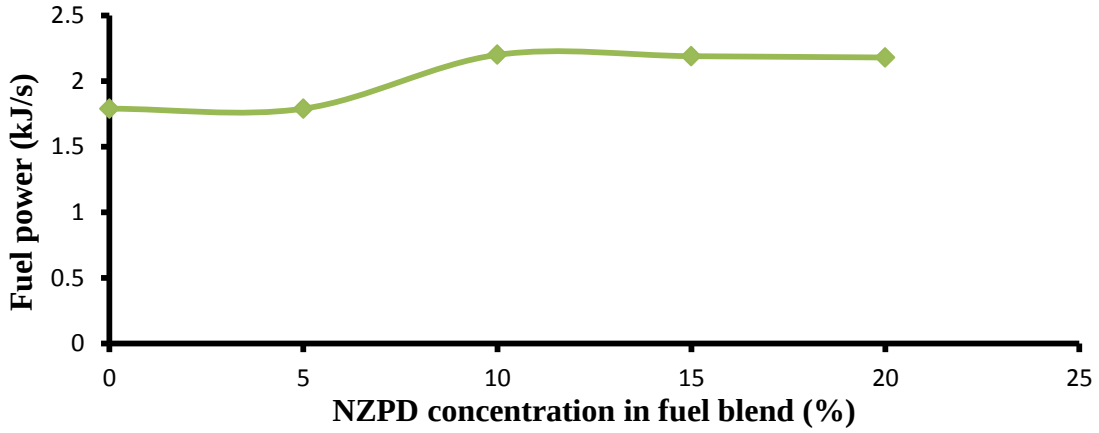

Figure 4.53: Curve showing the fuel power as a function of NZPD concentration in the fuel blend

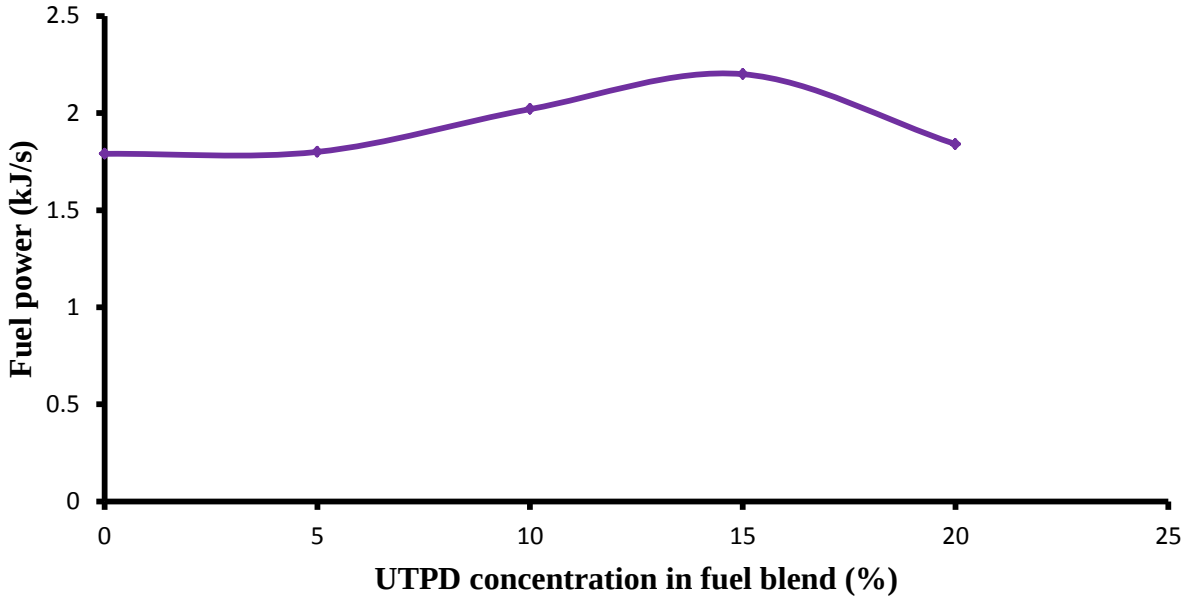

Figure 4.54: Curve showing the fuel power as a function of UTPD concentration in the fuel blend

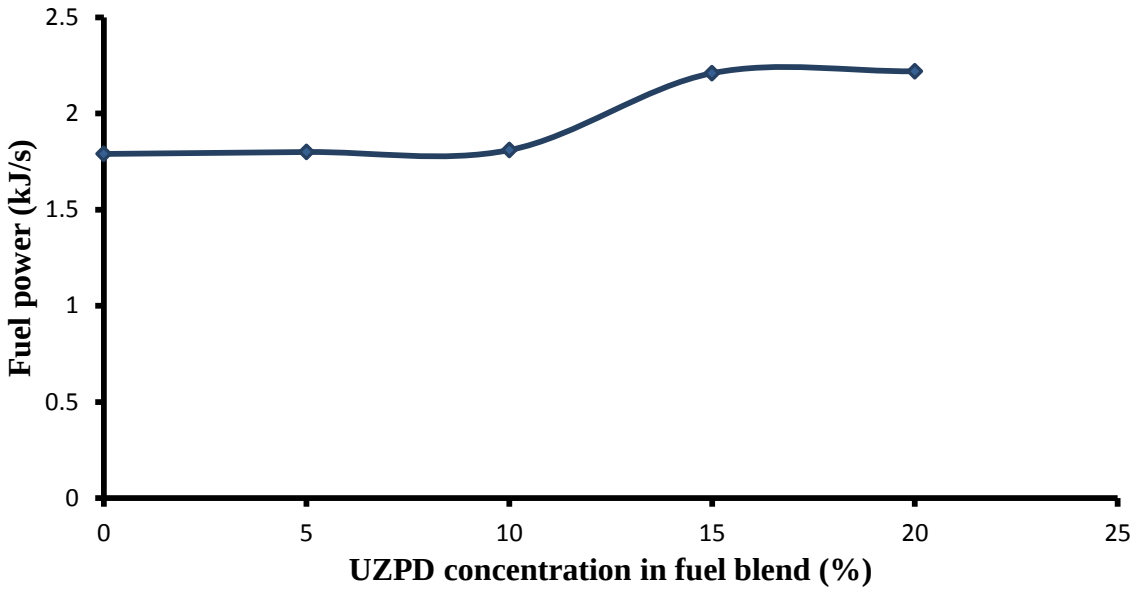

Figure 4.55: Curve showing the fuel power as a function of UZPD concentration in the fuel blend

In summary, the PD obtained from the thermal and catalysed pyrolytic oil from NR and UT combusted successfully in the blend ratio of 0, 5, 10, 15 and 20 % with commercial Petrol in a spark ignition combustion engine without engine modification. This is a different approach from the use of compression ignition engine normally reported by other researchers in literature [17, 55].

From the Figures (Figure 4.44, 4.46, 4.48 and 4.50) shown above for the entire PD-Petrol blend mixture fuel consumption rate against generator run time, there was an increase in the fuel consumption rate as the percentage concentration of the different PD increases in the fuel mixture. Nevertheless, the difference in the rate of fuel consumption did not deviate much from that of the commercial Petrol which had a value of 4.03×10^{-5} kg/s

while the highest amount of 5.08 x 10^{-5} kg/s was recorded for UZPD-Petrol fuel blend indicating 25.56% increase. This closeness of the different fuel mixture consumption rate with the Petrol fuel could be attributed to the closeness in the higher heating value of NRPD, 43.20 MJ/kg, NZPD 43.22 MJ/kg, UTPD, 41.40 MJ/kg, UZPD, 41.41 MJ/kg and 44.39 MJ/kg for Petrol fuel. Hence low amount of commercial petrol will be required for blending with PD to obtain similar engine performance.

The fuel consumption rate for the observed optimum PD-Petrol blend fuel compared with commercial Petrol as represented in Figure 4.51, the order of fuel consumption with respect to generator run time can be concluded as UZPD-Petrol blend >UTPD-Petrol blend >NZPD-Petrol blend >NRPD-Petrol blend. It is can be said that the distillates-Petrol blends obtained from natural rubber gave better comparative behaviour with the commercial petrol and lower fuel consumption rate than that obtained from UT distillates-Petrol blends. This could be associated with the HHV of NR pyrolytic oil distillates which were within the Petrol HHV range and above that of the UT pyrolytic oil distillates. The amount of aliphatic hydrogen and aromatic hydrogen in the NR as revealed by the ^{1}H and ^{13}C NMR analysis are closer in chemical shift range to that of commercial Petrol than that presented by the UT distillates. This is in agreement with the ^{1}H and ^{13}C NMR of commercial Petrol reported by Deavanni [55] and other researchers in literature that commercial Petrol is composed of a mixture of hydrogen attached to aliphatic and aromatic within the chemical shift of 0.8 – 1.8 and 2.1-2.8 ppm while the aliphatic and aromatic carbon lie within 10-50 ppm and 100-160 ppm.

Furthermore, the outcome of the fuel power for the different PD composition in the PD-Petrol fuel blend in the generator revealed that as the various PD composition increases in the PD-Petrol blend fuel, there is an increase in the generator fuel power. In addition, the optimum fuel power values as a function of the composition of PD in the PD-Petrol fuel mixture was obtained at the same composition that gave optimum fuel consumption rate values for each of the PD in PD-Petrol fuel blend. This satisfies the equation relationship that fuel power is dependent on the product of the mass of fuel consumed and the heating value of the fuel used.

4.10 Mathematical Modeling and Simulation of Pyrolysis of the Rubber

As highlighted in Chapter two above, thermogravimetric analysis, TGA, is the standard technique used in the study of the thermal degradation behavior of tyre rubber. It normally relates the weight loss of the material with constant rate (θ) of change in temperature over time. This implies that temperature and time have a linear relationship at a constant heating rate of θ/time as in equation (4.14).

$$T(t) = \theta t + T_0 \tag{4.14}$$

A TGA curve for used tyres (UT), in terms of weight loss against temperature at a heating rate of 15^{o}C/min over a temperature range of 30 to 800 ^{o}C is shown in Fig 4.56.

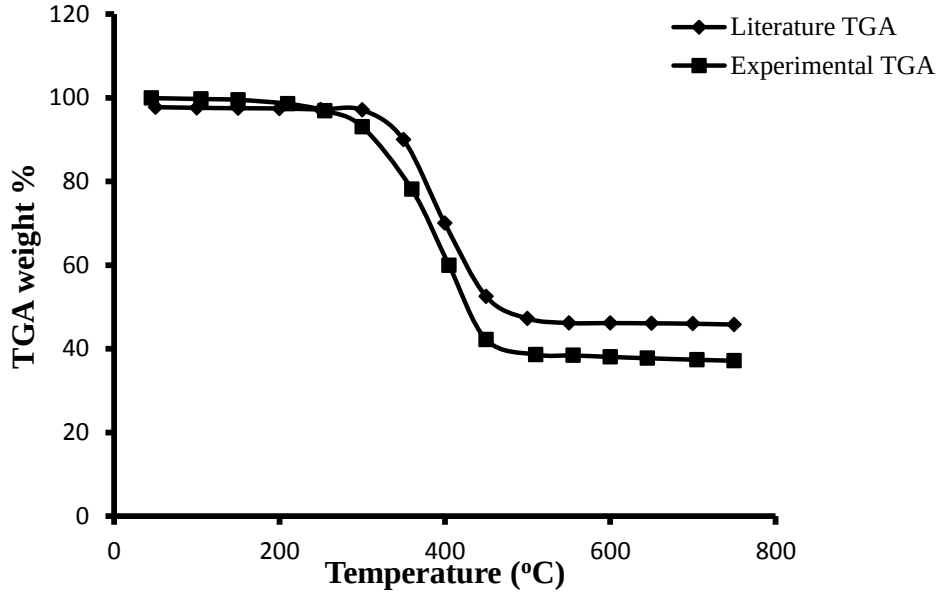

Figure 4.56: TGA curve of UT weight loss versus temperature at 15°C/min heating rate (where (A) is experimental data of this work, while (B) is data from literature [56]

As a result, this makes it difficult to study the weight change of a material as it degrades with time at a fixed temperature using the TGA. This section is therefore aimed at developing a mathematical model to adopt TGA as a dynamic apparatus to predict weight change of a material as it degrades with time at a fixed temperature. Thus experimental data from TGA (presented in Appendix E, Table E11) can be used to simulate the thermal degradation behavior of used tyres with changes in time at a particular temperature.

The degradation process as shown in Figure 4.57 is assumed to pass through three phases for the purpose of proper mathematical modeling. The phases are all assumed to be piece-wise continuous mathematically since the end of a phase is the beginning of the succeeding phase. The phases were classified into three time zones $0 \leq t \leq t_1$, $t_1 \leq t \leq t_2$ and $t \leq t_2$ for t_2 being a large time.

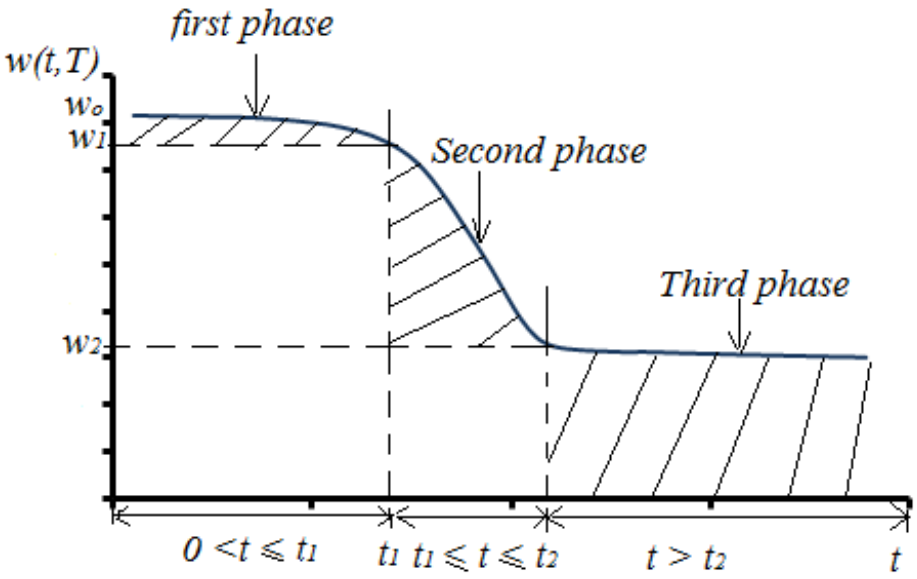

Figure 4.57: Three phase thermal degradation of weight change with time

Mathematical Derivation

First phase degradation model derivation:

$$\frac{dw(t)}{dt} = \alpha(t)w(t) \tag{4.15}$$

Equation (4.15) defines the relationship between changes in weight with time where

$$\alpha(t) = -\sigma_1 t T_0 + c_1 \tag{4.16}$$

and $\sigma_1>0$, is the rate of change (in degradation) at a fixed temperature, T_0, at this phase.

Imposing the initial condition $\alpha(0) = 0$ gives $c_1 = 0$

$$\therefore \alpha(t) = -\sigma_1 t T$$

Substituting for c_1 in equation 4.16,

$$\therefore \alpha(t) = -\sigma_1 t T_0 \tag{4.17}$$

Substituting equation (4.17) into equation (4.15) gives

$$\frac{dw(t)}{dt} = -\sigma_1 t T_0 w(t)$$

$$\int_0^t \frac{dw(t)}{w(t)} = \int_0^t (-\sigma_1 t T_0) dt$$

$$\ln w(t) = -\sigma_1 \frac{t^2 T_0}{2} + c_1$$

Taking the exponential of both sides,

$$w(t) = e^{(-\sigma_1 \frac{t^2 T_0}{2} + c_1)} \qquad \text{Where } A = e^{c_1}$$

$$\therefore w(t) = Ae^{-\sigma_1 \frac{t^2 T_0}{2}}$$

At $t = 0$, $\quad w(t) = w(0) = w_0 = Ae^0$

$$\Rightarrow A = w_0$$

$$\therefore w(t) = w_0 e^{-\sigma_1 \frac{t^2 T_0}{2}} \tag{4.18}$$

Equation 4.18 is the general model equation for the first phase of degradation (weight loss of rubber with time) at a fixed Temperature, T_0.

At boundary conditions, $w(t_1) = w_1 = w_0 \beta_1$ where $0 \le \beta_1 \le 1$ represents the proportion of the overall weight (w_0) remaining at time t_1

Simplifying,

$$-\sigma_1 \frac{t_1^{\,2}}{2} T_0 = \ln \beta_1$$

$$\sigma_1 = \frac{-2 \ln \beta_1}{t_1^{\,2} T_0} \tag{4.19}$$

Recall from equation (4.14) that at $t = t_1$,

$$T_1 = T(t_1) = \theta t_1 + T_0$$

Then for a fixed temperature, heating rate, $\theta = 0$

$$\Rightarrow T_1 = T_0$$

So, T_1 can be substituted for T_0 in equation 4.19

Second phase degradation model derivation:

At this phase, the weight loss with time is described to have satisfied a logistic model equation of the form:

$$\frac{dw}{dt} \propto T(t)\left(1-\frac{w}{k}\right)w \tag{4.20}$$

With a minimal weight value, k, where $T(t) = \theta t + T_0$

Introducing constant of proportionality, σ_2, equation (4.20) becomes

$$\frac{dw}{dt} = \sigma_2 T(t)\left(1-\frac{w}{k}\right)w \tag{4.21}$$

Expanding equation 4.21 gives

$$\frac{dw}{dt} = \sigma_2 T(t)w - \frac{\sigma_2 T(t)w^2}{k}$$

$$\frac{dw}{dt} - \sigma_2 T(t)w = \frac{-\sigma_2 T(t)w^2}{k} \tag{4.22}$$

The first order Non-homogenous Non linear ordinary differential equation (4.22) that is non linear in $w(t)$, was linearized using the method of change of variable. Let

$$v = \frac{1}{w} = w^{-1}$$

$$\therefore \frac{dv}{dw} = -w^{-2}$$

By chain rule,

$$\frac{dv}{dt} = \frac{dv}{dw}\frac{dw}{dt} = \frac{dw}{dt} = (\frac{dv}{dt}) / (\frac{dv}{dw})$$

$$\frac{dw}{dt} = -w^2(\frac{dv}{dt}) = -(\frac{1}{v^2})(\frac{dv}{dt}) \tag{4.23}$$

Substituting equation (4.23) into equation (4.22),

$$-\frac{1}{v^2}(\frac{dv}{dt}) - \sigma_2 T(t)\frac{1}{v} = \frac{-\sigma_2 T(t)}{kv^2} \tag{4.24}$$

Multiplying both sides of equation (4.24) by $-v^2$,

$$\frac{dv}{dt} + \sigma_2 T(t)v = \frac{\sigma_2 T(t)}{k} \tag{4.25}$$

Using technique of integrating factor for a first order differential equation of the form,

$$\frac{dv}{dt} + p(t)v = q(t)$$

Where integrating factor,

$$\mu(t) = e^{\int p(t)dt} = e^{\sigma_2 \int T(t)dt} = e^{\sigma_2 \int (\theta t + T_0)dt}$$

$\mu(t) = e^{\sigma_2(\frac{\theta t^2}{2} + T_0 t)}$, and $q(t) = \frac{\sigma_2 T(t)}{k}$

By change of variable method, let $z(t) = \frac{\theta t^2}{2} + T_0 t$

Using $v(t) = \frac{1}{\mu(t)}[\int^t \mu(t) q(t) dt + c_3]$ (4.26)

Substituting for $\mu(t)$ and $q(t)$ in equation (4.26),

$$v(t) = e^{-\sigma_2 z}[\int^t e^{\sigma_2 z(t)} \frac{\sigma_2 T(t)}{k} dt + c_3]$$

$$v(t) = e^{-\sigma_2 z}\left[\int e^{\sigma_2 z} \frac{\sigma_2 T(t)}{k} dt + c_3\right] \quad (4.27)$$

From $z(t) = \frac{\theta t^2}{2} + T_0 t$

$$\frac{dz}{dt} = \theta t + T_0$$

$$dt = \frac{dz}{(\theta t + T_0)}$$

Substituting for $d(t)$ in equation (4.27),

$$v(t) = e^{-\sigma_2 z}\left[\int^z e^{\sigma_2 z} \frac{\sigma_2 (\theta t + T_0)}{k} \frac{dz}{(\theta t + T_0)} + c_3\right]$$

$$v(t) = e^{-\sigma_2 z}\left[\frac{1}{k}\int^{z} e^{\sigma_2 z}\sigma_2 dz + c_3\right]$$

$$v(t) = e^{-\sigma_2 z}\left[\frac{\sigma_2}{k}\int^{z} e^{\sigma_2 z} dz + c_3\right]$$

$$v(t) = e^{-\sigma_2 z}\left[\frac{e^{\sigma_2 z}}{k} + c_3\right]$$

$$v(t) = \left[\frac{1 + c_4 k e^{-\sigma_2 z}}{k}\right] \quad \text{Where } c_4 = c_3 e^{-\sigma_2 z} \tag{4.28}$$

Recall, $w(t) = \frac{1}{v(t)}$

$$\therefore w(t) = \frac{k}{(1 + k c_4 e^{-\sigma_2 z})} \tag{4.29}$$

Imposing initial conditions, $z_1 = z(t_1), w(z_1) = w(z(t_1))$

$$w_1 = \frac{k}{(1 + k c_4 e^{-\sigma_2 z})} \tag{4.30}$$

Making c_4 subject of formula, equation (4.30) becomes

$$c_4 = \frac{(k - w_1)e^{\sigma_2 z_1}}{k w_1} \tag{4.31}$$

Substituting equation (4.31) into (4.29)

$$w(t) = \frac{k}{1 + \frac{(k - w_1)e^{\sigma_2 z_1} k e^{-\sigma_2 z}}{k w_1}} \tag{4.32}$$

Multiplying through with w_1, equation (4.32) becomes

$$w(t) = \frac{w_1 k}{w_1 + (k - w_1)e^{-\sigma_2 (z - z_1)}} \tag{4.33}$$

Recall,

$$z(t) = z = \frac{\theta t^2}{2} + T_0 t$$

$$z(t_1) = z_1 = \frac{\theta t_1^{\,2}}{2} + T_0 t_1$$

$$\therefore z(t) - z(t_1) = z - z_1 = \frac{\theta (t^2 - t_1^2)}{2} + T_0 (t - t_1) \tag{4.34}$$

Substituting equation (4.34) into equation (4.33) and simplifying,

$$w(t) = \frac{\beta_1 w_0 k}{\beta_1 w_0 + (k - \beta_1 w_0)e^{-\sigma_2 (\frac{\theta}{2}(t^2 - t_1^2) + T_0 (t - t_1))}} \tag{4.35}$$

For a fixed temperature, θ which is the heating rate = 0, equation (4.35) becomes,

$$w(t) = \frac{\beta_1 w_0 k}{\beta_1 w_0 + (k - \beta_1 w_0)e^{-\sigma_2 T_0 (t - t_1)}} \tag{4.36}$$

Equation (4.36) is the general model equation for the second phase of degradation (weight loss of rubber with time) at a fixed TemperatureT_0.

In order to determine σ_2, the rate of weight loss with time for the second phase, where $\sigma_2 > 0$, it is assumed that weight loss at $w(t_2) = w_2$,

$$w(t) = w_2 = w_0\beta_2 = \frac{\beta_1 w_0 k}{\beta_1 w_0 + (k - \beta_1 w_0)e^{-\sigma_2 T_0 (t_2 - t_1)}}$$

Cross multiply,

$$w_0\beta_1 + (k - w_0\beta_1)e^{-\sigma_2 T_0 (t_2 - t_1)} = \frac{w_0\beta_1 k}{w_0\beta_2}$$

$$(k - w_0\beta_1)e^{-\sigma_2 T_0 (t_2 - t_1)} = \frac{\beta_1 k}{\beta_2} - w_0\beta_1$$

$$e^{-\sigma_2 T_0 (t_2 - t_1)} = \frac{\beta_1 (k - \beta_2 w_0)}{\beta_2 (k - \beta_1 w_0)}$$

$$-\sigma_2 T_0 (t_2 - t_1) = \ln\left[\frac{\beta_1 (k - \beta_2 w_0)}{\beta_2 (k - \beta_1 w_0)}\right]$$

$$\therefore \sigma_2 = \frac{-1}{T_0 (t_2 - t_1)} \ln\left[\frac{\beta_1 (k - \beta_2 w_0)}{\beta_2 (k - \beta_1 w_0)}\right] \qquad (4.37)$$

Third phase degradation model derivation

At this phase, it is assumed that the limit of weight loss (for the general equation 4.36) is as t tends to ∞

$$\lim_{t\to\infty} w(t) = \lim_{t\to\infty} \frac{\beta_1 w_0 k}{\beta_1 w_0 + (k - \beta_1 w_0)e^{-\sigma_2 T_0 (t_2 - t_1)}}$$

$$= \frac{\beta_1 w_0 k}{\beta_1 w_0 + 0} = k$$

This implies that at the third phase, k is the value at which change in weight loss with time is negligible

Thus mathematically, $k = |w_{k+1} - w_k| \to 0$

Model application and interpretation

Figure 4.58 was drawn using the UT weight change with time for different fixed temperature using the first phase model equation (4.18), the second phase model equation (4.36) and given that $w(t) \to k$ as t tends to ∞. Python programming language was used to generate the plotted data for varying temperature (as presented in Appendix E, Table E12) from the general equation of the different degradation phases.

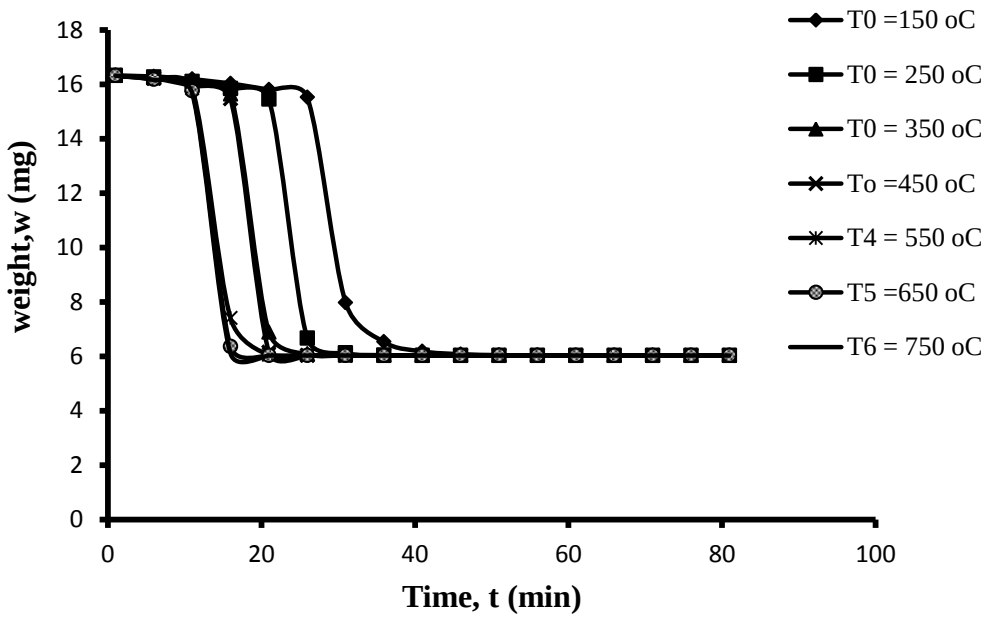

Figure 4.58: First, second and third phase weight loss versus time at different fixed temperature

At the first phase, w_o which is the initial weight of the UT, t_1 the total time for the first phase of degradation and any fixed temperature, $T_i \in i = 0,1,2,3...n$ were used where w_0 and t_1 are known values from the TGA. Also, it is assumed that weight changes occur with every other temperature at the same rate of σ_1 calculated from equation (4.19) at β_1 (weight fraction remaining at the end of first phase obtained from the TGA) and T_0. The second phase also has the same rate of σ_2 calculated from equation (4.37). The value of t_2, which is the total time for the completion of the second phase, was gotten from the TGA as well. Once these values of σ_1, and σ_2 are known, the time for the completion of the first phase and second phase degradation for the other different fixed temperatures were derived by making time t_1 and t_2 subject of formula in equation (4.19) and (4.37). Table 4.15 shows the calculated completion time, t_1 and t_2 for the different fixed temperature with known values of w_o = 16.32 mg, $\sigma_1 = 1.07 \times 10^{-6}$ and $\sigma_2 = 1.534 \times 10^{-3}$

Table 4.15: First and second phase total degradation time for different fixed temperature

Time (min)	T_o (150 ^oC)	T_1 (250 ^oC)	T_2 (350 ^oC)	T_3 (450 ^oC)	T_4 (550 ^oC)	T_5 (650 ^oC)	T_6 (750 ^oC)
t_1	25.97	20.12	17.00	14.99	13.56	12.48	11.61
t_2	75.65	55.78	47.26	42.53	39.52	37.43	35.91

From Figure 4.58, the degradation of the material occurred faster as the value of the fixed temperature increases. This is in accordance with the reduction in the completion time of degradation (from Table 4.15) for the first and second phases as the value of the fixed temperature increases.

The graph of the experimental TGA and the model is shown in Figure 4.59. Although that of the experimental TGA weight change occurred with time at a linear rate with temperature, the model which varied with time at different fixed temperature displayed similarity in weight degradation behaviour.

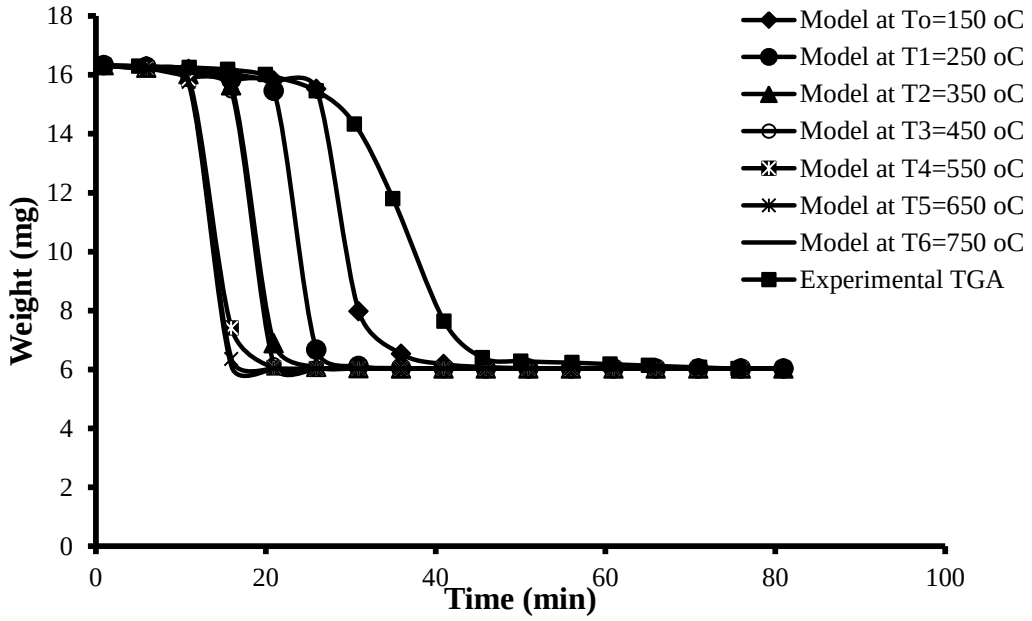

Figure 4.59: First, second and third phase weight loss versus time at different fixed temperature with the experimental TGA

This similarity in pattern between the experimental TGA and the model will enable the prediction of the material weight over a certain time for any fixed temperature using the model. For instance, when the initial weight of UT (16.32 mg) for a temperature of 450 ^{o}C in the TGA was compared with the predicted weight at a fixed temperature of 450 ^{o}C in the theoretical data generated using the mathematical model; it was 6.89 mg after 42.52 min while the weight of 6.54 mg was recorded after 18 min. This is probably due to the material being exposed to a higher temperature (450 ^{o}C) from the very onset of the degradation unlike in the case of the TGA where the material was gradually heated at a steady heating rate from a low temperature till it got to 450 ^{o}C. Therefore, in terms of percentage with reference to proportion of weight loss over time, it took 42.52 min for the material to lose 57.78% using the TGA while the material had a predicted weight loss of 60% after 18 min, a considerable shorter time at a fixed temperature of 450 ^{o}C.

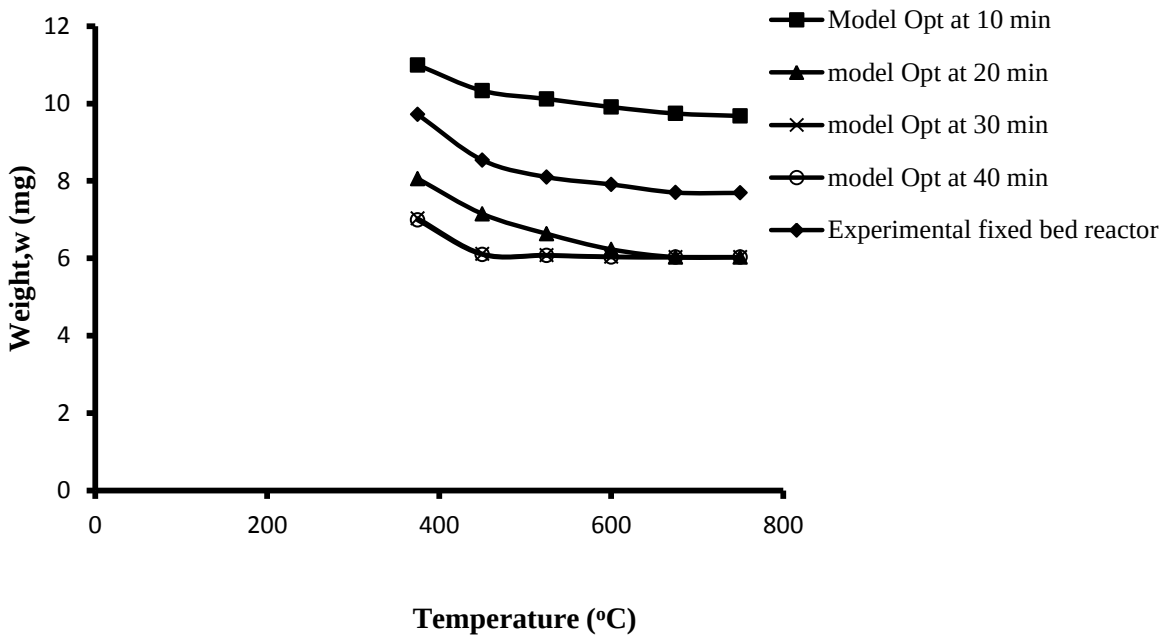

Figure 4.60: UT Weight against temperature for the model fixed operating time and the experimental in a fixed bed reactor

Furthermore, the weight change that occurred in the fixed bed reactor used for the pyrolysis of UT, experimental data were plotted against different operating model time, (Opt) as shown in Figure 4.60. The experimental weight loss had a characteristic pattern fitted closely to the second phase degradation of the mathematical model. In order to predict an optimum operating time for the pyrolysis, standard deviation (STD) was calculated between the model and the experimental data as presented in Table 4.16.

Table 4.16: Standard deviation of model from experimental data at different operating time

Tempt (^oC)	Experimental weight, w (mg)	Weight, w for opt of 10 min	Weight, w for opt of 20 min	Weight, w for opt of 30 min	Weight, w for opt of 40 min
375	9.72	10.99	8.06	7.03	6.98
450	8.54	10.33	7.15	6.11	6.09
525	8.10	10.11	6.63	6.08	6.07
600	7.91	9.90	6.23	6.04	6.03
675	7.70	9.74	6.03	6.03	6.03
750	7.69	9.67	6.03	6.03	6.03
STD		1.14	1.11	1.22	1.23

An operating time of 20 minutes gave the least STD between the mathematical model and the experimental data. Thus it can be predicted mathematically that the optimum time of 20 minutes is suitable for the fixed bed pyrolysis.

Therefore the mathematical model can be used to predict weight with time at a fixed temperature using some known parameters from the TGA and the optimum operating time for pyrolysis in the fixed bed reactor.

References

[1] Kovo, A.S., 2011. Development of Zeolites and Zeolite Membranes from Ahoko Nigerian Kaolin. **(**Doctoral dissertation, *University of Manchester,* Manchester, UK)

[2] Chandrasekhar, S. and Pramada, P.N., 2004. Kaolin-based zeolite Y, a precursor for cordierite ceramics. *Applied Clay Science*, *27*(3), pp. 187-198.

[3] Zi, G., Dake, T. and Ruiming, Z., 1988. Hydrothermal crystallization of zeolite Y from Na_2O-Fe_2O_3-Al_2O_3-SiO_2-H_2O system. *Zeolites*, *8*(6), pp. 453-457.

[4] Franco, F., Pérez-Maqueda, L.A. and Pérez-Rodrí, J.L., 2003. The influence of ultrasound on the thermal behaviour of a well ordered kaolinite.*Thermochimica Acta*, *404*(1), pp.71-79

[5] Sang, S., Liu, Z., Tian, P., Liu, Z., Qu, L. and Zhang, Y., 2006. Synthesis of small crystals zeolite NaY. *Materials Letters*, *60*(9), pp. 1131-1133.

[6] González, J.F., Encinar, J.M., Canito, J.L. and Rodríguez, J.J., 2001. Pyrolysis of automobile tyre waste. Influence of operating variables and kinetics study. *Journal of Analytical and Applied Pyrolysis*, *58*, pp. 667-683.

[7] Chang, Y.M., 1996. On pyrolysis of waste tyre: degradation rate and product yields. *Resources, Conservation and Recycling*, *17*(2), pp. 125-139.

[8] Juma, M., Koreňová, Z., Markoš, J., Annus, J. and Jelemenský, L., 2006. Pyrolysis and combustion of scrap tyre. *Petroleum and Coal*, *48*(1), pp. 15-26.

[9] Islam, M.R., Tushar, M.S.H.K. and Haniu, H., 2008. Production of liquid fuels and chemicals from pyrolysis of Bangladeshi bicycle/rickshaw tyre wastes. *Journal of Analytical and Applied Pyrolysis*, *82*(1), pp. 96-109.

[10] Kar, Y., 2011. Catalytic pyrolysis of car tyre waste using expanded perlite. *Waste Management*, *31*(8), pp. 1772-1782.

[11] Williams, P.T., 2013. Pyrolysis of waste tyres: a review. *Waste Management*, *33*(8), pp.1714-1728.

[12] Quek, A. and Balasubramanian, R., 2013. Liquefaction of waste tyres by pyrolysis for oil and chemicals—a review. *Journal of Analytical and Applied Pyrolysis*, *101*, pp.1-16.

[13] Karthikeyan, S., Sathiskumar, C. and Moorthy, R.S., 2012. Effect of process parameters on tyre pyrolysis: a review. *Journal of Scientific and Industrial Research*, *71*(5), pp. 309-315.

[14] Haydary, J., Koreňová, Z., Jelemenský, Ľ. and Markoš, J., 2008. Thermal decomposition of waste polymers. *Thermophysics 2008*, pp. 62.

[15] Juma, M., Koreňová, Z., Markoš, J., Jelemensky, L. and Bafrnec, M., 2007. Experimental study of pyrolysis and combustion of scrap tyre. *Polymers for Advanced Technologies*, *18*(2), pp. 144-148.

[16] Williams, P.T., Besler, S. and Taylor, D.T., 1990. The pyrolysis of scrap automotive tyres: The influence of temperature and heating rate on product composition. *Fuel*, *69*(12), pp. 1474-1482.

[17] Pradhan, D. and Singh, R.K., 2011. Thermal pyrolysis of bicycle waste tyre using batch reactor. *International Journal of Chemical Engineering and Applications*, *2*(5), pp. 332.

[18] Cypres, R. and Bettens, B., 1989. Production of benzoles and active carbon from waste rubber and plastic materials by means of pyrolysis with simultaneous post-cracking. *Pyrolysis and Gasification*, pp. 209-229.

[19] Cunliffe, A.M. and Williams, P.T., 1998. Composition of oils derived from the batch pyrolysis of tyres. *Journal of Analytical and Applied Pyrolysis*, *44*(2), pp. 131-152.

[20] Asadullah, M., Rahman, M.A., Ali, M.M., Rahman, M.S., Motin, M.A., Sultan, M.B. and Alam, M.R., 2007. Production of bio-oil from fixed bed pyrolysis of bagasse. *Fuel*, *86*(16), pp. 2514-2520.

[21] Bridgwater, A.V., 1999. Principles and practice of biomass fast pyrolysis processes for liquids. *Journal of Analytical and Applied Pyrolysis*, *51*(1), pp. 3-22.

[22] Shen, B., Wu, C., Wang, R., Guo, B. and Liang, C., 2006. Pyrolysis of scrap tyres with zeolite USY. *Journal of Hazardous Materials*, *137*(2), pp.1065-1073.

[23] Williams, P.T. and Brindle, A.J., 2003. Aromatic chemicals from the catalytic pyrolysis of scrap tyres. *Journal of Analytical and Applied Pyrolysis*, *67*(1), pp.143-164.

[24] Roy, C and Unsworth, J., 1989. Pilot plant demonstration of used tyres vacuum pyrolysis. In Pyrolysis and Gasification. *Elsevier Applied Science* London. pp. 180-189.

[25] Kawakami, S., Inoue, K., Tanaka, H. and Sakai, T., 1980. Pyrolysis process for scrap tyres. In *American Chemical Society Symposium Serminar;(United States)*, 130, No. CONF-790917-P5). Kobe Steel, Ltd., Japan.

[26] Martínez, J.D., Veses, A., Mastral, A.M., Murillo, R., Navarro, M.V., Puy, N., Artigues, A., Bartrolí, J. and García, T., 2014. Co-pyrolysis of biomass with waste tyres: upgrading of liquid bio-fuel. *Fuel Processing Technology*, *119*, pp. 263-271.

[27] Frigo, S., Seggiani, M., Puccini, M. and Vitolo, S., 2014. Liquid fuel production from waste tyre pyrolysis and its utilisation in a Diesel engine. *Fuel*, *116*, pp. 399-408.

[28] Aguado, R., Olazar, M., Vélez, D., Arabiourrutia, M. and Bilbao, J., 2005. Kinetics of scrap tyre pyrolysis under fast heating conditions. *Journal of Analytical and Applied Pyrolysis*, *73*(2), pp. 290-298.

[29] Barbooti, M.M., Mohamed, T.J., Hussain, A.A. and Abas, F.O., 2004. Optimization of pyrolysis conditions of scrap tyres under inert gas atmosphere. *Journal of Analytical and Applied Pyrolysis*, *72*(1), pp. 165-170.

[30] Islam, M.R., Haniu, H. and Beg, M.R.A., 2008. Liquid fuels and chemicals from pyrolysis of motorcycle tyre waste: product yields, compositions and related properties. *Fuel*, *87*(13), pp. 3112-3122.

[31] Dai, X., Yin, X., Wu, C., Zhang, W. and Chen, Y., 2001. Pyrolysis of waste tyres in a circulating fluidized-bed reactor. *Energy*, *26*(4), pp. 385-399.

[32] Dombrovsky, L.A., Sazhin, S.S., Sazhina, E.M., Feng, G., Heikal, M.R., Bardsley, M.E.A. and Mikhalovsky, S.V., 2001. Heating and evaporation of semi-transparent diesel fuel droplets in the presence of thermal radiation. *Fuel*, *80*(11), pp. 1535-1544.

[33] Brammer, J.G. and Bridgwater, A.V., 1999. Drying technologies for an integrated gasification bio-energy plant. *Renewable and Sustainable Energy Reviews*, *3*(4), pp. 243-289.

[34] Rofiqul, I.M., Haniu, H. and Rafiqul, A.B.M., 2007. Limonene-rich liquids from pyrolysis of heavy automotive tyre wastes. *Journal of Environment and Engineering*, *2*(4), pp. 681-695.

[35] Jahirul, M.I., Rasul, M.G., Chowdhury, A.A. and Ashwath, N., 2012. Biofuels production through biomass pyrolysis—a technological review. *Energies*, *5*(12), pp.4952-5001.

[36] Undri, A., Rosi, L., Frediani, M. and Frediani, P., 2014. Upgraded fuel from microwave assisted pyrolysis of waste tyre. *Fuel*, *115*, pp. 600-608.

[37] Boxiong, S., Chunfei, W., Cai, L., Binbin, G. and Rui, W., 2007. Pyrolysis of waste tyres: The influence of USY catalyst/tyre ratio on products. *Journal of Analytical and Applied Pyrolysis*, *78*(2), pp. 243-249.

[38] de Marco Rodriguez, I., Laresgoiti, M.F., Cabrero, M.A., Torres, A., Chomon, M.J. and Caballero, B., 2001. Pyrolysis of scrap tyres. *Fuel Processing Technology*, *72*(1), pp. 9-22.

[39] Kyari, M., Cunliffe, A. and Williams, P.T., 2005. Characterization of oils, gases, and char in relation to the pyrolysis of different brands of scrap automotive tyres. *Energy and Fuels*, *19*(3), pp.1165-1173.

[40] Pakdel, H., Pantea, D.M. and Roy, C., 2001. Production of dl-limonene by vacuum pyrolysis of used tyres. *Journal of Analytical and Applied Pyrolysis*, *57*(1), pp. 91-107.

[41] Pakdel, H., Roy, C., Aubin, H., Jean, G. and Coulombe, S., 1991. Formation of dl-limonene in used tyre vacuum pyrolysis oils. *Environmental Science and Technology*, *25*(9), pp.1646-1649.

[42] Pakdel, H. and Roy, C., 2003. Recovery of bitumen by vacuum pyrolysis of Alberta tar sands. *Energy and Fuels*, *17*(5), pp.1145-1152.

[43] Laresgoiti, M.F., Caballero, B.M., de Marco, I., Torres, A., Cabrero, M.A. and Chomón, M.J., 2004. Characterization of the liquid products obtained in tyre pyrolysis. *Journal of Analytical and Applied Pyrolysis*, *71*(2), pp. 917-934.

[44] Ucar, S., Karagoz, S., Ozkan, A.R. and Yanik, J., 2005. Evaluation of two different scrap tyres as hydrocarbon source by pyrolysis. *Fuel*, *84*(14), pp.1884-1892.

[45] Li, S.Q., Yao, Q., Chi, Y., Yan, J.H. and Cen, K.F., 2004. Pilot-scale pyrolysis of scrap tyres in a continuous rotary kiln reactor. *Industrial and Engineering Chemistry Research*, *43*(17), pp. 5133-5145.

[46] Chen, J.H., Chen, K.S. and Tong, L.Y., 2001. On the pyrolysis kinetics of scrap automotive tyres. *Journal of Hazardous Materials*, *84*(1), pp. 43-55.

[47] Llompart, M., Sanchez-Prado, L., Lamas, J.P., Garcia-Jares, C., Roca, E. and Dagnac, T., 2013. Hazardous organic chemicals in rubber recycled tyre playgrounds and pavers. *Chemosphere*, *90*(2), pp. 423-431.

[48] Olazar, M., Lopez, G., Arabiourrutia, M., Elordi, G., Aguado, R. and Bilbao, J., 2008. Kinetic modelling of tyre pyrolysis in a conical spouted bed reactor. *Journal of Analytical and Applied Pyrolysis*, *81*(1), pp. 127-132.

[49] Ceylan, S. and Topçu, Y., 2014. Pyrolysis kinetics of hazelnut husk using thermogravimetric analysis. *Bioresource Technology*, *156*, pp. 182-188.

[50] Gersten J, Fainberg V, Hetsroni G, Shindler Y. Kinetic study of the thermal decomposition of polypropylene, oil shale, and their mixture. *Fuel*, *79*(13), pp.1679-86.

[51] Rotliwala, Y.C. and Parikh, P.A., 2011. Thermal degradation of rice-bran with high density polyethylene: A kinetic study. *Korean Journal of Chemical Engineering*, *28*(3), pp.788-792.

[52] Parekh, D.B., Rotliwala, Y.C. and Parikh, P.A., 2009. Synergetic pyrolysis of high density polyethylene and Jatropha and Karanj cakes: A thermogravimetric study. *Journal of Renewable and Sustainable Energy*,*1*(3), pp. 033107.

[53] Leung, D.Y.C. and Wang, C.L., 1998. Kinetic study of scrap tyre pyrolysis and combustion. *Journal of Analytical and Applied Pyrolysis*, *45*(2), pp.153-169.

[54] Pilusa, T.J., Shukla, M. and Muzenda, E., 2013. Tyre Derived Fuel as an Alternative fuel for CI engines. *International Conference on Environment, Agriculture and Food Sciences (ICEAFS'2013)* Kuala Lumpur, Malaysia.

[55] Deenanath, E.D., 2014. Production and characterization of bioethanol derived from cashew apple juice for use in internal combustion engine. (Doctoral dissertation, *University of the Witwatersrand*, Johannesburg,South Africa).

[56] Ayanoğlu, A. and Yumrutaş, R., 2016. Production of gasoline and diesel like fuels from waste tyre oil by using catalytic pyrolysis. *Energy*, *103*, pp. 456-468.

CHAPTER 5

CONCLUSION AND RECOMMENDATIONS

5.1 Conclusion

A comparative study between pyrolytic oil obtained from used tyres and natural rubber (*Hevea brasiliensis*) was investigated. In order to have an optimum condition, pyrolysis process was studied for a feed particle size of 2, 4, 6, 8 and 10 mm and for an operating temperature range of 375 to 750 ^{o}C at a heating rate of 15 ^{o}C. The concentration of catalyst: feedstock ratio of 1, 2.5, 5, 6, 7.5 and 10 % was used for the catalytic pyrolysis. The zeolite NaY catalyst used for the catalytic pyrolysis was synthesised using Lawani Benin River Nigeria kaolin (LBK) as the source for silica and alumina. The produced pyrolytic oil was distilled and blended with commercial petrol in different ratios of 0, 5, 10, 15 and 20 % which were then tested in a spark ignition combustion engine.

Although pyrolytic oil was produced at different temperatures, an optimum yield was obtained at an operating temperature of 600 ^{o}C at a heating rate of 15^{o}C/min for a feed size of 6 mm. The used tyres and natural rubber gave maximum pyrolytic oil yield of 34.40 ± 2.18 and 75.93 ± 2.88 wt. % respectively. A maximum pyrolytic oil yield of 21.80 ± 2.42 and 65.87 ± 0.73 wt. % was obtained at catalyst: feedstock of 7.5 % concentration for catalytic pyrolysis of used tyres and natural rubber. Hence the zeolite NaY catalyst did not increase the yield of the pyrolytic oil from both studied materials. Nevertheless, its effect was seen on pyrolytic oil composition in terms of the biogasoline

range by the various particle sizes of the synthesised zeolites. The particle size of 0.648 nm obtained at 6 h ageing gave the highest biogasoline hydrocarbon yield of 85.73 wt. % which was higher than that obtained with the use of commercial zeolite NaY.

From the results, NR gave pyrolytic oil yield (75.93 ± 2.88 wt.%) which was almost thrice that obtained for the thermal pyrolysis of used tyres. This yield is almost twice the amount obtained from pyrolysis of used tyres and other polyisoprene based materials reported in literature. Also the low solid residue of 0.43 ± 0.12 wt. % observed for natural rubber relative to that of used tyres, 48.47 ± 0.29 wt. %, implies lower amount of char will need to be managed after the process.

From the physical properties such as density, viscosity, flash point, pour point, and HHV of pyrolytic oil produced from used tyres and natural rubber in this study, and their distillates, their properties were comparable with that of other pyrolytic liquids reported in literature by Islam et al (2008), Pradhan and Sighn (2011) and that of commercial diesel. This revealed that the materials can be a source of liquid fuel for energy. Also sulphur content which is a limiting factor in the direct combustion of UT pyrolytic liquid was absent in NR pyrolytic oil. This is an added advantage for NR pyrolytic oil in direct combustion.

The FTIR, NMR, and GC-MS analyses of both pyrolytic oil chemical properties, results revealed that the pyrolytic oil is a complex mixture of aliphatic and aromatic

hydrocarbons. The presence of carbon chain length of between C_5-C_{30} with majority being in the range of C_8-C_{10} was observed for NR and UT pyrolytic oil. The thermal and catalytic natural rubber pyrolytic oil had a lower amount of aromatic and PAHs, a main pollution source, than those of the used tyres pyrolytic oil. The presence of limonene an important industrial compound in high concentration of over 60% in natural rubber pyrolytic oil is an added advantage for the pyrolysis of natural rubber.

The distillates derived from the vacuum distillation of the different pyrolytic oil produced in this study presented a distillation temperature range of 50 to 175 ^{o}C for natural rubber pyrolytic oil and 30 to 251 ^{o}C for used tyres pyrolytic oil. Majority of the distillates were obtained at the temperature range similar to that of petrol and diesel. The GC-MS analysis results of the distillates also showed a composition of aliphatic and aromatics as the main compounds.

The combustion performance of the Pyrolytic oil distillates (from both pyrolytic oil) blended with commercial petrol combustion in a spark ignition petrol engine was operated successfully for the 5, 10, 15 and 20 % blend ratio without engine modification. For fuel consumption with respect to generator run time, it was observed that an optimum of 20 % NRPD-Petrol blend gave comparative fuel consumption behavior than the others with that of commercial petrol. The order of fuel consumption for the Pyrolytic oil distillates can be concluded as UZPD-Petrol blend >UTPD-Petrol blend >NZPD-Petrol blend >NRPD-Petrol blend.

From the outcome of the fuel power in the generator studied for the different distillates composition in the petrol blend, it was observed that as the concentration of the Pyrolytic oil distillates increased in the blended fuel, there was an increase in the generator fuel power. Also the optimum generator fuel power was obtained at the same composition of distillates that gave the optimum fuel consumption.

It can be concluded that the production of pyrolytic oil from natural rubber through pyrolysis had fuel properties that can make them serve as a source of alternative energy compared to that of used tyres. If further treatment is done on the pyrolytic oil and its distillates, it may serve as fuel alternative, additives and chemicals synthesis. This can also address the environmental issues that accompany the disposal of used tyres and reawaken the interest in natural rubber farming as a source of income. The Lawani Benin River Nigeria kaolin (LBK) used as a source for silica and alumina in the synthesis of zeolite NaY could open another economic channel for the beneficiation of the material.

A mathematical model which adopts thermogravimetry analyser (TGA) as a dynamic apparatus to predict weight change of a material as it degrades with time at a fixed temperature was developed. The proposed models phases were all assumed to be piece-wise continuous mathematically since the end of a phase is the beginning of the succeeding phase. The general model equation for the first phase of degradation was $w(t) = w_0 e^{-\sigma_1 \frac{t^2 T_0}{2}}$, while the second phase model was $w(t) = \frac{\beta_1 w_0 k}{\beta_1 w_0 + (k - \beta_1 w_0) e^{-\sigma_2 T_0 (t - t_1)}}$ and at the third phase, it was assumed that the limit of weight loss (in the second phase

equation) as t tends to ∞ gives a value k, at which change in weight loss with time is negligible. The proposed model was used to plot a graph of weight loss versus time at different fixed temperature which fitted well with the experimental TGA and fixed bed reactor.

5.2 Recommendations

Based on challenges encountered during the course of this study and the need to investigate beyond the set aim of this research, the following recommendations are made:

- Analysis of Pyrolytic oil distillates concentration of natural rubber and used tyres from 25 to 100% for generator fuel consumption and fuel power in petrol blend is recommended. This will assist in determining the further benefits of higher concentration of pyrolytic oil distillates compared to that already studied.
- Study of the effect of operating temperature on limonene presence in natural rubber at lower temperatures can be performed to get the optimum temperature for high limonene yield in natural rubber. Also the possible way of extracting such useful chemical compounds can be investigated.
- The distillation of the different pyrolytic oil using fractional distillation column at atmospheric pressure can give a better report of the various fractions obtainable form the pyrolytic oil at specific temperatures than that of the batch distillation method used in this study.

- An emission study from the combustion of the different pyrolytic oil distillates and petrol blend fuel in the generator can be performed to determine the environmental impact of such fuel mixture.

APPENDIX A

Zeolite NaY synthesis from Lawani river Benin kaolin (LBK) using external silica source

The synthesis of Zeolite NaY from the LBK Metakaolin using external silica source was performed using molar ratio stated in the Table below:

Constituent	Na_2O	SiO_2	Al_2O_3	H_2O
Verified molar ratio	15	15	1	450

Elements and their relative molecular weight are stated below;

Na = 22.99

Al = 26.98

O = 16

Si = 28.09

H = 1.01

Na_2O = 61.98

NaOH = 40.0

H_2O = 18.01

SiO_2 = 60.08

Al_2O_3 = 101.96

Na_2SiO_3 = 122.07

Using the SiO_2/Al_2O_3 ratio of the LBK metakaolin of approximately 3 obtained from the XRF analysis, the above molar ratio for the constituent can be rewritten to show the amount of additional silica provided by anhydrous Na_2SiO_3 in the table below;

Constituent	Na_2O	SiO_2	Al_2O_3	Additional Silica	H_2O
Verified molar ratio	15	3	1	12	450

From the table, the mass of the various constituents can be calculated as shown below;

Mass of LBK metakaolin

LBK metakaolin needed for the synthesis of Zeolite NaY is 282.2g.

Additional silica

The mass of additional Silica needed from external source was calculated based on the weight percent of the silica present in the Na_2SiO_3 used. The Na_2SiO_3 containing 47% SiO_2 and 52% NaO_2 that served as the external source of silica was supplied by Sigma-Aldrich.

Therefore, assuming 10g of Na_2SiO_3 was collected, this implies that 4.7g SiO_2 which is same as 0.078 mole SiO_2 is contained in it.

So, if 10g NA_2SiO_3 gives 0.078 mol of SiO_2 then xg is contained in 12 mol of SiO_2 for the extra silica.

Calculating for xg of Na_2SiO_3 by proportion gives 12 x 10/0.078 = 1538.46g of Na_2SiO_3

Since 52% of Na_2O is contained in Na_2SiO_3, this means that (52 x 1538.46)/100 = 799.99g Na_2O.

When expressed in mole it is 12.91 mol of Na_2O. This means that the use of Na_2SiO_3 provided additional 12.91 mol of Na_2O to the synthesis mixture. In to account for this extra, it must be subtracted from the recipe composition. Hence outstanding Na_2O is 15 – 12.91 = 2.09 mol.

Mass of Na_2O

NaOH pellet which is 99%w/w supplied by Sigma Aldrich was used as the source of Na_2O since Na_2O does not exist and is derived according to the equation:

$$Na_2O + H_2O \longrightarrow 2\ NaOH$$

This means the supplied Sodium hydroxide pellets gives 0.099 mol of water as shown on the balanced equation. This will also be subtracted from the water constituent in the mixture recipe.

Hence, if 1g of NaOH is collected, the actual NaOH collected is 0.99g which is same as 0.0248mol NaOH solute.

Using proportion, the corresponding mass equivalent to the amount of NaOH can be calculated.

Hence 1g ≡ 0.0248mol NaOH

xg = 4.18mol NaOH from outstanding Na_2O

This means 168.55g NaOH pellets is needed.

Mass of H_2O

Balance water is; 450 – 2.09 = 447.91mol H_2O ≡ 8066.86g H2O

Determined mass of constituent required for the zeolite Y synthesis is given below;

LBK metakaolin: 282.2g

Additional silica (Na_2SiO_3): 1538.46g

NaOH: 168.55g

H_2O: 8066.86g

The calculated individual quantity precursor needed for the zeolite NaY synthesis was then reduced using a multiplier factor of 28.59/8066.86 to get;

LBK metakaolin: 1g

Additional Silica (Na_2SiO_3): 5.45g

NaOH: 0.60g

H_2O: 28.59g

Appendix B

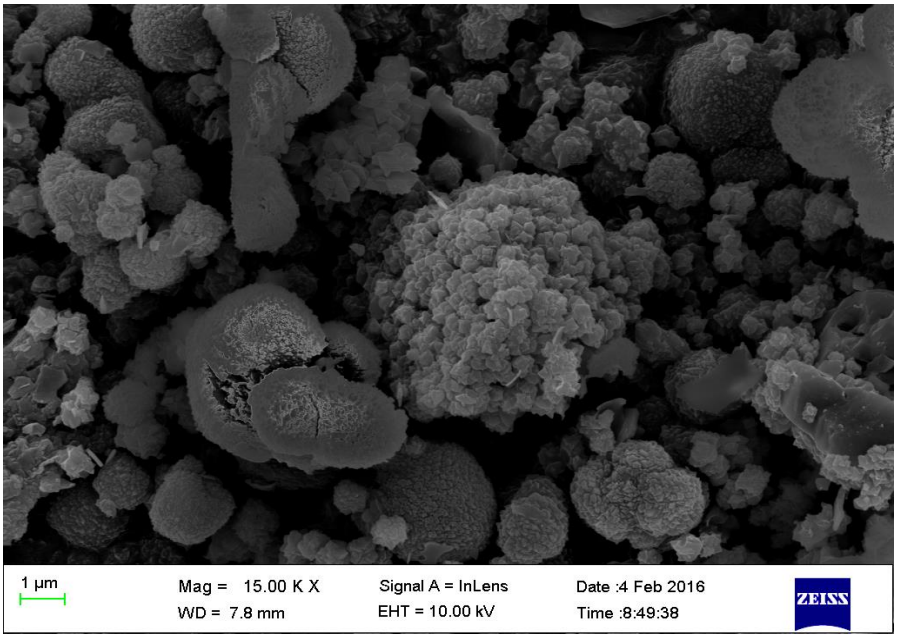

Figure B1: SEM image of 0 h ageing time synthesised zeolite NaY at a scale bar of 1 µm

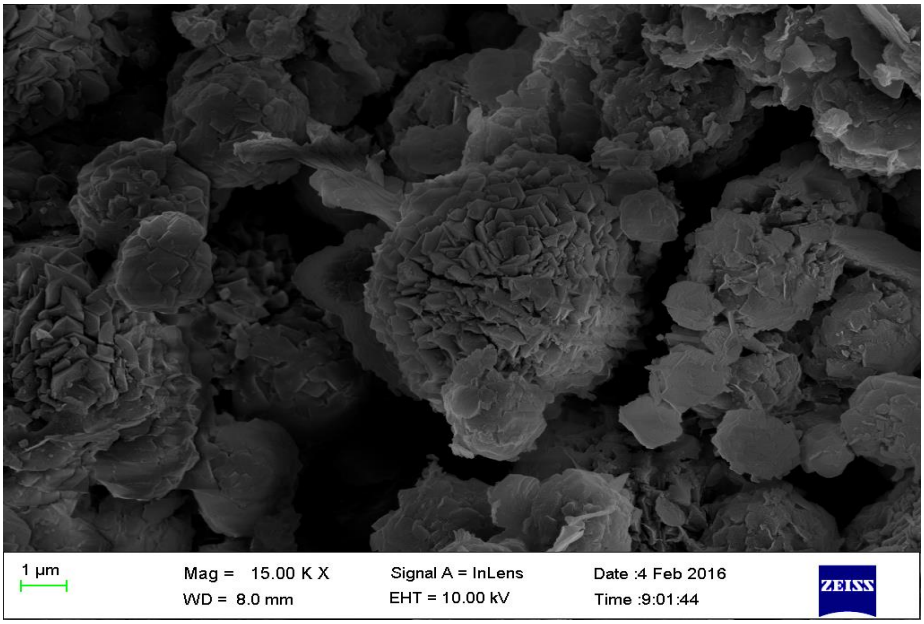

Figure B2: SEM image of 0.5 h ageing time synthesised zeolite NaY at a scale bar of 1 µm

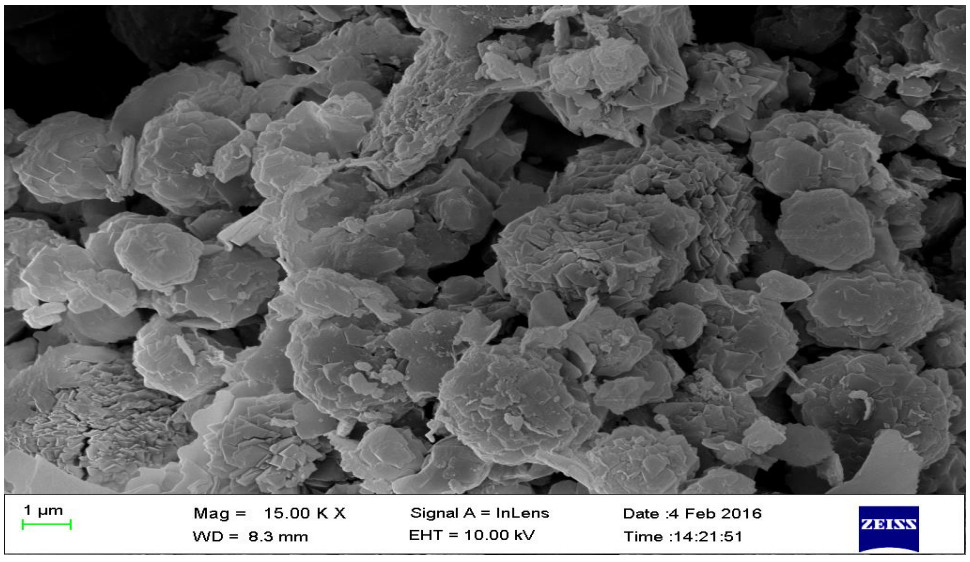

Figure B3: SEM image of 1 h ageing time synthesised zeolite NaY at a scale bar of 2 µm

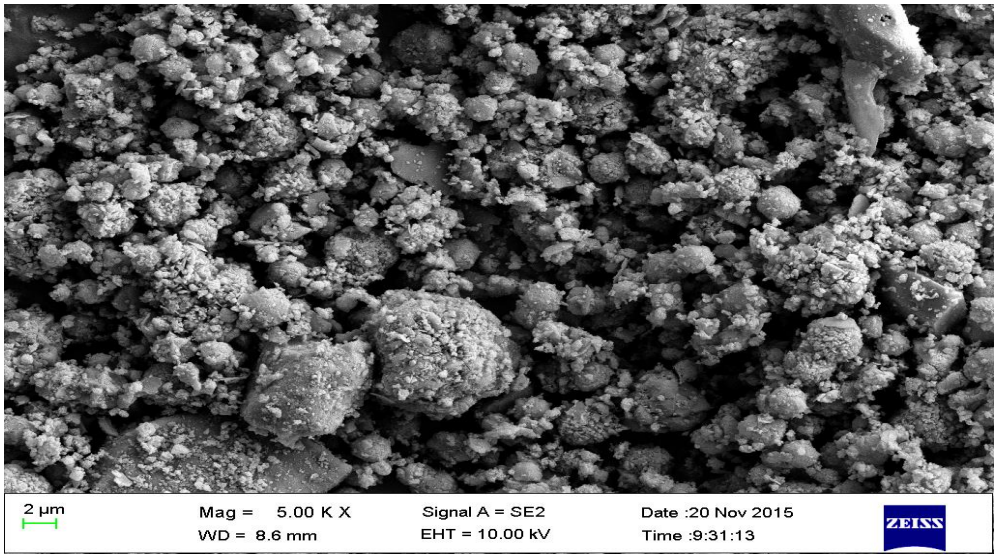

Figure B4: SEM image of 3hrs ageing time synthesised zeolite NaY at a scale bar of 2 µm

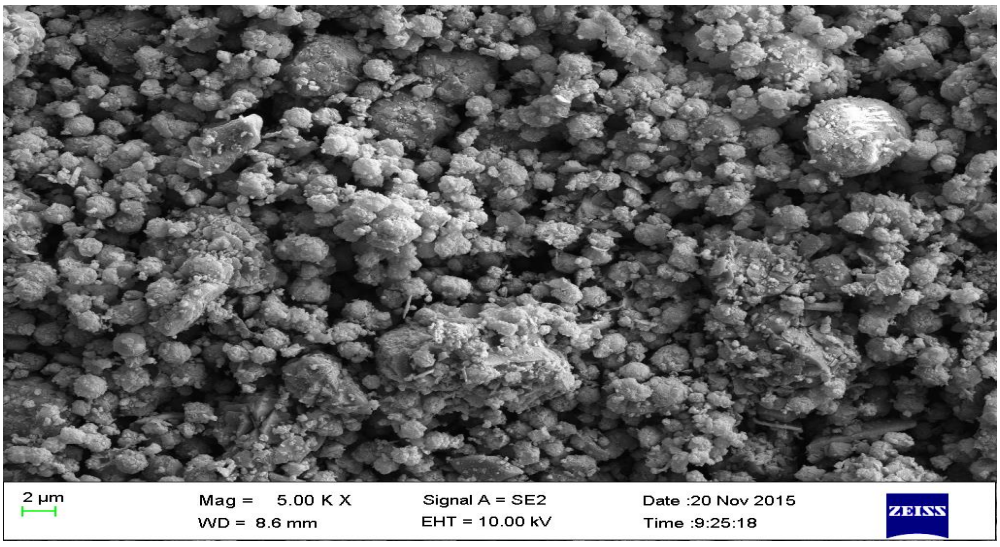

Figure B5: SEM image of 6hrs ageing time synthesised zeolite NaY at a scale bar of 2 µm

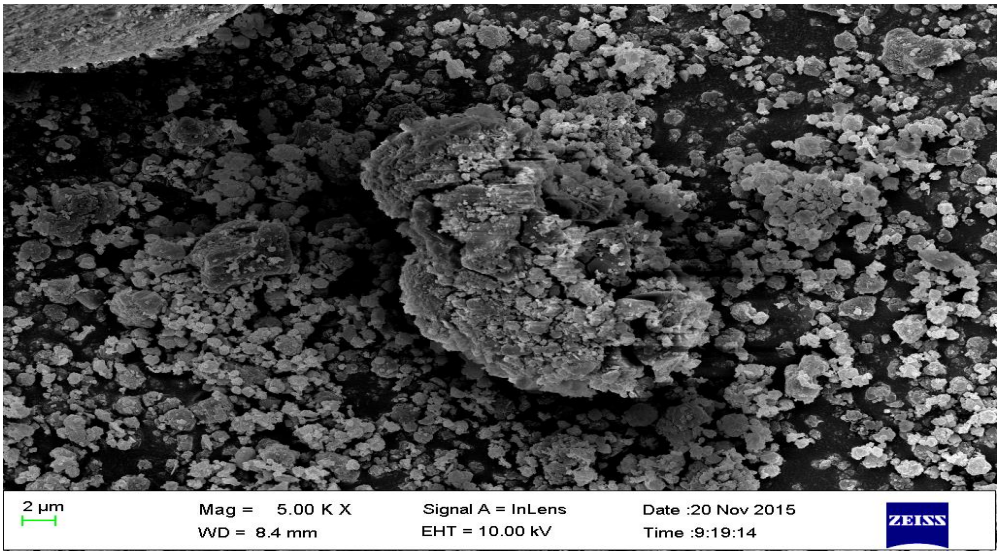

Figure B6: SEM image of 9hrs ageing time synthesised zeolite NaY at a scale bar of 2 µm

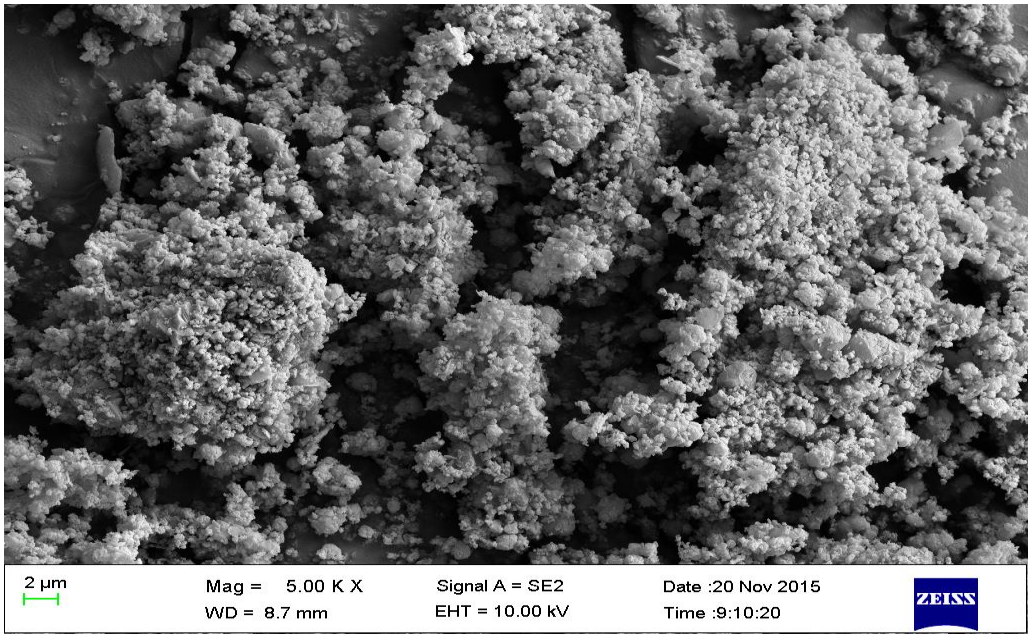

Figure B7: SEM image of 12hrs ageing time synthesised zeolite NaY at a scale bar of 2 µm

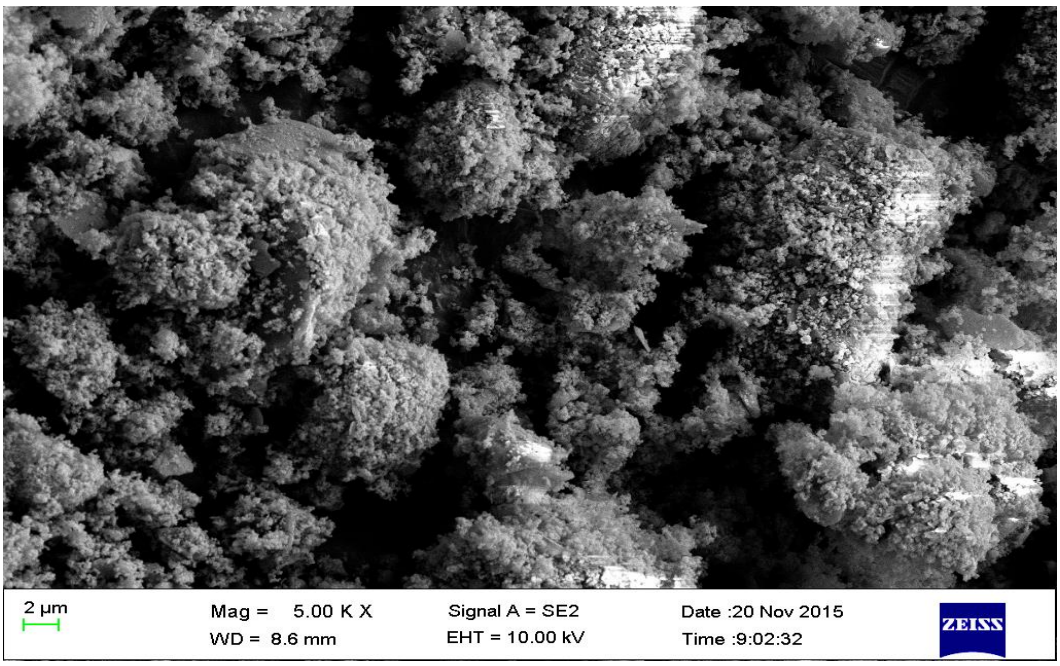

Figure B8: SEM image of 24hrs ageing time synthesised zeolite NaY at a scale bar of 2 µm

Table B1: Ageing effect on zeolite NaY particle size

Ageing (h)	Zeolite NaY Particle size (nm)
0	302 ± 0.11
0.5	455 ± 0.13
1	522 ± 0.10
3	603 ± 0.09
6	648 ± 0.10
9	652 ±0.17
12	669 ± 0.11
24	830 ± 0.12

Appendix C

Determination of optimum heating rate and operating temperature on the pyrolysis of used tyres and natural rubber products yield.

Fixed parameters:

Particle size = 2mm

Mass of sample = 10g

Table C1 Determination of optimum heating rate and operating temperature

	Operating Temperature (^oC)	Pyrolytic oil (wt. %)	Solid Char (wt. %)	Gas (wt. %)
Heating rate of 5°C/min	375	3.82 ± 1.91	54.10 ± 0.49	42.08 ± 2.11
	450	9.10 ± 1.20	46.28 ± 1.61	44.62 ± 0.55
	525	12.28 ± 0.74	41.81 ± 0.22	45.91 ± 0.10
	600	18.88 ± 0.11	37.79 ± 0.03	43.33 ±0.12
	675	14.45 ±1.05	36.89 ± 0.01	48.66 ± 0.64
	750	11.31 ±0.77	36.55 ± 0.05	52.14 ±0.22

	Operating Temperature (^oC)	Pyrolytic oil (wt. %)	Solid Char (wt. %)	Gas (wt. %)
Heating rate of 10°C/min	375	4.01 ± 1.10	53.79 ± 0.32	42.20 ± 2.01
	450	11.70 ± 0.55	44.57 ±0.41	43.73 ±0.66
	525	16.38 ±0.33	39.98 ±0.19	43.64 ±0.25
	600	22.89 ±0.10	34.36 ±0.44	42.75 ± 0.39
	675	16.44 ±0.11	33.89 ±1.21	49.67 ±0.89
	750	13.62 ±0.21	33.74 ±0.01	52.64 ±0.15

	Operating Temperature (^oC)	Pyrolytic oil (wt. %)	Solid char (wt. %)	Gas (wt. %)
Heating rate of 15°C/min)	375	4.24 ± 1.64	49.31 ± 0.17	46.45 ± 2.43
	450	14.22 ±0.32	42.05 ± 1.0	43.73 ±0.66
	525	20.61 ±0.11	38.40 ±0.14	40.99 ± 0.34
	600	24.5 ± 0.17	33.0± 0.10	42.5± 0.10
	675	18.32 ± 0.23	32.9± 0.54	48.78±0. 19
	750	10.95 ± 0.05	32.30 ± 0.15	56.75 ± 0.04

From the results on the Table above, the heating rate of 15^{o}C/min gave optimum yield of pyrolytic oil at particle size of 2mm and mass of 10g of sample pyrolysed.

This will be used to determine other parameter effect in this study.

Determination of optimum mass of sample for the fixed-bed reactor pyrolysis of used tyres and natural rubber products yield.

Fixed parameters:

Operating temperature: 600 ^{o}C (from the experiment result)

Heating rate: 15 ^{o}C/min (from the experiment result)

Particle size = 2mm

Table C2 Determination of optimum mass of sample for the fixed-bed reactor pyrolysis

Used Tyres			
Mass (g)	Pyrolytic oil (wt %)	Solid char (wt %)	Gas (wt %)
10	24.5 ± 0.17	33.0 ± 0.10	42.5 ± 0.10
15	31.18 ± 6.70	33.11 ± 0.12	35.71 ± 6.81
20	36.62 ± 2.20	33.13 ± 0.08	30.25 ± 2.61
NR			
10	75.93 ± 1.06	0.43 ± 0.12	23.63 ± 2.99
15	84.4 ± 2.44	0.18 ± 0.11	15.4 ± 1.47
20	83.72 ± 2.26	0.38 ± 0.02	15.9 ± 2.23

From the results on the Table above, although increase in the sample mass lead to an increase in the pyrolytic oil yield, but there is less accuracy for the 15 and 20g of used tyres and natural rubber as seen in the standard deviation values. Hence the mass of 10g was adopted due to its minimal standard deviation value.

Table C3 Effect of particle sizes on used tyres pyrolysis

Particle size (mm)	Pyrolytic oil (wt. %)	Solid char (wt. %)	Gas fraction (wt. %)
2 mm	24.5 ± 0.17	33.0± 0.10	42.5 ± 0.10
4 mm	27.83± 2.55	49.03± 0.35	21.13 ± 3.38
6 mm	34.4± 2.18	48.47± 0.29	17.13 ± 2.24
8 mm	33.17± 5.45	50.0± 0.14	16.83 ± 5.48
10 mm	30.22 ± 2.11	54.01 ±0.16	15.77 ± 3.23

Table C4 Effect of Temperature on product yield distribution of used tyres pyrolysis

Temperature (^{o}C)	Pyrolytic oil (wt. %)	Char (wt. %)	Gas (wt. %)
375	6.49± 0.21	59.58± 6.98	33.93± 5.46
450	22.15± 1.85	52.3± 4.3	25.55± 1.55
525	30.1± 2.1	49.62± 2.62	20.28± 1.28
600	34.4± 2.18	48.47± 0.29	17.13± 2.24
675	30.32± 0.17	47.18± 0.18	22.5± 0.14
750	14.03± 0.13	47.12± 0.16	38.85± 0.07

Table C5 Effect of Temperature on product yield distribution of natural rubber pyrolysis

Temperature (^{o}C)	Pyrolytic oil (wt. %)	Solid char (wt. %)	Gas fraction (wt. %)
375	55.6 ± 1.29	2.57 ± 0.28	42.26 ± 1.0
450	53.8 ± 1.56	0.47 ± 0.10	45.73 ± 1.65
525	51.33 ± 4.04	0.43 ± 0.04	48.24 ± 4.04
600	75.93 ± 2.88	0.43 ± 0.12	23.63 ± 2.99
675	55.17 ± 5.90	0.17 ± 0.08	44.67 ± 5.93
750	44.23 ± 1.80	0.16 ± 0.04	55.58 ± 1.23

Table C6 Effect of catalyst concentration on used tyres pyrolysis product distribution

Zeolite Y (wt. %)	Pyrolytic oil (wt. %)	Solid char (wt. %)	Gas fraction (wt. %)
1	21.73± 2.30	34.67 ± 0.20	43.6 ± 2.22
2.5	20.45 ± 1.83	35.0 ± 0.88	45.30 ± 2.36
5	17.73 ± 3.03	36.4 ± 1.14	45.83 ± 2.49
6	19.70 ± 1.69	37.68 ± 0.87	43.86 ± 2.18
7.5	21.3± 2.42	39.9 ± 0.54	38.8 ± 2.45
10	20.33 ± 1.96	42.1 ± 0.54	37.57 ± 2.48

Table C7 Effect of catalyst concentration on natural rubber pyrolysis product distribution

Zeolite Y (wt. %)	Pyrolytic oil (wt. %)	Solid char (wt. %)	Gas fraction (wt. %)
1	59.2± 5.85	0.57 ± 0.24	40.4 ± 5.73
2.5	59.80 ± 4.12	1.99 ± 0.33	37.86 ± 6.10
5	62.23 ± 6.98	3.53 ± 0.54	34.20 ± 7.50
6	63.79 ± 1.21	3.98 ± 0.63	32.50 ± 1.12
7.5	65.87 ± 0.73	4.37 ± 0.74	29.77 ± 0.33
10	65.87 ± 0.62	5.67 ± 0.42	28.45 ± 1.02

Appendix D

Table D1: GCMS characterisation of derived NR pyrolytic oil obtained at 600 ^{o}C

Peak #	Name	R.T. (min:sec)	Area %	Formula
1	1,3,6-Heptatriene, 2,5,5-trimethyl-	04:01.5	0.4426	C10H16
27	2,6-Dimethyl-1,3,6-heptatriene	05:01.5	0.98112	C9H14
52	1-Penten-3-yne, 2-methyl-	07:01.4	0.20269	C6H8
28	1,3-Cyclopentadiene, 5,5-dimethyl-2-propyl-	05:04.9	0.3613	C10H16
71	1,7-Octadiene, 2,7-dimethyl-3,6-bis(methylene)-	10:00.2	0.12479	C12H18
29	2,6-Dimethyl-1,3,5,7-octatetraene, E,E-	05:05.5	0.15227	C10H14
43	1,3,5-Cycloheptatriene, 3,7,7-trimethyl-	06:06.1	0.30222	C10H14
89	Furan, 3-(4,8-dimethyl-3,7-nonadienyl)-, (E)-	11:01.1	1.0142	C15H22O
2	2-Cyclohexen-1-ol, 4-ethyl-1,4-dimethyl-	04:10.5	0.84296	C10H18O
113	cis-à-Bisabolene	12:03.8	0.10683	C15H24
90	(3S,6R)-3-Hydroperoxy-3-methyl-6-(prop-1-en-2-yl)cyclohex-1-ene	11:06.3	0.45876	C10H16O2
91	Naphthalene, 1,7-dimethyl-	11:07.0	0.13136	C12H12
137	1,3-Bis-(2-cyclopropyl,2-methylcyclopropyl)-but-2-en-1-one	17:01.3	0.18517	C18H26O
131	Squalene	16:02.5	0.87178	C30H50
31	Benzene, 1-ethyl-2-methyl-	05:14.6	0.56069	C9H12
3	Cyclohexene, 1-methyl-4-(1-methylethenyl)-, (S)-	04:16.2	8.207	C10H16
32	Cyclohexene, 3-methyl-6-(1-methylethyl)-	05:16.0	0.31605	C10H18
33	(1S)-2,6,6-Trimethylbicyclo[3.1.1]hept-2-ene	05:16.6	1.5327	C10H16
92	(3E,7E)-4,8,12-Trimethyltrideca-1,3,7,11-tetraene	11:10.7	1.5109	C16H26
93	ç-Elemene	11:11.0	0.17198	C15H24
4	Benzene, 1-ethyl-2-methyl-	04:18.4	0.33184	C9H12
46	Benzene, 1-methyl-4-(1-methylethenyl)-	06:17.5	0.29391	C10H12
7	Benzene, 1,2,3-trimethyl-	04:21.2	0.26541	C9H12
117	Cyclohexane, 1-ethenyl-1-methyl-2,4-bis(1-methylethenyl)-	12:13.8	0.32085	C15H24
118	anti-10-Methyl-endo-tricyclo[5.2.1.0(2.6)]decane	12:14.3	0.76028	C11H18
145	Diisooctyl phthalate	22:04.4	6.7325	C24H38O4
8	1,3-Dimethyl-1-cyclohexene	04:23.2	0.243	C8H14
34	Limonene	05:22.9	42.609	C10H16
36	Benzene, 1,2,3-trimethyl-	05:24.9	0.15205	C9H12
9	Benzene, 1,2,3-trimethyl-	04:26.0	0.18654	C9H12
37	2-Methyl-1-nonene-3-yne	05:25.1	1.8495	C10H16
61	1,3-Cyclopentadiene, 5,5-dimethyl-	08:22.2	0.18216	C7H10
94	2,6,9,11-Dodecatetraenal, 2,6,10-trimethyl-, (E,E,E)-	11:20.0	0.16973	C15H22O

10	Santolina triene	04:27.4	0.34267	C10H16
95	2,4-Dinitrophenyl crotonate	11:20.4	0.70125	C10H8N2O6
119	Santolina triene	12:19.6	0.25014	C10H16
47	1,8-Nonadiene, 2-methyl-5,7-dimethylene-	06:26.3	0.11479	C12H18
132	1,3-Bis-(2-cyclopropyl,2-methylcyclopropyl)-but-2-en-1-one	16:16.6	0.12813	C18H26O
11	3,4-Nonadiene	04:29.8	0.26051	C9H16
38	Cyclohexene, 4-methyl-1-(1-methylethenyl)-	05:29.5	0.15709	C10H16
56	Bicyclo[2.2.1]hept-2-ene, 1-methyl-	07:28.1	0.26864	C8H12
66	1H-Indene, 1-ethylidene-	09:26.4	0.26325	C11H10
73	1,2,3-Trimethylindene	10:28.3	0.19982	C12H14
12	Benzene, 1,2,3-trimethyl-	04:34.3	0.3834	C9H12
39	á-Ocimene	05:33.5	0.13488	C10H16
140	2-Benzofurancarboxylic acid, 2,4,5,6,7,7a-hexahydro-4,4,7a-trimethyl-, methyl ester, cis-	19:19.6	0.10223	C13H20O3
139	3,5,9-Trimethyl-deca-2,4,8-trien-1-ol	17:23.2	0.23571	C13H22O
120	1,3,8-p-Menthatriene	12:28.4	0.10124	C10H14
74	1,7-Octadiene, 2,7-dimethyl-3,6-bis(methylene)-	10:30.5	0.13273	C12H18
14	cis-2,6-Dimethyl-2,6-octadiene	04:36.5	1.856	C10H18
48	Benzene, (1,1-dimethylpropyl)-	06:34.9	0.47721	C11H16
16	2,4,6-Octatriene, 2,6-dimethyl-, (E,Z)-	04:37.5	1.8909	C10H16
40	1-Propyne, 3-phenyl-	05:37.0	0.15202	C9H8
101	2,6,9,11-Dodecatetraenal, 2,6,10-trimethyl-, (E,E,E)-	11:31.0	0.21776	C15H22O
121	Naphthalene, 1,4,6-trimethyl-	12:31.9	0.16646	C13H14
18	Bicyclo[2.2.1]heptane, 2,2-dimethyl-5-methylene-	04:40.3	0.26732	C10H16
49	1,3,8-p-Menthatriene	06:38.7	0.25463	C10H14
41	Benzeneacetaldehyde, à-methyl-	05:39.9	0.33762	C9H10O
19	trans-1,4-Hexadiene	04:40.9	0.7593	C6H10
20	1,5-Heptadiene, 3,3,5-trimethyl-	04:41.2	1.0763	C10H18
103	p-Mentha-1,8-dien-7-ol	11:35.5	0.15823	C10H16O
67	Naphthalene, 1-methyl-	09:39.8	0.16776	C11H10
21	1-Pentene, 5-(2,2-dimethylcyclopropyl)-2-methyl-4-methylene-	04:45.1	0.10583	C12H20
42	1,3,5-Cycloheptatriene, 3,7,7-trimethyl-	05:45.9	0.34851	C10H14
50	Benzene, 4-ethyl-1,2-dimethyl-	06:45.5	0.34838	C10H14
22	Phenol, 2-(1-methylethyl)-	04:48.3	0.61016	C9H12O
77	(R)-1-Methyl-4-(6-methylhept-5-en-2-yl)cyclohexa-1,4-diene	10:42.6	0.26951	C15H24
23	Hydratropic acid, 3-methylbut-2-en-1-yl ester	04:48.6	2.7211	C14H18O2
24	1H-Indene, 2,3,4,7-tetrahydro-	04:49.6	0.25378	C9H12
80	(3S,6R)-3-Hydroperoxy-3-methyl-6-(prop-1-en-2-yl)cyclohex-1-ene	10:45.0	0.11153	C10H16O2
133	Santolina triene	16:39.1	0.79998	C10H16
51	2,4,6-Octatriene, 2,6-dimethyl-, (E,Z)-	06:50.0	0.11087	C10H16

58	Naphthalene	07:49.4	0.22286	C10H8
62	1H-Indene, 2,3-dimethyl-	08:48.8	0.13147	C11H12
68	Tricyclo[3.3.0.0(2,8)]octan-3-one, 4-methyl-4-(2-methyl-2-propenyl)-	09:48.1	0.39299	C13H18O
26	1,3,7-Octatriene, 3,7-dimethyl-	04:54.3	0.30341	C10H16
82	1,4-Methanocycloocta[d]pyridazine, 1,4,4a,5,6,9,10,10a-octahydro-11,11-dimethyl-, (1à,4à,4aà,10aà)-	10:48.6	1	C13H20N2
69	Tetracyclo[5.2.1.0(2,6).0(3,5)]decane, 4,4-dimethyl-	09:51.7	0.32584	C12H18
63	1H-Indene, 2,3-dimethyl-	08:53.3	0.15932	C11H12
59	1H-Indene, 2,3-dihydro-1,1-dimethyl-	07:55.7	0.16511	C11H14
86	(3R,6R)-3-Hydroperoxy-3-methyl-6-(prop-1-en-2-yl)cyclohex-1-ene	10:54.2	0.15029	C10H16O2
127	Cyclopropane, 1-(2-methylene-3-butenyl)-1-(1-methylenepropyl)-	12:53.2	0.11303	C12H18
129	3-Heptyne, 5-ethyl-5-methyl-	12:54.3	1.12	C10H18
87	Naphthalene, 2,3-dimethyl-	10:57.3	0.19102	C12H12
134	Bicyclo[5.2.0]nonane, 4-methylene-2,8,8-trimethyl-2-vinyl-	16:51.8	0.24664	C15H24
130	1,5,9-Undecatriene, 2,6,10-trimethyl-, (Z)-	15:56.3	0.62954	C14H24
141	trans-Geranylgeraniol	19:52.6	0.39486	C20H34O
136	1,5,5-Trimethyl-6-methylene-cyclohexene	16:57.8	0.38966	C10H16
143	trans-Geranylgeraniol	19:56.8	0.63136	C20H34O

Table D2: GC/MS characterisation of derived NRZ pyrolytic oil obtained at 600 ^{o}C

Peak #	Name	R.T. (min:sec)	Area %	Formula
1	1,3,6-Heptatriene, 2,5,5-trimethyl-	04:01.6	0.30856	C10H16
20	2,6-Dimethyl-1,3,6-heptatriene	05:01.5	0.87031	C9H14
34	2,4,6-Octatriene, 2,6-dimethyl-, (E,Z)-	07:01.5	0.21984	C10H16
37	1,7-Octadiene, 2,7-dimethyl-3,6-bis(methylene)-	10:00.1	0.79883	C12H18
21	2,6-Dimethyl-1,3,5,7-octatetraene, E,E-	05:05.4	0.11845	C10H14
44	(3E,7E)-4,8,12-Trimethyltrideca-1,3,7,11-tetraene	11:00.9	0.85701	C16H26
2	2-Cyclohexen-1-ol, 4-ethyl-1,4-dimethyl-	04:10.5	0.21119	C10H18O
61	anti-10-Methyl-endo-tricyclo[5.2.1.0(2.6)]decane	12:05.4	0.33091	C11H18
73	trans-Farnesol	16:02.5	0.74242	C15H26O
22	Mesitylene	05:14.6	0.306	C9H12
3	Cyclohexene, 1-methyl-4-(1-methylethenyl)-, (S)-	04:16.1	6.5379	C10H16
23	Cyclohexene, 3-methyl-6-(1-methylethyl)-	05:15.9	0.29224	C10H18
63	Bicyclo[3.1.1]heptane, 6,6-dimethyl-3-methylene-	12:08.9	0.32341	C10H16
24	(1S)-2,6,6-Trimethylbicyclo[3.1.1]hept-2-ene	05:16.5	0.33779	C10H16
79	4,8,12-Tetradecatrien-1-ol, 5,9,13-trimethyl-	17:04.6	0.23275	C17H30O
46	Cyclohexane, 1-ethenyl-1-methyl-2,4-bis(1-methylethenyl)-	11:10.6	1.3417	C15H24
4	Benzene, 1,2,3-trimethyl-	04:18.4	0.14847	C9H12
30	Benzene, 1-methyl-4-(1-methylethenyl)-	06:17.3	0.12066	C10H12
6	Benzene, 1,4-diethyl-	04:21.2	0.22763	C10H14
64	Cyclohexene, 1-methyl-4-(1-methylethenyl)-, (S)-	12:13.9	0.19425	C10H16
65	5-Hepten-1-ol, 2-ethenyl-6-methyl-	12:14.2	0.45075	C10H18O
85	Diisooctyl phthalate	22:04.2	3.893	C24H38O4
7	trans,cis-1,7-Dimethylspiro[4.5]decane	04:23.3	0.15007	C12H22
25	Limonene	05:22.7	66.274	C10H16
47	2,6,9,11-Dodecatetraenal, 2,6,10-trimethyl-, (E,E,E)-	11:19.9	0.13224	C15H22O
48	1,5-Heptadiene, 2,6-dimethyl-	11:20.3	0.4911	C9H16
9	Bicyclo[2.2.1]heptane, 2,2-dimethyl-3-methylene-, (1R)-	04:27.4	0.28681	C10H16
74	1,3-Bis-(2-cyclopropyl,2-methylcyclopropyl)-but-2-en-1-one	16:16.2	0.28873	C18H26O
49	1-Cyclohexyl-1-pentyne	11:21.8	0.11196	C11H18
10	3,4-Octadiene	04:29.8	0.1834	C8H14
27	Cyclohexene, 4-methyl-1-(1-methylethenyl)-	05:29.4	0.12879	C10H16
11	trans-3-Caren-2-ol	04:35.2	0.26577	C10H16O
51	(3E,7E)-4,8,12-Trimethyltrideca-1,3,7,11-tetraene	11:28.7	0.64462	C16H26
82	(1,2,3-Trimethyl-cyclopent-2-enyl)-methanol	17:23.2	0.16199	C9H16O
12	2,6-Octadiene, 2,6-dimethyl-	04:36.5	1.4042	C10H18
31	Benzene, 1-methyl-4-(1-methylpropyl)-	06:34.7	0.22654	C11H16
13	Cyclohexene, 1,5,5-trimethyl-3-methylene-	04:37.4	0.72094	C10H16

52	2,6,9,11-Dodecatetraenal, 2,6,10-trimethyl-, (E,E,E)-	11:30.8	0.13578	C15H22O
15	Cyclohexene, 4-methyl-1-(1-methylethenyl)-	04:40.2	0.20784	C10H16
32	1,3,8-p-Menthatriene	06:38.5	0.15693	C10H14
16	1,6-Octadiene, 3,7-dimethyl-	04:40.9	0.55922	C10H18
53	(-)-Aristolene	11:34.0	0.14577	C15H24
67	Cyclohexane, 1-ethenyl-1-methyl-2,4-bis(1-methylethenyl)-	12:33.3	0.18358	C15H24
54	(1R,4R,5S)-1,8-Dimethyl-4-(prop-1-en-2-yl)spiro[4.5]dec-7-ene	11:35.1	0.17586	C15H24
55	Bicyclo[2.2.2]octane, 1-bromo-4-methyl-	11:39.0	0.12752	C9H15Br
39	(R)-1-Methyl-4-(6-methylhept-5-en-2-yl)cyclohexa-1,4-diene	10:42.4	0.15201	C15H24
56	(R)-1-Methyl-4-(6-methylhept-5-en-2-yl)cyclohexa-1,4-diene	11:42.6	0.14561	C15H24
75	Santolina triene	16:38.9	0.7325	C10H16
33	2,4,6-Octatriene, 2,6-dimethyl-, (E,Z)-	06:49.8	0.29482	C10H16
35	1,7-Octadiene, 2,7-dimethyl-3,6-bis(methylene)-	09:47.9	0.11178	C12H18
19	1,3,7-Octatriene, 3,7-dimethyl-	04:54.3	0.20465	C10H16
60	à-Farnesene	11:48.0	0.48983	C15H24
43	1,3-Cyclopentadiene, 1,3-bis(1-methylethyl)-	10:54.1	0.10731	C11H18
69	cis-à-Bisabolene	12:53.2	0.14325	C15H24
71	3,3,5,5-Tetramethylcyclopentene	12:54.0	0.7523	C9H16
76	Bicyclo[5.2.0]nonane, 4-methylene-2,8,8-trimethyl-2-vinyl-	16:51.8	0.23486	C15H24
72	1,5,9-Undecatriene, 2,6,10-trimethyl-, (Z)-	15:56.4	0.10566	C14H24
77	1,3-Bis-(2-cyclopropyl,2-methylcyclopropyl)-but-2-en-1-one	16:55.5	0.22381	C18H26O
78	Tricyclo[2.2.1.0(2,6)]heptane-3-methanol, 2,3-dimethyl-	16:57.8	0.39648	C10H16O
84	trans-Farnesol	19:56.7	0.1048	C15H26O

Table D3: GC/MS characterisation of derived UT pyrolytic oil obtained at 600 ^{o}C

Peak #	Name	R.T. (min:sec)	Area %	Formula
1	1,3,6-Heptatriene, 2,5,5-trimethyl-	04:01.9	0.27622	C10H16
2	Camphene	04:02.8	0.1468	C10H16
46	2-Methyl-1-nonene-3-yne	05:01.9	0.36244	C10H16
115	2,4,6-Octatriene, 2,6-dimethyl-, (E,Z)-	07:01.9	0.25266	C10H16
80	p-Cresol	06:03.2	0.3688	C7H8O
170	4-Isopropyl-1-phenyl-hexa-1,5-dien-3-ol	09:00.4	0.10126	C15H20O
5	1,1,3,3,5-Pentamethylcyclohexane	04:06.2	0.23291	C11H22
116	Benzene, 1,3-dimethyl-5-(1-methylethyl)-	07:04.6	0.11268	C11H16
6	1,2-Cyclohexanedimethanol	04:07.9	0.12666	C8H16O2
117	Benzene, 1-methyl-2-(2-propenyl)-	07:04.9	0.44496	C10H12
83	Benzene, 1-methyl-3-(1-methylethyl)-	06:06.4	0.53243	C10H14
237	1,4-Hexadiene, 3-ethyl-	11:02.3	0.6724	C8H14
203	2-Pentene, 3,4,4-trimethyl-	10:03.7	1.3313	C8H16
48	1,3-Cyclohexadiene, 1-methyl-4-(1-methylethyl)-	05:09.4	0.35476	C10H16
8	1-Propanol, 3-(phenylmethoxy)-	04:10.8	0.43918	C10H14O2
9	Benzene, propyl-	04:12.4	0.18523	C9H12
205	Isomyocorene	10:07.7	0.17025	C10H16
118	1,2,3,4,5,8-Hexahydronaphthalene	07:11.0	0.11379	C10H14
85	Benzene, 2-ethyl-1,3-dimethyl-	06:12.2	0.32995	C10H14
119	Phenol, 2,3-dimethyl-	07:11.4	0.2892	C8H10O
10	Allylidenecyclohexane	04:14.7	0.34278	C9H14
338	Squalene	16:02.8	0.36331	C30H50
86	Cyclohexene, 1-methyl-4-(1-methylethylidene)-	06:13.4	0.39596	C10H16
51	Benzene, 1,2,3-trimethyl-	05:14.9	1.6238	C9H12
176	1H-Indene, 2,3-dihydro-4,7-dimethyl-	09:11.0	0.26573	C11H14
348	1,2-Benzenedicarboxylic acid, butyl 2-ethylhexyl ester	17:03.1	0.40947	C20H30O4
120	1H-Indene, 2,3-dihydro-4-methyl-	07:13.4	0.72509	C10H12
12	Cyclohexene, 1-methyl-4-(1-methylethenyl)-, (S)-	04:16.5	2.5857	C10H16
88	o-Isopropenyltoluene	06:14.6	0.46476	C10H12
324	Sulfurous acid, butyl cyclohexylmethyl ester	14:06.9	0.90262	C11H22O3S
277	1,3,6,10-Dodecatetraene, 3,7,11-trimethyl-, (Z,E)-	12:09.0	0.21258	C15H24
121	Naphthalene, 1,2-dihydro-	07:14.3	0.33148	C10H10
13	Cyclohexene, 1-methyl-4-(1-methylethenyl)-, (S)-	04:17.3	0.59849	C10H16
52	Cyclohexene, 3-methyl-6-(1-methylethyl)-	05:16.4	0.24432	C10H18
304	Sulfurous acid, cyclohexylmethyl hexyl ester	13:08.6	0.50938	C13H26O3S
122	5H-5-Methyl-6,7-dihydrocyclopentapyrazine	07:15.0	0.12562	C8H10N2
243	3-Cyclohexene-1-carboxaldehyde, 2,4,6-trimethyl-	11:11.0	0.72537	C10H16O

53	o-Cymene	05:17.3	3.7413	C10H14
14	Benzene, 1-ethyl-2-methyl-	04:18.8	0.33273	C9H12
91	Benzene, 1-methyl-4-(1-methylethenyl)-	06:17.8	0.56752	C10H12
54	2-Decene, 5-methyl-, (Z)-	05:19.3	0.91225	C11H22
55	Limonene	05:19.8	1.3456	C10H16
124	Benzene, pentyl-	07:18.4	0.22583	C11H16
149	Benzene, 1-methyl-3-(1-methyl-2-propenyl)-	08:17.5	0.13419	C11H14
378	Heptacosane	24:01.8	0.14024	C27H56
92	Ethyl (E)-hex-3-enyl carbonate	06:19.9	0.19085	C9H16O3
19	1,3-Dimethyl-1-cyclohexene	04:23.6	0.60479	C8H14
179	Ethyltetramethylcyclopentadiene	09:19.4	0.1047	C11H18
57	Limonene	05:23.5	14.275	C10H16
180	Benzene, 4-(2-butenyl)-1,2-dimethyl-, (E)-	09:19.9	0.14735	C12H16
366	Diisooctyl phthalate	22:07.2	6.6322	C24H38O4
210	1,3,7-Octatriene, 2,7-dimethyl-	10:20.2	0.16743	C10H16
59	Cyclohexene, 4-methyl-1-(1-methylethenyl)-	05:25.9	0.30454	C10H16
250	trans-Farnesol	11:20.7	0.38808	C15H26O
23	Furane-2-carboxylic acid, (2-chloro-5-furanoyloxy)phenyl ester	04:28.1	0.32025	C16H9ClO6
96	Benzene, 1-methyl-4-(2-methylpropyl)-	06:26.5	0.32148	C11H16
251	Quinoline, 1,2-dihydro-2,2,4-trimethyl-	11:21.7	0.3798	C12H15N
308	Phenol, 4-(1,1,3,3-tetramethylbutyl)-	13:19.9	1.1232	C14H22O
127	Naphthalene, 1,2,3,4-tetrahydro-	07:26.0	0.18229	C10H12
128	Benzenepropanenitrile, á-oxo-	07:26.6	0.16716	C9H7NO
60	Indane	05:28.6	0.56503	C9H10
153	Benzothiazole	08:25.9	1.3622	C7H5NS
253	Quinoline, 2,4-dimethyl-	11:23.0	0.395	C11H11N
24	1,6-Octadiene, 2,6-dimethyl-, (Z)-	04:30.1	0.28775	C10H18
184	Benzothiazole, 2-methyl-	09:25.3	0.25988	C8H7NS
325	Nonadecane	14:20.6	0.25733	C19H40
98	Butane, 2-bromo-	06:28.6	1.0183	C4H9Br
61	2-Methyl-1-nonene-3-yne	05:29.8	0.49174	C10H16
370	Sulfurous acid, cyclohexylmethyl isobutyl ester	23:12.0	0.32198	C11H22O3S
25	1-Pentanol, 2,2,4-trimethyl-	04:31.6	0.56286	C8H18O
186	Naphthalene, 1-methyl-	09:26.7	0.292	C11H10
154	Benzene, (1-ethyl-1-propenyl)-	08:28.0	0.27577	C11H14
188	Propanedinitrile, (2,3-dihydro-1-methyl-1H-inden-1-yl)-	09:27.7	0.15573	C13H12N2
62	Benzene, 3-butenyl-	05:33.4	0.21653	C10H12
213	1,2,3-Trimethylindene	10:28.6	0.16406	C12H14
26	Benzene, 1-ethyl-2-methyl-	04:34.6	0.1816	C9H12
255	(1R,4R,4aS,8aR)-4,7-Dimethyl-1-(prop-1-en-2-yl)-	11:27.7	0.15341	C15H24

	1,2,3,4,4a,5,6,8a-octahydronaphthalene			
27	Phosphonic acid, (p-hydroxyphenyl)-	04:35.0	0.56475	C6H7O4P
100	Bicyclo[6.1.0]nonane, 9-(1-methylethylidene)-	06:33.2	0.15734	C12H20
256	trans-Farnesol	11:29.1	0.60724	C15H26O
101	Phenol, 2,6-dimethyl-	06:34.6	0.15098	C8H10O
214	2,6,9,11-Dodecatetraenal, 2,6,10-trimethyl-, (E,E,E)-	10:30.7	0.12149	C15H22O
28	2,6-Dimethyl-2-trans-6-octadiene	04:36.8	1.313	C10H18
131	Benzene, 1-methyl-3-(1-methylethyl)-	07:34.0	0.10318	C10H14
102	Benzene, 1-methyl-4-(1-methylpropyl)-	06:35.2	0.63709	C11H16
29	Benzene, 2-propenyl-	04:37.3	0.27457	C9H10
371	Tetracosane	23:18.9	0.13726	C24H50
30	2,4,6-Octatriene, 2,6-dimethyl-, (E,Z)-	04:37.9	0.84727	C10H16
65	1-Propyne, 3-phenyl-	05:37.3	0.29231	C9H8
288	2-Cyclopentene-1-carboxylic acid, 1,2,3-trimethyl-, ethyl ester, (.+-.)-	12:31.4	0.2832	C11H18O2
104	Tricyclo[4.2.1.0(2,5)]nonane, 3-ethenyl-	06:37.5	0.13689	C11H16
217	Disulfide, bis(1,1,3,3-tetramethylbutyl)	10:33.6	1.1142	C16H34S2
32	Benzonitrile	04:40.1	0.33602	C7H5N
66	Cyclohexene, 1-methyl-4-(1-methylethylidene)-	05:39.2	0.1281	C10H16
289	Naphthalene, 2,3,6-trimethyl-	12:32.2	0.28107	C13H14
218	Biphenyl	10:34.5	0.23838	C12H10
132	Benzene, 2-ethenyl-1,3,5-trimethyl-	07:38.1	0.16155	C11H14
67	Benzene, 1-methyl-3-propyl-	05:40.1	0.52949	C10H14
33	1,6-Octadiene, 3,7-dimethyl-	04:41.2	0.69256	C10H18
34	Cyclopentaneethanol, á,2,3-trimethyl-	04:41.6	0.10267	C10H20O
69	Phenol, 2-methyl-	05:43.3	0.61858	C7H8O
192	Naphthalene, 1-methyl-	09:40.1	0.22718	C11H10
70	2-Hexene, 5,5-dimethyl-, (Z)-	05:44.7	1.7714	C8H16
71	Benzene, n-butyl-	05:45.4	0.33907	C10H14
352	Sulfurous acid, cyclohexylmethyl hexyl ester	17:33.6	0.657	C13H26O3S
72	Benzene, 1-methyl-3-(1-methylethyl)-	05:46.2	0.39523	C10H14
159	1H-Indene, 2,3-dihydro-4,7-dimethyl-	08:43.4	0.13511	C11H14
107	Benzene, 1,2,3,4-tetramethyl-	06:45.7	0.29505	C10H14
368	Sulfurous acid, cyclohexylmethyl tetradecyl ester	22:29.9	0.19794	C21H42O3S
223	trans-à-Bergamotene	10:42.8	0.20461	C15H24
38	Hydratropic acid, 3-methylbut-2-en-1-yl ester	04:48.9	1.9197	C14H18O2
74	1,6-Octadiene, 3,7-dimethyl-	05:48.1	0.21803	C10H18
263	2-Ethyl-3-methylene-indan-1-one	11:42.3	0.10976	C12H12O
360	Sulfurous acid, cyclohexylmethyl isobutyl ester	20:33.3	0.43157	C11H22O3S
137	Benzoic acid	07:46.8	3.3161	C7H6O2
264	(1R,4R,5S)-1,8-Dimethyl-4-(prop-1-en-2-yl)spiro[4.5]dec-7-	11:43.0	0.10831	C15H24

	ene			
39	1-(2-Methylphenyl)ethanol	04:50.0	0.40424	C9H12O
342	Santolina triene	16:39.3	0.36447	C10H16
138	1H-Indene, 2,3-dihydro-1,6-dimethyl-	07:48.3	0.54522	C11H14
196	Naphthalene, 1-ethyl-1,2,3,4-tetrahydro-	09:46.4	0.10646	C12H16
109	1,3-Cyclohexadiene, 1,3,5,5-tetramethyl-	06:50.2	0.1682	C10H16
139	Naphthalene	07:49.6	0.65259	C10H8
161	1H-Indene, 2,3-dimethyl-	08:49.0	0.11394	C11H12
162	Bicyclo[6.4.0]dodeca-9,11-diene	08:49.6	0.11584	C12H18
198	Naphthalene, 1,2,3,4-tetrahydro-1,1-dimethyl-	09:48.8	0.28122	C12H16
344	Sulfurous acid, cyclohexylmethyl hexyl ester	16:41.8	0.36824	C13H26O3S
42	Bicyclo[2.2.1]heptane, 2,2-dimethyl-3-methylene-, (1R)-	04:54.6	0.26529	C10H16
141	1H-Indene, 1-ethyl-2,3-dihydro-	07:52.4	0.12489	C11H14
76	Benzeneacetaldehyde, à-methyl-	05:54.4	0.19853	C9H10O
318	Phenol, 2-methyl-4-(1,1,3,3-tetramethylbutyl)-	13:46.7	0.59983	C15H24O
111	10-Dodecyn-1-ol	06:54.1	0.14509	C12H22O
43	3-Heptene, 2,2,4,6,6-pentamethyl-	04:57.1	0.25127	C12H24
165	1H-Indene, 2,3-dimethyl-	08:53.5	0.17374	C11H12
44	Bicyclo[2.2.1]heptane, 2,2-dimethyl-3-methylene-, (1R)-	04:57.9	0.17727	C10H16
113	1,5,6,7-Tetramethylbicyclo[3.2.0]hepta-2,6-diene	06:57.0	0.19221	C11H16
142	1H-Indene, 2,3-dihydro-1,6-dimethyl-	07:56.0	0.50994	C11H14
230	Pentane, 1-chloro-5-(methylenecyclopropyl)-	10:53.3	0.11279	C9H15Cl
361	1,4-Benzenediamine, N-(1,3-dimethylbutyl)-N'-phenyl-	20:43.4	0.68379	C18H24N2
200	Benzene, 3-cyclohexen-1-yl-	09:55.0	0.25154	C12H14
298	cis-à-Bisabolene	12:52.9	0.11813	C15H24
114	Benzeneacetic acid, à-oxo-, methyl ester	06:59.0	0.44336	C9H8O3
357	2,4,4-Trimethyl-1-pentanol, trifluoroacetate	19:46.6	0.26518	C10H17F3O2
379	Hentriacontane	24:43.3	0.14932	C31H64
169	Z-3,4,4-Trimethyl-2-pentene	08:59.3	0.64245	C8H16
232	Naphthalene, 2,6-dimethyl-	10:57.5	0.13362	C12H12
274	Hexadecane	11:59.5	0.13248	C16H34
337	4,8,12-Tetradecatrien-1-ol, 5,9,13-trimethyl-	15:56.6	0.26214	C17H30O
347	1,5,5-Trimethyl-6-methylene-cyclohexene	16:58.1	0.12839	C10H16
358	trans-Geranylgeraniol	19:57.2	0.16937	C20H34O
377	Benzothiazole, 2-butyl-	23:56.3	0.11424	C11H13NS

Table D4: GC/MS characterisation of derived UTZ pyrolytic oil obtained at 600 ^{o}C

Peak #	Name	R.T. (min:sec)	Area %	Formula
1	1,3,6-Heptatriene, 2,5,5-trimethyl-	04:02.1	0.24514	C10H16
46	2-Methyl-1-nonene-3-yne	05:01.9	0.34847	C10H16
2	2-Methyl-1-nonene-3-yne	04:03.0	0.11745	C10H16
109	2,4,6-Octatriene, 2,6-dimethyl-, (E,Z)-	07:01.9	0.25173	C10H16
79	Benzyl alcohol	06:03.2	0.18381	C7H8O
162	4-Isopropyl-1-phenyl-hexa-1,5-dien-3-ol	09:00.4	0.10059	C15H20O
163	1H-Indene, 2,3-dimethyl-	09:00.9	0.10958	C11H12
187	Tricyclo[3.3.0.0(2,8)]octan-3-one, 4-methyl-4-(2-methyl-2-propenyl)-	10:00.4	0.11512	C13H18O
110	3,4-Dimethylcumene	07:04.6	0.10434	C11H16
111	1H-Indene, 2,3-dihydro-4-methyl-	07:04.9	0.46408	C10H12
5	10-Undecyn-1-ol	04:08.1	0.12379	C11H20O
80	Benzene, 1-methyl-3-(1-methylethyl)-	06:06.4	0.47361	C10H14
219	1,4-Hexadiene, 3-ethyl-	11:02.4	0.77006	C8H14
188	3-Penten-1-ol, 2,2,4-trimethyl-	10:03.7	1.1644	C8H16O
48	1,3-Cyclohexadiene, 1-methyl-4-(1-methylethyl)-	05:09.5	0.34969	C10H16
7	2-Cyclohexen-1-ol, 4-ethyl-1,4-dimethyl-	04:10.9	0.40641	C10H18O
164	Biphenylene, 1,2,3,6,7,8,8a,8b-octahydro-, trans-	09:06.5	0.10273	C12H16
49	Thiophene, 3-(1,1-dimethylethyl)-	05:11.3	0.21543	C8H12S
8	Benzene, propyl-	04:12.5	0.18357	C9H12
112	Benzene, 1-ethenyl-4-methoxy-	07:10.9	0.12998	C9H10O
83	Benzene, 2-ethyl-1,4-dimethyl-	06:12.2	0.34156	C10H14
113	2,5-Cyclohexadien-1-one, 4-ethyl-3,4-dimethyl-	07:11.3	0.11231	C10H14O
9	7-Propylidene-bicyclo[4.1.0]heptane	04:14.9	0.31585	C10H16
330	Squalene	16:02.9	0.39697	C30H50
84	ç-Terpinene	06:13.4	0.44049	C10H16
51	Benzene, 1-ethyl-2-methyl-	05:14.9	1.4766	C9H12
167	1H-Indene, 2,3-dihydro-4,7-dimethyl-	09:11.0	0.27705	C11H14
344	Dibutyl phthalate	17:03.2	0.22591	C16H22O4
114	1H-Indene, 2,3-dihydro-4-methyl-	07:13.3	0.74024	C10H12
10	Cyclohexene, 1-methyl-4-(1-methylethenyl)-, (S)-	04:16.6	2.4334	C10H16
86	Indan, 1-methyl-	06:14.7	0.45638	C10H12
307	Sulfurous acid, butyl cyclohexylmethyl ester	14:07.1	1.0533	C11H22O3S
115	Naphthalene, 1,2-dihydro-	07:14.3	0.38102	C10H10
11	Hept-2-ene, 2,4,4,6-tetramethyl-	04:17.4	0.42065	C11H22
52	Cyclohexene, 3-methyl-6-(1-methylethyl)-	05:16.5	0.24473	C10H18
285	Sulfurous acid, cyclohexylmethyl hexyl ester	13:08.8	0.55595	C13H26O3S
354	Benzoyl isothiocyanate	19:02.9	0.34016	C8H5NOS

116	5H-5-Methyl-6,7-dihydrocyclopentapyrazine	07:15.1	0.11195	C8H10N2
225	4,8,12-Tetradecatrien-1-ol, 5,9,13-trimethyl-	11:11.1	0.78057	C17H30O
53	o-Cymene	05:17.3	3.6405	C10H14
12	Benzene, 1-ethyl-2-methyl-	04:18.9	0.32468	C9H12
346	Cyclohexane, 1-bromo-4-methyl-	17:06.0	0.13808	C7H13Br
88	Benzene, 1-methyl-4-(1-methylethenyl)-	06:17.8	0.64512	C10H12
55	D-Limonene	05:19.9	0.87397	C10H16
118	Benzene, pentyl-	07:18.4	0.23006	C11H16
142	1H-Indene, 2,3-dihydro-1,1-dimethyl-	08:17.5	0.14803	C11H14
15	Benzene, 1-ethyl-3-methyl-	04:21.5	0.5109	C9H12
89	Ethyl (Z)-hex-3-enyl carbonate	06:19.9	0.18779	C9H16O3
378	Heptacosane	24:02.1	0.22435	C27H56
16	Benzene, 1-ethyl-3-methyl-	04:22.6	0.19155	C9H12
18	5,5-Dimethyl-1,3-hexadiene	04:23.7	0.498	C8H14
367	Diisooctyl phthalate	22:06.2	3.888	C24H38O4
56	Limonene	05:23.3	14.059	C10H16
359	trans-Geranylgeraniol	20:08.7	0.13648	C20H34O
195	1,3,7-Octatriene, 2,7-dimethyl-	10:20.2	0.20135	C10H16
19	Benzene, 1,2,3-trimethyl-	04:26.5	0.17429	C9H12
58	Cyclohexene, 4-methyl-1-(1-methylethenyl)-	05:25.5	0.80498	C10H16
231	Geranyl bromide	11:20.7	0.41664	C10H17Br
265	Doconexent	12:19.8	0.12797	C22H32O2
22	Bicyclo[2.2.1]heptane, 2-(1-buten-3-yl)-	04:28.2	0.24402	C11H18
92	Benzene, 1-methyl-4-(2-methylpropyl)-	06:26.5	0.11491	C11H16
121	Naphthalene, 1,2,3,4-tetrahydro-	07:26.0	0.19377	C10H12
290	Phenol, 4-(1,1,3,3-tetramethylbutyl)-	13:20.1	1.5378	C14H22O
59	Indane	05:28.5	0.6012	C9H10
122	Benzene, (1-nitroethyl)-	07:26.6	0.16071	C8H9NO2
145	Benzothiazole	08:25.8	1.3712	C7H5NS
23	1,6-Octadiene, 2,6-dimethyl-, (Z)-	04:30.2	0.27612	C10H18
173	Benzothiazole, 2-methyl-	09:25.4	0.29634	C8H7NS
234	Quinoline, 2,4-dimethyl-	11:23.5	0.95999	C11H11N
94	Butane, 2-bromo-	06:28.6	0.72067	C4H9Br
310	1-Iodo-2-methylundecane	14:20.7	0.198	C12H25I
60	2-Methyl-1-nonene-3-yne	05:29.8	0.4471	C10H16
174	1-Phenyl-1-pentyne	09:26.3	0.22953	C11H12
370	Sulfurous acid, cyclohexylmethyl tetradecyl ester	23:12.3	0.4611	C21H42O3S
175	Naphthalene, 1-methyl-	09:26.6	0.33154	C11H10
24	1-Pentanol, 2,2,4-trimethyl-	04:31.7	0.33469	C8H18O
146	Benzene, (1-ethyl-1-propenyl)-	08:28.0	0.2894	C11H14
177	Propanedinitrile, (2,3-dihydro-1-methyl-1H-inden-1-yl)-	09:27.7	0.15683	C13H12N2

61	à-Phellandrene	05:33.4	0.19375	C10H16
197	1,2,3-Trimethylindene	10:28.6	0.18705	C12H14
25	Benzene, 1-ethyl-4-methyl-	04:34.7	0.21885	C9H12
96	Bicyclo[6.1.0]nonane, 9-(1-methylethylidene)-	06:33.3	0.15726	C12H20
237	1,5,9-Undecatriene, 2,6,10-trimethyl-, (Z)-	11:29.2	0.67903	C14H24
27	2,6-Octadiene, 2,6-dimethyl-	04:36.9	1.2412	C10H18
98	Benzene, 1-methyl-4-(1-methylpropyl)-	06:35.1	0.11047	C11H16
28	à-Methylstyrene	04:37.3	0.30354	C9H10
29	1,3-Cyclohexadiene, 1,3,5,5-tetramethyl-	04:37.9	0.8272	C10H16
371	Tetracosane	23:19.2	0.24949	C24H50
62	1-Propyne, 3-phenyl-	05:37.3	0.40377	C9H8
99	Tricyclo[4.2.1.0(2,5)]nonane, 3-ethenyl-	06:37.5	0.15258	C11H16
269	Lycorenan, 9,10-dimethoxy-1-methyl-	12:31.5	0.3246	C18H23NO3
201	Disulfide, bis(1,1,3,3-tetramethylbutyl)	10:33.6	0.98431	C16H34S2
31	Benzonitrile	04:40.1	0.37646	C7H5N
270	Naphthalene, 2,3,6-trimethyl-	12:32.3	0.35881	C13H14
32	á-Pinene	04:40.7	0.12119	C10H16
202	Biphenyl	10:34.7	0.27951	C12H10
125	Benzene, 2-ethenyl-1,3,5-trimethyl-	07:38.1	0.17069	C11H14
64	Benzene, 1-methyl-3-propyl-	05:40.2	0.47867	C10H14
33	5-Hexenal, 4-methylene-	04:41.3	0.67908	C7H10O
34	6-Dodecene, (Z)-	04:41.6	0.69036	C12H24
315	2,4,4-Trimethyl-1-pentanol, trifluoroacetate	14:33.1	0.11295	C10H17F3O2
67	Phenol, 2-methyl-	05:43.2	0.32225	C7H8O
297	2-Aminobiphenyl	13:35.7	0.1098	C12H11N
179	Naphthalene, 1-methyl-	09:40.1	0.28394	C11H10
68	1-Pentene, 4,4-dimethyl-	05:44.7	1.1493	C7H14
69	Benzoic acid, 2,4,5-trichlorophenyl ester	05:45.0	0.42232	C13H7Cl3O2
70	Benzene, (2-methylpropyl)-	05:45.4	0.18807	C10H14
349	Sulfurous acid, cyclohexylmethyl isobutyl ester	17:33.8	0.90716	C11H22O3S
71	p-Menthane, 2,3-dibromo-8-phenyl-	05:46.2	0.32932	C16H22Br2
151	1H-Indene, 2,3-dihydro-4,7-dimethyl-	08:43.4	0.14356	C11H14
102	Benzene, 1-methyl-3-(1-methylethyl)-	06:45.7	0.2353	C10H14
368	Sulfurous acid, cyclohexylmethyl tetradecyl ester	22:29.9	0.2747	C21H42O3S
72	ç-Terpinene	05:47.4	0.26646	C10H16
207	trans-à-Bergamotene	10:42.8	0.11104	C15H24
37	2,6-Octadiene, 2,6-dimethyl-	04:49.0	1.8627	C10H18
336	3-Ethylbenzothiazolin-2-thione	16:37.1	0.10639	C9H9NS2
73	3,4-Decadiene	05:48.1	0.19673	C10H18
245	1H-Indene, 3-ethenyl-2,3-dihydro-1,1-dimethyl-	11:42.5	0.1043	C13H16
360	Sulfurous acid, cyclohexylmethyl isobutyl ester	20:33.5	0.63789	C11H22O3S

39	1-(2-Methylphenyl)ethanol	04:50.1	0.44334	C9H12O
337	2,6,9,11-Dodecatetraenal, 2,6,10-trimethyl-, (E,E,E)-	16:39.3	0.24171	C15H22O
130	1H-Indene, 2,3-dihydro-1,1-dimethyl-	07:48.3	0.51996	C11H14
103	1,3-Cyclohexadiene, 1,3,5,5-tetramethyl-	06:50.2	0.21969	C10H16
132	Naphthalene	07:49.6	0.69414	C10H8
369	Heptacosane	22:34.7	0.22463	C27H56
153	1H-Indene, 2,3-dimethyl-	08:49.1	0.11602	C11H12
210	1,2,3-Trimethylindene	10:47.1	0.18057	C12H14
154	Benzene, hexyl-	08:49.6	0.12843	C12H18
185	Naphthalene, 1,2,3,4-tetrahydro-1,1-dimethyl-	09:48.9	0.31271	C12H16
133	Benzoic acid	07:50.9	4.0738	C7H6O2
340	Sulfurous acid, cyclohexylmethyl hexyl ester	16:42.0	0.47234	C13H26O3S
275	cis-à-Bisabolene	12:46.1	0.11436	C15H24
42	Bicyclo[2.2.1]heptane, 2,2-dimethyl-3-methylene-, (1R)-	04:54.7	0.2677	C10H16
301	Phenol, 2-methyl-4-(1,1,3,3-tetramethylbutyl)-	13:47.0	0.96707	C15H24O
105	Bicyclo[10.1.0]tridec-1-ene	06:54.1	0.15005	C13H22
43	1-Hexen-3-yne, 2-tert-butyl-	04:57.2	0.15814	C10H16
44	Bicyclo[3.1.1]heptane, 6,6-dimethyl-2-methylene-, (1S)-	04:57.9	0.17125	C10H16
107	1,5,6,7-Tetramethylbicyclo[3.2.0]hepta-2,6-diene	06:56.9	0.18657	C11H16
136	1H-Indene, 2,3-dihydro-1,6-dimethyl-	07:55.9	0.49871	C11H14
213	4-Decyne	10:53.3	0.30997	C10H18
76	1,3-Cyclohexadiene, 1,5,5,6-tetramethyl-	05:58.7	0.12262	C10H16
137	o-Cymene	07:56.8	0.16672	C10H14
361	1,4-Benzenediamine, N-(1,3-dimethylbutyl)-N'-phenyl-	20:43.8	1.0925	C18H24N2
77	Tricyclo[3.2.1.0(1,5)]octane	05:59.1	0.221	C8H12
186	Benzene, 3-cyclohexen-1-yl-	09:55.1	0.3175	C12H14
108	Benzeneacetic acid, à-oxo-, methyl ester	06:58.9	0.37675	C9H8O3
356	2,4,4-Trimethyl-1-pentanol, trifluoroacetate	19:46.8	0.3764	C10H17F3O2
253	Allylidenecyclohexane	11:55.4	0.11656	C9H14
161	3-Penten-1-ol, 2,2,4-trimethyl-	08:59.3	0.524	C8H16O
216	Naphthalene, 2,6-dimethyl-	10:57.6	0.13792	C12H12
379	Heptacosane	24:43.6	0.24445	C27H56
366	Tetracosane	21:48.5	0.19771	C24H50
217	1H-Indole, 2,3-dihydro-1,2,3,3-tetramethyl-	10:59.7	0.18266	C12H17N
256	Hexadecane	11:59.6	0.17687	C16H34
329	Squalene	15:56.7	0.27969	C30H50
350	2,4,4-Trimethyl-1-pentanol, heptafluorobutyrate	17:56.8	0.10707	C12H17F7O2
362	2,4,4,6,6,8,8-Heptamethyl-1-nonene	20:54.3	0.10685	C16H32
343	cis-8-Ethyl-bicyclo[4.3.0]non-3-ene	16:58.3	0.15156	C11H18
363	Hexanedioic acid, bis(2-ethylhexyl) ester	20:55.0	0.39126	C22H42O4
380	Sulfurous acid, cyclohexylmethyl tetradecyl ester	24:55.4	0.20853	C21H42O3S

Table D5: GC/MS characterisation of NR distillates

Peak #	Name	R.T. (min:sec)	Area %	Formula
1	o-Xylene	03:23.6	1.5707	C8H10
2	2-Cyclopentene-1-carboxylic acid, 1-methyl-, methyl ester	03:33.1	3.336	C8H12O2
4	2,6-Dimethyl-1,3,6-heptatriene	03:45.6	0.72303	C9H14
5	Limonene	04:00.1	0.99676	C10H16
6	2,6-Dimethylbicyclo[3.2.1]octane	04:08.6	0.18841	C10H18
7	2-Cyclohexen-1-ol, 4-ethyl-1,4-dimethyl-	04:12.9	0.23233	C10H18O
8	1,5-Heptadiene, 3,3,6-trimethyl-	04:16.4	2.05	C10H18
9	3-Nonyne	04:18.9	0.10115	C9H16
10	Limonene	04:21.7	1.1582	C10H16
12	Limonene	04:37.4	1.6898	C10H16
16	Cyclotetrasiloxane, octamethyl-	04:49.4	0.8073	C8H24O4Si4
19	1,5-Heptadiene, 3,3,5-trimethyl-	04:57.2	6.7424	C10H18
20	limonene-	04:59.2	1.3768	C10H16
21	9-Dodecyn-1-ol	05:04.4	0.10536	C12H22O
22	4-Methyl-1,5-Heptadiene	05:10.4	9.6609	C8H14
25	2,6-Dimethyl-1,3,6-heptatriene	05:24.8	1.7657	C9H14
27	1-Pentanol, 2-ethyl-4-methyl-	05:39.5	1.998	C8H18O
29	Limonene	06:00.9	0.11978	C10H16
30	Limonene	06:01.3	0.16093	C10H16
33	Benzene, 1-methyl-3-propyl-	06:06.3	0.36138	C10H14
38	Benzene, 2-ethyl-1,4-dimethyl-	06:10.7	0.37757	C10H14
39	Limonene	06:13.2	0.57458	C10H16
47	Benzene, 2-ethyl-1,3-dimethyl-	06:29.3	0.39076	C10H14
48	3,7-Decadiene, 2,9-dimethyl-	06:30.1	0.58762	C12H22
49	Benzene, 1-methyl-4-(1-methylethenyl)-	06:31.3	0.10036	C10H12
50	Benzene, 1-methyl-3-(1-methylethyl)-	06:34.7	0.16145	C10H14
51	Santolina triene	06:36.7	0.27725	C10H16
55	Limonene	06:38.6	0.41088	C10H16
56	Benzene, 1-methyl-4-(1-methylethenyl)-	06:40.2	0.5065	C10H12
58	9,12,15-Octadecatrienal	06:41.8	0.14129	C18H30O
59	Cyclopropane, 2-(1,1-dimethyl-2-propenyl)-1,1-dimethyl-	06:42.8	0.22571	C10H18
62	Decane	06:46.1	0.23074	C10H22
63	Benzene, 1-methyl-4-(2-methylpropyl)-	06:49.2	0.19829	C11H16
64	Limonene	06:49.9	0.19352	C10H16
68	2-tert-Butyltoluene	06:53.4	0.2038	C11H16
69	3,4-Decadiene	06:56.0	0.19571	C10H18

70	Benzene, 1-methyl-4-(1-methylpropyl)-	06:57.7	0.11426	C11H16
72	2,6-Dimethyl-1,3,5,7-octatetraene, E,E-	07:01.1	0.18502	C10H14
74	Cyclohexene,3-(2-propenyl)-	07:03.9	0.74374	C9H14
78	Limonene	07:12.4	0.1211	C10H16
79	2-[(Trimethylsilyl)oxy]-2-{4-[(trimethylsilyl)oxy]phenyl}ethanamine	07:14.4	2.3627	C14H27NO2Si2
83	1-methyl-1-indanol	07:19.3	0.11474	C10H12O
87	Limonene	07:24.1	0.16573	C10H16
91	Benzene, 1-methyl-3-(1-methylethyl)-	07:29.8	0.10467	C10H14
92	exo-7-(2-Propenyl)bicyclo[4.2.0]oct-1(2)-ene	07:31.9	0.10197	C11H16
95	Benzene, (1-methylene-2-propenyl)-	07:36.8	0.12615	C10H10
97	3,4-Octadiene	07:39.6	0.36285	C8H14
98	Benzene, (1-methyl-2-cyclopropen-1-yl)-	07:40.7	0.12837	C10H10
101	Pentanoic acid	07:58.2	0.3793	C5H10O2
102	Benzene, 2-ethenyl-1,3,5-trimethyl-	07:59.4	0.22423	C11H14
103	3-Octyn-2-one	08:01.1	0.38521	C8H12O
107	1H-Indene, 2,3-dihydro-1,1-dimethyl-	08:09.9	0.50706	C11H14
112	9-Octadecen-12-ynoic acid, methyl ester	08:16.5	0.16767	C19H32O2
113	Benzene, (1-methyl-1-butenyl)-	08:17.5	0.47881	C11H14
117	Benzene, (1,3-dimethylbutyl)-	08:26.6	0.23138	C12H18
119	Bicyclo[6.1.0]nonane, 9-(1-methylethylidene)-	08:31.2	0.14361	C12H20
121	Geijerene	08:34.1	0.22055	C12H18
123	Geijerene	08:37.2	0.21337	C12H18
131	6-Methyl-6-hepten-4-yn-3-ol	08:50.9	0.40961	C8H12O
132	1H-Cycloprop[e]azulene, decahydro-1,1,4,7-tetramethyl-, [1aR-(1aà,4á,4aá,7á,7aá,7bà)]-	08:53.5	0.10924	C15H26
138	3,3,5,5-Tetramethylcyclopentene	09:01.0	0.50065	C9H16
139	7-Methyl-1,2,3,5,8,8a-hexahydronaphthalene	09:03.8	0.12584	C11H16
144	1H-Indene, 4,7-dimethyl-	09:10.1	0.208	C11H12
149	Cycloheptane, 1-methyl-4-methylene-	09:16.6	0.26452	C9H16
153	Benzene, 1,3-dimethyl-5-(1-methylethyl)-	09:22.2	0.57065	C11H16
158	1,2,3-Trimethylindene	09:31.2	0.19914	C12H14
164	Cyclohexasiloxane, dodecamethyl-	09:42.3	0.48213	C12H36O6Si6
166	Tridecane	09:43.6	0.58466	C13H28
167	Cyclopropane, (2-methylenebutyl)-	09:45.2	0.22575	C8H14
168	1H-Indene, 1-ethylidene-	09:47.4	0.3218	C11H10
175	1-Dodecen-3-yne	09:53.6	0.1745	C12H20
188	6,7-Dimethyl-1,2,3,5,8,8a-hexahydronaphthalene	10:14.2	0.1122	C12H18
189	Bicyclo[2.2.1]heptane, 2-(1,1-dimethyl-2-propenyl)-	10:15.3	0.14137	C12H20
192	2-Pentene, 1-bromo-3,4-dimethyl-	10:20.3	0.17435	C7H13Br
196	1,2-Di(prop-2-ynyl)cyclohexane	10:27.3	0.11217	C12H16

199	Carbamic acid, (2,6-dichlorophenyl)-, 2-furanylmethyl ester	10:30.5	1.0704	C12H9Cl2NO3
203	1H-3a,7-Methanoazulene, octahydro-1,4,9,9-tetramethyl-	10:35.2	0.14726	C15H26
204	Tricyclo[7.2.0.0(3,8)]undec-4-ene, 4,8,11,11-tetramethyl-	10:37.7	0.1334	C15H24
207	1,2-Dibromo-5-hexene	10:43.1	1.4872	C6H10Br2
212	1,2,3-Trimethylindene	10:50.6	0.44068	C12H14
215	8-Nonenoic acid, 5,7-dimethylene-, methyl ester	10:54.4	0.33268	C12H18O2
222	Bicyclo[3.1.1]hept-2-ene, 2,6-dimethyl-6-(4-methyl-3-pentenyl)-	11:06.4	0.2128	C15H24
223	1,4-Methanophthalazine, 1,4,4a,5,6,7,8,8a-octahydro-9,9-dimethyl-, (1à,4à,4aà,8aà)-	11:09.4	0.2648	C11H18N2
225	Naphthalene, 1,2,3,4,4a,5,6,8a-octahydro-4a,8-dimethyl-2-(1-methylethenyl)-, [2R-(2à,4aà,8aá)]-	11:13.3	0.12336	C15H24
227	Butane, 1-chloro-4-(methylenecyclopropyl)-	11:18.0	1.7529	C8H13Cl
232	Farnesol isomer a	11:26.8	0.10266	C15H26O
238	2-Octene, 2-methyl-6-methylene-	11:36.1	3.1066	C10H18
243	Benzene, 1-(1,3-dimethyl-2-butenyl)-4-(trifluoromethyl)-	11:47.1	1.619	C13H15F3
249	1,5-Heptadiene, 3,3-dimethyl-, (E)-	11:55.7	1.6173	C9H16
262	ç-Elemene	12:12.8	0.14588	C15H24
270	(2S,4R)-p-Mentha-[1(7),8]-diene 2-hydroperoxide	12:21.0	0.54587	C10H16O2
274	Tridecane	12:24.4	0.1901	C13H28
275	trans-Calamenene	12:27.5	0.10267	C15H22
282	4-Tridecen-6-yne, (Z)-	12:34.0	0.1397	C13H22
284	Cyclopentane, 1,1,3-trimethyl-3-(2-methyl-2-propenyl)-	12:36.0	0.21118	C12H22
291	(Z,Z)-à-Farnesene	12:44.1	0.12223	C15H24
301	trans-p-mentha-1(7),8-dien-2-ol	12:53.1	0.11798	C10H16O
302	Naphthalene, 2,3,6-trimethyl-	12:55.7	0.37516	C13H14
317	Limonene	13:14.8	1.187	C10H16
336	(-)-cis-Myrtanol	13:44.2	0.20888	C10H18O
342	Mercaptoacetic acid, 2TMS derivative	13:51.7	1.2631	C8H20O2SSi2
365	Tridecane	14:42.0	0.17701	C13H28
376	Naphthalene, 1,2,3,4-tetramethyl-	15:02.4	0.10342	C14H16
385	Nonanamide	15:21.7	0.1069	C9H19NO
388	Furane-2-carboxylic acid, (2-chloro-5-furanoyloxy)phenyl ester	15:29.6	0.31216	C16H9ClO6
390	Mercaptoacetic acid, 2TMS derivative	15:32.8	0.44058	C8H20O2SSi2
392	Fluorene, 9-benzenesulfonyl-	15:36.2	0.34272	C19H14O2S
395	2-Decene, 2-methyl-	15:44.4	0.18723	C11H22
416	(Z,Z)-à-Farnesene	16:20.6	0.20515	C15H24
425	Pentadecanenitrile	16:49.1	0.12911	C15H29N
430	1,2,4-Oxadiazole-5-carboxamide, 3-(5-bromo-2-furanyl)-N-[2-(2-methoxyphenyl)ethyl]-	16:53.8	0.1805	C16H14BrN3O4
441	Elemene isomer	17:19.3	0.27152	C15H24
450	Cyclopentane, 2-ethylidene-1,1-dimethyl-	17:43.8	0.47606	C9H16

451	2-Methyl-1-tetradecene	17:44.7	0.10512	C15H30
464	2-Benzofuranmethanol, 2,4,5,6,7,7a-hexahydro-4,4,7a-trimethyl-, cis-	19:26.0	0.23326	C12H20O2
467	2-Benzofurancarboxylic acid, 2,4,5,6,7,7a-hexahydro-4,4,7a-trimethyl-, methyl ester, cis-	19:37.9	0.1196	C13H20O3
471	Hexanedioic acid, bis(2-ethylhexyl) ester	21:12.3	0.42582	C22H42O4
472	Bis(2-ethylhexyl) phthalate	22:21.4	0.96216	C24H38O4
473	(R)-2,7,8-Trimethyl-2-((3E,7E)-4,8,12-trimethyltrideca-3,7,11-trien-1-yl)chroman-6-ol	23:12.3	0.13418	C28H42O2

Table D6: GC/MS characterisation of NRZ distillates

Peak #	Name	R.T. (min:sec)	Area %	Formula
1	Cyclobutane, 1,2-diethenyl-	03:01.9	0.40137	C8H12
3	1,5-Dimethyl-1,4-cyclohexadiene	03:03.6	0.12079	C8H12
13	Benzene, 1,3-dimethyl-	03:24.4	0.52015	C8H10
17	9-Tetradecen-1-ol, acetate, (E)-	03:35.0	0.12879	C16H30O2
20	1,3,5,7-Cyclooctatetraene	03:41.2	0.36751	C8H8
22	2,2-Dimethyl-3-heptanone	03:43.6	0.23019	C9H18O
25	Furan, 4-methyl-2-propyl-	03:51.9	0.34827	C8H12O
37	Cyclohexene, 1,5,5-trimethyl-3-methylene-	04:22.9	0.51818	C10H16
42	1,3,7-Octatriene, 2,7-dimethyl-	04:35.4	0.34497	C10H16
43	D-Limonene	04:38.0	2.7002	C10H16
44	Hept-2-ene, 2,4,4,6-tetramethyl-	04:39.3	1.3628	C11H22
47	Benzene, (1-methylethyl)-	04:42.1	2.6945	C9H12
48	trans,trans-1,7-Dimethylspiro[4.5]decane	04:45.3	0.22845	C12H22
52	1-Pentanol, 2,2,4-trimethyl-	04:53.6	2.9929	C8H18O
53	Benzene, 1,2,3-trimethyl-	04:55.8	0.26773	C9H12
54	Benzeneethanol, á-ethenyl-	04:56.9	0.17116	C10H12O
56	Benzonitrile	04:59.6	1.4412	C7H5N
57	1,1'-Bicyclopropyl, 1,1'-dimethyl-	05:02.8	0.76456	C8H14
61	Hydratropic acid, 3-methylbut-2-en-1-yl ester	05:10.7	0.43875	C14H18O2
65	2,6-Dimethyl-1,3,6-heptatriene	05:24.6	3.8154	C9H14
68	Benzene, 1,2-diethyl-	05:38.2	0.74297	C10H14
73	2-Pyrrolidinone, 1-methyl-	05:52.8	0.52368	C5H9NO
77	1-(2-Methylphenyl)ethanol	05:54.8	0.32377	C9H12O
83	3-Nonyne	05:58.3	0.11038	C9H16
88	Indene	06:00.7	0.51456	C9H8
96	Phenol, 2-methyl-	06:06.2	1.2309	C7H8O
100	Heptane, 2,2,6,6-tetramethyl-4-methylene-	06:09.5	5.0042	C12H24
103	3,4-Nonadiene	06:11.7	0.28482	C9H16
109	2,4-Nonadiyne	06:17.3	0.95228	C9H12
117	p-Cresol	06:23.0	0.71081	C7H8O
123	Benzene, 1-ethyl-2,4-dimethyl-	06:28.7	0.75216	C10H14
125	Benzene, 1-methyl-3-(1-methylethenyl)-	06:31.3	0.15794	C10H12
127	Benzene, 1-ethyl-2,4-dimethyl-	06:34.4	0.35744	C10H14
131	Cyclohexene, 1-methyl-4-(1-methylethylidene)-	06:36.8	0.43489	C10H16
132	4-Dodecene, (E)-	06:38.2	0.11911	C12H24
133	Benzene, 1-methyl-4-(1-methylethenyl)-	06:40.3	0.71549	C10H12

134	2-Methylbicyclo[4.3.0]non-1(6)-ene	06:41.3	0.16568	C10H16
139	Undecane	06:46.1	0.51949	C11H24
142	4-Methylphenyl acetone	06:49.0	0.52874	C10H12O
148	Phenol, 2,3-dimethyl-	06:54.3	0.24349	C8H10O
151	Cyclopropane, 2-(1,1-dimethyl-2-propenyl)-1,1-dimethyl-	06:56.0	0.31837	C10H18
152	Benzene, 1-methyl-4-(1-methylpropyl)-	06:57.9	0.94916	C11H16
155	Diazoadamantane	07:00.8	0.34289	C10H14N2
165	13-Methyltetradecanal	07:10.2	0.13332	C15H30O
173	Butyraldehyde, 4-(methylenecyclopropyl)-	07:16.9	0.31326	C8H12O
176	1,5,6,7-Tetramethylbicyclo[3.2.0]hepta-2,6-diene	07:19.4	0.33923	C11H16
177	Benzoylacetonitrile	07:20.6	1.1295	C9H7NO
181	1,3-Cyclohexadiene, 1,3,5,5-tetramethyl-	07:24.4	0.13042	C10H16
185	1-Phenyl-1-butene	07:27.4	1.0489	C10H12
189	Phenol, 2,4-dimethyl-	07:30.1	0.35768	C8H10O
194	Formic acid, 2-phenylethyl ester	07:33.8	0.2284	C9H10O2
197	Indan, 1-methyl-	07:36.2	1.3467	C10H12
203	2-Pentyn-4-one	07:40.1	0.19555	C5H6O
205	Benzene, (2-methylbutyl)-	07:41.1	0.52924	C11H16
206	Naphthalene, 1,2-dihydro-	07:41.6	0.57281	C10H10
217	Naphthalene, 1,2,3,4-tetrahydro-	07:48.4	0.45848	C10H12
222	Benzene, (1-methylene-2-propenyl)-	07:51.6	0.13838	C10H10
223	Benzoic acid, ethyl ester	07:52.6	0.24481	C9H10O2
228	Benzene, 1-methyl-4-(1-methylpropyl)-	07:56.2	0.28927	C11H16
233	Benzene, 2-ethenyl-1,3,5-trimethyl-	08:00.0	0.11985	C11H14
234	Di-tert-butyl peroxide	08:00.8	1.5685	C8H18O2
240	Spiro[2.9]dodeca-4,8-diene	08:05.1	0.15348	C12H18
245	Cyclopropane, 1-methyl-2-octyl-	08:09.3	0.18739	C12H24
247	1H-Indene, 2,3-dihydro-1,1-dimethyl-	08:10.7	0.87555	C11H14
248	Naphthalene	08:11.5	0.77105	C10H8
252	2,2-Dimethylindene, 2,3-dihydro-	08:14.1	0.13279	C11H14
254	1H-Indene, 1-ethyl-2,3-dihydro-	08:14.8	0.35084	C11H14
257	Tridecane	08:16.9	0.53161	C13H28
260	Benzene, 1-methyl-4-(1-methyl-2-propenyl)-	08:18.5	0.7841	C11H14
265	2-Hexene, 6-nitro-	08:23.9	0.14398	C6H11NO2
287	trans-1-Phenyl-1-pentene	08:41.7	0.23035	C11H14
300	Benzene, (1-ethyl-1-propenyl)-	08:50.2	0.68432	C11H14
303	Benzene, 1-(1-methylethenyl)-3-(1-methylethyl)-	08:54.5	0.15545	C12H16
314	1(3H)-Isobenzofuranone, 3a,4,5,7a-tetrahydro-4-hydroxy-3a,7a-dimethyl-, (3aà,4á,7aà)-(ñ)-	09:01.3	0.11045	C10H14O3
315	2-Cyclopentene-1-tridecanoic acid, (S)-	09:01.7	0.11782	C18H32O2
317	5,6,7,8,9,10-Hexahydrobenzocyclooctene	09:03.9	0.24718	C12H16

326	1H-Indene, 4,7-dimethyl-	09:10.5	0.19721	C11H12
328	Benzene, hexyl-	09:11.5	0.37618	C12H18
334	1H-Indene, 2,3-dimethyl-	09:15.1	0.25709	C11H12
338	Naphthalene, 2-ethyl-1,2,3,4-tetrahydro-	09:18.3	0.13309	C12H16
350	Naphthalene, 5-ethyl-1,2,3,4-tetrahydro-	09:28.4	0.15557	C12H16
351	(1-Methylbuta-1,3-dienyl)benzene	09:28.9	0.10436	C11H12
356	Benzene, (2-methyl-1-butenyl)-	09:32.7	0.10027	C11H14
361	Thymol	09:36.9	0.23571	C10H14O
367	Tridecane	09:42.9	0.27184	C13H28
372	1H-Indene, 1-ethylidene-	09:47.3	0.26392	C11H10
377	1-Hexanol, 2,2-dimethyl-	09:49.9	1.5621	C8H18O
387	Heptane, 2,2,6,6-tetramethyl-4-methylene-	09:58.9	0.78194	C12H24
390	Naphthalene, 1-methyl-	10:00.5	0.2346	C11H10
400	Naphthalene, 1-ethyl-1,2,3,4-tetrahydro-	10:07.5	0.16874	C12H16
402	1H-Indene, 2,3-dihydro-1,1,3-trimethyl-	10:09.6	0.25265	C12H16
410	Benzene, 3-cyclohexen-1-yl-	10:16.0	0.20172	C12H14
413	Heptane, 2,2,6,6-tetramethyl-4-methylene-	10:19.0	0.45488	C12H24
469	Farnesene epoxide, E-	11:03.4	0.13459	C15H24O
478	3-Octyne, 5-methyl-	11:13.9	0.10085	C9H16
485	Geranyl nitrile	11:21.8	0.20929	C10H15N
486	1,4-Heptadiene, 3-methyl-	11:22.7	0.23257	C8H14
494	1,5,9-Undecatriene, 2,6,10-trimethyl-, (Z)-	11:31.3	0.2523	C14H24
495	(3-tert-Butyl-5-hydroxymethyl-cyclohex-2-enyl)-methanol	11:32.1	0.40203	C12H22O2
503	2-Octene, 2-methyl-6-methylene-	11:41.0	0.1237	C10H18
510	trans-Farnesol	11:49.2	0.14613	C15H26O
545	Undecanoic acid	13:07.0	0.34048	C11H22O2
547	Cyclopropane, 3-chloro-1,1,2,2-tetramethyl-	13:29.5	0.382	C7H13Cl
550	Phenol, 4-(1,1-dimethylpropyl)-	13:36.8	0.33942	C11H16O
554	Phenol, 2-methyl-4-(1,1,3,3-tetramethylbutyl)-	14:04.1	0.16362	C15H24O
568	Undecanoic acid	17:23.2	0.1378	C11H22O2
582	á-Sitosterol	25:23.3	0.16379	C29H50O

Table D7: GC/MS characterisation of UT distillates

Peak #	Name	R.T. (min:sec)	Area %	Formula
1	1,4-Cyclohexadiene, 1,2-dimethyl-	03:13.3	0.54435	C8H12
2	p-Xylene	03:23.6	3.0225	C8H10
3	Cyclohexene,3-(2-propenyl)-	03:33.3	0.26358	C9H14
5	Cyclopentane, 1-methylene-3-(1-methylethylidene)-	03:37.5	0.27	C9H14
6	Ethylbenzene	03:41.1	0.16048	C8H10
7	2,6-Dimethyl-1,3,6-heptatriene	03:45.7	0.54355	C9H14
8	1,3-Cyclohexadiene, 1,3,5,5-tetramethyl-	03:59.5	0.26099	C10H16
13	1,6-Octadiene, 3,7-dimethyl-, (S)-	04:19.6	0.18084	C10H18
16	D-Limonene	04:37.4	9.7651	C10H16
17	Benzene, (1-methylethyl)-	04:42.3	0.2741	C9H12
18	2,6-Dimethyl-1,3,5,7-octatetraene, E,E-	04:42.7	0.41269	C10H14
20	Spiro[4.4]nonane, 1-methylene-	04:47.9	0.87969	C10H16
21	trisiloxane, 1,1,1,5,5,5-hexamethyl-3-[(trimethylsilyl)oxy]-	04:48.6	0.76815	C9H28O3Si4
22	1,6-Octadiene, 2,6-dimethyl-, (Z)-	04:49.9	0.17828	C10H18
23	Benzene, 1-methyl-3-(1-methylethyl)-	04:55.7	0.20382	C10H14
26	1,6-Octadiene, 2,6-dimethyl-, (Z)-	05:03.0	1.6353	C10H18
28	2,6-Octadiene, 2,6-dimethyl-	05:10.2	10.167	C10H18
31	Bicyclo[2.2.1]heptane, 7,7-dimethyl-2-methylene-	05:24.1	0.73	C10H16
32	Urea, (phenylmethoxy)-	05:25.2	0.70722	C8H10N2O2
33	Ethylenediamine, N,N'-bis(à-methylbenzyl)-	05:32.7	0.64012	C18H24N2
37	D-Limonene	05:49.9	0.16872	C10H16
38	Bicyclo[2.2.1]heptane, 7,7-dimethyl-2-methylene-	05:54.7	0.49678	C10H16
39	D-Limonene	05:58.4	0.39654	C10H16
43	Cyclohexene, 4-methyl-1-(1-methylethenyl)-	06:00.4	0.13982	C10H16
44	1,3,6-Octatriene, 3,7-dimethyl-, (Z)-	06:00.9	0.19989	C10H16
49	Benzene, 1-methyl-3-propyl-	06:05.9	0.36138	C10H14
56	Benzene, 1-methyl-3-(1-methylethyl)-	06:10.3	0.25563	C10H14
58	1,5-Cyclooctadiene, 1,3-dimethyl-	06:12.8	0.58046	C10H16
62	2-Cyclohexen-1-ol, 4-ethyl-1,4-dimethyl-	06:18.0	0.27626	C10H18O
70	Cyclohexane, 1-butenylidene-	06:27.0	0.25039	C10H16
72	2,6-Dimethyl-1,3,5,7-octatetraene, E,E-	06:29.0	0.35476	C10H14
73	1-Pentene, 3-ethyl-3-methyl-	06:30.0	0.10045	C8H16
76	o-Cymene	06:34.4	0.14782	C10H14
79	(-)-cis-Myrtanol	06:36.8	0.17694	C10H18O
81	2-Cyclohexen-1-ol, 4-ethyl-1,4-dimethyl-	06:38.5	0.64011	C10H18O
83	Benzene, 1-methyl-4-(1-methylethenyl)-	06:40.0	0.51752	C10H12

86	Ethyl (E)-hex-3-enyl carbonate	06:42.7	0.29316	C9H16O3
90	Decane	06:45.9	0.17037	C10H22
93	Cyclooctene, 3-ethenyl-	06:49.8	0.2492	C10H16
97	6,6-Dimethyl-2-vinylidenebicyclo[3.1.1]heptane	06:53.4	0.25673	C11H16
99	3,4-Octadiene	06:56.0	0.15239	C8H14
100	Benzene, 1-methyl-4-(1-methylpropyl)-	06:57.7	0.1253	C11H16
101	(E)-4,8-Dimethylnona-1,3,7-triene	06:58.1	0.62688	C11H18
102	Benzene, 1-methyl-4-(1-methyl-2-propenyl)-	06:59.9	0.10011	C11H14
104	2,6-Dimethyl-1,3,5,7-octatetraene, E,E-	07:01.2	0.32087	C10H14
106	1,4-Pentadiene, 3,3-dimethyl-	07:03.9	0.95673	C7H12
110	Benzene, 1-ethyl-2,4-dimethyl-	07:07.6	0.3958	C10H14
113	3-Octen-5-yne, 2,7-dimethyl-, (E)-	07:12.5	0.18836	C10H16
115	Cyclopentasiloxane, decamethyl-	07:14.3	0.31295	C10H30O5Si5
117	Pinocarvone	07:17.0	1.2787	C10H14O
123	2,4,6-Octatriene, 2,6-dimethyl-, (E,E)-	07:24.1	0.73881	C10H16
126	1,3,8-p-Menthatriene	07:30.0	0.23351	C10H14
129	1H-Indene, 1-ethylideneoctahydro-, trans-	07:33.6	0.20948	C11H18
130	3-Undecyne	07:34.1	0.11325	C11H20
135	1,5-Cyclooctadiene, 1,3-dimethyl-	07:39.6	0.47227	C10H16
146	2-Methylenebornane	07:59.0	0.11073	C11H18
147	Benzene, 2-ethenyl-1,3,5-trimethyl-	07:59.4	0.2876	C11H14
148	2-(5-Methyl-furan-2-yl)-propionaldehyde	08:01.2	0.69818	C8H10O2
154	1H-Indene, 2,3-dihydro-1,1-dimethyl-	08:09.9	0.67763	C11H14
161	Bicyclo[2.2.1]heptane, 2-(1-methylpropyl)-	08:15.9	0.19138	C11H20
163	1H-Indene, 2,3-dihydro-1,1-dimethyl-	08:17.5	0.67983	C11H14
170	Benzene, (1,3-dimethylbutyl)-	08:26.6	0.38531	C12H18
174	1,2-Cyclohexanedimethanol	08:31.5	0.6135	C8H16O2
180	1-(3-Methyl-cyclopent-2-enyl)-cyclohexene	08:37.3	0.28134	C12H18
181	Benzene, (3-methyl-2-butenyl)-	08:39.0	0.24477	C11H14
190	Cyclopentane, 2-ethylidene-1,1-dimethyl-	08:47.2	0.12333	C9H16
193	6-Methyl-6-hepten-4-yn-3-ol	08:51.0	0.54505	C8H12O
203	Benzeneacetic acid, à-methoxy-, (ñ)-	08:58.9	0.31459	C9H10O3
207	1-(1,2,3-Trimethyl-cyclopent-2-enyl)-ethanone	09:01.3	0.66469	C10H16O
219	Cycloheptane, 1-methyl-4-methylene-	09:16.8	0.37073	C9H16
223	6,6-Dimethyl-2-vinylidenebicyclo[3.1.1]heptane	09:22.5	0.76632	C11H16
225	1,3-Benzenediol, O-(2-furoyl)-O'-propargyloxycarbonyl-	09:23.9	0.55522	C15H10O6
233	9,12,15-Octadecatrienoic acid, (Z,Z,Z)-	09:35.3	0.11486	C18H30O2
238	Cyclohexasiloxane, dodecamethyl-	09:42.8	0.31684	C12H36O6Si6
240	Bicyclo[4.1.0]heptane, 3,7,7-trimethyl-, [1S-(1à,3à,6à)]-	09:45.9	0.2976	C10H18
241	Naphthalene, 1-methyl-	09:47.6	0.4273	C11H10
242	Benzene, 1,4-bis(1-methylethenyl)-	09:49.6	0.17886	C12H14

246	6,7-Dimethyl-1,2,3,5,8,8a-hexahydronaphthalene	09:53.7	0.44391	C12H18
270	1,2-Dibromo-5-hexene	10:31.5	1.6836	C6H10Br2
278	1,2-Dibromo-5-hexene	10:44.0	1.752	C6H10Br2
282	1,2,3-Trimethylindene	10:51.5	0.53044	C12H14
284	cis-à-Bergamotene	10:55.4	0.27307	C15H24
297	1,5-Heptadiene, 2,6-dimethyl-	11:29.4	0.10991	C9H16
301	2-Butene, 1-bromo-3-methyl-	11:38.2	0.24315	C5H9Br
306	Geranyl nitrile	11:50.3	2.1001	C10H15N
312	(1R,4R,4aS,8aR)-4,7-Dimethyl-1-(prop-1-en-2-yl)-1,2,3,4,4a,5,6,8a-octahydronaphthalene	12:04.2	0.48108	C15H24
321	(1R,4R,4aS,8aR)-4,7-Dimethyl-1-(prop-1-en-2-yl)-1,2,3,4,4a,5,6,8a-octahydronaphthalene	12:12.5	0.11668	C15H24
329	aR-Himachalene	12:20.6	0.10801	C15H22
335	Undecane, 3,5-dimethyl-	12:26.6	0.19195	C13H28
337	trans-Calamenene	12:29.8	0.15767	C15H22
339	(1R,4R,4aS,8aR)-4,7-Dimethyl-1-(prop-1-en-2-yl)-1,2,3,4,4a,5,6,8a-octahydronaphthalene	12:31.3	0.19766	C15H24
348	1H-3a,7-Methanoazulene, octahydro-3,6,8,8-tetramethyl-, [3R-(3à,3aá,6à,7á,8aà)]-	12:42.4	0.24216	C15H26
355	Cyclohexene, 1-methyl-4-(1-methylethenyl)-, (S)-	12:48.0	0.20725	C10H16
363	2-Cyclopentene-1-carboxylic acid, 1,2,3-trimethyl-, ethyl ester, (.+-.)-	12:57.5	0.60048	C11H18O2
364	Naphthalene, 2,3,6-trimethyl-	12:57.9	0.54418	C13H14
373	Naphthalene, 1,4,6-trimethyl-	13:07.4	0.12684	C13H14
376	Naphthalene, 1,4,6-trimethyl-	13:10.5	0.14635	C13H14
439	2-Benzofuranmethanol, 2,4,5,6,7,7a-hexahydro-4,4,7a-trimethyl-, cis-	14:32.8	0.1096	C12H20O2
444	Hexadecane	14:42.2	0.34375	C16H34
455	Naphthalene, 1,2,3,4-tetramethyl-	15:02.7	0.19189	C14H16
471	3-Undecene, 2-methyl-, (Z)-	15:44.2	0.11741	C12H24
486	Carbamic acid, (2,6-dichlorophenyl)-, 2-furanylmethyl ester	16:27.7	0.19264	C12H9Cl2NO3
498	1,3-Bis-(2-cyclopropyl,2-methylcyclopropyl)-but-2-en-1-one	16:53.4	0.10514	C18H26O
500	2,6,9,11-Dodecatetraenal, 2,6,10-trimethyl-, (E,E,E)-	17:00.6	0.18966	C15H22O
501	Cyclopentaneundecanoic acid, methyl ester	17:02.5	0.11428	C17H32O2
510	Cyclopentane, 2-ethylidene-1,1-dimethyl-	17:43.2	0.25915	C9H16

Table D8: GC-MS characterisation of UTZ distillates

Peak #	Name	R.T. (min:sec)	Area %	Formula
1	Cyclobutane, 1,2-diethenyl-	03:02.7	0.46777	C8H12
6	Ethylbenzene	03:16.9	0.12337	C8H10
7	5,5-Dimethyl-1,3-hexadiene	03:20.7	0.96105	C8H14
10	Benzenesulfonamide, N-benzyl-2-ethoxy-5-(tetrazol-1-yl)-	03:25.4	0.20959	C16H17N5O3S
11	(3-Methylphenyl) methanol, 2-methylbutyl ether	03:26.2	0.89396	C13H20O
18	1,3,5,7-Cyclooctatetraene	03:41.7	2.8165	C8H8
19	o-Xylene	03:43.5	1.4729	C8H10
20	Acetic acid, trifluoro-, 3-methylbutyl ester	03:45.0	0.10882	C7H11F3O2
22	Cyclopentadiene, 2,5,5-trimethyl-	03:49.4	0.2428	C8H12
32	4-Hexen-3-one, 2,2-dimethyl-	04:17.3	0.22528	C8H14O
34	Cyclohexene, 1,5,5-trimethyl-3-methylene-	04:22.8	0.78328	C10H16
39	1,5-Cyclooctadiene, 1,5-dimethyl-	04:35.8	0.40348	C10H16
40	Cyclohexene, 1-methyl-4-(1-methylethenyl)-, (S)-	04:36.3	0.12134	C10H16
46	Benzonitrile	05:02.3	2.1851	C7H5N
65	1-(2-Methylphenyl)ethanol	06:01.5	0.23055	C9H12O
71	Phenol, 2-methyl-	06:04.6	0.94419	C7H8O
74	Indene	06:06.3	0.48915	C9H8
77	Benzene, 1-methyl-3-propyl-	06:07.9	0.60174	C10H14
87	2,4,4-Trimethyl-1-pentanol, pentafluoropropionate	06:14.1	6.1552	C11H17F5O2
90	Bicyclo[6.1.0]nonane, 9-(1-methylethylidene)-	06:15.9	0.32162	C12H20
96	2-(Methylsulfonyl)acetophenone	06:20.7	1.2559	C9H10O3S
99	p-Cresol	06:22.6	0.75831	C7H8O
101	Cyclohexene, 4-methyl-1-(1-methylethenyl)-	06:24.7	0.11471	C10H16
110	Benzene, 1-ethyl-2,4-dimethyl-	06:31.7	0.81831	C10H14
112	Benzene, 1-methyl-3-(1-methylethenyl)-	06:33.9	0.24659	C10H12
117	trans-Verbenyl caprate	06:37.3	0.3913	C20H34O2
120	ç-Terpinene	06:40.0	0.52277	C10H16
125	Benzene, 1-methyl-4-(1-methylethenyl)-	06:43.4	0.76197	C10H12
126	Ethanol, 2-(3,3-dimethylcyclohexylidene)-, (Z)-	06:44.2	0.12994	C10H18O
128	cis-3-Hexenyl cis-3-hexenoate	06:45.4	0.47778	C12H20O2
133	Decane	06:49.1	0.69878	C10H22
135	(3-Methylphenyl) methanol, 1-methylpropyl ether	06:51.7	0.25193	C12H18O
140	Phosphinous chloride, tert-butylisopropyl-	06:55.8	4.0761	C7H16ClP
141	Chloroacetic acid, 3-ethylphenyl ester	06:56.4	0.23246	C10H11ClO2
145	Ethyl (Z)-hex-3-enyl carbonate	06:58.5	0.41715	C9H16O3
148	Benzene, 1-methyl-4-(1-methylpropyl)-	07:00.6	0.91183	C11H16

151	Bicyclo[4.2.0]oct-1-ene, 7-exo-ethenyl-	07:03.5	0.37451	C10H14
174	1,5,6,7-Tetramethylbicyclo[3.2.0]hepta-2,6-diene	07:21.8	0.29881	C11H16
175	Benzoylacetonitrile	07:23.0	1.3728	C9H7NO
178	2,4,6-Octatriene, 2,6-dimethyl-, (E,E)-	07:26.8	0.1453	C10H16
181	Methoxyacetic acid, 3-phenyl-2-propenyl ester	07:29.7	0.98264	C12H14O3
184	Phenol, 2,4-dimethyl-	07:32.6	0.31094	C8H10O
187	2-Heptyne-4-one	07:34.2	0.79781	C7H10O
190	Benzene, 4-pentenyl-	07:36.6	0.27984	C11H14
193	Indan, 1-methyl-	07:38.9	1.3049	C10H12
194	Naphthalene, 1,2-dihydro-	07:40.5	0.11017	C10H10
198	Benzene, pentyl-	07:43.7	0.57062	C11H16
199	Benzene, 1-butynyl-	07:44.2	0.50095	C10H10
209	Naphthalene, 1,2,3,4-tetrahydro-	07:50.9	0.46627	C10H12
215	Benzoic acid, ethyl ester	07:54.8	0.27332	C9H10O2
221	o-Cymene	07:58.2	0.3042	C10H14
225	Benzene, 2-ethenyl-1,3,5-trimethyl-	08:02.1	0.13822	C11H14
226	Di-tert-butyl peroxide	08:03.1	1.4618	C8H18O2
232	Spiro[2.9]dodeca-4,8-diene	08:07.2	0.42448	C12H18
234	2,2-Dimethylindene, 2,3-dihydro-	08:09.1	0.16671	C11H14
237	Cyclopropane, 1-methyl-2-octyl-	08:11.7	0.1564	C12H24
245	1H-Indene, 1-ethyl-2,3-dihydro-	08:16.9	0.31716	C11H14
249	Tridecane	08:19.0	0.41619	C13H28
257	1-Cyclohexyl-1-pentyne	08:25.1	1.1795	C11H18
262	1,2,4-Trioxolane, 3,5-diphenyl-	08:29.0	0.20102	C14H12O3
279	trans-1-Phenyl-1-pentene	08:44.4	0.14324	C11H14
287	Benzothiazole	08:50.7	3.0778	C7H5NS
289	Benzene, (1-ethyl-1-propenyl)-	08:52.6	0.59929	C11H14
295	Naphthalene, 1,2,3,4-tetrahydro-1,8-dimethyl-	08:56.5	0.17462	C12H16
308	Benzene, (1,3-dimethylbutyl)-	09:06.2	0.10644	C12H18
315	1H-Indene, 1,3-dimethyl-	09:12.6	0.18926	C11H12
327	Benzene, 4-pentynyl-	09:20.4	0.19017	C11H12
332	Sulfurous acid, cyclohexylmethyl dodecyl ester	09:25.5	0.82695	C19H38O3S
338	Naphthalene, 6-ethyl-1,2,3,4-tetrahydro-	09:30.5	0.16561	C12H16
347	Benzene, cyclohexyl-	09:36.7	0.10873	C12H16
358	Tridecane	09:44.8	0.27444	C13H28
363	Benzothiazole, 2-methyl-	09:48.3	0.41216	C8H7NS
368	Propanedinitrile, (2,3-dihydro-1-methyl-1H-inden-1-yl)-	09:51.0	0.2047	C13H12N2
370	1-Pentanol, 2,2,4-trimethyl-	09:51.9	1.439	C8H18O
383	Naphthalene, 1-methyl-	10:02.5	0.30224	C11H10
394	Naphthalene, 1-ethyl-1,2,3,4-tetrahydro-	10:09.1	0.21141	C12H16
396	1H-Indene, 2,3-dihydro-1,1,3-trimethyl-	10:11.2	0.28186	C12H16

404	à-Santoline alcohol	10:14.8	0.15641	C10H18O
407	Benzene, 3-cyclohexen-1-yl-	10:17.6	0.33231	C12H14
411	Heptane, 2,2,6,6-tetramethyl-4-methylene-	10:20.5	0.6033	C12H24
419	3-Penten-1-ol, 2,2,4-trimethyl-	10:28.8	1.0729	C8H16O
441	Bicyclo[4.1.0]heptan-3-ol, 4,7,7-trimethyl-, (1à,3á,4à,6à)-	10:42.4	0.17614	C10H18O
452	1,2,3-Trimethylindene	10:50.1	0.11923	C12H14
459	Biphenyl	10:55.5	0.24734	C12H10
461	Disulfide, bis(1,1,3,3-tetramethylbutyl)	10:57.4	2.7224	C16H34S2
463	1,2-Benzenediol, o-(3-cyclopentylpropionyl)-o'-(2-methylbenzoyl)-	11:00.1	0.10488	C22H24O4
494	2-Methylallyl methacrylate	11:22.9	0.33547	C8H12O2
495	1,4-Heptadiene, 3-methyl-	11:23.8	0.36208	C8H14
504	1,4-Hexadiene, 3,3,5-trimethyl-	11:32.3	0.37039	C9H16
508	1,5,9-Decatriene, 2,3,5,8-tetramethyl-	11:35.9	0.14377	C14H24
515	Quinoline, 1,2-dihydro-2,2,4-trimethyl-	11:41.3	0.15505	C12H15N
516	Geranyl nitrile	11:41.9	0.21044	C10H15N
525	trans-Farnesol	11:50.1	0.2614	C15H26O
571	Cyclopropane, 3-chloro-1,1,2,2-tetramethyl-	13:29.7	0.40996	C7H13Cl
572	Phenol, 4-(1,1,3,3-tetramethylbutyl)-	13:37.5	0.29747	C14H22O
576	Phenol, 2-methyl-4-(1,1,3,3-tetramethylbutyl)-	14:04.6	0.14324	C15H24O
579	Sulfurous acid, cyclohexylmethyl hexyl ester	14:27.8	0.56345	C13H26O3S
583	Disulfide, bis(1,1,3,3-tetramethylbutyl)	14:53.4	0.30325	C16H34S2
588	Urea, N-cyclohexyl-N'-phenyl-	16:46.9	0.13188	C13H18N2O
590	Undecanoic acid	17:23.9	0.15378	C11H22O2
594	Sulfurous acid, cyclohexylmethyl hexyl ester	17:53.2	0.16343	C13H26O3S
486	Carbamic acid, (2,6-dichlorophenyl)-, 2-furanylmethyl ester	16:27.7	0.19264	C12H9Cl2NO3
498	1,3-Bis-(2-cyclopropyl,2-methylcyclopropyl)-but-2-en-1-one	16:53.4	0.10514	C18H26O
500	2,6,9,11-Dodecatetraenal, 2,6,10-trimethyl-, (E,E,E)-	17:00.6	0.18966	C15H22O
501	Cyclopentaneundecanoic acid, methyl ester	17:02.5	0.11428	C17H32O2
510	Cyclopentane, 2-ethylidene-1,1-dimethyl-	17:43.2	0.25915	C9H16

Appendix E

Plot values for fuel consumption of the different concentration of the various fuel blend as a function of generator run time is presented in TableE1 to TableE4 in this section. Also the plot value for the fuel power as a function of the PD composition in the PD-Petrol fuel blend and other parameters such as the different PD densities, HHV, mass of fuel consumed e.tc.

Table E1

NRPD-petrol blends					
Fuel blend (%)	**5**	**10**	**15**	**20**	**0**
Time (min)	Volume(ml)				
0	200	200	200	200	200
5	189.0909	181.8182	181.8182	154.5455	160
10	181.8182	174.5455	172.7273	145.4545	145.4545
15	163.6364	163.6364	152.7273	127.2727	118.1818
20	160	138.1818	138.1818	109.0909	109.0909
25	145.4545	118.1818	120	90.90909	90.90909
30	141.8182	112.7273	109.0909	54.54545	81.81818
35	109.0909	90.90909	101.8182	43.63636	72.72727
40	100	81.81818	90.90909	36.36364	65.45454
45	90.90909	63.63636	54.54545	25.45455	54.54545
50	49.09091	36.36364	36.36364	18.18182	36.36364

Table E2

NZPD-petrol blends					
Fuel blend (%)	**5**	**10**	**15**	**20**	**0**
Time (min)	volume(ml)				
0	200	200	200	200	200
5	181.8182	163.6364	181.8182	181.8182	160
10	163.6364	145.4545	163.6364	163.6364	145.4545
15	154.5455	127.2727	145.4545	145.4545	118.1818
20	138.1818	116.3636	127.2727	138.1818	109.0909
25	127.2727	98.18182	116.3636	123.6364	90.90909
30	109.0909	72.72727	109.0909	109.0909	81.81818
35	90.90909	54.54545	90.90909	87.27273	72.72727
40	72.72727	36.36364	72.72727	72.72727	65.45454
45	54.54545	1.818182	36.36364	36.36364	54.54545
50	36.36364	0.727273	0.727273	0.727273	36.36364

Table E3

UTPD-Petrol blends					
Fuel blend (%)	**5**	**10**	**15**	**20**	**0**
Time (min)	volume(ml)				
0	200	200	200	200	200
5	185.4545	189.0909	174.5455	181.8182	160
10	174.5455	174.5455	156.3636	167.2727	145.4545
15	160	160	145.4545	152.7273	118.1818
20	145.4545	145.4545	127.2727	138.1818	109.0909
25	127.2727	123.6364	101.8182	127.2727	90.90909
30	116.3636	109.0909	72.72727	109.0909	81.81818
35	105.4545	72.72727	54.54545	90.90909	72.72727
40	90.90909	54.54545	36.36364	65.45454	65.45454
45	72.72727	36.36364	25.45455	36.36364	54.54545
50	36.36364	0.727273	18.18182	14.54545	36.36364

Table E4

UZPD-Petrol blends					
Fuel blend (%)	**5**	**10**	**15**	**20**	**0**
Time (min)	Volume(ml)				
0	200	200	200	200	200
5	181.8182	181.8182	181.8182	174.5455	160
10	174.5455	170.9091	167.2727	163.6364	145.4545
15	152.7273	152.7273	149.0909	145.4545	118.1818
20	138.1818	145.4545	134.5455	130.9091	109.0909
25	127.2727	127.2727	120	116.3636	90.90909
30	109.0909	116.3636	101.8182	105.4545	81.81818
35	94.54545	98.18182	90.90909	90.90909	72.72727
40	72.72727	72.72727	65.45454	72.72727	65.45454
45	54.54545	54.54545	36.36364	54.54545	54.54545
50	36.36364	36.36364	0.363636	1.454545	36.36364

Table E5

NRPD-Petrol blend (%)	Fuel power (KJ/s)
0	1.79
5	1.65
10	1.8
15	1.79
20	2.02

Table E6

NZPD-Petrol blend (%)	Fuel power (KJ/s)
0	1.79
5	1.79
10	2.2
15	2.19
20	2.18

Table E7

UTPD-Petrol blend (%)	Fuel power (KJ/s)
0	1.79
5	1.8
10	2.02
15	2.2
20	1.84

Table E8

UZPD-Petrol blend (%)	**Fuel power (KJ/s)**
0	1.79
5	1.8
10	1.81
15	2.22
20	2.2

Table E9

Distillate	**Density (Kg/m^3)**	**HHV (MJ/kg)**
Petrol	737.22	44.39
NRPD	823.0	43.20
NZPD	821.5	43.22
UTPD	885.0	41.40
UZPD	884.6	41.41

Table E10

Fuel blend (%)	Density (Kg/m^3)	Mass of fuel consumed (kg)	Mass of fuel consumed(Kg/s)	HHV (MJ/kg)	Fuel power (MJ/s)	Fuel power (KJ/s)
Petrol 100%	737.22	0.121	4.03 x 10-5	44.39	0.00179	1.79
NRPD5%	741.62	0.112	3.73 x 10-5	44.30	0.00165	1.65
NRPD10%	745.87	0.122	4.07 x 10-5	44.25	0.00180	1.80
NRPD15%	750.19	0.123	4.09 x 10-5	44.19	0.00179	1.79
NRPD20%	754.66	0.137	4.57 x 10-5	44.11	0.00202	2.02
NZPD5%	741.62	0.121	4.05 x 10-5	44.31	0.00179	1.79
NZPD10%	745.66	0.149	4.95 x 10-5	44.26	0.00219	2.19
NZPD15%	749.57	0.149	4.98 x 10-5	44.21	0.00220	2.20
NZPD20%	753.98	0.150	5.01 x 10-5	44.14	0.00221	2.21
UTPD5%	744.55	0.122	4.06 x 10-5	44.33	0.00180	1.80
UTPD10%	751.88	0.150	4.99 x 10-5	44.08	0.00202	2. 20
UTPD15%	759.59	0.138	4.6 x 10-5	43.91	0.00220	2.02
UTPD20%	766.93	0.125	4.2 x 10-5	43.82	0.00184	1.84
UZPD5%	744.49	0.122	4.06 x 10-5	44.33	0.00180	1.80
UZPD10%	751.88	0.123	4.1 x 10-5	44.15	0.00181	1.81
UZPD15%	759.59	0.152	5.05 x 10-5	43.96	0.00222	2.22
UZPD20%	766.93	0.152	5.08 x 10-5	43.31	0.00220	2.20

Table E11

Experimental TGA

Time min	Temperature °C	weight mg	Weight %
2.04	45	16.31	99.92
3.48	60	16.3	99.86
5.07	75	16.29	99.8
6.56	90	16.28	99.76
8.06	105	16.27	99.71
9.56	120	16.26	99.66
11.05	135	16.25	99.6
12.55	150	16.24	99.51
14.05	165	16.22	99.36
15.54	180	16.18	99.17
17.03	195	16.14	98.9
18.52	210	16.08	98.56
20	225	16.01	98.13
21.5	240	15.93	97.58
22.99	255	15.81	96.88
24.48	270	15.66	95.94
25.97	285	15.46	94.71
27.47	300	15.19	93.09
28.97	315	14.83	90.89
30.47	330	14.33	87.79
31.98	345	13.63	83.51
33.49	360	12.75	78.13
35	375	11.79	72.24
36.51	390	10.82	66.29
38.01	405	9.79	59.96
39.51	420	8.68	53.17
41.02	435	7.63	46.76
42.52	450	6.89	42.21
44.02	465	6.53	39.99
45.53	480	6.4	39.22
47.04	495	6.34	38.86
48.55	510	6.3	38.63
50.06	525	6.28	38.46
51.56	540	6.25	38.31
53.07	555	6.27	38.42
54.57	570	6.25	38.3
56.08	585	6.23	38.19
57.58	600	6.21	38.07
59.08	615	6.19	37.95
60.58	630	6.18	37.85

62.08	645	6.16	37.75
63.59	660	6.14	37.65
65.09	675	6.13	37.56
66.6	690	6.12	37.47
68.11	705	6.1	37.39
69.62	720	6.09	37.3
71.13	735	6.07	37.22
72.63	750	6.06	37.14
74.14	765	6.05	37.05
75.65	780	6.03	36.95

Python programming language procedure used is as follows:

```
#Thermal Weight-loss of used tyre with time at a fixed temperature.

Import numpy as np

From matplotlib import pyplot as plt

def pcf(t, phase1_time, phase2_time, temp = 150):

if (t <= phase1_time):

func = w0 * np.exp(-sig1*temp*(t**2/2))

elif(t <= phase2_time):

func = (w0*beta1*k)/(w0 * beta1 + (k - w0*beta1)*np.exp(-sig2 * temp*(t - phase1_time)))

elif(t > phase2_time):

func = k

return func

w0 = 16.32

phase1_time = [25.97, 20.12, 17.00, 14.99,13.56, 12.48,11.61]

phase2_time = [75.97, 55.78,47.26, 42.53,39.52,37.43,35.91]

beta1 = 0.9471
```

```
beta2 = 0.3695

w2 = 6.0302

k = 6.0302

sig1 = (-2*np.log(beta1))/(25.97**2 * 150)

sig2 = (-1/(150*(75.65-25.97)))*np.log((beta1*(k - beta2*w0))/((beta2*(k - beta1*w0))))

exp_time = np.arange(0.97,80.97,1)


#Temperature 1

w150 = []

temp1 = 150

For i in range(len(exp_time)):

w150 += [pcf(exp_time[i], phase1_time[0],phase2_time[0],temp1)]

plt.plot(exp_time, w150)


#Temperature 2

w250 = []
```

```
temp1 = 250
for i in range(len(exp_time)):
w250 += [pcf(exp_time[i], phase1_time[1],phase2_time[1],temp1)]
plt.plot(exp_time, w250)

#Temperature 3
w350 = []
temp1 = 350
for i in range(len(exp_time)):
w350 += [pcf(exp_time[i], phase1_time[2],phase2_time[2],temp1)]
plt.plot(exp_time, w350)

#Temperature 4
w450 = []
temp1 = 450
for i in range(len(exp_time)):
```

```
w450 += [pcf(exp_time[i], phase1_time[3],phase2_time[3],temp1)]
plt.plot(exp_time, w450)

#Temperature 5
w550 = []
temp1 = 550
for i in range(len(exp_time)):
w550 += [pcf(exp_time[i], phase1_time[4],phase2_time[4],temp1)]
plt.plot(exp_time, w550)

#Temperature 6
w650 = []
temp1 = 650
for i in range(len(exp_time)):
w650 += [pcf(exp_time[i], phase1_time[5],phase2_time[5],temp1)]
plt.plot(exp_time, w650)
```

```
#Temperature 7

w750 = []

temp1 = 750

for i in range(len(exp_time)):

w750 += [pcf(exp_time[i], phase1_time[6],phase2_time[6],temp1)]

plt.plot(exp_time, w750)


##Plotting the graphs

plt.legend(["T = 150","T = 250","T = 350","T = 450","T = 550","T = 650","T = 750"])

plt.axis([0,80,4,18])

plt.xlabel("time(t)")

plt.ylabel("Weight(w)")

plt.show()

plt.ion()
```

Table E12: Chart for weight at time, t for different fixed temperatures, T

Time, t = [0.97 1.97 2.97 3.97 4.97 5.97 6.97 7.97 8.97 9.97 10.97 11.97 12.97 13.97 14.97 15.97 16.97 17.97 18.97 19.97 20.97 21.97 22.97 23.97 24.97 25.97 26.97 27.97 28.97 29.97 30.97 31.97 32.97 33.97 34.97 35.97 36.97 37.97 38.97 39.97 40.97 41.97 42.97 43.97 44.97 45.97 46.97 47.97 48.97 49.97 50.97 51.97 52.97 53.97 54.97 55.97 56.97 57.97 58.97 59.97 60.97 61.97 62.97 63.97 64.97 65.97 66.97 67.97 68.97 69.97 70.97 71.97 72.97 73.97 74.97 75.97 76.97 77.97 78.97 79.97]

Weight at 150 = [16.318762607270866, 16.314896770519265, 16.308403174925669, 16.299284958971295, 16.287546528260783, 16.273193551974657, 16.256232958306263, 16.23667292888835, 16.214522892215513, 16.189793516069962, 16.162496698959089, 16.132645560574499, 16.100254431283151, 16.065338840662459, 16.027915505092171, 15.988002314416862, 15.94561831769402, 15.900783708043539, 15.853519806615543, 15.803849045694317, 15.75179495095713, 15.697382122907543, 15.640636217503751, 15.581583926003283, 15.520252954046244, 15.456672000000001, 11.698524443581826, 9.8045433820329464, 8.6871358804819785, 7.9658510258870541, 7.4728935927819347, 7.12269683424267, 6.8670252908068337, 6.6766174409616914, 6.5327045680426279, 6.4227148187487888, 6.3379340534336261, 6.2721552579451263, 6.2208597852724701, 6.180700097303947, 6.1491612207311093, 6.1243323070428621, 6.1047483688705926, 6.0892781123718125, 6.0770428730115107, 6.0673570476196304, 6.0596837028105197, 6.0536011010397086, 6.0487772105535216, 6.0449501372089873, 6.041913002276873, 6.0395021925773413, 6.0375881906408129,

6.0360683928658885, 6.0348614685285353, 6.0339029188320339, 6.0331415742382841, 6.0325368277509455, 6.0320564469327431, 6.0316748419649615, 6.0313716936636235, 6.031130865988839, 6.0309395436431608, 6.0307875479098536, 6.0306667937284173, 6.0305708587468674, 6.0304946411903426, 6.0304340882000815, 6.0303859801015376, 6.0303477590705716, 6.0303173930500833, 6.0302932676580596, 6.0302741003252391, 6.0302588720881545, 6.0302467734055298, 6.0302371611137895, 6.0302, 6.0302, 6.0302, 6.0302]

Weight at T=250 = [16.317937730907385, 16.311495504101284, 16.300676536673929, 16.285489541282153, 16.265946741705591, 16.242063856450276, 16.213860077679584, 16.181358045512045, 16.144583817734262, 16.103566834985614, 16.058339881479831, 16.00893904133688, 15.955403650606511, 15.897776245072794, 15.836102503936566, 15.770431189480192, 15.700814082826181, 15.62730591590808, 15.549964299778804, 15.468849649387762, 10.772931164619083, 8.6150595025025378, 7.5802523359070921, 7.0066686819883408, 6.6630549313720566, 6.4475593644312266, 6.3085078783804853, 6.2171272625876481, 6.156350881991056, 6.1156064149638123, 6.0881455418974433, 6.069571053915042, 6.056976819442534, 6.0484233955159752, 6.0426078222415063, 6.0386507470947075, 6.035956855879463, 6.034122268989714, 6.0328725845859852, 6.0320211855777952, 6.0314410705528605, 6.031045769548375, 6.0307763903272544, 6.0305928144922101, 6.0304677087278451, 6.0303824485549846, 6.0303243426965194, 6.0302847425381083, 6.0302577541985558, 6.0302393610137193, 6.0302268255978744, 6.0302182823842605, 6.0302124599543543,

6.0302084918087298, 6.0302057874072856, 6.0302]

Weight at T=350 = [16.317112896239529, 16.308094946766136, 16.292953559169231, 16.271705799783078, 16.244375599782565, 16.210993710266372, 16.171597644597373, 16.126231608151514, 16.074946415659401, 16.017799396356921, 15.954854287192722, 15.886181114371025, 15.811856063537912, 15.731961338947958, 15.646585011975565, 15.555820859361742, 15.459768191612076, 9.4566182173045128, 7.650862411173887, 6.8825303559083615, 6.5008611644062579, 6.2967198103328128, 6.1832052898333529, 6.1187178507329802, 6.0816361578758853, 6.0601647161438486, 6.0476820493999526, 6.0404081567712922, 6.0361637538787045, 6.0336851300973757, 6.0322370064387627, 6.031390718555885, 6.0308960671777498, 6.0306069190165363, 6.0304378885101517, 6.0303390733778786, 6.0302813050452526, 6.0302475327254488, 6.030227788745921, 6.0302162459745947, 6.0302094977981779, 6.0302055526500817, 6.0302032462188322, 6.0302018978214411, 6.0302011095144055, 6.0302006486502124, 6.0302003792173497, 6.0302]

Weight at T=375 = [16.316906694087258, 16.307244918209218, 16.291023386581514, 16.268261687654721, 16.238987285572854, 16.203235464950698, 16.161049260002223, 16.112479368219397, 16.057584048843758, 15.996429006415328, 15.929087259724756, 11.96015450282481, 8.3631878726113609, 7.1528543607899486, 6.6142843996625338, 6.3454699598910072, 6.2036162459782247,

6.1265579289944716, 6.0840379962027988, 6.0603732715230594, 6.0471394406978991, 6.0397190120129505, 6.0355520257641606, 6.0332100638035211, 6.031893194910726, 6.0311525322325572, 6.030735890100889, 6.030501498330703, 6.0303696295351923, 6.0302954381881486, 6.0302536964082316, 6.030230211313123, 6.0302169978779849, 6.0302095635741386, 6.0302053807892788, 6.0302]

Weight at T=450 = [16.316288103265187, 16.304695098365993, 16.285234240677173, 16.257933724591567, 16.222833064504528, 16.179982999508436, 16.129445371171254, 16.07129297481136, 16.005609384769233, 15.932488754263076, 15.852035590499266, 15.764364505789484, 15.669599945504157, 15.567875893765919, 15.459335557857226, 8.7406623372573922, 7.1406773720444354, 6.5402795116169461, 6.2756550094125023, 6.1508477095464755, 6.0901073798610721, 6.0600955200977937, 6.0451556536766828, 6.0376910045933148, 6.0339544167055577, 6.0320822572220978, 6.0311438058592044, 6.0306732820727884, 6.0304373418544062, 6.0303190246953813, 6.0302596903429029, 6.0302299345820671, 6.030215012167198, 6.0302075285982442, 6.0302037755925459, 6.0302018934605135, 6.0302009495710225, 6.0302004762101937, 6.0302002388195843, 6.0302001197681099, 6.030200060063752, 6.0302000301219936, 6.0302, 6.0302, 6.0302, 6.0302, 6.0302, 6.0302, 6.0302, 6.0302, 6.0302, 6.0302, 6.0302, 6.0302, 6.0302, 6.0302,

6.0302, 6.0302]

Weight at T=525 = [16.315669535894539, 16.302145677215577, 16.279447151992294, 16.247612318272033, 16.206694913333529, 16.156763902534482, 16.097903285616372, 16.030211861227937, 15.953802950591404, 15.868804081393156, 15.775356633133129, 11.093115055408649, 7.5757776225392259, 6.6353206869888011, 6.2864734702156557, 6.1421262048623397, 6.0797237322662259, 6.0522374815931324, 6.0400310896283846, 6.0345906293399603, 6.0321618618739965, 6.0310768125963881, 6.0305919118012685, 6.0303751818920972, 6.0302783066627352, 6.0302350035487668, 6.0302156468587604, 6.0302069942800731, 6.0302031265056657, 6.0302013975764543, 6.0302006247294786, 6.0302002792598195, 6.0302001248317101, 6.0302000558009246, 6.0302000249435279, 6.0302]

Weight at T=550 = [16.31546335198226, 16.301295958753066, 16.277518579464186, 16.24417330583346, 16.201319097934682, 16.14903161047987, 16.087402970263241, 16.016541505683318, 15.936571429454707, 15.847632475810228, 15.749879493676632, 15.643481997481599, 15.528623677415704, 10.608231594566048, 7.4049464184512992, 6.5536154194491898, 6.2447586877900108, 6.1206678225310673, 6.0687888859306449, 6.0467404156527769, 6.0373044924601498, 6.0332542634111688, 6.031513548316827,

6.0307650111711437, 6.0304430517386667, 6.0303045571270673, 6.0302449794597006, 6.0302193498352645, 6.0302083241780586, 6.0302035810130468, 6.0302015405317011, 6.0302006627282134, 6.0302002851020333, 6.0302001226493314, 6.0302000527630701, 6.0302000226983834, 6.0302000097647204, 6.0302000042007284, 6.0302000018071302, 6.0302]

Weight at T= 600 = [16.315050991974417, 16.299596654695627, 16.273662119795823, 16.237297464533547, 16.190572816073836, 16.133578126143398, 16.066422882477607, 15.989235758354971, 15.902164201789228, 15.805373966214823, 15.699048584756518, 10.727762169041737, 7.3046560457612655, 6.480715500988107, 6.2019825368136896, 6.0974916814680462, 6.0568328377195204, 6.0407834390440565, 6.0344124060207074, 6.0318776812636949, 6.0308683415584676, 6.0304662754967824, 6.0303060916878071, 6.0302422706039929, 6.0302168421803328, 6.0302067105678914, 6.030202673749244, 6.030201065325322, 6.0302004244669636, 6.030200169124126, 6.0302000673856231, 6.0302000268490508, 6.0302000106977047, 6.0302000042623813, 6.0302000016982973, 6.0302]

Weight at T= 650 = [16.314638642388633, 16.297897527779583, 16.269806573797506, 16.230424533642967, 16.179833662186532, 16.118139429701571, 16.045470155483788, 15.961976563138819, 15.867831259695198, 15.76322814106209, 15.648381726698041, 15.523526426685814, 9.6358276915301939, 6.9962914711943016, 6.3539836743329667, 6.1457696043295273, 6.0723387687915009, 6.0456820923968042, 6.0359040743328327, 6.0323037035724045, 6.0309761532062804, 6.0304863984647472, 6.0303056856857671, 6.0302390004722488, 6.0302143921803397, 6.0302053110994898, 6.030201959939629, 6.0302007232710855, 6.0302002669067569, 6.0302000984958779, 6.0302000363476678, 6.0302000134132818, 6.030200004949867, 6.0302000018266355, 6.0302000006740784, 6.0302000002487528, 6.0302000000917966, 6.0302]

Weight at T=675 = [16.314432471503935, 16.297048030743813, 16.267879143356971, 16.226989159216181, 16.174466756755344, 16.110425622518449, 16.035004041131344, 15.948364397766211, 15.850692595604148, 15.742197391220799, 15.623109651220378, 10.399157699986636, 7.0877329968789269, 6.3676198340542127, 6.1458599615061518, 6.070774331655346, 6.0445475579328951, 6.0352876715473425, 6.032005883581415, 6.0308412284615089, 6.0304277140953682, 6.0302808697761652, 6.0302287203274911, 6.0302101998775104, 6.0302036224415376, 6.0302012864950489, 6.0302004568934811, 6.030200162263875, 6.0302000576273613, 6.0302000204661255, 6.0302000072684621, 6.0302000025813651, 6.0302000009167607, 6.0302000003255838, 6.0302000001156291,

6.0302, 6.0302]

Weight at T=750 = [16.313813974482205, 16.294499805297814, 16.262098221945209, 16.216687398162644, 16.158376719423824, 16.087306343911525, 16.003646641189853, 15.907597511721551, 15.799387591034401, 15.679273342970935, 15.547538047054264, 10.102265104756583, 6.9121901674437378, 6.2840272467109894, 6.1083039380864603, 6.0547074186020629, 6.0379365094993833, 6.0326469018047746, 6.0309743694866986, 6.0304451106781798, 6.0302775893798879, 6.0302245612562242, 6.0302077750193872, 6.0302024612357332, 6.0302007791215271, 6.0302002466364604, 6.0302000780745306, 6.0302000247150493, 6.0302000078237246, 6.030200002476656, 6.0302000007840029, 6.0302000002481808, 6.0302000000785627, 6.0302000000248688, 6.0302000000078726, 6.0302]